INTEGRATING MULTI-SOURCE DATA TO QUANTIFY CHANGES IN BIOMASS AND SOIL ORGANIC CARBON DUE TO LAND-USE CHANGE IN THE BOREAL PLAINS ECOZONE, CANADA

A Dissertation Submitted to the College of Graduate and Postdoctoral Studies

in Partial Fulfillment of the Requirements

for the Degree of Doctor of Philosophy

in the Department of Soil Science

University of Saskatchewan

Saskatoon

By

Thuan Van Ha

PERMISSION TO USE

In presenting this dissertation in partial fulfillment of the requirements for a Postgraduate degree from the University of Saskatchewan, I agree that the Libraries of this University may make it freely available for inspection. I further agree that permission for copying of this dissertation in any manner, in whole or in part, for scholarly purposes may be granted by the professor or professors who supervised my dissertation work or, in their absence, by the Head of the Department of Soil Science or the Dean of the College of Agriculture and Bioresources. It is understood that any copying or publication or use of this dissertation or parts thereof for financial gain shall not be allowed without my written permission. It is also understood that due recognition shall be given to me and to the University of Saskatchewan in any scholarly use that may be made of any material in my dissertation. Requests for permission to copy or to make other uses of materials in this dissertation, in whole or part, should be addressed to:

Head, Department of Soil Science
University of Saskatchewan
Saskatoon, Saskatchewan
Canada, S7N 5A8

DISCLAIMER

Reference in this dissertation to any specific commercial products, process, or service by trade name, trademark, manufacturer, or otherwise, does not constitute or imply its endorsement, recommendation, or favouring by the University of Saskatchewan. The views and opinions of the author expressed herein do not state or reflect those of the University of Saskatchewan, and shall not be used for advertising or product endorsement purposes.

ABSTRACT

Land use and cover change (LUCCs) is the second largest source of global carbon emission and there has been a growing interest in LUCCs to mitigate climate change effects. Global land-use change associated with cropland expansion, which is a major carbon source, was dominant in the last century. Abandoned cropland typically is a carbon sink and was observed in many regions in the recent decades. However, there has been little research on carbon balance resulting from LUCCs in agricultural landscapes, especially under abandoned cropland in Canada. Information on carbon balance resulting from LUCCs is necessary for national greenhouse gas (GHG) inventories as well as emission mitigation options. The primary objective of the study is to quantify carbon stocks and dynamics as consequences of LUCCs in the Boreal Plains Ecozone, Canada. Field measurement on carbon stocks in abandoned cropland was assessed at field sites in Saskatchewan. Vegetation C ranged from 7.6 to 90.1 Mg C ha^{-1} and increased linearly with stand age. Ecosystem C increased from 74.2 to 137.6 Mg C ha^{-1} after 41 years of abandonment (or net C sink of 1.9 Mg C ha^{-1} yr^{-1}). In the agriculture region of the Boreal Plains Ecozone, land-use change accounted for 6.5% of the total area during the 1990-2000 period. Forest to cropland conversion was dominant on well-drained Chernozemic and Luvisolic soil orders. Abandoned cropland occurred mainly on poorly drained and acidic parent materials. LUCCs in agriculture region was estimated to be a net C sink of 0.76 ±0.3 Mg C ha^{-1} yr^{-1} during this period. In the agriculture-forest transition region of the Boreal Plains Ecozone, substantial land-use changes occurred in pasture (+76%) and summer fallow (-87.8%) over a 27-year period (1984 - 2011). The shrub and forest area was reduced -31.6% and -16.4%, respectively. Forest disturbances occurred mainly during 2005 – 2011. Substantial changes of summer fallow to annual cropland took place on the higher soil capability land and annual cropland to pasture conversion was more likely on lower capability soil classes. We estimated that LUCCs in the region was a net C source of approximately 552.7 Gg C across the research period or 0.07 Mg C ha^{-1} yr^{-1}.

ACKNOWLEDGEMENTS

I would like to express my special appreciation and thanks to my supervisors, Professor Dr. Daniel J. Pennock and Dr. Murray J. Bentham, for the continuous support and mentorship of my Ph.D. study, for their patience, motivation, and immense knowledge. I would like to acknowledge the valuable guidance and insightful comments from my supervisory committee, Dr. Mark Johnston, Dr. Brian McConkey, Dr. Xulin Guo, and Dr. Ted Huffman. Special thanks to Dr. Frank Larney for his willingness to be my external examiner and his contributions to the enhancement of this dissertation.

My sincere thanks also goes to Dr. Colin Laroque, who helped to decode information from tree rings, and Dr. Xulin Guo, who gave access to the sophisticated device, Plant Canopy Analyzer. Many thanks to the Department of Soil Science for allowing me access to the laboratory and research facilities. Without the precious support, it would not be possible to conduct this research.

The completion of this research would not have been possible without help from Darrel Cerkowniak, Paul Krug, Rob Alary, Mihai Voicu, Jiangui Liu, Leah Brannen, Kendra Purton, Jeremy Kiss, Thuan Chu, and Tung Nguyen. Warm thanks for all your help, guidance, and support.

I am so grateful to the Vietnam International Education Development (VIED) and College of Graduate Studies and Research scholarship scheme and the Department of Soil Science, College of Agriculture and Bioresources, University of Saskatchewan for making it possible for me to study here.

DEDICATION

This dissertation is dedicated to my parents, Dzung Ha and Thich Ha, who motivated and shaped me into the person I am today. I also dedicate this work to my wife, Elise Dang, who has supported and encouraged me through this adventure. This thesis is also dedicated to my parents-in-law, Bich Nguyen and Cuong Dang, and my children, Hannah Ha and Mayah Ha, who bring happiness into my life when times are dark and gloomy.

TABLE OF CONTENTS

LIST OF FIGURES

LIST OF TABLES

LIST OF ABBREVIATIONS

AAFC	Agriculture and Agri-Food Canada
AFOLU	Agriculture, Forestry and Other Land Use
AGB	Aboveground biomass
AVHRR	Advanced Very High Resolution Radiometer
BGB	Belowground biomass
BPE	Boreal Plains Ecozone
CLI	Canada Land Inventory
CBM-CFS	Carbon Budget Model of the Canadian Forest Sector
CO_2	Carbon dioxide
CO_2e	Carbon dioxide equivalent
DBH	Diameter at breast height
DOC	Dissolved organic carbon
DOM	Dead organic matter
GHG	Greenhouse gases
GIS	Geographic information system
IPCC	The Intergovernmental Panel on Climate Change
LAI	Leaf Area Index
LUCC	Land use and cover change
NBP	Net Biome Productivity
NBR	Normalized Burn Ratio
NDVI	Normalized Difference Vegetation Index
NEP	Net Ecosystem Productivity
NPP	Net Primary Productivity
Rh	Heterotrophic respiration
RothC	Rothamsted Carbon Model
SOC	Soil organic carbon
UNEP	United Nations Environment Program
UNFCCC	The United Nations Framework Convention on Climate Change
WMO	World Meteorological Organisation

1. GENERAL INTRODUCTION

Since the Industrial Revolution (1880s) the global temperature has increased by approximately 0.8 ˚C and the rate of increase (0.15 – 0.2 ˚C per decade) has been faster since 1975 (GISTEMP Team, 2016; Hansen et al., 2010). A recent study estimated that average global temperature could increase between 0.72 and 0.85 ˚C over the period 2003 - 2012 (IPCC, 2013). The impacts of global warming and climate change include increases in the risk of drought, forest fire, and floods, alterations in land cover and land use, and increases in heat-related illness and diseases; overall "the net damage costs of climate change are likely to be significant and to increase over time" (IPCC, 2007b).

Scientific evidence indicates that changes in climate have been caused by both natural processes (i.e. volcanism, solar emissions, and troposphere aerosols) and human influences. However, human activities such as burning of fossil fuels and alternations in land use have increased greenhouse gas (GHG) concentration in the atmosphere, and are the leading cause of global warming (Cox et al., 2000; Crowley, 2000; IPCC, 2013). Among the six GHGs covered under the Kyoto Protocol, CO_2 is of primary concern because the higher concentration of this gas, and its association with human activities, has caused most of the warming (IPCC, 2007a). GHG emissions have increased substantially in the recent decades, from 27 to 49 Gt CO_2 equivalents per year during 1970 – 2010. GHG emissions from agriculture, forests and other land use contributed 24% of the global annual emission, which is the second largest source (after the energy sector) (IPCC, 2013). Canada contributed an estimated 1.6% of global emissions (CAIT, 2015).

The Intergovernmental Panel on Climate Change (IPCC) was established by the World Metrological Organisation (WMO) and United Nations Environment Program (UNEP) in 1988 with the participation of many scientists and parties to provide an objective source of information about climate change. The main aims of the IPCC are to assess scientific information relevant to human-induced climate change, its impacts, and options for adaptation and mitigation and to produce assessment reports every five to six years. Each member country has to provide an annual

National Greenhouse Gas Inventory following the 2006 IPCC guidelines under the obligations of the United Nations Framework Convention on Climate Change (UNFCCC).

The terms land use and land cover are often used interchangeably although formally each term has a specific meaning. Land use refers to the purpose the land serves - for example, recreation, wildlife habitat, or agriculture (Brown, 2006). Land cover refers to the bio-physical cover of the earth's surface, for example, vegetation, urban infrastructure, water, or bare soil. Under the IPCC guidelines, information on annual emission and removals of the key GHGs (CO_2, N_2O, CH_4) from the Agriculture, Forestry and Other Land Use (AFOLU) sector is required (IPCC, 2006). This includes CO_2 emissions and removals resulting from C stock changes in biomass, dead organic matter (DOM) and mineral soils. The land-use categories defined in the IPCC Guidelines are Forest, Cropland, Grassland, Wetlands, Settlements, and Other Land. C stocks and changes should be reported under land remaining in the same category and land converted from one category to another (i.e., land use and land-use change). However, some C stock changes are not associated with land-use change. The commercial harvest of managed forest, for example, which is included in the IPCC Guidelines, is not a land-use change. C stocks and dynamics under changes in land use and cover are included in this study and therefore land-use change and land-cover change may be used interchangeably under the term land-use and cover change (LUCC).

Although Canada's GHG emissions accounts for a small portion of the global GHG (1.6%), it ranks as one of the highest GHG emitting countries per capita (20.4 Mg CO_2e per person). The major contributions are from transportation, oil and natural gas, and electricity generation sectors. C fluxes in the land use, land-use change and forestry category act as a C source of approximately 0.072 Gt C in 2014, accounting for about 9.8% the total national GHG emissions (CAIT, 2015; Environment Canada, 2013).

The exchanges of GHGs between terrestrial and the atmosphere are directly affected by LUCC. Depending on conversion types, a region could act as C sink or source. Land conversion from forest to cropland, for example, causes a reduction in C stocks (Houghton et al., 2012). On the contrary, some changes such as tree plantation (Houghton and Goodale, 2004), natural succession in abandoned cropland (Johannes and Tilman, 2000; Silver et al., 2000), and reducing tillage and efficient use of fertilizer (McConkey et al., 2003; Smith et al., 1998a), show high

potential C accumulation in both biomass and soil. Nonetheless, C uptake rates under a land conversion type are dependent on site conditions and time scales (Goodale et al., 2002; Guo and Gifford, 2002).

The transition region between agricultural and forestry along the southern edge of the Canadian boreal forest, is likely to have experienced considerable changes in land use and C storage. The forest cover of the region has been shown to be susceptible to climate change. The massive dieback of trembling aspen (*Populus tremuloides*) due to increased drought stress (Hogg et al., 2008; Michaelian et al., 2011), freeze-thaw damage (Hanninen, 2006), increased fire frequency (Flannigan et al., 2009) have been important in the recent decades. Consequently, it has been predicted that the boreal forest could shift to the northeast rapidly through a process called "savanification" (Frelich and Reich, 2010). Additionally, because it is a transition region between forest and agriculture, LUCCs such as forest clearing for agriculture, could be prevalent. The importance of this region, and the lack of integrated information on LUCC in the region, highlights the need for studies to explore the spatial distribution of the changes as well as the potential impacts on the carbon budget for this region.

Since the 1950s, a considerable area (0.64 million km^2) of cropland has been abandoned in North America, covering central and eastern Canada (Ramankutty and Foley, 1999b). As it is no longer used for cultivation, abandoned cropland typically reverts to natural vegetation, and biomass and SOC can be accumulated (Schierhorn et al., 2013). The large areas of abandoned cropland in Russia (45.5 Mha) and Kazakhstan (12.9 Mha), for instance, could accumulate C with the estimated annual rates of 3.4 Mg C yr^{-1} and 2.4 Mg C yr^{-1}, respectively (Kurganova et al., 2015). In Canada, abandoned cropland also shows high potential for C sequestration. Amichev et al. (2012) reported that long-term willow plantation on agriculturally marginal land could accumulate 5.5 Mg C ha^{-1} yr^{-1}. Information on C stock and dynamics on abandoned farmland, which might have regenerated into shrub or forest, is limited. Meanwhile, information on C stocks, emissions, and removals of GHGs associated with LUCCs, including abandoned cropland is expected in national reports to the UNFCCC (IPCC, 2006). The information is also particularly important to enhance our knowledge of the role that land use and cover change could influence Canada's carbon budget. My study is focused on quantifying the vegetation spatial distribution and ecosystem C dynamics in the transition region of the boreal plains ecozone.

At the national level, Huffman et al. (2015) estimated aboveground woody C stocks and dynamics in the agriculture region during 1990 and 2000 (excluding forest). Canada's cropland acted as a C sink of 78.3 Gg yr^{-1} during the study period. In forest region, Kurz et al. (2013) concluded that managed boreal forest acts as a C sink of 28 Tg C yr^{-1} during 1990 - 2000. Data from multiple sources, including field measurements and remote sensing detailing the effect of LUCCs on C stocks and dynamics in Boreal Plains Ecozone (BPE), will lead to more accurate estimation of on terrestrial C budgets, which in turn will support policy and management decisions.

The general objective of the study presented in this dissertation is to estimate C stocks and dynamics resulting from LUCCs in the Agri-Forest transition region of the Boreal Plains Ecozone. Field experiments, geographic information systems (GIS), remote sensing techniques, and C modelling studies were used to achieve the following objectives:

1. Quantification of C stocks, distributions, and dynamics in abandoned cropland using a field sampling study in the BPE in Saskatchewan.
2. Characterization of LUCCs in the agriculture region of the BPE and exploration of the links between the land use transitions and soil characteristics.
3. Estimation of C stocks and dynamics under changes in LUCCs for the research region over a period of 15 years using the Carbon Budget Model of the Canadian Forest Sector (CBM-CFS3).
4. Detection of LUCCs over a period of 27 years (time-series data) and extraction of information on location, magnitude, and duration of the LUCCs in the Agri-Forest transition region of central Saskatchewan.
5. Extraction of major land transitions based on bi-temporal change detection technique and documentation of the association between the transitions and soil capability classes.

This dissertation reports LUCCs and C stock changes in the BPE in plot, field, and regional scale. The research outcome presented in this dissertation is organized a manuscript-based format with seven chapters. Following this introduction and literature review (Chapter 2), the three subsequent chapters (Chapter 3 – 5) detail research studies examining LUCCs and C stock changes. Specifically, Chapter 2 comprises an in-depth review of the literature in relation to

LUCCs and C stock changes. This chapter covers the background on C implications of LUCCs and provides a detailed review on approaches to quantify LUCCs and C density based on C pools. Chapter 3 details the field study that measured C stock under three dominant types of land use (forest, cropland, and abandoned cropland) with the main focus on quantifying C stock and dynamics in abandoned cropland using a chronosequence approach. Chapter 4 presents my research outcomes on LUCCs at field scale and their association to soil characteristics. An estimation of ecosystem C changes as a result of LUCCs for the agriculture region of the Boreal Plains Ecozone is included in this chapter. Chapter 5 integrates the research findings on LUCCs in the Agri-Forest transition region of the BPE in Saskatchewan, Canada. The research outcomes on location, magnitude, and duration of LUCCs described in Chapter 5 provide insights into LUCCs from long-term monitoring at a broad spatial scale. Chapter 6 summarises some key findings from each research study and recommendations for future research.

2. LITERATURE REVIEW

2.1. Global Carbon Cycle

High concentrations of GHGs such as CO_2 are expected to have significant impacts on the global weather pattern (climate change) in the immediate future. Evidence from long-term monitoring studies indicates that the global temperature (one type of climate change) has increased, at an accelerating rate, by approximately 0.8 ˚C since 1975 (GISTEMP Team, 2016; Hansen et al., 2010). Climate change is driven by both natural processes and human influences, but human activities such as burning of fossil fuels and changes in land use speed up GHG concentrations in the atmosphere, a leading cause of climate change and global warming (Cox et al., 2000; Crowley, 2000; IPCC, 2013). According to a current estimation, the GHG emissions from agriculture, forest and other land use are the second largest source of GHG (after the industrial sector) contributing 24% of the global annual emissions (IPCC, 2013). Thus, accurate quantification of C stock and dynamics among C pools is important to understand the global carbon cycle, support the development of climate change policies, and predict future climate change.

Earth's atmosphere, oceans, land, and fossil fuels are the main pools for C stocks, and C exchange between the pools is termed the carbon cycle. Current estimates by the Intergovernmental Panel on Climate Change (IPCC, 2007a) report that, excluding C in the Earth's crust, the largest amount of C is in the ocean pool, 38000 Gigatonnes C (Gt C). Soil and vegetation (terrestrial ecosystem) store 2300 Gt C. Global soil organic carbon was estimated to be in a range from 1388.5 to 1460.5 Gt C (Scharlemann et al., 2014). Carbon stocks in the atmosphere are estimated at 762 Gt C. A recent estimation of C fluxes among the pools, indicate that the exchange rates of CO_2 accumulation are larger than can be balanced by natural processes. In the period 2005-2014, the sinks associated with land and ocean accumulated 3.0±0.8 Gt C yr^{-1} and 2.6±0.5 Gt C yr^{-1}, respectively. Meanwhile, the release rates associated with the industrial sector and the use of fossil fuels were estimated to be 9.0±0.5 Gt C yr^{-1} and 0.9±0.5 Gt C yr^{-1} from land-use change. On average, the growth rate of C in the atmosphere was estimated to be 4.4 Gt C yr^{-1} during the

research period (Le Quéré et al., 2015). Although this is much less C than that contained in the C pools, the continuous accumulation rate of CO_2 in the atmosphere is concerning because of its influence on the greenhouse effect and climate change (Allen et al., 2009; IPCC, 2007a; Shakun et al., 2012; Tans and Dlugokencky, 2015).

The amount of C stored in each pool varies over time, as a result of several fluxes, adding and removing C simultaneously. Through the photosynthesis process, plants utilise sunlight, atmospheric CO_2, and water from the soil to create carbohydrates that are stored in the structure of plants at an estimated rate of 120 Gt C yr^{-1}. Correspondingly, nearly 50% of this amount is released back into the atmosphere through the respiration process, and a similar portion is sequestered in the soil profile (known as soil organic carbon, SOC) at a rate of 60 Gt C yr^{-1}. From the soil pool, approximately 55 - 60 Gt C yr^{-1} is released into the atmosphere through the decomposition process, as a result of biological activities. It is estimated that soil carbon is transferred into the oceanic pool via sediment at a rate of 0.4 to 0.6 Gt C yr^{-1} (Houghton, 2007; Lal, 2008). Therefore, reducing C emissions and maintaining C sequestration, especially soil C, are required to mitigate global warming and climate change for coming decades.

In the last decades, attempts have been made for a better estimation on trends and amount of anthropogenic GHG emissions from different sectors, including agriculture, forest and other land uses (AFOLU). According to a current estimation (Tubiello et al., 2015), the share of anthropogenic GHG emissions from AFOLU declined from 23.6 ± 2.1 % during the 1990s to 21.2 ± 1.5 % in 2010. Specifically, global GHG emission from AFOLU declined slightly from 11.1 ± 0.8 Gt CO_{2e} in the 1990s to 10.6 ± 1.2 Gt CO_{2e} in 2000s, and to 10.3 ± 0.9 Gt CO_{2e} in 2010. The major contribution to the decline was from forest and other land use (FOLU) sub-categories (Tubiello et al., 2015). In another study on the global forest emission, Federici et al. (2015) estimated a decline in C emissions from 1.09 Gt C yr^{-1} during 2001 – 2010 to 0.79 Gt C yr^{-1} during 2011 – 2015. Indeed, the emission from agriculture continued to increase in the last decades, from 4.8 ± 0.3 in 1990s to 5.1 ± 0.3 in 2000s, and to 5.4 ± 0.3 CO_{2e} in 2010 (Tubiello et al., 2015). As understanding trends of GHG emissions is required to support our mitigation options pertaining to global warming and climate change (Houghton, 2007; Lal, 2008), further studies to update as well as enhance current estimations on AFOLU are needed (Houghton et al., 2012).

Forest and soils are recognized as important C sinks as they have great potential to sequester atmospheric CO_2, which is expected to be the main cause of climate change. Recent research shows evidence and opportunities for mitigation of global warming through C sequestration in terrestrial ecosystems, including soils and vegetation. Living biomass of forest plays an important role in the global C budget and ecological function (Moran et al., 2000). Soil has the potential to sequester three times more C than the atmosphere (Batjes, 1996). Many factors have been identified in the literature as affecting C stock and dynamics in soils; these include land-use and land-cover change (LUCC) (Guo and Gifford, 2002), soil types and soil characteristics (Meersmans et al., 2012), and disturbance history (Moroni et al., 2010). A number of studies have been conducted on C quantification of natural forest and agriculture soils, but fewer studies have focused on forest regrowth from abandoned cropland.

Canada contributed 1.6% of the worldwide GHG emissions in 2012 (CAIT, 2015). A recent report indicates that C fluxes in land use, land-use change and forestry category act as a C source, which amounted to an emission of 0.072 Gt C in 2014, accounting for approximately 9.8% the total national GHG emissions (Environment and Climate Change Canada, 2016). According to Stinson et al. (2011) the managed boreal forest has acted as a C sink of 0.028 Gt C yr^{-1} during 1990 to 2008; bark beetle outbreak, wild fires, and forest harvesting are the major causes of the low C sequestration, as well as its variability, over this period. In agricultural regions, Huffman et al. (2015) estimated that woody vegetation covers, such as trees and shrubs, which are not considered as “forest”, acted as a C sink at a rate of 78.3 Gg C yr^{-1}, and the formerly abandoned farmland had contributed significantly to the estimated rate. Although the current estimations have provided a general view of C stock and its dynamics, the estimated outcomes have large uncertainty, requiring further studies on C emission at different spatial scales on land-use change in order to reduce the uncertainty (Houghton et al., 2012; Huffman et al., 2015).

Historically, cropland abandoned in Canada has occurred in central and eastern Canada since the 1950s (Ramankutty and Foley, 1999b); and some studies associated with C quantification were conducted. In eastern Canada, Benjamin et al. (2005) investigated the vegetation composition of abandoned farmland. Foote and Grogan (2010) also assessed the capability of abandoned cropland on soil C accumulation under different soil orders. In the western part of Canada, afforestation on marginal lands, including abandoned cropland, shows very high potential for C

sequestration under willow plantation, which could accumulate up to 4.6 Mg C ha^{-1} yr^{-1} in the boreal plains ecozone (Amichev et al., 2012). In the same eco-region, a recent study also suggests the potential of C removal under a woody biomass transition in agriculture areas (Huffman et al., 2015). However, information on the extent, C stocks, and the potential for C sequestration under natural regeneration in both ecosystem and individual pools has not been explicitly investigated. Additionally, under the IPCC guidelines for National Greenhouse Gas Inventory, abandoned croplands are also required to be reported (IPCC 2006).

2.2. Carbon Implications of Land-use Change and Land-cover Change

Under growing world demands for food, fibre, and fuel, global land use and land cover have experienced a substantial change. According to current estimations, the global ice-free land area is 13,300 million ha (M ha). Forest and pasture were the two major land covers with an estimated area of 4,000 and 3,410 M ha, respectively. The remaining area includes cropland at roughly 10-12% of the land area (1,500 – 1,600 M ha), built-up areas (351 M ha), and unused land (445 M ha) (Lambin and Meyfroidt, 2011). The global expansion of cultivated lands has disturbed approximately 600 M ha of forest and nearly 500 M ha of grassland and savannas (Ramankutty and Foley, 1999a). In recent decades, while forest area in North America and European countries was stable, Southeast Asia and the Amazon basin have become hotspots of deforestation (Lepers et al., 2005). These include an annual removal of approximately 3 M ha and 1 M ha in the Brazilian and Indonesian tropical forest during the period of 2000 – 2012 (Hansen et al., 2013). Similarly, natural vegetation in sub-Saharan Africa has been lost at an estimated rate of 5 M ha per year during 1975 – 2000 (Brink and Eva, 2009). While forest to cropland was the major land use transition during the last half past century, the area of cropland was shrunk to compensate for other types of land use such as abandoned cropland, build-up, and land degradation. It is estimated that nearly 200 M ha of cropland has been abandoned in different parts of the world, including eastern North America (Ramankutty and Foley, 1999b). According to the recent assessment report of the United Nations Environment Program (UNEP) on worldwide land use, this transition trajectory is expected to continue in the next decades (UNEP, 2014). Scientific evidence indicates that historical LUCC has contributed to changes in the global climate, and it is thus essential to include LUCC in any assessment of climate processes.

Land-use and cover change are considered one of the major causes that alter the amount of carbon held in soil and vegetation over time and change the flux rate of GHGs between terrestrial ecosystems and the atmosphere (Houghton and Goodale, 2004). In a recent estimation, LUCC in the last decade contributed approximately 10% of annual the global GHG emissions (Le Quéré et al., 2015) and thus is a contributor to climate change. Depending on types of conversion and ecosystem region, land-use change can be a C source or sink (IPCC, 2003). Conversions of forest to agriculture or build-up, for instance, release C (also other GHGs) held in biomass and soil into the atmosphere and also accelerate the decay rate of dead wood and litter (IPCC, 2001). In the tropical regions, the gross emissions of C from deforestation could be equivalent to 40% (or 3.0 Pg C yr^{-1}) of the global fossil-fuel emissions (Pan et al., 2011). Including C accumulated under other uses of land such as abandoned agriculture and regrowth after harvesting, the net emissions of C from deforestation in tropical regions are reported to be 1.0 Pg C yr^{-1} during 2000 – 2010 (Baccini, 2004). Additionally, current land use and practices under cropland and pasture of the region were estimated to be a C source of 1.4 and 0.48 Pg C yr^{-1} during the 1900s, respectively (Houghton and Goodale, 2004). In the boreal and temperate regions, although natural disturbances such as wildfire and insect outbreak were dominant (McCullough et al., 1998), the forest region acts as a sink of 1.3 Pg C yr^{-1} (Pan et al., 2011). Some land use and practices, such as tree plantations, fire suppression, and woody encroachment (Houghton and Goodale, 2004) or reducing tillage and efficient use of fertilizer (McConkey et al., 2003; Smith et al., 1998a), have also contributed to the changes in the agriculture region of the boreal and temperate zones.

The consequences of LUCC are known to impact the balance of the Earth system, causing changes in the patterns of precipitation, evapotranspiration, soil moisture, and surface temperature (Bonan, 1997; Ray et al., 2006). Deforestation of the Amazon for agriculture purposes, for example, has caused a significant increase in mean surface temperature (2.5 $^{\circ}$C), reduction in annual evapotranspiration (30%), and precipitation (25%) (Nobre et al., 1991). However, the effects of LUCC on climate appear to be different depending on location and type of ecosystem. Precipitation in the Northern Hemisphere, for example, appears to increase about 0.5 to 1% in the mid- and high-latitude but decrease approximately 0.3% in the sub-tropical area (IPCC, 2001). The global LUCC has also induced an estimated reduction of 5% annual terrestrial evapotranspiration (Sterling et al., 2013). Moreover, scientific evidence indicates that the global

temperature has increased at an accelerating rate by 0.8 ˚C since 1975 (GISTEMP Team, 2016; Hansen et al., 2010). Change in the global climate pattern is evident in many negative consequences such as sea-level rise, flooding, severe droughts, more severe wildfires, and more destructive storms and hurricanes (Foley et al., 2005; Hansen et al., 2012; Walther et al., 2002). Given that the global terrestrial C stocks in vegetation and soil pools are very large (2,477 Gt C to the depth of 1 m (IPCC, 2007a)) and some LUCCs hold potential for C accumulation, a better understanding of the changes is important for optimizing land use options as well as helping to prevent significant climate change.

2.3. Land use and Cover Change Detection using Remote Sensing Techniques

Carbon fluxes in the terrestrial ecosystem and other C pools continue to occur at different spatial and temporal scales all around the world. Scientific evidence has indicated the impacts of natural events and anthropogenic activities on the continuous changes on global land surface (Nepstad et al., 1999; van der Werf et al., 2010), and vice versa (Frey et al., 2004; Michaelian et al., 2011). Intensifying efforts toward enhancing timely quantification accuracy on changes in land use and land cover have become important tasks for in-depth understanding of cover characteristics (such as type and amount) and dynamics (such as cover type, change rate) through space and time.

Change detection is "the process of identifying differences in the state of an object or phenomenon by observing it at different times" (Singh, 1989). Changes in land use and cover can be quantified by detecting two types of change: conversion and modification. Land cover conversion involves abrupt changes with a replacement of one cover by another cover class, such as forest to cropland. Land cover modification is a subtle change that causes changes in the cover attribute without changing the original class, such as a moderate insect outbreak in a forest. Although in recent decades there are more readily available remote sensing techniques to explore these changes, challenges still exist in monitoring ecosystem change from space due to complexity of cover changes under different disturbance agents over time and place (Coppin et al., 2004).

To monitor land-cover change, Earth Observation (EO) instruments, which offer a rich and historical archived data, play an important role in the assessment and monitoring of LUCC in spatial and temporal fashion (Goward et al., 2006). Landsat imagery is available in large volumes, offering free-of-charge pre-processed data with a suitable spatial and temporal resolution. In

association with advances in image processing methods and computation capacity, Landsat time series data have stimulated widespread use for many LUCC applications and shows the greatest opportunity for LUCCs monitoring (Coppin et al., 2004). There are significant advantages of using this data source, including the extraction of additional information allowing a more comprehensive understanding of LUCC (Cohen et al., 2010; Kennedy et al., 2010; Wulder et al., 2010). For these reasons, Landsat time series data is very valuable to studies on spatial, temporal, and severity of changes in land cover at a landscape scale.

Many change detection techniques using digital images have been developed in the recent decades (Coppin et al., 2004; Lu et al., 2004; Singh, 1989). Change detection techniques can be grouped into binary change detection, multiclass change detection, and change detection using time series images.

Binary change detection is a simple method and uses a group of techniques that focus on detection of change and no-change features using two date images. Some additional techniques in this group include image differencing, image rationing, image regression, vegetation index differencing, principal component analysis, and background subtraction (Lu et al., 2004; Singh, 1989). Quick result generation with limited input data is one of the advantages of using these techniques. According to Lu et al. (2004), selecting image bands (or vegetation indices) and suitable thresholds for change detection are critical in this group of techniques. Singh (1989) recommended image regression using MSS image band 2 for abrupt change detection and concluded that more sophisticated techniques did not improve change detection results. However, the drawbacks of these techniques include the difficulties in identifying the true change areas and detecting change areas due to phenological variation from time to time of some land covers (Lu et al., 2004). Moreover, detailed information on cover changes such as time and change trajectory is not available. Therefore, this technique would be suitable for abrupt change detection with a small number of land-cover types.

Multi-class change detection is suitable for extracting "from-to" information of cover change with a scarcity of input data. This technique can generate change maps based on classified results from images taken at different dates. The sub-category includes post-classification comparison, spectral and temporal combined analysis, unsupervised change detection, hybrid

change detection, and artificial neural networks (Lu et al., 2004). The advantages of these methods are the ability to provide “from-to” information and the capability of reducing external impacts such as atmospheric effects encountered at the pixel level (Hansen et al., 2008; Jensen, 2005; Song et al., 2001). The approach also allows integration of data from different sensors if data from the same sensor and season are not available (Lu et al., 2008). However, change detection results strongly depend on the quality of training samples or classification outputs (Serra et al., 2003). Change detection accuracy may be degraded by errors accumulated due to miss-registration (Coppin et al., 2004).

Time series change detection comprises methods for analysing multi-date imagery to extract meaningful information. Changed areas are detected by observations of the landscape over time rather than the differences between two or more images collected from different dates. The application of multi-temporal data with trajectory analysis shows the greatest opportunity for LUCC monitoring (Coppin et al., 2004). The significant advantages of this approach over the above techniques are that additional information on conversions and modifications, such as rate, time, extent of change, pre-event, and post-event, can be derived (Kennedy et al., 2010). However, the major drawback of time series change detection inherently associates coarse spatial resolution imagery and the available time series length (Coppin et al., 2004).

The common techniques used in time-series data analysis include image classification-based and trajectory-based change detection. In the first approach, each image is classified separately, and post-classification techniques are then used to identify the changes. In the Boreal Plains Ecozone of Canada, Schroeder et al. (2011) detected forest disturbances by harvest and fire using supervised minimum-distance-to-mean classifier. The authors concluded that the accuracy of the output maps varied with input spectral variables (bands and indices) and that input variable selection is an important step to achieving good results. The advantages of this approach include reduced time for radiometric calibration and atmospheric correction of the input images although the lack of ground truth samples may introduce errors to final products via misclassification and misregistration (Coppin et al., 2004). Kennedy et al. (2010) introduced a model using a trajectory-based change detection approach, namely Landsat-based detection of trends in disturbance and recovery (Landtrendr). In another study, Huang et al. (2010a) introduced an automated approach for tracking forest disturbance history. By applying temporal segmentation of spectral indices

extracted from Landsat time-series data, the model allows us to capture all changes due to natural and artificial forest disturbances with associated characteristics (Griffiths et al., 2012; Kennedy et al., 2012; Meigs et al., 2011). Although the trajectory-based change detection, such as Landtrendr, offers a robust approach for monitoring forest disturbance and recovery (Kennedy et al., 2007; Piciarelli et al., 2008), its application to a more sophisticated land cover such as the transition regions of the boreal forest and cropland remains to be examined.

2.4. Carbon Density and Carbon Change in the Agricultural-Forest Transition Zone

In the boreal plains ecozone of Canada, forest, shrub, pasture, and cropland are the major land uses and covers. High variations in ecosystem C density under different land use and cover types have been observed in this region. In the boreal forest of Saskatchewan, Fitzsimmons (2003) reported the total ecosystem C to 45 cm soil depth was 158 Mg C ha^{-1}. Price et al. (1999) show ecosystem C to 20 cm soil depth in central Canada ranged from 108 - 154 Mg C ha^{-1}. This estimated range is comparable to 163.6 Mg C ha^{-1} quantified by Seedre et al. (2014) in a 27-year secondary succession stand. In a native aspen stand in Alberta, Arevalo et al. (2009), estimated ecosystem C to be 223 Mg C ha^{-1}. Overall in a recent synthesis, Kurz et al. (2013) estimated ecosystem C in the boreal forest to be 193 Mg C ha^{-1}.

The conversion of the boreal forest into cultivated land was estimated to cause a loss of all biomass C and approximately 30% in soil C in a period of 20 – 50 years after conversion (Wei et al., 2014). It reveals, based on previous studies, that the range of ecosystem C in the forest would be from 100 to 223 Mg C ha^{-1}. Assuming the soil C in the transition zone is 82 Mg C ha^{-1}, agricultural clearing could cause an annual loss rate of 0.5 Mg C ha^{-1} yr^{-1} from the soil pool.

Ecosystem C density in shrub cover may be much lower than that in forest; however, no intensive study has been conducted in our research area to quantify ecosystem C density in shrub cover. Pinno and Wilson (2011) reported that C density in shrub (to 60 cm depth) cover was 92.4 Mg C ha^{-1} under woody encroachment in the northern Great Plains, Canada. The C density of 11.8 Mg C ha^{-1} estimated in biomass pools may be comparable to that in post-harvesting stands, 7.6 Mg C ha^{-1} (Peng et al., 2002). Assuming C in the soil pool in the mixed forest of the boreal forest is 82 Mg C ha^{-1} (Kurz et al., 2013; Pennock and van Kessel, 1997b; Stinson et al., 2011), the average C density in shrub could be roughly 92 Mg C ha^{-1} in the research region. C loss under shrub to

cropland conversion has not been investigated in the boreal ecozone, but the conversion could cause a loss of all C biomass and a certain amount of soil C.

Carbon density in pasture cover is lower than that found in the shrub cover. Current studies estimate C density in pasture varies from 61 Mg C ha^{-1} (to 45 cm depth) in Cookson, central Saskatchewan (Fitzsimmons et al., 2004), 80.7 Mg C ha^{-1} in Regina, Saskatchewan (Pinno and Wilson, 2011), to 121 Mg C ha^{-1} (to 50 cm depth) in central Alberta (Arevalo et al., 2009). These study results suggest that ecosystem C density of the cover could range from 63 to 121 Mg C ha^{-1}. C under this cover is found mainly in soil as only a small amount (approximately 1 Mg C ha^{-1}) was observed in the biomass pool (Fitzsimmons et al., 2004).

In cropland, the median values of C density in soil to 45 cm depth were reported to be 65 to 83 Mg C ha^{-1} (Fitzsimmons et al., 2004; Pennock and van Kessel, 1997b). Including the biomass pool, the C density of cultivated land (50 cm depth) was reported to be 132 Mg C ha^{-1} (Arevalo et al., 2009). This value seems to be comparable to the previous value reported for Saskatchewan cropland where soil C was quantified to 50 cm instead of 45 cm depth and biomass pool was included (Pennock and van Kessel, 1997a). These studies also concluded that ecosystem C in the forest is higher than in the cropland and the difference between C density in the cultivated and pasture group is not significant. In Canada, Smith et al. (2001) estimated an accumulated rate of soil C to be 0.44 Mg C ha^{-1} yr^{-1} in the top 20 cm of soil due to the conversion of cropland to pasture. However, the gain rate depends on many other factors such as soil group, texture, fertiliser, and cropland rotation (Smith et al., 2001).

A rate of 0.13 Mg C ha^{-1} yr^{-1} could be sequestered in the top 20 cm of soil by changing from conventional-tillage to no-tillage management (Smith et al., 2001). Lemke et al. (2012) estimated in the Chernozemic soil of Saskatchewan that the same land-use change over long term could accumulate soil C at a mean rate of 0.18 Mg C ha^{-1} yr^{-1} in the top 15 cm, and suggested the accumulation rate could be higher over short term. Bremer et al. (2002) observed that the added amount in SOC was 0.50 Mg C ha^{-1} yr^{-1} due to the same LUCC conversion in the short term.

A similar C accumulation rate may be achieved under fallow to cropland and cropland to pasture conversions. McConkey et al. (2000), for instance, estimated that the accumulation rate ranges from 0.2 to 0.6 Mg C ha^{-1} yr^{-1} in the top 40 cm depth after 10 years of the conversion from

fallow to cropland. Under the same conversion but over a longer period, Boehm and Kulshreshtha (2000) reported the accumulated rate of 0.1 to 0.5 Mg C ha^{-1} yr^{-1}. It is concluded that a similar amount of C can be sequestered through the conversion of summer fallow to cropland or pasture, as would be obtained from cropland to pasture, with the mean rate being as much as 0.3 Mg C ha^{-1} yr^{-1}.

Abandoned cropland, which includes the conversions of summer fallow to forest, summer fallow to shrub, cropland to shrub, and cropland to forest, is expected to increase total C. Using a chronosequence approach on 19 fields disused for cultivation from 1927 to 1982, Johannes and Tilman (2000) found that the average C accumulation rate was 1.67% per year (over 12 years) with an average amount of 19.7 g C m^{-2} y^{-1} (or 0.197 Mg C ha^{-1} yr^{-1}) and that vegetation composition had a significant influence on soil C accumulation. In another study on changes in ecosystem C storage over 40 years in east-central Minnesota, it was shown that soil C accumulation contributed to 11% net storage and annual SOC accumulation rate was 1.1 Mg C ha^{-1} (Johnston et al., 1996). Meanwhile, Hooker and Compton (2003) reported that in an 115-year period after agricultural abandonment in Rhode Island, USA, the annual mean rate of C in mineral soil (20 - 70 cm) was 1.26 Mg C ha^{-1}. They examined the changes in ecosystem C and N during the first century of agricultural abandonment using a chronosequence approach. Agricultural abandonment was identified by comparison among cover types, land use history, climate conditions, and soil type, and by examination of the Ap horizon. Foote and Grogan (2010) used a chronosequence approach on abandoned croplands in southeastern Ontario, Canada and found that the rates of C accumulation were not significantly influenced by soil types. The total C stocks to 10 cm depth of Podzol, Brunisol, and Luvisol were 8.5, 10.3, 11.4 g C m^{-2} y^{-1} (0.085 – 0.114 Mg C ha^{-1} yr^{-1}) and approximately 70% of the C accumulation occurred in the top 5 cm. The authors also reported that time since cropland abandonment is more important than soil type for SOC sequestration and the highest sequestration potential could be reached by 80 – 100 years after abandonment.

Other land cover conversions, which could release terrestrial C into the atmosphere, include forest to pasture, forest to shrub, and shrub to pasture (Grünzweig et al., 2015; Huffman et al., 2015; Murty et al., 2002). The conversion of native forest into pasture may result in a slight increase in the world SOC (Guo and Gifford, 2002) or no change (Martin et al., 2005). In contrast, observations in the boreal forest of Saskatchewan indicate that deforestation for cultivation could

result in a potential decrease of 50 Mg C ha^{-1} total C in a short term (Fitzsimmons et al., 2004; Houghton, 1999b) and a substantial loss of approximately 30% of SOC (Murty et al., 2002).

No study has investigated the effect of forest to shrub conversion on ecosystem C dynamics. Nonetheless, a loss of 13 Mg C ha^{-1} in soil C was observed under mature forest to early successional cover in less than 20 years (Pennock and van Kessel, 1997a). Assuming the amount of aboveground biomass in shrub is equal to that of a 30-year stand (7.6 Mg ha^{-1}) and forest reaches maturing at 120 years (27.4 Mg C ha^{-1}), the conversion from forest to shrub could result in a loss of at least 20 Mg C ha^{-1} in biomass C (Peng et al., 2002). A release rate of 33 Mg C ha^{-1} of ecosystem C due to the conversion from forest to shrub can be inferred from the above studies. Similarly, shrub to cropland and shrub to pasture have not been investigated in the Boreal Plains Ecozone. Assuming these conversions cause a minor loss or no change in SOC, at least an amount of roughly 7.6 to 8.6 Mg C ha^{-1} in biomass C is expected to be lost under these conversions (Peng et al., 2002).

2.5. Carbon Stocks and Dynamics in Forest Ecosystems

The study of C pools is important to understand how C is cycled and likely to change in the future. For C stocks and dynamics, five C pools need to be included according to IPCC guideline (IPCC, 2006): aboveground biomass (AGB), belowground biomass (BGB), dead wood, litter, and soil organic matter (SOM). AGB is composed of all biomass of living vegetation above the soil including stems, stumps, branches, bark, seeds, and foliage. Fixing atmospheric CO_2 during photosynthesis and transferring C across different C pools are the important roles played by AGB. Hence, changes in land use will impact C pool accumulation. BGB is all living biomass of roots that have root diameter greater than 2 mm (IPCC, 2006). Root biomass contributes a significant proportion (about 50%) of terrestrial C being cycled and about 33% of the global annual primary production (Jackson et al., 1996). It also has an important role in the C cycle by transferring and storing C in the soil. Recent studies found that BGB could account for 20% (Cairns et al., 1997) to 26% (Santatonio et al., 1977) of the total biomass. For all ecosystems, approximately 70% of root biomass is distributed in the top 40 cm of the soil surface (Jackson et al., 1996). Dead wood includes all non-living woody biomass, having a size greater than 10 cm in diameter that is not contained in the litter, standing, lying on the ground, or in the soil. Fallen stems (logs), standing

dead trees (snags and stumps), dead branches, dead coarse roots are the main sources of coarse woody debris (IPCC, 2006) and are important components of forest ecosystems (Bond-Lamberty et al., 2002). However, they contribute a relatively small proportion to the C stocks of forests (Ravindranath and Ostwald, 2007). Litter includes all non-living biomass having a size from 2 mm to 10 cm in diameter in various stages of decomposition. Although litter is not a major C pool, contributing only a relatively small amount of C, it plays an important role in defining C density and governing the release of CO_2 into the atmosphere. Soil organic matter (SOM) is a generic term for all organic compounds in soil, excluding living roots and animals. This organic component of soil consists of plant and residues at various stages of decompositions (active or labile, stable, and inert or recalcitrant). The concentration of SOM in soil varies from 1% (upland soil) to 18% (organic soil), and SOM is estimated to contain approximate 58% (Gallardo et al., 1987).

2.5.1. Aboveground Biomass

Understanding trends in biomass and production during the secondary succession is essential for the estimation of C stock and dynamics. Conceptually, after forest harvest, C accumulated in aboveground biomass could be zero or higher, depending on the harvest methods. In the first period after harvesting, grass is the dominant cover, but shrubs soon replace this cover. In time, short sprouts and small trees grow in the shelter of the shrubs, forming a young forest. The trees become taller and more complex over time, forming mature forests (Aide et al., 2000; Carmona et al., 2002; Guariguata and Ostertag, 2001).

It was observed that without disturbance, C accumulates in aboveground biomass of a succession forest, in the sigmoid pattern (Finegan, 1984; Seedre et al., 2011). In the boreal forest, C is accumulated predominantly during the first and second succession stages (grass and shrubs). In the first 20 years, C stock in living plants yields low amount of C, but this rate continues to increase until the last stage of succession (about 150 years). Under a logging chronosequence of the Manitoba Mixedwood forests, Martin et al. (2005) observed that C content in AGB increased from 6.3 Mg C ha^{-1} in an 11-year-old stand to 26.9 Mg C ha^{-1} in an 18-year-old stand, and to 50.3 Mg C ha^{-1} in a 60-year-old stand. Changes in site conditions after cover changes, which result in the improvement of soil nutrients, soil temperature, water regimes, and the photosynthesis process, are probably the main causes of the high growth rates and C storage in the living plant as well as

other C pools (Goulden et al., 2011). In the tropical region, the young forest succession stage also has the highest growth rates. In AGB only, secondary forests can yield up to 100 Mg ha^{-1} during the first two decades, but the accumulation trends were associated with disturbance history (Brown and Lugo, 1990). Furthermore, differences in site conditions (such as water, soil fertility, temperature, soil type), species composition, disturbance type, and time scale, certainly influence the C storage, dynamic rates, and even patterns in each C pool. In a review, Silver et al. (2000) concluded that forests growing on abandoned agricultural land accumulate biomass faster than on pasture, and natural succession could produce aboveground biomass at a rate of 6.2 Mg ha^{-1} yr^{-1} and 2.9 Mg ha^{-1} yr^{-1} during 20 and 80 years of regrowth, respectively.

Carbon in the litter follows an increasing pattern under non-disturbed conditions over time, but it may decrease gradually after disturbance events such as stand replacement. This pattern flattens in the last succession stage (Goulden et al., 2011). In the boreal Mixedwood stand, litter C decreased from 43.8 Mg C ha^{-1} after a decade of logging, to 24.9 Mg C ha^{-1} after six following decades, suggesting an estimated decline rate of 0.35 Mg C ha^{-1} yr^{-1} (Martin et al., 2005). Higher rates of decomposition and lack of detritus input from live plants are the main reasons for the decrease.

2.5.2. Belowground Biomass

Belowground biomass is dominated by coarse and fine roots. It was observed that fine roots contributed a significant proportion of annual net primary productivity, but this biomass pool has a short turnover time, resulting in a small proportion of total C storage in any given forest stand (Goulden et al., 2011; Pinno et al., 2010). The development pattern of fine roots is an annual cycle and depends on temperature and soil moisture (season). A critical review by Yuan and Chen (2010) showed that the mean of fine root biomass in the boreal forest was 5.28 Mg ha^{-1}, and the fine root biomass increases with stand age until 70 years in broad-leaved stands and 90 years in conifer stands, before it declines. In mature forests in Europe, Helmisaari and Hallbäcken (1999) estimated the fine-root biomass to 30 cm depth to range from 2.3 to 5.8 Mg ha^{-1}. In the boreal plains ecozone of Saskatchewan, fine root biomass ranged from 1.6 Mg ha^{-1} to 3.1 Mg ha^{-1} depending on forest stand (Kalyn and Van Rees, 2006). Steele et al. (1997) found that fine root growth was mainly regulated by temperature, and the average Net Primary Productivity (NPP) was estimated to be

0.6 Mg ha^{-1} yr^{-1} and 2.6 Mg ha^{-1} yr^{-1} for aspen *(P. tremuloides)*, and spruce *(P. glauca)* stand, respectively. In another study on trembling aspen stand, Pinno et al. (2010) found that biomass of fine root in parkland (23.2 Mg ha^{-1}) was significantly higher than that in the boreal forest (5.4 Mg ha^{-1}).

Coarse root biomass, including living roots and dead roots, has longer turnover times compared to fine roots. The living coarse roots grow continuously overtime with the development of aboveground living trees and accumulate C in the same pattern as AGB (Li et al., 2003a). The decomposition rates of coarse roots after harvesting are influenced by tree species and site conditions. Tree species affect the C residence time of coarse roots by the sizes of roots, how deep they are in soil, regeneration capability, and quality of the roots. Site conditions influence water regimes, temperature, soil fauna, tree density, soil fertility, clay content, and topographical characteristics. According to Cairns et al. (1997), AGB explains 83% of the variation in root biomass. Diameter at breast height (DBH) and tree height were the reliable predictors of coarse root biomass (Brassard et al., 2011). In Canada, allometric equations were used intensively for quantifying the coarse root biomass (Lambert et al., 2005; Li et al., 2003b). Additionally, C storage in roots can also be predicted from stem diameters based on root:shoot ratio (Mokany et al., 2006). Under succession after logging in the boreal mixedwood stands, coarse root stocks ranged from 2.2 Mg ha^{-1} to 9.9 Mg ha^{-1} (Martin et al., 2005). Although coarse roots accounted for a small proportion of total ecosystem C (approximately 6% of NPP, (Li et al., 2003b), the total biomass in this pool can reach 30% of total biomass in forest ecosystems (Brassard et al., 2011). In summary, BGB is a considerable C pool and plays an important role in C sequestration over time.

2.5.3. Dead wood biomass

Dead wood biomass includes all non-living woody biomass, having a size greater than 10 cm in diameter. Fallen stems (logs), standing dead trees (snags and stumps), dead branches, dead coarse roots are the main pools of coarse woody debris (IPCC, 2006). After a disturbance event such as forest fire, insect break, or logging, coarse woody debris remains on site and decomposes slowly, and this process releases CO_2 into the atmosphere at varying rates (Boulanger and Sirois, 2006; Knohl et al., 2002; Tinker and Knight, 2001). For quantification of dead wood C at field-based sites, time series and chronosequence studies are the two primary methods used. The

quantification attributes may include decay classes, volume, biomass, or C concentration (Russell et al., 2015). Some key factors that influence the decay rate of woody debris include decomposer community, environment (such as temperature and precipitation), and debris quality.

The quality of woody debris is an important factor regulating decomposition rates. Organic matter with a high proportion of cellulose, lignin, and polyphenol and a low proportion of protein and nutrient content will decompose more slowly. In contrast, organic matter having high nutrient content and low lignin and polyphenol concentrations will decompose rapidly and begin the mineralization process early. According to an estimation from Zhang et al. (2008), a combination of total nutrient content (N, P, K, Ca, Mg) and C:N ratio (debris quality factor) could explain 70.2% of the total variation in decomposition. On average, plant residues that contain a C/N ratio of 14:1 are suitable for microbial activities, supporting decomposition rates. It was estimated in the boreal forest ecosystem that annual decomposition rates range from 3.3 to 4.5% depending on forest stands (Krankina and Harmon, 1995).

Temperature and moisture play a significant part in the decomposition rates of dead woody (Liu et al., 2013b). It was observed that the decomposition of woody debris decreases with decreasing mean annual temperature (Yatskov et al., 2003). In the boreal forest, Hagemann et al. (2010) indicated that buried woody debris, which has a low temperature and respiration rate, and a high water content, results in slower decomposition rates compared to that of woody debris lying on the ground surface.

Additionally, size of organic materials and distances to decomposers are also important factors controlling decomposition rates (Boddy et al., 1989; Yatskov et al., 2003; Zell et al., 2009). In wood of similar residue quality, decomposition rates will be higher if residues are located in the upper layer (A horizon), so that decomposers can approach easily to break down residues. Studies also show that the highest decomposition rates occur in the top six inches of soil, since moisture and oxygen are available for microorganism activities. Hence, the greater the distance of plant residues to the soil surface, the slower the decomposition rates. The difference in decomposition rates of standing and lying dead trees in the same forest is a good example of this. Surfaces of substrates or sizes of residues also influence the rate of decomposition – the smaller the residue particle, the faster the decomposition rate. The smaller particles facilitate water-soluble capacity

of organic matter into forms that are easy to break down by decomposers. Smaller residue particle size also exposes more surface areas to a decomposition process such as hydrolysis and oxidization (Shorohova and Kapitsa, 2016). This explains why decomposition rates of dead branches are higher than those of dead stumps.

Dead wood biomass (also coarse woody debris) is normally accumulated from three sources: (1) previous stands, (2) its introduction during disturbance, and (3) self-thinning during regeneration. The coarse woody debris dynamic pattern varies with site condition and types of disturbance. However, the general pattern of C dynamics in coarse woody debris follows the U-shape pattern. According to Janisch and Harmon (2002), total woody debris C immediately after disturbances may be higher than the original forest stands as woody debris may be contributed from the two other sources (source number 1 and 2). The C stock in this pool decreases with time from when the disturbance occurred, because of the ease of debris contribution from live trees. This trend normally lasts about 40 – 60 years, according to the authors. These results also agree with an observation in boreal forests in Newfoundland, Canada, in which coarse woody debris was decomposed completely within 40 – 60 years after disturbances (Moroni, 2006). The recovery stage occurs when self-thinning of live trees contributes to the biomass pool. It takes approximately 150 years to reach a peak, which is equivalent to total mass of coarse woody debris of an old-growth stand (Janisch and Harmon, 2002). A synthesis study conducted by Kurz et al. (2013) indicates that C density in the dead wood pool amounts to 20 Mg C ha^{-1} in the Canada's boreal forest and that this pool accounts for approximately 20% of the total C.

2.5.4. Litter

The litter (also forest floor) comprises small dead woody debris, leaf litter, and duff layers beyond the mineral soil, and includes all non-living biomass with sizes ranging from 2 mm to 10 cm in diameter, and is in various stages of decomposition (IPCC, 2006). The litter plays a significant role in regulating soil C, nutrient content, heterotrophic respiration, and sources of dissolved organic C. Although the litter is not a major forest C pool, contributing only a relatively small portion of soil C, (i.e. 11.5% in aspen stand of Saskatchewan (Kalyn and Van Rees, 2006)), it plays an important role in defining C density and governing the release of CO_2 to the atmosphere.

The dynamics of organic material storage in the litter vary with stand ages and is influenced by many factors such as disturbance, vegetative productivity, decomposition rate, and litter quality. The litter's continuous layer of bryophyte (mosses and liverworts) may also influence soil temperature and water content, and thereby decomposition rates of SOM. It was observed in a boreal forest of Saskatchewan that the total foliage-litter production in litter was approximately 20 Mg ha^{-1}, and the storage was stable over 80 years of simulation under non-disturbance conditions; and the litter stores more litter and C in the south with warmer climate than further north, and more C storage were found in the productive sites compared to nutrient-poor sites (Zhang et al., 2011). There was a high positive correlation found between C in litter and stand age. C accumulated in aspen stands (27.8 Mg C ha^{-1}) was significantly higher than that in pine *(P. banksiana)* stands (13.1 Mg C ha^{-1}) in western boreal forest (Nalder and Merriam, 1995). Following afforestation, C in litter increased with stand ages during the first 60 years (Niu and Duiker, 2006).

Disturbance history also affects the amount of biomass and thus, the amount of C accumulated in litter. Simard et al. (2001) reported that litters were thickest under clear-cut harvesting, followed by undisturbed stands, and burn stands. Fire disturbance may consume up to 100% of the litter, depending on fire severity and fire substrate composition (such as size of debris, presence of bryophyte). After forest fire disturbance, the C in the litter normally resets to zero, then increases gradually with the rise of live biomass from trees reaching a plateau, and then stabilizes once the forest matures. In contrast, organic matter and C dynamics in litter after harvesting are different. Immediately after harvesting, organic material in the harvested litter is normally higher than before harvesting because of the addition of dead biomass from live branches and leaves. However, input debris from living trees to the litter will decrease and decomposition rates may increase due to changes in sunlight and surface temperature. According to Nave et al. (2010), harvesting caused an average loss of 8% in soil C in temperate forest and the highest loss occurred in litter (-30%) regardless of soil type, tree species, and time since harvesting, suggesting soil C in litter is more vulnerable to forest harvesting than that in mineral soil. The study also highlighted that harvesting induced C losses in hardwoods (-36%) which was significantly higher than the coniferous/mixed stands (-20%). Organic material in the litter pool stabilizes when the input mass is equal to decomposition rate. Organic material increases with the addition of input material from new stands, which are greater than decomposition rates. The variations of C in the

litter are dependent upon many factors such as disturbance history, vegetation productivity, decomposition rate, and litter quality.

2.5.5. Soil Organic Carbon

The stock of soil organic carbon (SOC) in a natural forest is normally stable because of the natural balances between input rates of litter biomass and rhizodeposition from forest stands, SOC decomposition rates, and leaching of dissolved organic carbon (DOC). In Canada's managed forest, the boreal plains ecozone was estimated to have the largest ecosystem C stock, at approximately 8 Pg C (Kurz et al., 2013). On average, soil C content was estimated to be 86 Mg ha^{-1} for boreal forest (Stinson et al., 2011).

Following disturbances, SOC stock and dynamics are influenced by a combination of processes, including C gains, C losses, C translocations, and C transformations. Soil C increases if the input rates of biomass increase, and therefore, the C input rates are more than C lost rates. The increase in the input rates may be the result of increases in aboveground and belowground detritus and belowground C exudation through root systems. Carbon may decline from hydrological losses by leaching, gaseous losses by microbial respiration and decomposition, and thermal combustion. Carbon translocation involves the movement of C with soil profiles. With the activity of soil organisms, the movement can be upward or downward. However, downward movements of C from upper layers to deeper layers are dominant, especially the downward movement of DOM through hydrological translocation. Carbon transformation involves modification of the chemical composition of SOC fractions in soils under changing environmental conditions. The transformations may be caused by the detritus of soil fauna through conversion of compounds with simple chemical structure into more complex compounds. The availability of oxygen in soils, formation of physical, chemical, and biological protection, as well as combustion, were observed to transform the chemical composition of SOC (Lal, 2005).

Forest disturbances may change one or more processes and normally cause a decline in soil C. For example, forest harvesting including logging, thinning regimes, and clear-cutting for agriculture purposes, cause huge losses in terrestrial C. Forest harvesting causes a decline in soil C in the first 10-20 years, followed by an accumulation period, which is known as the Covington curve (Covington, 1981). Johnson et al. (1995) noted that there are three main pathways of soil C

decline after harvesting: (1) the removal of biomass from sites (stems and branches), (2) the increase in decomposition rate due to changes in soil micro-climate, and (3) the acceleration of water flux by reducing cover, resulting in leaching of DOM and particle organic matter (POM).

It is obvious that the input rates of C from litterfall and rhizodeposition decline rapidly after harvesting. However, C storage in soil tends to increase briefly in the upper layer of soil profile because of the abundance of woody materials left on-site on the litter. Nevertheless, the removal of vegetation may also cause a change in soil temperature and moisture, resulting in changes in decomposition rates of SOM. It was observed that rising temperature caused an exponential increase in decomposition rates at favourable moisture conditions. Under comparable conditions, SOC and nitrogen content vary with soil moisture content to form a parabolic relationship. Accordingly, decomposition rates increase with soil moisture content to a maximum rate at intermediate levels, then decline because of low oxygen concentration in high soil moisture content, where only anaerobic organisms regulate the decomposition process. Many anaerobic organisms produce acids during metabolism that limit the growth of many other organisms. Moisture also influences leaching as the organic matter may contain soluble substances. When hydrologic condition is changed, soluble substances are rapidly lost by leaching or microbial consumption. Recent incubation studies found that the influences of temperature and moisture interact, and that different temperature and moisture patterns resulted in the inconsistent proportion of products (amount of nitrogen per gram carbon). Recent studies by Thomsen et al. (1999) and Fitzsimmons et al. (2004) found that water (including groundwater) was the main factor in controlling the degradability of soil C. Soil texture has indirect effects on decomposition and through soil structure defines the ability of the soil to retain water. In addition to soil moisture and temperature, soil pH at severe levels (<4 or >9) and toxic levels of elements in the organic matter, may reduce decomposition rates.

The amount of organic matter in soils is known to be a significant factor influencing rates of decomposition. The high amount of organic material creates a better environment where soil microbes can develop and exist in large numbers. While there is a decline in soil C due to the removal of biomass after forest harvesting, the effects of decomposition rates on the dynamics of soil C after forest harvesting are not consistent. Some studies show that after forest harvesting, soil temperature increases for a short period affecting decomposition rates (Houghton et al., 1987).

However, the results of other observations varied. It was reported that after harvest, soil temperature increases, causing a decrease in soil moisture and thereby reducing decomposition rates. Hence, vegetation removal plays a more significant role in the decline of SOM after harvesting (Miegroet and Olsson, 2011).

Soil C loss can also occur following forest harvesting through the acceleration of leaching rates of DOC fraction. It was observed by Piirainen et al. (2007) that clear-cutting of the boreal forest had significant influence on water fluxes and resulted in leaching of DOC to groundwater. The average loss of DOC was 36.5 kg ha^{-1} annually, and could last up to five years. However, this amount was minor compared to the loss from other pathways. Clear-cutting also causes changes in the input of organic matter, the substrate quality, soil solution, and microbial activity, which all influence DOC dynamics (Cronan, 1990).The accumulation rates of SOC vary depending on many factors including input rates of organic matter, successional time, and disturbance regimes, soil texture, and climate (Hooker and Compton, 2003; Johnston et al., 1996; Post and Kwon, 2000).

In research on soil C pools in relation to climate, Post et al. (1982) found that soil C density increases with increasing precipitation and decreasing temperature. To gain an appreciation of the effects of land-use change on soil C stocks, Guo and Gifford (2002) conducted a meta-analysis from 74 papers and the results indicated that soil C stocks decline after land-use changes from pasture to plantation (for timber production in managed forest, −10%), native forest to plantation (−13%), native forest to cropland (−42%), and pasture to cropland (−59%). Soil C stocks increase after land-use changes from native forest to pasture (+ 8%), cropland to pasture (+ 19%), cropland to the plantation (on managed forest, + 18%), and cropland to secondary forest (+ 53%). Under similar land use and climate conditions, soil with high clay content tends to have a higher SOC as organic matter can be inaccessible to micro-organisms thereby slowing decomposition processes. Soil C stocks are also influenced by litter decomposition rate (the higher the litter decomposition rate, the faster C releases from soils), which is controlled by environmental conditions such as humidity, temperature, micro-organisms (Zhang et al., 2008).

Considerable research indicates, however, that soil C mass per area and the changes caused by disturbance are site specific. In forest soil of Prince Albert, Saskatchewan, Peng et al. (2002) reported an estimated value of 41.72 Mg C ha^{-1}. This estimated value is lower than 57.5 Mg C ha^{-1}

observed by Pennock and van Kessel (1997a) in the mixedwood forest of Saskatchewan. In the same region, Fitzsimmons et al. (2004) observed that soil C density to 45 cm depth in the forest of the boreal plains ecozone, varied from 97 to 114 Mg C ha^{-1} with the median value of 83 Mg C ha^{-1}. Carbon density in the managed boreal forests was estimated to be 87 Mg C ha^{-1} (Kurz et al., 2013). Evapotranspiration, slope and aspect, landscape position, latitude, changes in land use and cover, and soil characteristics are believed to be the key factors controlling SOC levels (Jobbagy and Jackson, 2000; Pennock et al., 1994; Thomsen et al., 1999).

2.6. Field Methods for Carbon Estimation

Quantification and mapping of biomass are important to quantify stocks in the C cycle. In article 2 of the Directive 2009/28/EC, biomass is defined by the European Community as "the biodegradable fraction of products", which include residues from agriculture and forestry (European Community, 2009). Under the IPCC guideline, ecosystem C is estimated from four different pools and C content in dried biomass has been assumed to be 50%.

2.6.1. Aboveground biomass estimation methods

Estimation of the AGB in forest ecosystems is important for evaluating productivity and sustainability of forests. It also gives us an idea of the potential amount of C that can be emitted or sequestered under different land uses, land covers and changes. This information supports decision making on forests. The literature shows that aboveground biomass can be estimated using field measurements and remote sensing techniques. In field measurement, Seidel et al. (2011) grouped aboveground biomass estimation approaches into three main categories: direct, indirect contact, and indirect non-contact methods.

A direct method involves partial or the whole destruction of a tree to identify biomass weight or volume of a tree or an area unit. This method includes allometric, stratified clipping, and litter traps. Allometric equations reflect the correlation between two or more biophysical parameters. One of the main purposes of building allometric equations is to estimate non-measurable (or difficult to measure, i.e. height) from measurable parameters. The advantage of this method is that once equations are established, formulas can be applied to other trees (Ash and Helman, 1990). Total biomass weight per tree is normally estimated using allometric or conversion factors derived from tree height and/or tree diameter at breast height. A variety of allometric

equations have been developed for different tree species. Ter-Mikaelian and Korzukhin (1997) summarised sixty-five biomass equations for North American tree species. For Canadian forest biomass and its component calculation, Stanek and State (1978) listed approximately 660 regression equations. The accuracy of allometric equations depends on the number of trees representative of the ecosystem type. A large number of sample trees are required, which may be time-consuming and laborious. Stratified clipping is complete harvesting of all parts of plants at defined interval height levels to obtain a vertical profile of the foliage density (Aber, 1979). This method is time-consuming and laborious so it is not suitable for large areas and dense understory. Hence, it is only applicable to small plants such as shrubs, grasses, understory, and litter at small areas or quadrats. Litter traps are another method to measure leaf area index and the dry weight to leaf area ratio. The procedure involves collecting leaves or needles in traps of various designs. This method is suitable for land covers that have autumn leaf fall such as deciduous forests but it would not be feasible for heterogeneous forest stands (Jonckheere et al., 2004).

Indirect methods involve attaining measurements without any contact with plants (Seidel et al., 2011). The indirect method includes indirect contact, which requires contact between the measuring instrument and the plant, and indirect non-contact, which operates without contact with the plant. Indirect contact consists of point quadrat and inclined point quadrat. Some parameters such as Leaf Area Index (LAI), cover percentage, green area index can be measured by piercing a vegetation canopy with a long thin needle under known elevation and azimuth angle for counting the number of hits or contacts of the point quadrat with green canopy elements. Although correlation was found between the actual and estimated LAI value using this method, it is time consuming and hard to implement in vegetation types with canopies higher than 1.5m due to the required physical length of the needle (Jonckheere et al., 2004). The advantages using these methods are that they are less time consuming and less expensive compared to destructive methods.

Digital techniques make data analysis easier than physical measurements. MacArthur and Horn Photography and Hemispherical Photography, for instance, quantify foliage biomass distribution based on photographs taken from a vertical camera. The photographs then allow calculation of the ratio of sky to plant area or foliage profile. Samples can be taken quickly with portable devices. The difficulties are associated with camera placement and with data analysis.

The accuracy of this method depends on foliage pattern (Fukushima et al., 1998). In order to overcome shortcomings in previous methods, Light Detection and Ranging (LiDAR) instruments, a remote sensing survey method to examine the surface of the Earth, have been used at quadrat level. Some biophysical parameters, such as tree height, DBH, plan area index, leaf area index, can be estimated. However, the applications are still under development and validation (Takeda et al., 2008). Terrestrial 3D laser scanner is a modern device that can measure many parameters simultaneously with very high accuracy for estimation of forest structure and biomass. Nevertheless, this technique is in the early stage of development and it is a less standardized method for data analysis (Seidel et al., 2011). Multiband Vegetation Image, introduced by Kucharik et al. (1998), can reduce estimation bias affected by branch, stem areas, defoliation, and non-random spatial distribution in canopy to leaf area index. By separating woody and non-woody elements, the technique makes it possible to improve leaf area index estimation and clump index that can be used for biomass estimation. Tracing Radiation and Architecture of Canopies is a new optical instrument for measuring LAI, clumping index, and Fraction of Photosynthetically Active Radiation absorbed by plant canopies and is based on gap size distribution, which contains information of canopy architecture. The Tracing Radiation and Architecture of Canopies device, can contribute to improving the accuracy of biomass estimation in heterogeneous patterns (Chen and Cihlar, 1995). However, it is not yet applicable to coniferous tree species on a scale larger than shoot level (Seidel et al., 2011).

Collecting data for biomass estimation using radiation measurement, such as Li-Cor Line Quantum sensor, Sunfleck Ceptonmeter, and Li-Cor LAI 2000 devices, may be the most common means used in the last decades. These are portable devices that allow easy operation in shrubs and forests. The Li-Cor LAI 2000 device offers comparative accuracy and comprehensive data. Furthermore, high correlation found between LAI and some vegetation indices achieved from satellite images in recent studies reveal the higher potential use of LAI for AGB estimation (Gupta et al., 2000; Madugundu et al., 2008; Wang et al., 2005). Because it requires above and below canopy data for LAI measurement, the study site must be close to an open field. The Li-Cor LAI 2000 can be used for collecting data in abandoned cropland and its direct approach provides high accuracy in forest biomass estimation, but it is labour and resource intensive, and time consuming. Direct contact measurements give us more accurate data without taking destructive samples, but

they are time consuming and only applicable to low vegetation canopies. The direct non-contact approach shows high potential for field measurement of forests because the data are in digital format and are collected using portable devices. Although field measurement provides high accuracy for biomass estimation, it has limitations that make it impossible to implement for biomass estimation at a broad spatial scale. Therefore, remote sensing is expected to be the alternative approach to overcome these limitations.

2.6.2. Belowground biomass estimation methods

According to Ravindranath and Ostwald (2008), there are five main methods for BGB estimation.

1) Excavation of roots involves digging to a certain depth interval and measuring the fresh weight of roots. Shoot/root ratio or equations can be generated to present the relationships between roots and other parameters for BGB estimation.

2) The second approach for BGB estimation is the monolith method. This approach estimates root biomass by digging a soil pit (1 x 1 x 1 m) and taking soil samples. Roots are separated using running water. Dry mass of roots per volume of soil and per hectare to depth are estimated. Soil coring for non-tree vegetation is normally applied to grass and shrub covers.

3) A soil core sampler is used to take soil samples at certain depths (30-40 cm); roots are separated from soil using running water and a sieve; they are weighed and then root mass per plot at each depth is extrapolated. Soil coring can be applied to root estimation of forest covers (Majdi et al., 2005) but a concern was raised by Sala et al. (1988) that results from this method are normally overestimated because of sampling errors.

4) The root to shoot ratio approach is quite similar to the excavation of roots approach but this is normally applied to certain species and stand ages. A review by Cairns et al. (1997) reported that root to shoot ratio ranges from 0.18 – 0.3. This value varies depending upon species, tree age, and site-specificity (Levy et al., 2004).

5) Using allometric equations is another approach to BGB estimation based on the relationship between root biomass and aboveground biomass. In the CBM-CFS3, Kurz et al.

(1996) introduced two equations for total root biomass estimation for softwood and hardwood using this approach.

Dynamics of BGB can be monitored by six common methods, namely sequential soil coring, ingrowth cores, minirhizotron, a nitrogen budget approach, biomass expansion factor, and a C flux method (Ravindranath and Ostwald, 2008), but biomass expansion factor is the most common. In this method, the ratio of total oven dry aboveground biomass of the inventory volume of non-destructive sampling provides reliable results (Qureshi et al., 2012). In recent research on Pinus, Sanquetta et al. (2011) concluded that it is reliable to use the biomass expansion factor and the shoot-to-root ratio, which relates tree age, tree height, and DBH, in regression equations. Mokany et al. (2006) found a negative relationship between root-to-shoot ratio and shoot biomass, precipitation, and soil clay content for forest/woodland. No correlation was found between root-to-shoot ratio and mean annual temperature. In shrub and grassland, root-to-shoot ratio and shoot biomass, precipitation, and mean annual temperature, show negative correlation, while no correlation was found between root-to-shoot ratio and soil clay content.

2.6.3. Coarse woody debris and litter biomass estimation methods

Coarse woody debris (CWD) is an important component of forest ecosystems and plays an important role in C storage (Bond-Lamberty et al., 2002). Total volume and mass of woody debris are the primary interest variables. To quantify CWD in forest, line-intercept and quadrat methods are the common sample designs. In the first approach, diameter of CWD is measured long transect lines (at point of interception) to estimate total volume of in a sample area. One of the advantages of the method is that time for data collection can be reduced by measuring only the diameter at the point of interception (Warren and Olsen, 1964; van Wagner, 1968). Random direction and transection length greater than 100 m are suggested to achieve acceptable results (Woldendorp et al 2004). The author also notes that high variability is associated with canopy cover (<50% cover), where the amount of CWD is relatively low. In the quadrat method, a full census of CWD on a fixed-area plot is conducted. The method is more time consuming, but it is effective under limited pieces of CWD per plot (Woldendorp et al 2004). With a limited plot size (under agriculture landscape) and low canopy cover (secondary stage), full census of CWD using the quadrat method should be considered.

The dominant factors that influence the amount of dead biomass include amount of input at the disturbance time, mortality rate, and decomposition rate. In a study of coarse wood debris in Douglas-fir forests in western Oregon and Washington, Spies et al. (1988) found that under forest fire disturbance, amounts of woody detritus at the time of the disturbance are more closely related to total coarse woody debris than stand age. The amount of woody debris found in the research was 92, 50, and 173 Mg ha^{-1} for stand age < 80, 80-100, and 400-500 respectively, to form a U-shaped pattern. Busing (2005) found the annual rate of mortality for tree DBH > 10 cm was 0.7%, but varied by forest stand and species. Changes in decomposition rates, which are influenced by climate, substrate quality, and size class, result in changes in mass loss and dead wood density. Over a period of 5 years, about 40% of mass was lost during the decomposition process of five tree species of western Australia forests (Brown et al., 1996). Results from a research study of dead wood density of five boreal tree species, conducted by Seedre et al. (2012), showed the influence of the rate of decomposition on the amount of dead wood. Decomposition rates of birch *(*B. papyrifera*)*, spruce *(P. glauca)*, and pine *(P. banksiana)* logs on biomass, volume, and density can be found in Harmon et al. (2000) using equation: $k = -[Ln(final) - Ln(initial)]/t$**;** where: k is decomposition rate; initial and final are the volume, density, or mass at the start and end of the time t that has been decomposing.

In the CBM-CFS3, dead wood pools include snag stem dead organic matter (DOM); dead standing stem wood of merchantable size, snag branch DOM (dead branch, stump, and small dead tree), medium DOM (coarse woody debris on the ground), and belowground fast DOM (dead coarse roots in mineral soil) (Kurz et al., 2009). Snag stems DOM and snag branches DOM of softwood and hardwood are separated. For practical purposes, one may use different definitions for each DOM pool. In Janisch and Harmon (2002), for example, coarse dead wood and fine dead wood are differentiated based on diameter and length of woody materials. Coarse dead wood includes logs (diameter > 10 cm and length > 1 m), stumps (standing cut tree boles and < 1.3 m in height), and snags (standing dead trees with >1.3 m in height). Fine dead wood includes snag, branches, and small dead trees, which are smaller and shorter than the defined coarse dead wood. Diameters of snags, stumps, and logs are normally measured by a caliper. Data on length and height of snags, stumps, and logs are acquired using a tape measure, clinometer, or digital rod (Harmon and Sexton, 1996; Janisch and Harmon, 2002). Aboveground fine wood is normally

estimated by harvesting in the plots then weighing it using a portable scale (Harmon and Sexton, 1996).

Woody volume and woody dry weight can be converted into C, based on C concentration and wood density. Wood density is calculated by dividing woody dry mass (g) by volume (cm^3) (Seedre et al., 2012). The default value for C concentration in coarse woody debris is 0.5 (IPCC, 2006). Carbon in coarse woody debris is calculated by multiplying C concentration, density, and volume (Weggler et al., 2012).

For wood detritus dynamics, chronosequence, time-series, and decomposition vector are the three main approaches. In chronosequence, woody detritus samples are normally collected once on sites of different ages. Janisch and Harmon (2002), for example, applied the chronosequence approach to estimate the changes of C stored in live and coarse woody debris in different forest successional stages of southwest Washington State. The mean of C stored in coarse woody detritus was 21 Mg ha^{-1} in a 60 year stand. This approach is favoured because it provides rapid estimation with short time for sampling. The results from the approach are comparable to others. However, there is some uncertainty about initial condition and tree size of woody detritus and the effects of local conditions on the decomposition rate (Harmon et al., 2000). Time series is another approach for woody debris estimation. In this approach, samples are collected in a specific time interval, ranging from 0.5 year to decades. In research conducted by Brown et al. (1996), time for data collection was set for 0.5, 2, and 5 years to examine the effects of climate conditions, substrate quality, and substrate size to decomposition rates on branches and boles material in western Australian forests. Different factors affected the changes in woody detritus such as mass change, substrate quality, size of substrate and nutrient concentration. However, it takes longer to collect data compared to previous methods. A hybrid approach between the two methods, or decomposition vector, was introduced by Harmon et al. (2000) to estimate woody detritus decomposition dynamics on three species of logs from north-western Russia. Data were collected twice in a 3 year interval (time 1 in 1993 and time 2 in 1996). Data on snags and logs of birch, spruce, and pine species in the range of 1 to 70 years of age from 12 permanent plots were collected. The results show that decomposition rates were 0.046, 0.033, and 0.035 for birch, spruce, and pine, respectively. The authors concluded that the decomposition vector is a useful approach that can reduce experiment time. However, the authors also raised concern about time

intervals. A comparison on performance of the two approaches suggested that although chronosequence approach provides a lower estimation result, it may be more suitable for long term and large areas with unknown temporal pattern of input (Harmon et al., 2000).

Litter is defined as all non-living biomass with a size of 2 mm to 10 cm in diameter, in different decomposition stages. It is a key component in defining soil C density, CO_2 release rate to the atmosphere and nutrient content. Current research on forest-litter dynamics in Canada's boreal forest, Zhang et al. (2011) calibrated field measurements of biomass growth and litterfall to estimate forest litter dynamics. The results showed that forest litter C storage was controlled by stand age, climate, and soil productivity, increasing with forest growth, and levelling out after about 100 years of succession. Prescott et al. (2000) used a field measurement approach and found no evidence of the effect of fertilization on foliar litter of boreal forests. The forest litter C storage ranges from 10 to 40 Mg ha^{-1}.

2.6.4. Soil Organic Carbon estimation methods

Quantifying the potential of SOC sequestration plays an important role in predicting the contribution of soil C sinks towards mitigating CO_2 emission. SOC is defined as the total organic C in a soil exclusive of C from un-decayed plants and animal residues or the amount of C bound in an organic compound (Grewal et al., 1991), including the fine root (< 2 mm in diameter). In a recent study, Qureshi et al. (2012) defines SOC as a mixture of dead plant residue in various stages of decomposition. Global soil C is estimated to be 1462–1548 Pg of C in the upper 100 cm (Batjes, 1996). The amount of C stock in soil depends on the balance of C input from plant production and C loss through decomposition. Climate, land use history, soil texture, and hydrology are considered as the primary variables that influence those two processes and C storage (Ju and Chen, 2005).

There are two distinct approaches to characterise SOC stock with Tier 3 (advanced estimation systems) method (IPCC, 2006), which are measurement-based and model-based approaches. Soil C stock inventory of the measurement-based is a traditional method based on performing direct measurement. Soil samples are collected in sampling network, and soil C mass per area is then estimated from soil samples in a laboratory processing. According to Qureshi et al. (2012), there are five common methods of laboratory processing for C quantification from soil samples namely (1) Nuclear magnetic Resonance Spectroscopy (NMR), (2) Diffuse Reflectance

Infrared Fourier Transform (DRIFT), (3) Walkley and Black procedure, (4) Dry combustion with automated analyzers, and (5) Hydrogen Peroxide Digestion. While NMR and DRIFT are not common as they are expensive, Walkley and Black is commonly used because it provides higher accuracy with simple technique and infrastructure. However, dry combustion with automated analyzers, which involves dry combustion of soils that are pre-combusted to remove organic matter in an O_2 stream (Rabenhorst, 1988), could be the most common technique to determine SOC. High accuracy, timely, and simple to process are some advantages of the method. Using automated analyzer instruments, such as the Leco CR-12 Carbon Analyser, are also widely used. This method involves heating the soil sample at high temperature to combust soil organic matter or carbonate and measuring weight losses (Wang and Anderson, 1998). Some advantages of using this technique includes simplicity, less expensive and less labour intensive compared to other methods (Wang et al., 2012).

After having C density at a plot scale, the data are then extrapolated to the desired spatial extent (e.g. field, landscape scale). It is normally used for local scales. The advantage of this method is that it gives high accuracy. But it does not provide spatial information (Foote and Grogan, 2010) and is expensive and inefficient for mapping and measuring a large area or deeper soil profiles (Miklos et al., 2010), especially in monitoring changes in soil carbon (de Gruijter et al., 2016; Rossel et al., 2016). Therefore, model-based, a process using imperial or other types of advanced models, are normally cooperated for having a rapid, practical, and cheap methods. The advantages of the model-based process include the capability to estimate C stock and changes, including effects of land-use change and management in the long term. However, measurement-based is still needed for model calibration and evaluation. The approach can address non-linearity of changes from carbon input (AGB, litter) and output (microbial decomposition) as well as transfer of C among pools, including soils (de Gruijter et al., 2016; IPCC, 2006). It is normally used for regional scale studies (Allen et al., 2010).

2.7. Modelling and Remote Sensing Approaches for Biomass Estimation

Although carbon estimation using the field measurement approach offers high accuracy results, it is expensive, time consuming, and not feasible for large spatial and time scale C

quantification. Other approaches, including modelling and remote sensing, can be used to supplement field measurements.

2.7.1. Modelling approach

Modelling methods can be used to monitor changes in biomass over time periods with certain basic input parameters. Landsberg (2003) used a process-based model that simulates the dynamics of biomass based on physiological process or forest growth such as leaf photosynthesis, litter fall, and mortality losses. Process-based models provide high accuracy of growth and biomass productivity (Korol et al., 1996). The advantages of this method include the ability to project future C stocks and supplement field measurement. However, the requirement for input data or parameters in each model should be taken into account. For this reason, the ability to apply these models to regional or global scale is limited (Ståhl et al., 2004). Because changes in AGB are not fully reflected in pixel values of imagery, calculation of biomass directly from remotely sensed data is impossible. Nevertheless, a number of canopy parameters that can be retrieved from remotely sensed data, such as tree height, crown diameter, canopy gap fraction, can provide a better estimation of AGB using models (Seidel et al., 2011). Many different models have been used for biomass estimation such as multiple regression analysis, K-Nearest Neighbour (KNN), neural networks, and vegetation canopy models. Among these models, regression models may be the most commonly used for relating canopy reflectance of remotely sensed data and tree parameters such as tree height, age, DBH, crown cover, LAI (Lu, 2006). Zheng et al. (2007) used regression models to relate vegetation indices of Landsat data and field measurement for biomass mapping. Using the moderate-resolution imaging spectroradiometer (MODIS) data, Potithepa et al. (2010) concluded that in evaluating long-term relationships of LAI and Normalized Different Vegetation Index (NDVI), LAI and Enhanced Vegetation Index (EVI) are reliable. In mountainous areas of Alberta, Soenen et al. (2010) executed the geometric optical canopy reflectance model in multiple forward mode (MFM) for mapping biomass density and distribution. The results showed that the MFM approach offered improved biomass density estimation compared to NDVI and spectral mixture analysis (SMA).

The above review of biomass estimation methods suggests it is difficult to use an individual method for quantifying biomass. Cover pattern is usually heterogeneity under different

contributing factors such as time and disturbance agents (Gellrich et al., 2007). A single approach to quantify biomass C at a landscape scale with different land covers, such as grass, shrub, and forest may not be adequate. A combination of field data (tree height, DBH, LAI), along with allometric equations, and remote sensing data should be more effective.

2.7.2. Remote sensing approach

Remote sensing is defined as "the measurement or acquisition of information of some property of an object or phenomenon, by a recording device that is not in physical or intimate contact with the object or phenomenon under study" (Colwell, 1993 qtt in Jensen 2005, p3). It is also recognised as the most cost-effective way of acquiring data over large areas. Remotely sensed data provide spatial, spectral, and temporal information in digital format that make it easy to obtain a synoptic view of the area of interest and to analyse data. It has been used widely for LUCC studies. However, optical remote sensing is not a means to provide all information for different research disciplines. In biomass estimation, remotely sensed data do not provide immediate information, but the spectral value can be calibrated with field-measured parameters to attain biomass information. Hence, remotely sensed data were widely used in recent decades for biomass estimation as spectral brightness value and vegetation indices are considered to be correlated with forest biomass (Tucker and Sellers, 1986). Field data are calibrated with biological variables derived from remotely sensed data, to present the relationship through different data statistical methods.

Depending on spatial scales and associated research purposes, different data sources in different spatial resolutions of remotely sensed data are collected for biomass studies (Houghton, 2005; Jenkins et al., 2003; Tømmervik, 2003). Lu (2006) grouped remotely sensed data associated with forest biomass estimation into four categories which are (1) fine spatial resolution derived from aerial photographs and IKONOS, (2) medium spatial resolution with Landsat and *Satellite Pour l'Observation de la Terre* (SPOT), (3) coarse spatial resolution with Indian Remote Sensing Satellite (IRS-1C), Advanced Very High Resolution Radiometer (AVHRR), and (4) radar data with Radar and LiDAR.

Fine spatial resolution data have resolution of less than 5 meters and are normally products of airborne and space-borne satellites such as QuickBird and IKONOS. A high correlation is found

between actual C density and parameters derived from high spatial resolution data. Using aerial photographs, De Jong et al. (2003) found a correlation between aboveground biomass and spectral indices. Similarly, a high correlation was found between NDVI of hyperspectral airborne satellite and field measured grass/herb biomass (Cho et al., 2007). By utilising the panchromatic bands and texture analysis of IKONOS, Proisy et al. (2007) found very high coefficients of determination (r^2=0.8) and accuracy for total biomass, trunk biomass, and branch biomass estimation. However, high spatial resolution data have limitations, that were identified by Lu (2006) including (1) high spatial variation, shadowing by the canopy, and topography which cause difficulties in developing a biomass estimation model; (2) lack of shortwave infrared images; and (3) difficulties in handling and storing data for large area application. Moreover, high-resolution data, such as Quickbird, costs much more than coarser data sources for acquisition, processing, and analysis (Hyde et al., 2006). In such cases, high spatial resolution images do not help to achieve better parameters such as LAI (Soudani et al., 2006). In short, high accuracy can be attained from high resolution data but this source is more suitable for small research areas.

Medium spatial resolution refers to remote sensing data that have a spatial resolution range from 10 to 100m. Data from Landsat, SPOT, IRS, CBERS, ASTER, and ALI have medium spatial resolution (Powell et al., 2007). Among them, Landsat data have the longest records, and thereby became the most frequently used for many different applications, including forest biomass estimation (Luther et al., 2006; Sader, 1989; Tømmervik, 2003; Zheng et al., 2008). Luther et al. (2006) used Landsat Thematic Mapper (Landsat TM) for mapping forest biomass in Newfoundland, Canada and found the accuracy of method is 70% for coniferous, broadleaf, and mixed forest areas. Landsat TM data also provide better aboveground biomass estimation in successional forest than in mature forests (Lu, 2005), although the accuracy is much lower for overall species-type mapping (Powell et al., 2007). The Landsat time-series images approach showed high potential for aboveground biomass estimation and biomass dynamics at a broad spatial scale (Powell et al., 2010). Unfortunately, Landsat Enhanced Thematic Mapper plus (Landsat ETM+) sensor has experienced a failure of the scan line corrector since 2003, resulting in an approximate 23% data loss. As a result, SPOT images, which have a full range of resolutions from 1 km global scale to 2.5 m local scale with high revisit frequencies, are used extensively for

vegetation mapping (Xie et al., 2008) and biomass estimation (Hasegawa et al., 2010; Nichol and Sarker, 2011; Tian et al., 2012).

Coarse spatial resolution refers to image data with a spatial resolution greater than 100m. Common coarse resolution data include AVHRR, SPOT vegetation, and Moderate Resolution Imaging Spectroradiometer (MODIS). Among these data sources, MODIS is the most suitable and the most extensively used for biomass estimation at continental scale providing a close relationship between the middle infrared spectral band and biophysical parameters. Moreover, MODIS is readily available (Lu, 2006). In short, Landsat imagery, with its moderate spatial and spectral resolution and ready availability, may be the most suitable for a landscape-scale study.

Radar and LiDAR data have been used extensively in recent years due to their advantages in acquisition irrespective of light and weather conditions. They are both active remote sensing techniques. A Radar system collects data by measuring time and angle of the reflected radio waves (or microwaves) sent by the transmitter. Some forest stand parameters can be retrieved from radar backscatter, such as tree height, tree age, DBH, basal area, and AGB. The correlation between predicted biomass and radar derived biomass found by Sun et al. (2002) is high (r^2=0.92). LiDAR data are collected based on measurements of the round-trip time (which can be inferred the distance) for a pulse of laser energy (laser light) to travel from sensor to targets and to reflect back to the instrument. Canopy height, vertical structure, and ground elevation, are some attributes that can be captured from a LiDAR system (Drake et al., 2002). Based on tree height, density, and intensity parameters derived from LiDAR data, Hudak et al. (2012) estimated aboveground biomass at the landscape scale successfully. However, they are considered to be the most expensive data sources that require a sophisticated process for data analysis, more skills, knowledge, and specific software (Lu, 2006; Wulder et al., 2012).

2.8. Models for Estimating Ecosystem Carbon Stocks and Changes

The stocks and changes of C in plants and soils are influenced by a number of factors including climate condition, ecosystem condition, decomposition rate, environmental conditions, and biological processes. A decrease of temperature, for instance, causes an increase in soil C storage (Post et al., 1982) and vice versa, mainly by stimulating the decomposition rate (Kirschbaum, 2000). As an example of ecosystem conditions, a land-use change from native forest

to cropland decreases total C stocks in soil by 42%, while the conversion from cropland to secondary forest increases total C stock in soil by 53% (Guo and Gifford, 2002). The main features to consider regarding environmental conditions associated with C release from soil are litter and SOM decomposition. Climate, moisture, temperature, litter quality, and the soil microbial community are the main factors that affect litter decomposition rate (Beare et al., 1992; Berg et al., 1993; Couteaux et al., 1995; Hobbie, 1996; Kirschbaum, 1995; Meentemeyer, 1978). Decomposition of SOC is also influenced by biological processes including priming effects (Kuzyakov et al., 2007), biodiversity, and root exudates (Langley and Hungate, 2003). Chemical and physical conditions such as C:N ratio and lignin content, and soil texture are also important factors controlling SOM decomposition rate (Dignac et al., 2002). As a result, the dynamics of SOM is a complex process and it is not fully understood.

Various methods have been developed to estimate the pools and fluxes of soil C. Modelling is a well-known approach to address the influences of the above factors on C sequestration potential and dynamics, by simulating and predicting different C pools, time scales, and spatial levels (Falloon and Smith, 2002; Kurz et al., 2009; Masera et al., 2003; Pueyo and Begueria, 2007). In the literature, there is no particular model that simulates C stocks and changes in forests under abandoned croplands. Hence, an evaluation with regard to input data requirements, the accuracy of estimation, time and spatial scale, availability for use in the same ecosystem, and so forth, is needed for model selection. As noted by Kurz et al. (2009), forest C dynamic models include process-based models, which predict C dynamics based on migration and transformation processes of C in different pools and empirical growth and yield curve models, which rely on data measured in the past.

Process-based models simulate the interacting processes of a number of factors in a system. Based on observation, causes and effects of different changes in a given factor on the system can be quantified. Therefore, this type of model can help us to describe and predict changes under future environment scenarios. However, these models require more field observation than the empirical models for data calibration and validation procedures (Peng and Wen, 2006). The common process-based models include CENTURY (Metherell et al., 1993) 3-PG (Landsberg and Waring, 1997), and RothC (Coleman et al., 1997).

In empirical growth and yield curve models, past survey data can be utilized to enhance the accuracy of predictions. Good simulation performance of human activities and natural disturbances are the important inclusions in the model. However, such models are limited by the slow response to global change factors, such as climate change (Kurz et al., 2009). CBM-CFS (Kurz et al., 2009), CO2FIX (Masera et al., 2003), and EFISCEN (Nabuurs et al., 2000) are examples of growth and yield curve models. Application of these models in relation to LUCC and C stocks and changes in different pools is reviewed in the following sections.

2.8.1. Process-based models: CENTURY, 3-PG, and RothC

CENTURY is a process-based ecosystem model to simulate C, N, P, S dynamics through an annual cycle over time. It was originally introduced by Parton et al. (1987) for soil under grasslands in the prairies of North America, but has been widely applied to arable (Leite et al., 2004; VandenBygaart et al., 2008) and forest soil (Peng and Apps, 1998; Peng et al., 2002). Input for the current version, CENTURY 5.0, includes meteorology, soil texture, plant cover, management, time step, and initial C, N, P, S. Three SOM pools (active, slow, and passive), that have different decomposition rates are linked together and associated with aboveground and belowground litter pools, and the surface microbial pool. The grassland sub-model and the forestland sub-model are combined to simulate the shrub ecosystem. CENTURY can also simulate the growth of deciduous or evergreen forest in different development stages (Ojima et al., 2002). In the boreal forest of central Canada, Peng and Apps (1997) used the CENTURY model to examine the sensitivity of boreal forest to climate change; in the study, the influence of different harvest regimes on C stocks and fluxes was investigated for boreal forests of Canada. A study on grasslands by Parton et al. (1987) concluded that aboveground plant production and soil C and N were predicted adequately using CENTURY 4.0. The authors also remarked on the expected overestimation of C and N levels for fine textured soils. Changes in soil C and N under land use conversion from cereal fields and vineyards to forest plantations were studied by Romanyà et al. (2000) using the CENTURY model. VandenBygaart et al. (2008) applied CENTURY to investigate soil C change factors (annual to perennial cropping, tillage to no-tillage, and summer fallow to continuous cropping) across Canada and asserted that Century is adequate to derive C change factors. The potential performance of the model for analyzing boreal forest by linking it to a GIS was examined by Peng and Apps (1997). The authors discussed the advantages that can be

taken from temporal dynamics in CENTURY and spatial integration benefits of GIS. According to Smith et al. (1997), there are nine models extensively used for SOC simulation for arable lands with the performance of each not being significantly different, but CENTURY is the preferred model that can be applied to different land covers including grass and forest.

Physiological Processes Predicting Growth (3-PG) is a process-based C balance model where biomass production is calculated from radian energy absorbed by forest canopies. BGB is estimated using an allometric ratio. The model was developed by Landsberg and Waring (1997) and tested on forests in Australia and New Zealand. Required input data include weather data (radiation, frost days per month, humidity, and precipitation), initial biomass value, available soil water, initial stem number, stand age and other parameter values. This model has become prevalent because it uses weather data and remote sensing data for parameterization (Landsberg and Waring, 1997). Data measured from scattered locations across landscapes and remotely sensed data, can be incorporated to generate new data forms in scalable and predictable relationships (Coops et al., 2001). The outputs from the model include: stem wood production, net production, mortality, live and dead stem biomass, leaf and root turnover, autotrophic (plant) respiration, and relative constraints of environment. Biomass estimation for scrub and forests of New Zealand conducted by White et al. (2000) found high correlation between simulated and plot-based estimation (r^2=0.98). 3-PG prediction also correlated with regional estimation of aboveground biomass or total vegetation biomass of the entire country. However, a slight underestimation of stem biomass and total biomass still existed at the broad scale due to some assumption factors for biomass allocation to roots, soil characteristics, and stand age. Amichev et al. (2012) used this model to quantify potential willow biomass yields on marginal land of Saskatchewan. In a recent study, 3-PG was also used for carbon estimation of six comment tree and shrub shelterbelts (hybrid poplar, white spruce, scots pine, Manitoba maple, green ash, and caragana) in Saskatchewan (Amichev et al., 2016). Vegetation indices such as the Normalized Difference Vegetation Index (NDVI) from AVHRR instrument (Coops et al., 2001) and SPOT images (Coops et al., 2002), or leaf area index (LAI) from Moderate Resolution Imaging Spectroradiometer (MODIS) satellite imagery (Mustafa et al., 2011) can all be used as input data.

The Rothamsted Carbon Model (RothC) is a process-based model and was originally developed to model the turnover of organic C in arable soils using long-term experiment data by

Jenkinson and Rayner (1977) at Rothamsted Research in the UK. RothC models the effects of soil types, temperature, moisture content, and plant covers of the turnover processes. This model is constructed to quantify organic C in four different active compartments (Decomposable Plant Material, Resistant Plant Material, Microbial Biomass, and Humified Organic Matter) of SOM and Inert Organic Matter based on their decomposition rates. Applications of this model have been extended to land use other than arable land including forest soils (Jenkinson et al., 1999), and grassland soils (Leifeld et al., 2009). The advantages of the model include low data input, long history, and applicability to spatial data. Monthly data required to execute the model include meteorology, clay content, soil cover, decomposability of input residue, input of plant residues, and depth of soil layer sampled (Coleman and Jenkinson, 1999). The model has been applied successfully in simulation of soil C stock under land-use change. Romanyà et al. (2000) conducted a simulation of the change in SOC after afforestation on Mediterranean agricultural soil using chronsequence data and found that the model was sensitive to previous land use. Recent research on 11 land-use change chronosequences, (Cerri et al., 2007) also found RothC to perform well in simulating the changes of SOC under “forest to pasture” conversion. The authors asserted that chronosequence data were the most useful source in illustrating trends of soil C dynamics. Moreover, RothC allows linking with spatial data such as soil attributes, meteorological conditions, and land uses. Falloon et al. (2006), for instance, utilized national spatial data from the UK in RothC to investigate the effects of land use change, land management, and climate on SOC stocks. However, a plant growth module is not included in the RothC model, requiring users to analyze by other means.

In summary, these process-based models show good performance in simulating C stock and change in forest ecosystems and linking with spatial data. RothC and CENTURY models were originally developed for soil C simulation, while 3-PG estimates the amount of C allocated belowground, based on allometric ratios. RothC is limited by not including plant growth during simulation. For simulating C stock and dynamics in Canada, CENTURY shows the greatest potential as this model was originally developed for prairie grassland and has been applied widely in Canada under different land use and land cover conversions.

2.8.2. Empirical yield curve models: CBM-CFS, CO2FIX, and EFISCEN

The CBM-CFS3 model (Carbon Budget Model of the Canadian Forest Sector version 3), is produced by the Canadian Forest Service, Natural Resources Canada. This empirical yield curve model was constructed for C accounting of forest ecosystems, which can calculate forest C stocks and stock changes for the past and into the future. Forest stand, defined as communities of trees that are homogeneous enough to be treated as a unit, is the smallest spatial scale for basic calculation. Forest stand includes attributes such as area, age, and land class. In CBM-CFS attribute data and parameters can be set by users or pre-set default parameters are used. Annual dynamics of C are aggregated from quantifications in each pool consisting of ten biomass pools and eleven DOM pools according to IPCC's requirements (Kurz et al., 2009) associated with disturbed characteristics (type and magnitude). Cover disturbance, such as forest fire, insect infestation, and harvesting, is the main component of the CBM-CFS. The advantages of the model include: (1) estimation of C stock and changes can be achieved in different spatial scales, from forest stand to local, landscape, regional, and national scales; (2) development of the model relied on a huge variety of literature covering almost all tree species, soil types (excluding peatland), eco-zones, types of disturbances, and inventory data in Canada and it can, therefore, be applied to a wide range of forest covers and relevant disturbances; (3) it is flexible in inputting data (i.e. mixed forest stand) and setting parameters (i.e. using curve-smoothing for non-merchantable volume or using biomass expansion factors where allometric equations are not available); and (4) the outputs are in both graphic and tabular data and meet IPCC's standards. However, some improvements for the model are being considered. For example, currently aboveground biomass is only estimated based on allometric equations derived almost entirely from merchantable trees, and DOM and soil C dynamics were derived from forest plot data, and thus the model cannot be applied directly to agriculture, grassland, and shrub ecosystems. In pursuit of better performance by CBM-CFS, studies have been conducted by Metsaranta and Kurz (2012) and Smyth et al. (2011). Similarly, for the model to enhance its accuracy, it would be valuable to consider specific parameters on forests regrown after agricultural disturbance. Li et al. (2002) applied the model successfully to estimate forest NPP in the three prairie provinces in western Canada (NPP varies from 72 to 293 g C m^{-2} $year^{-1}$ depending on eco-climate, forest type, age, and site productivity). By adding tree-ring data of merchantable jack pine *(P. banksiana)* stands, Metsaranta and Kurz (2012) estimated

net ecosystem productivity (NEP), NPP, and heterotrophic respiration (Rh) annually from 1975 to 2004 using CBM-CFS in Saskatchewan and Manitoba. CBM-CFS was used to study impacts of harvest and fire on C dynamics (Luckai et al., 2012) and simulating C fluxes of coppice willow plantations on marginal lands in Saskatchewan (Amichev et al., 2012).

CO2FIX, a carbon budget model, was originally developed for quantifying C stocks and fluxes of mono-species stands in the Netherlands as part of the CASFOR project – C Sequestration in Afforestation and Sustainable Forest Management. In 1999 the most recent version, CO2FIX V3.1, was made available for the Windows Operation System in the CASFOR II project with financial support from the European Commission program (Mohren and Goldewijk, 1990). This yield-curve model can quantify C stocks and fluxes in three different pools, forest biomass, SOM, and wood products chain, and it can apply to forest stand, landscape, and ecosystem levels. The model also includes a bio-energy module to compare benefits related to GHG emission projects, a financial module to determine the benefit of a forest project, and a C accounting module to quantify C credit (Schelhaas et al., 2004). It is a user-friendly model (Masera et al., 2003) and can be applied to a large variety of forest types and project applications. Using this model, Nabuurs and Schelhaas (2002) conducted research on sixteen typical forest types in Europe, and Masera et al. (2003) modelled C sequestration in afforestation, agroforestry and a forest management project, for both temperate and tropical conditions. This parameterized model allows estimation of C stocks and fluxes under different disturbances such as fire, storm damage, pest and diseases, and climate change using default parameters or parameters input by users. However, improvements are needed as some uncertainties exist in the model (Groen et al., 2006). Sources of uncertainty were noted by Nabuurs and Schelhaas (2002) for SOM dynamics and the C content of dry matter. Furthermore, modelling for a non-forest system such as grassland and cropland was introduced, but no literature was found. Some research in this regard has been conducted successfully in Canada. For instance, Neilson et al. (2007) integrated the model with a timber supply model for forest management planning in New Brunswick. Gaboury et al. (2009) estimated the net C balance of the woodland afforestation of boreal forest in Quebec, Canada. However, the effects of climatic factors when applying the model to central Canada were overestimated due to the different relationships between annual mean temperature and growing season temperatures in this area (Nabuurs and Schelhaas, 2002).

EFISCEN, the European Forest Information Scenario model, is an area-based matrix model originally developed by Ola Sallnas in the 1990s at the Swedish Agriculture University. The European Forest Institute (EFI), in collaboration with other scientists made improvements (Nabuurs et al., 2001; Schelhaas et al., 2007; Thurig and Schelhaas, 2006). The model focuses on sustainable management regimes, wood production possibilities, nature orientated management, climate change impacts, natural disturbances, and C balance issues. Carbon stock and dynamics can be estimated from wood volume using a biomass expansion factor. This soil C module was inherited from a dynamic soil carbon model, YASOO (Schelhaas et al., 2007). To enhance the performance of EFISCEN, a number of studies have been conducted. Nabuurs et al. (2000) validated the EFICEN model by adding regrowth boost after thinning practice. Schelhaas et al. (2002) included natural disturbances of fire, storm, snow, insect, and aging that cause tree mortality. New modules under climate change scenarios and un-recovered wood after disturbance scenarios were also added. The advantages of the model are that it requires little input data and is applicable to different spatial scales (Thurig and Schelhaas, 2006). In addition, forest management regimes were included in the model, making it suitable for forest management project options (Nabuurs et al., 2001). However, in a case study for model evaluation in heterogeneous forests of Switzerland, Thurig and Schelhaas (2006) concluded that modelling forest growth and increment stocks did not function well at the regional scale. Mortality function and forest management practice options in the EFISCEN model should be improved as EFISCEN is currently designed for even-aged managed forests (Schelhaas et al., 2007). It can predict for only a 50-year forest development period (Nabuurs et al., 2001) and thereby modelling estimates for longer time periods have limitations. A comparison of potential and efficiency of three different models (EFISCEN, forest growth model – MELA, and forest ecosystem model - SIMA) on CO_2 mitigation options was conducted by Nuutinen and Kellomaki (2001) which revealed that interactions between growth and forest management are not well simulated in EFISCEN resulting in its inadequacy to search and suggest effective forest management applications. Underestimation of C accumulation rate was also noted (Nuutinen and Kellomaki, 2001).

In summary, all of the above yield-curve models include disturbance attributes due to land-use change, but conversion of cropland to forest has been omitted. The models require comparable input data and provide aspatial outputs. Growth yield curves were retrieved mainly from forest

stands, so this would be more suitable for estimation of C stock in AGB. In time scale and spatial scale, EFISCEN does not perform well with forest age over 50 years nor at stand level or landscape levels. CO2FIX is a good model, but overestimation of C stock for west-central Canada was acknowledged due to the effects of climatic pattern on the model (Nabuurs and Schelhaas, 2002). CBM-CFS has good performance when applied to Canadian forest ecosystems, but it is more suitable for merchantable forests. Hence, of the three models, CBM-CFS could be the most suitable for modelling C stock and fluxes for vegetation covers of abandoned cropland in Canada, but an additional module for non-forest vegetation may be needed.

3. QUANTIFYING CHANGES IN BIOMASS AND SOIL ORGANIC CARBON IN ABANDONED CROPLANDS IN SASKATCHEWAN, CANADA

3.1. Preface

The need to harmonize between land use and environmental sustainability, including reducing carbon emissions, is one of the most pressing issues facing humanity. Although major land transitions in the last century accelerated terrestrial carbon emission, abandoned cropland in recent decades could lead to carbon accumulation in both soil and vegetation. However, carbon sequestration in abandoned cropland is not well understood, especially in western Canada. Estimating carbon stocks in such land will help enhance our understanding of carbon sequestration potential and provide valuable data for carbon estimation studies associated with agricultural land-use change. The primary objective of this study was to quantify carbon stocks and dynamics in abandoned cropland. Carbon stocks in abandoned cropland and those in adjacent cultivated fields and forest were compared to estimate carbon accumulation rate in the soil pool. A study with field sampling of properties such as vegetation biomass, and soil organic carbon at three locations, was conducted in the Boreal Plains Ecozone, Saskatchewan, Canada.

3.2. Abstract

Abandoned cropland is expected to serve as a substantial C sink in the future because of its natural regeneration of vegetation and its potential increase in SOC. Little is known about the quantity, distribution, and dynamics of this potential sink for the Boreal Plains Ecozone in Canada. The main objective of this study was to determine C stock, distribution, and changes in the Boreal Ecozone in Saskatchewan, Canada. Historical air photos were used to detect abandoned fields and to apply a chronosequence approach to quantify ecosystem C stocks and dynamics. The field study was conducted at six sites with stand ages ranging from 9 to 41 years in the Boreal Plains Ecozone, north of Saskatoon, Saskatchewan. All abandoned sites had similar characteristics including soil order (Chernozem), dominant tree species (trembling aspen, *populus tremuloides*), disturbance history (cultivated), and ecozone - located in the Boreal Plain with similar environmental

conditions - but differing in stand ages. The means of ecosystem C ranged from 60.09 to 138.61 Mg C ha^{-1} and increased with stand age although no linear relationships were evident. After four decades of abandonment, vegetation C ranged from 9.49 to 100 Mg C ha^{-1} and increased linearly with stand age, forming a C sink with a rate of 1.41 Mg C ha^{-1} yr^{-1}. Mean values of soil C ranged from 44.15 to 86.85 Mg C ha^{-1}. Soil C increased over time but linear correlation was not observed. However, compared to adjacent cultivated sites, SOC accumulation rates in abandoned cropland revealed a small potential C sink, especially in the short term. Dead wood, belowground, aboveground, and litter biomass increased with stand age. Aboveground biomass was the main sink and increased linearly with stand age. Means of tree volume ranged from 2.08 to 117.92 m^3 ha^{-1} and correlated with stand age suggesting a yield-curve model might be used for broader scale C estimation. All C pools contributed to ecosystem C dynamics since abandonment but tree biomass was the main contributing pool.

3.3. Introduction

Global temperature has increased over the 20th century and is projected to continue to rise in the 21st century. Land-use and land-cover change associated with changes in terrestrial C stocks has significantly contributed to the increase of greenhouse gases (GHG) in the atmosphere and global temperature (IPCC, 2013). The most recent IPCC report estimated that global CO_2 emissions from LUCC, including deforestation and other land-use changes, was 0.9±0.5 Gt C yr^{-1} during 2004 – 2013. Alternatively, C uptake by forest has removed 2.9 ±0.8 Gt C yr^{-1} from the atmosphere or approximately one third of annual C from anthropogenic fossil fuel use (8.9 ±0.4 Gt C yr^{-1}) (Le Quéré et al., 2014). Therefore, understanding C stocks and dynamics under LUCC is particularly important for predicting potential climate change as well as developing mitigation strategies.

National inventory on GHGs emission and sequestration are required to be reported to the United Nations Framework Convention on Climate Change (UNFCCC). In Canada, Agriculture and Agri-Food Canada (AAFC) and Canadian Forest Services (CFS, Natural Resources Canada) are responsible for reporting GHGs associated with land-use changes in agriculture and forestry. Carbon stocks and dynamics at operational, provincial, national scales in the past, present, and future have relied on inventory data and simulation models, such as CBM-CFS3.

Under 2006 IPCC guidelines for National Greenhouse Gas Inventory, GHGs emission and removal under abandoned cropland are reported in designated categories depending on the conversions, such as cropland to forest or cropland to grass (IPCC, 2006). However, carbon stocks and dynamics from abandoned croplands have not been monitored and reported separately in most of national GHGs reports. In the United States, the Environmental Protection Agency (EPA) is responsible for the annual US GHG inventory report. According to the recent EPA report, abandoned cropland was included in the "other lands converted to grassland" category. This conversion resulted in a net uptake of 8.8 million Mg CO_2 (or 2.4 million Mg C) in 2013 (EPA, 2014). In Europe, the European Environment Agency is responsible for greenhouse gases inventory reporting based on input from the European Union members. In the recent report of European Environment Agency, grassland (including abandoned cropland) increased by 14% between 1990 and 2012, and abandoned cropland contributed 82% of the change, resulting in a C sink of 19.89 Gg CO_2 in 2012 (EEA, 2014). In Japan, the C sink in abandoned cropland has not been quantified separately but included under Other Land category in the national GHG inventory. In 2010, this land category became a C source of 382 Gg CO_2, but C stock changes as a result of abandoned cropland were not reported (NIES, 2014). In short, although abandoned cropland has not generally been monitored and reported separately at the national scale, recent reports suggest C accumulation results from abandoned cropland.

In Canada, an AAFC and CFS collaborative project to quantify C stocks and dynamics under LUCCs from agriculture has been conducted to determine C stock and dynamics in Canada's agricultural region. Extracting cover change information from air photo interpretation and biomass productivity from reference data, C accumulated in the aboveground biomass (which is not defined as forest) was estimated at ecozone level. Accordingly, aboveground woody biomass of the boreal plains during 1990 - 2000 was estimated at a rate of 51.2 Gg yr^{-1} (Huffman et al., 2015). Abandoned cropland and associated regrowth of wood biomass has been studied in Canada (Benjamin et al., 2005; Foote and Grogan, 2010), but there has been no comprehensive study examining the distribution, stocks and dynamics of C from the whole C pools in this type of land-cover. Hence, having a comprehensive study, which quantifies C stocks and dynamics in all C pools, at a field scale on abandoned croplands, is necessary. Such a study would play an important role in C estimation at a broader scale.

The main objective of this study was to characterize the C distribution and to quantify C stock and changes under abandoned croplands in Saskatchewan, Canada. Abandoned cropland in our study refers to land where cultivation activities have ceased for at least nine years and regeneration to shrub or forest has begun (Keenleyside and Tucker, 2010). As the information on municipal taxes on this land has not been included, the closest alternative term for this land could be unused cropland. We focused primarily on the fringe area of the Boreal Plains Ecozone in Saskatchewan on landscapes associated with the Chernozem soil order.

3.4. Materials and Methods

3.4.1. Site selection and descriptions

Aerial photographs, available since the 1960s from the archive of Saskatchewan Geospatial Imagery Collaborative (SGIC), and recent online map layers from SGIC Flysask website (http://www.flysask.ca/), were used to detect and select the sample sites. ArcMap tools were used to pre-process data including geometric correction of aerial photographs and the map layers. Abandoned cropland was detected from field to field using visual interpretation or an on-screen change detection approach with support of the ArcMap Swipe tool. Suspected abandoned cropland was sketched into potential abandoned site map layer. Field surveys were then conducted to confirm if the potential sites were in fact abandoned croplands.

The criteria used as evidence for abandoned cropland included: (1) confirmation from landowners, (2) plough layer (Ap) present in soil pits, (3) historical agriculture use in air photos, and (4) vegetation cover without any recent significant disturbances such as grazing, forest fire or harvesting.

Study areas were located around Bright Sand Lake (the north sites), and Redberry (the south sites), in the Boreal Transition Ecozone of Saskatchewan, Canada, approximately 200 km north of City of Saskatoon (Fig. 3.1.). Total area of the abandoned cropland was approximately 160 ha. The specific abbreviation names, locations of each study site in UTM coordinate system, stand age, and soil orders are presented in the Table 3.1. Of the six abandoned cropland sites, three were near Bright Sand Lake (BSN-09, BSL-24, BSE-27) and two were in the Redberry region (RED-10, RET-15). The sixth abandoned site near Witchekan Lake (WAL-41) was chosen due to difficulty in locating an older stand in the Bright Sand Lake and Redberry regions. However, all

sample sites were in close geographic proximity and in the same ecozone. Permanent cropland and forest sites, used as references, were located adjacent to each abandoned site.

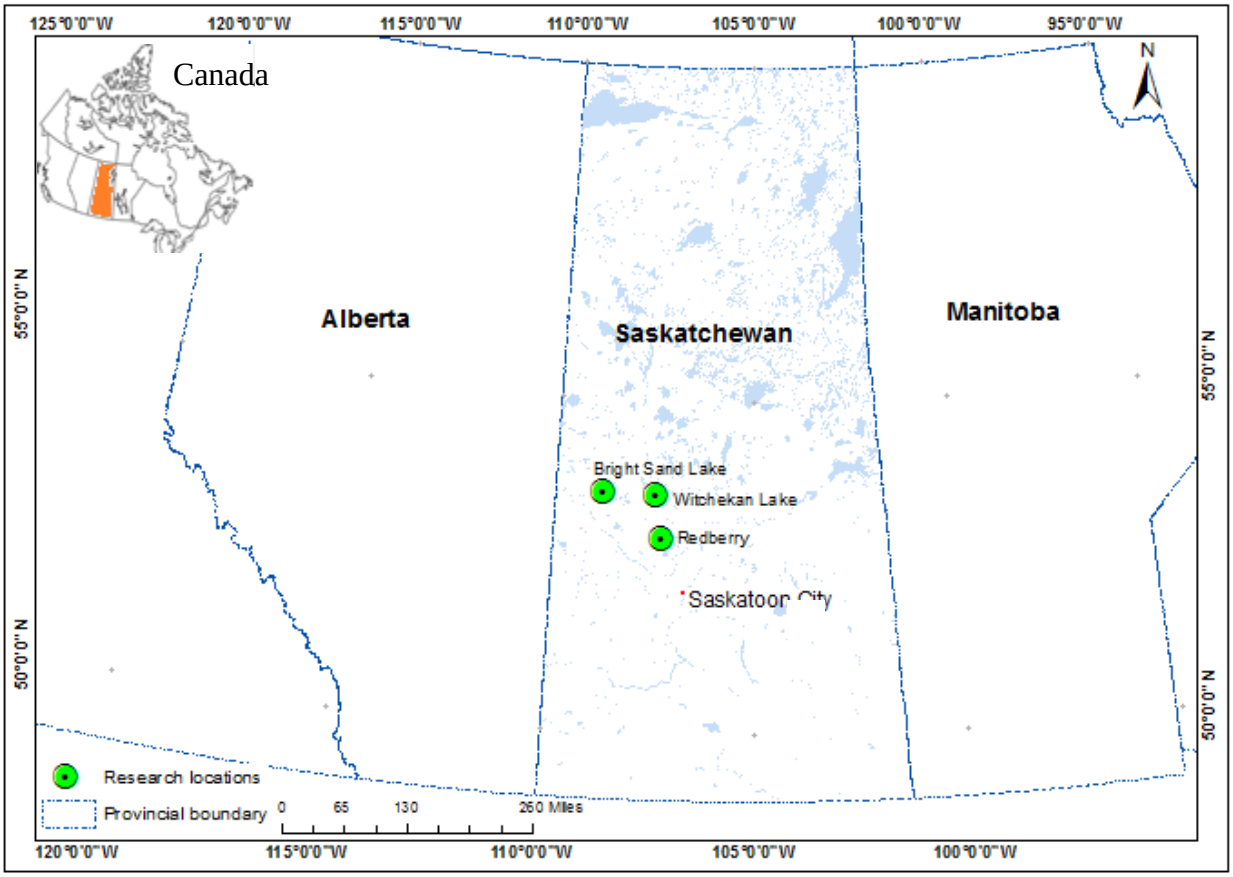

Fig. 3.1 Sample locations of the cropland, abandoned cropland, and forest sites at Bright Sand Lake, Witchekan Lake, and Redberry, Saskatchewan, Canada.

Table 3.1 Summary information about the research sites.

Site	UTM[#] coordinates		Sampling grid	Stand age	Area	Soil orders
	x	y				
	m			*Year*	*ha*	
Cropland						
C-BSN	250769	5947566	3 x 3			
C-RED	347880	5867986	3 x 3			Chernozem
C-BSL	248003	5939625	3 x 3			Chernozem
C-BSE	246705	5946661	3 x 3			Chernozem
Abandoned cropland						
BSN-09	249330	5950552	3 x 3	9	17.61	Chernozem
RED-10	346774	5866702	3 x 3	10	7.08	Chernozem
RET-15	347325	5866659	3 x 3	15	32.37	Chernozem
BSL-24	246875	5944682	3 x 3	24	39.07	Chernozem
BSE-27	246375	5946378	3 x 3	27	15.31	Chernozem
WLA-41	339304	5939888	3 x 3	41	11.49	No sampling[$]
Mature forest						
F-BSN	249718	5951166	1			Brunisol
F-RED	347000	5866632	1			Chernozem
F-BSS	249432	5941399	1			Chernozem
F-BSE	246396	5945756	1			Chernozem
F-BSL	246828	5944938	1			Chernozem

[#] All sites are in UTM zone 13.
[$] Cancelled soil sampling due to soil disturbance before the soils could be sampled.

3.4.2. Sampling design

The experimental design consisted of a systematic grid of nine sub-sample points in 150 x 150 m with 3 x 3 parallel transects (nine subplots in each field). An area of 100 m^2 was selected to quantify tree biomass (tree plot). Shrub and detritus samples were collected in a 3 x 3 m quadrat inside the tree plot (shrub plot). Similarly, inside each shrub plot was a 0.25 m^2 quadrat for collecting litter and herb samples (herb plot). Soil samples were collected in the center of the sample points (Fig. 3.2). Field measurements were conducted in August, 2012 on fifteen study sites including six abandoned croplands, four croplands, and five mature forests. The abandoned croplands were characterized by sparse vegetation of grass, shrub, or young forest stands following

natural regeneration after cultivation ceased. The tree canopy of forest sites was dominated by a mixture of trembling aspen (*P. tremuloides*), balsam poplar (*P. balsamifera*), white spruce (*P. glauca*), beaked willow (*S. bebbiana*), and chockcherry (*P. virginiana*).

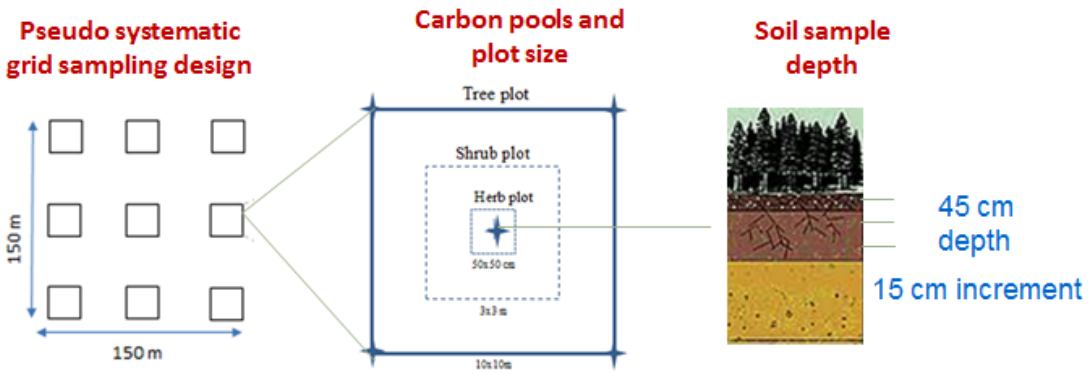

Fig. 3.2 Sample plot outline for studying C stocks in abandoned cropland.

3.4.3. Terrestrial carbon pools

The five major C pools defined in the LUCC protocol are aboveground biomass, belowground biomass, dead wood biomass, litter, and soil organic matter. Aboveground biomass (AGB) comprises biomass of all living vegetation above the soil including grass, shrub, and trees. Belowground biomass (BGB) is living roots of trees excluding fine roots < 2 mm diameter. Dead wood biomass is a combination of standing and fallen dead wood (coarse detritus). Litter biomass comprises dead organic surface material on top of mineral soil. SOC is the decomposition of plant and animal residues, root exudates, living and dead microorganisms, and soil biota (IPCC 2006). Our study sampled all these C pools with ecosystem C equalling the total C stock in the different pools.

3.4.4. Data collection and laboratory analysis

Biomass of living trees was estimated from tree height and tree DBH using allometric equations. Tree height and stem diameter were measured in tree sample plots (100 m^2) using a tree height measuring pole and tree diameter calliper; tree species were also recorded.

Biomass from living tree and coarse roots was estimated using allometric equations adapted from Lambert et al. (2005) and Li et al. (2003b), respectively. Shrub biomass was estimated using a destructive sample collection approach. Shrub samples (small trees with height 0.5 to 4 m) were harvested in 4 m^2 quadrats. The fresh samples (g m^{-2}) were mixed and oven dried to a constant weight within 0.5 to 1 kg at 60 ˚C and converted to Mg ha^{-1}. A boreal forest biomass-to-carbon conversion factor of 0.5 was used (Fitzsimmons et al., 2004). The same sample collection and analysis protocol were used for grass samples within a 0.25 m^2 quadrat. The volume of dead wood biomass was estimated by using the equation for calculating the volume of a cylinder. e

In tree plots, dead wood biomass >10 cm in diameter were measured in two parts, above and below breast height (Eq. 3.1, 3.2). The conversion factor of volume to oven-dry mass of 0.36 Mg m^{-3} was used (Fitzsimmons et al., 2004).

$$\mathbf{V = \pi r^2 h} \textit{ for } h \leq 1.3m \qquad \text{(Eq. 3.1)}$$

$$\mathbf{V = [\pi r^2 (1.3)] + [\pi r^2 (h-1.3)/3]} \textit{ for } h \geq 1.3m \qquad \text{(Eq. 3.2)}$$

Where: V = volume; h: height (m); r = 0.5 dbh (m)

Detritus (dead branches) of 2 to 10-cm diameter was measured in 4 m^2 quadrat (shrub plots) using destructive methods. In each quadrat, approximately 0.3 kg subsamples were collected and oven dried to constant weight.

For litter biomass, all fine detritus with diameter < 0.2 cm was collected in 0.25 m^2 quadrat and oven-dried to constant weight. Biomass from all vegetation pools were calculated and converted to Mg ha^{-1}. Stand age of the abandoned sites were based on the tree coring samples taken at 45 cm above ground from nine tallest trees at each site.

Soil samples were collected at the center of the tree plots from six abandoned croplands, five mature forests, and four cropland sites at three depth intervals (0-15, 15-30, and 30-45 cm) using a fixed volume corer (4.0 cm radius) or truck-mounted hydraulic punch (2.75 cm radius). Biomass sampling was conducted on WLA-41 site (Witchekan Lake) but soil sampling at the site was cancelled due to the landowner introducing elk *(C. canadensis)* onto the land before the soils could be sampled. Fine roots were included in soil samples (diameter < 1 cm). The soil order was

identified from a soil pit dug at each sample site using the Canadian system of the soil classification guideline (Soil Classification Working Group, 1987).

Soil bulk density, C density, and particle size were measured in the laboratory. Bulk density was determined from soil samples dried at 105 ˚C for a minimum of 48 hours to constant weight and calculated using soil dry mass (g) divided by total volume (cm^3). Soil C was determined using a 2 mm sieve and then thoroughly mixing the material before using the Leco CR-12 Carbon Analyser (dry combustion method) to quantify C density (Wang and Anderson, 1998).

To understand the impact of abandoned cropland on soil carbon accumulation, the SOC stocks to a fixed depth and fixed mass were used. The SOC stock is assessed to a fixed depth, which is the product of the sample depth, carbon concentration, and soil bulk density. The SOC stocks at fixed depth were calculated following Ellert et al. (2006) as:

The SOC at fixed depth:

$$\mathbf{SOC_{FD}} = \sum_1^n \boldsymbol{Dcs} * \boldsymbol{Ccs} * \boldsymbol{Lcs} * \mathbf{0.1} \quad \text{(Eq. 3.3)}$$

Where: SOC_{FD} is soil organic carbon for fixed depth (Mg C ha^{-1}); Dsc is the density of core segment (g cm^{-3}); Ccs is the organic C concentration of core segment (mg C g^{-1} dry soil); Lcs is the length of core segment (cm); n is the core segment.

The SOC stock to a fixed depth method has been considered to introduce substantial bias due to the spatial and temporal variability in bulk density (Ellert et al., 2006; VandenBygaart and Angers, 2006). The interpretation of SOC stock changes following a land-use conversion, which causes changes in bulk density, can lead to errors. SOC stocks on an equivalent soil mass or fixed mass is therefore required to correct the calculation.

For SOC stocks at fixed mass calculation, mass of soil to the designated depth (M_{soil}) is calculated as: $M_{soil} = \sum_1^n \boldsymbol{Dcs} * \boldsymbol{Lcs} * \mathbf{100}$; and the lowest soil mass from all sample cores (M_{ref}) are needed to identify. The SOC stocks at fixed mass were calculated as (Ellert et al., 2006):

The SOC at fixed mass:

$$\mathbf{SOC_{FM}} = \mathbf{SOC_{FD}} - \mathbf{M_{ex}}\ \mathbf{C_{sn}}/\mathbf{1000} \quad \text{(Eq. 3.4)}$$

Where: SOC_{FM} is mass SOC per ha of soil having M_{ref} (Mg C ha^{-1}) and SOC_{FD} is SOC at fixed depth; Mex is the excess mass of soil, which needs to be subtracted so that mass of soil is equivalent in all sample sites. It is calculated as $M_{ex} = M_{soil} - M_{ref}$; Csn is the SOC concentration in deepest soil core segment.

Soil particle size was measured using pipette method (Indorante et al., 1990). Leaf Area Index (LAI), defined as the total one-side area of leaf tissue per unit ground area, was measured for biomass estimation and for land-use classification at a broader scale, if required, using vegetation indices.

Mean and standard deviation were reported for each field because subsamples were collected at each sample site. All Pairs Tukey-Kramer test was applied to compare means at 0.05 level of significance. Linear correlation was used to assess the relationships among variables.

3.5. Results

3.5.1. Characteristics of the sample sites

The Chernozemic soil order was dominant in 12 of 13 sample sites (Table 3.1). The Brunisolic soil order was found at the mature forest site BSN. In the abandoned sites, Orthic Black Chernozem and Orthic Dark Brown Chernozem were the dominant soil subgroups.

Measured soil characteristics are presented in Table 3.2. The mean thickness of the A horizon (A_p) ranged from 11.1 to 17.7 cm at the north and the south sites, respectively. The A_p thickness in the abandoned sites was not significantly different from forest and cropland sites. Loam was the dominant soil texture class among the sample sites. Sand fractions in northern abandoned sample sites ranged between 49 to 54% and in the south sites between 33 and 36%. No significant difference in mean sand fraction values was evident between abandoned cropland and forest sites for both north and south sample areas. There was significantly higher clay fraction found in the south sites (26%) compared to the north (19%). Mean values of bulk density (BD) in abandoned cropland ranged from 1.5 to 1.8 g cm^{-3} with mean values for north and south site were 1.6 and 1.5 g cm^{-3} and the pair of means are significantly different.

Table 3.2 Means and standard deviations (in parentheses) of soil fraction, bulk density (BD), and SOC stock in the cropland, abandoned, and forest.

Region	Land-use	n	Ah/Ap thickness¥	Sand fraction	Clay fraction	Bulk density	SOC to 45 cm depth	SOC in equivalent soil mass
			cm	*%*	*%*	*g cm^{-3}*	*Mg C ha^{-1}*	*Mg C ha^{-1}*
North	Cropland	27	11.1	49.5 a	19.7 a	1.7 a	54.0 c	49.9
			(2.4)	(5.34)	(3.3)	(0.1)	(9.1)	(8.6)
	BSN-9§	9	13.1	48.5 a	20.1 a	1.8 a	66.6 bc	50.6
			(3.0)	(6.3)	(4.0)	(0.2)	(13.0)	(15.4)
	BSL-24	9	14.7	50.6 a	17.8 a	1.7 a	60.8 c	44.2
			(3.1)	(6.4)	(5.0)	(0.1)	(11.5)	(10.6)
	BSE-27	8	14.6	50.7 a	17.8 a	1.6 a	58.8 c	48.7
			(3.4)	(8.4)	(3.1)	(0.1)	(12.5)	(8.0)
	Forest	4	13.9	50.2 a	22.5 a	1.7 a	59.8 bc	46.3
			(6.7)	(5.3)	(4.9)	(0.2)	(7.4)	(9.5)
South	Cropland	9	14.4	33.7 a	23.2 a	1.4 a	75.8 bc	78.9
			(3.7)	(11.3)	(5.6)	(0.1)	(28.1)	(29.2)
	RED-10	9	15.3	37.1 a	24.2 a	1.5 a	113.71 a	79.9
			(5.8)	(9.2)	(4.2)	(0.2)	(39.0)	(33.2)
	RET-15	9	17.7	34.8 a	27.5 a	1.5 a	96.5 a	86.9
			(5.4)	(9.3)	(5.1)	(0.2)	(29.4)	(29.4)
	Forest	1	17.0	34.3 a	25.8 a	1.5 a	97.5 a	97.5
			(0.0)	(0.0)	(0.0)	(0.0)	(0.0)	(0.0)

§BSN-9: Abandoned site name – Stand age; ¥: A_h for forest, A_p for cropland and abandoned cropland. Means in a given column with the same letter are not significantly different (P = 0.05);

3.5.2. SOC in abandoned croplands

Means of SOC density to 45 cm depth (SOC_{FD}) and SOC in equivalent soil mass (SOC_{FM}) are shown in Table 3.3. Accordingly, SOC_{FD} and SOC_{EMS} ranged from 58.9 to 113.7 Mg C ha^{-1} and from 44.1 to 86.9 Mg C ha^{-1}, respectively, for the abandoned sites.

In the North, the mean values of SOC_{FD} for abandonment (62.2 Mg C ha^{-1}) was higher than that in cropland (54 Mg C ha^{-1}) and forest (59.8 Mg C ha^{-1}), but it was not significantly different between the means. The mean value of SOC_{FD} in abandoned cropland in the South (105.1 Mg C ha^{-1}) was higher than 75.8 Mg C ha^{-1} found in cropland and 97.5 Mg C ha^{-1} in forest. The comparisons show that mean value of SOC_{FD} in the South, which are thicker in Ap horizon and higher in clay content, was significantly higher than that in the North.

The SOC_{FM} in abandoned cropland of the North is 47.82 Mg C $ha^{-1}$and significantly lower than 83.4 Mg C ha^{-1} in the South. Compared to other land-use types, SOC_{FM} of the abandoned cropland in the North was slightly lower than that in cropland, but it was higher than the forest. In the South, the mean value of SOC_{FM} of abandoned cropland is lower than the forest and higher than that in cropland. However, the different in means of SOC_{FM} among the land-use types were not significant.

3.5.3. SOC dynamics in abandoned cropland

SOC dynamics were examined based on tree stand ages at abandoned sites. The results showed no correlation between SOC stock and the tree stand ages which may have been attributed to differences in historical cultivation practices and high variation of SOC concentration at the sample sites. Consequently, each sample site might have had different SOC levels at the stating point regardless of the function of time.

For having a rough estimation on SOC accumulation after cropland abandonment, pair-comparison between SOC stocks in abandoned cropland and that in adjacent cropland sites were conducted for the first sample depth (15 cm). The pair-comparison was made with the assumption that the starting points of SOC in abandoned cropland are equal to that in adjacent cultivated cropland. Table 3.3 shows that abandoned cropland have higher SOC stocks compared to cultivated site in most cases. The table also suggests that a small amount of SOC has accumulated

since abandonment at the first soil depth. The table also shows that the SOC data is variable and there is no clear temporal pattern of SOC accumulation. Over the average period of 17 years, the mean change of SOC is 0.36 Mg ha^{-1} yr^{-1}.

Table 3.3 Means and standard deviations (in parentheses) of SOC mass in cropland and abandoned sites in the 0-15 cm soil depth.

Site code	Stand age	SOC stock in ESMs		
		Cropland	Abandoned cropland	Annual C change
	Year		*Mg C ha^{-1}*	*Mg C ha^{-1} yr^{-1}*
BSN	9	29.1 (4.6)	36.7 (9.7)	0.8
RED	10	57.6 (10.1)	63. 5 (19.1)	0.6
RET[¥]	15	57.6 (10.1)	59.9 (19.0)	0.2
BSL	24	31.3 (6.1)	36.1 (5.9)	0.2
BSE	27	31.3 (6.1)	31.3 (4.3)	0.0

[¥] RET and RED for cropland are the same site (one reference site)

3.5.4. Biomass density and its dynamics

Means of biomass in the different pools are shown in Table 3.4. It shows that herb biomass in abandoned cropland ranged from 1.8 to 3.6 Mg ha^{-1}. No linear correlation between herb biomass and stand age was evident. Mean values of biomass in detritus (dead branches) ranged from 0.1 to 2.9 Mg ha^{-1}. These values increased with stand age but the relationship was not significant (Fig.3.3).

The means of the biomass in the shrub pool ranged from 1.1 Mg ha^{-1} to 8.7 Mg ha^{-1}. The dead stand pool contributed to total biomass only after 15 years of abandonment. The mean values of this pool range from 0.1 to 6.4 Mg ha^{-1} with a positive trend over time although the linear fit between the variables was not significant.

The range of biomass in litter pool was from 4.6 to 19.9 Mg ha^{-1} with a mean of 13.5 Mg ha^{-1} (for 9 to 41-year stands). Table 3.4 shows that litter biomass increases with stand age but the linear correlation was not significant.

For tree biomass, high variation was found among sites with dissimilar stand ages. The live tree biomass of the 9-year site was 2.9 Mg ha^{-1} while the value of the 15-year site was approximately ten times of that at 24.2 Mg ha^{-1} with both being located in the south region. In the north region, live tree biomass ranged from 2.5 to 121.5 Mg ha^{-1}. For the entire time sequence, live tree biomass increases over time following linear correlation (Fig. 3.3)

Tree biomass = 4.02*Age -33.2; r = 0.96; $P < 0.05$ (Eq. 3.5)

Where: Tree biomass is aboveground dry biomass of the trees greater than 2 m in height; Age is number of years since regeneration (stand ages).

Trembling aspen is the dominant species in BSN (77%), RED (70%), RET (12%), BSL (59%), and BSE (36%). Balsam poplar *(P. balsamifera)* also presents in almost all abandoned sites, including BSN (6%), RED (30%), RET (23%), BSL (35%), BSE (24%). RET and WLA are dominated by chokecherry (*P. virginiana*, 33%) and birch willow (71%), respectively. Birch willow also accounts high proportion in RET (32%). Spruce shows in BSE with a considerable proportion (18%).

Table 3.4 Means and standard deviations (in parentheses) of biomass in different vegetation pools of the abandoned croplands.

Site name	Stand age	Biomass					
		Herb	Detritus	Shrub	Dead stand	Litter	Tree
	Year	*Mg ha^{-1}*					
BSN-9	9	2.6 (0.3)	0.1 (0.3)	1.1 (2.4)	0.0 (0.0)	4.6 (2.9)	2. 5 (4.9)
RED-10	10	1.8 (3.1)	1.7 (1.3)	8. 7 (5.0)	0.0 (0.0)	10.5 (7.6)	2.9 (2.9)
RET-15	15	5.0 (3.4)	0.5 (0.7)	4.4 (3.6)	0.1 (0.2)	9.4 (4.4)	24.2 (17.2)
BSL-24	24	1.9 (0.6)	1.8 (1.6)	2.4 (1.4)	1.7 (3.6)	6.3 (6.5)	54.0 (64.0)
BSE-27	27	0.9 (0.9)	2.9 (3.0)	1.9 (2.4)	6.4 (4.8)	19.9 (11.6)	102.0 (54.1)
WLA-41	41	3.6 (0.6)	2.9 (3.2)	2.1 (1.4)	1.8 (1.3)	19.8 (7.1)	121.5 (128.2)

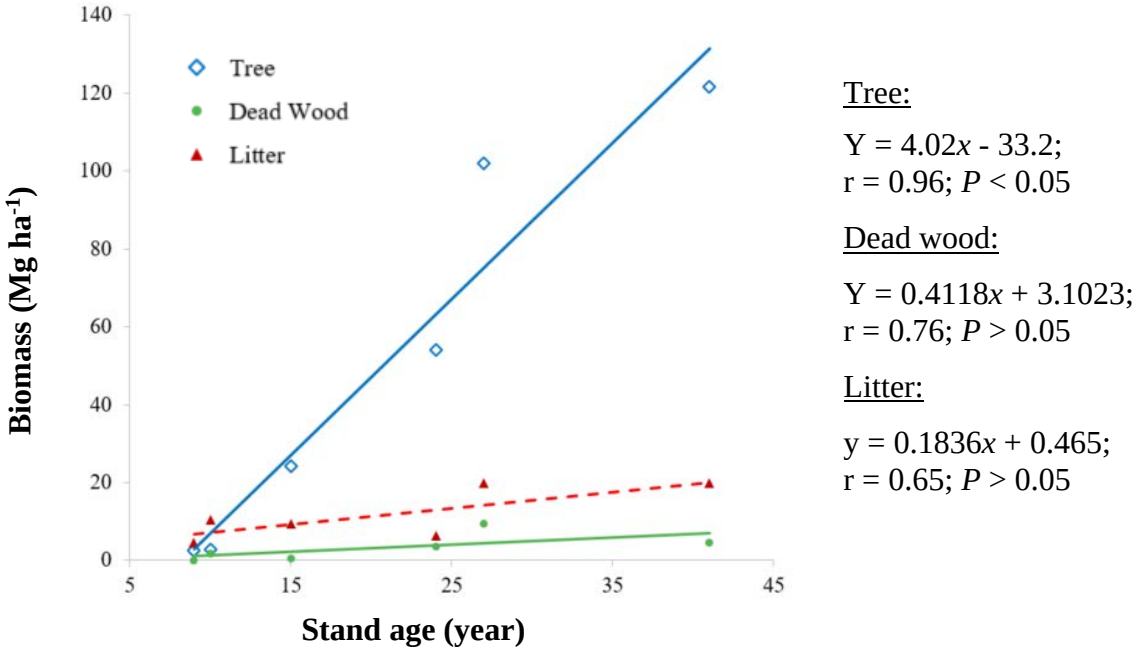

Fig. 3.3 Relationship between biomass (Mg ha^{-1}) from tree (blue diamond), dead wood (red triangle), and litter (green dots) with stand age (years).

Means and standard deviations of biomass in different vegetation pools of abandoned croplands are presented in Table 3.5. In this table, aboveground biomass values were obtained by adding the biomass content in herbaceous, shrubs, and trees. Similarly, Deadwood is the sum of Detritus and Dead stand. In a range of 9 to 41 abandoned years, ABG values range from 6.2 to 127.2 Mg ha^{-1}. Aboveground biomass was positively correlated with stand age (Fig. 3.4) and followed the linear relation as:

Aboveground biomass = 3.92*Age – 25.17; r = 0.98; $P < 0.05$ (Eq. 3.6)

Where: Aboveground biomass is aboveground dried biomass from tree, shrub, and detritus; Age is number of years since regeneration (stand ages).

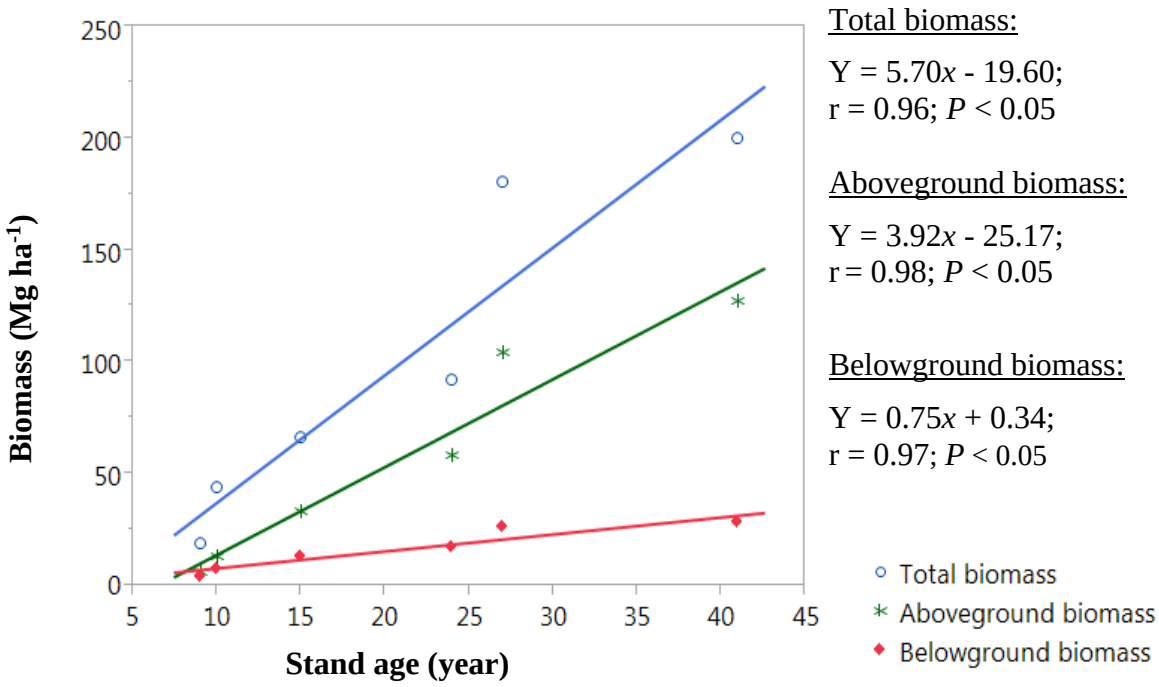

Fig. 3.4 Relationship between biomass (Mg ha^{-1}) from total biomass (blue circle), aboveground biomass (green asterisk), and belowground biomass (red diamond) with stand age (year).

Mean values of the BGB ranged from 4.4 in the 9-year site to 28.5 Mg ha^{-1} in the 41-year site. High positive linear correlation was found between belowground biomass and stand ages (r = 0.97; $P < 0.05$). Total vegetation biomass is the sum of biomass from litter, detritus, dead wood, belowground, and aboveground biomass. Total biomass increased from 19.0 Mg ha^{-1} to 200 Mg ha^{-1} after four to 41 years of regeneration, respectively. Total biomass found positively correlates with abandoned years (Fig. 3.4) as:

Total biomass = 5.70*Age – 19.6; r = 0.96; $P < 0.05$ (Eq. 3.7)

Where: Total biomass is an addition of biomass from litter, dead wood, belowground, and aboveground biomass; Age is number of years since regeneration (stand ages).

Table 3.5 and Fig. 3.3 also show that dead wood biomass increases with abandoned years but the trend was not significant.

Table 3.5 Means and standard deviations (in parentheses) of biomass in different vegetation pools of the abandoned croplands.

Site name	**Stand age**	**Biomass**									
		Aboveground biomass		Belowground biomass		Dead wood biomass		Litter		Total biomass	
	Year	*Mg ha^{-1}*									
BSN-9	9	6.2 (6.8)	a§	4.4 (2.8)	a	0.1 (0.3)	b	4.6 (2.9)	a	15.2 (12.0)	c
RED-10	10	13.4 (6.2)	a	7.6 (2.1)	a	1.7 (1.3)	b	10.5 (7.6)	ab	33.1 (12.3)	c
RET-15	15	33.5 (17.4)	ab	13.3 (4.4)	ab	0.5 (0.7)	b	9.4 (4.4)	a	56.7 (24.26)	bc
BSL24	24	58.3 (63.4)	ab	17.3 (11.3)	ab	3.5 (4.9)	b	6.3 (6.5)	a	85.4 (78.8)	abc
BSE27	27	104.8 (54.5)	bc	26.5 (10.0)	bc	9.3 (6.5)	a	19.9 (11.6)	b	160.4 (71.6)	ab
WLA-41	41	127.2 (127.8)	c	28.5 (16.8)	c	4.8 (4.0)	ab	19.8 (7.1)	b	180.2 (145.4)	a

§Means in a given column with the same letter are not significantly different (P = 0.05);
Dead wood = Dead detritus + Dead stand

The proportion of each biomass pool in total vegetation biomass is illustrated in Fig. 3.5. It shows that AGB was the main contribution to total vegetation biomass.

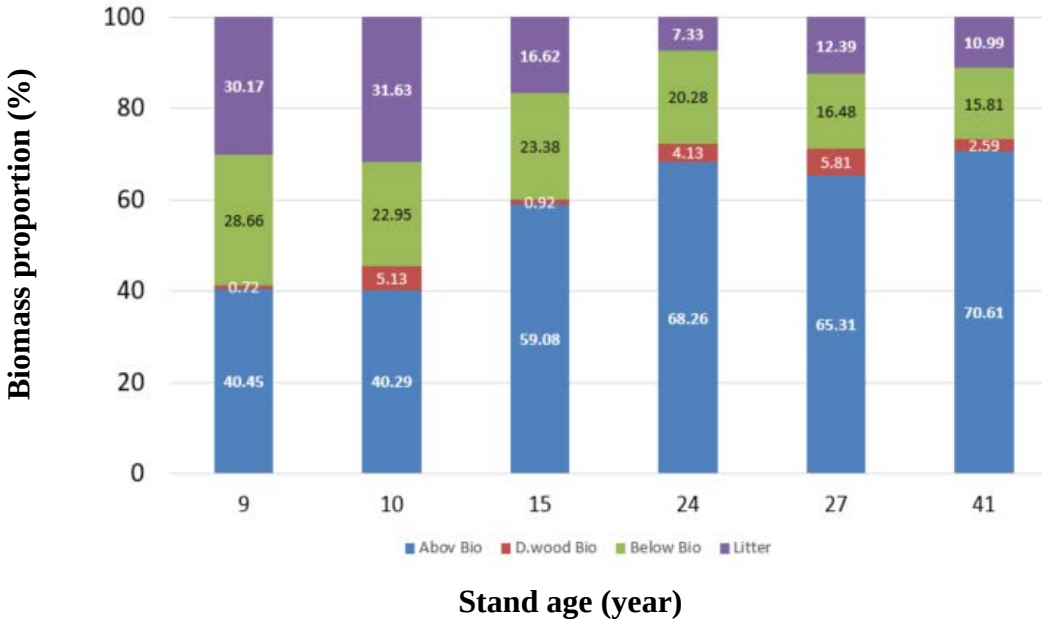

Fig. 3.5 Proportion of biomass (%) from litter, dead wood, BGB, AGB to total vegetation biomass in the different stand ages.

In order to estimate AGB at a spatially broader scale using vegetation index, Leaf Area Index (LAI) and tree volume were measured during field sampling. Vegetation index (LAI) is associated with biomass data, species component, tree volume, stand age, and is valuable information for biomass estimation and LUCC detection projects. Our primary result on relationships between LAI and total biomass is presented in Fig.3.6. It illustrates that a high correlation relationship exists between LAI and total biomass ($r = 0.77$, $P< 0.05$) and that LAI is a good parameter for total biomass estimation.

Tree volume was estimated from biomass of tree boles. A conversion factor of 2.2 Mg m^{-3} was applied to convert tree biomass to tree volume. Mean values of the tree volume ranged from 2.1 m^{-3} in the 9-year site to 117.9 m^3 ha^{-1} in 27-year site. The relationship between stand ages and tree volume is shown in Fig. 3.7, which illustrates that the relationship between tree volumes and years of abandoned followed a linear model ($r = 0.84$; $P < 0.05$).

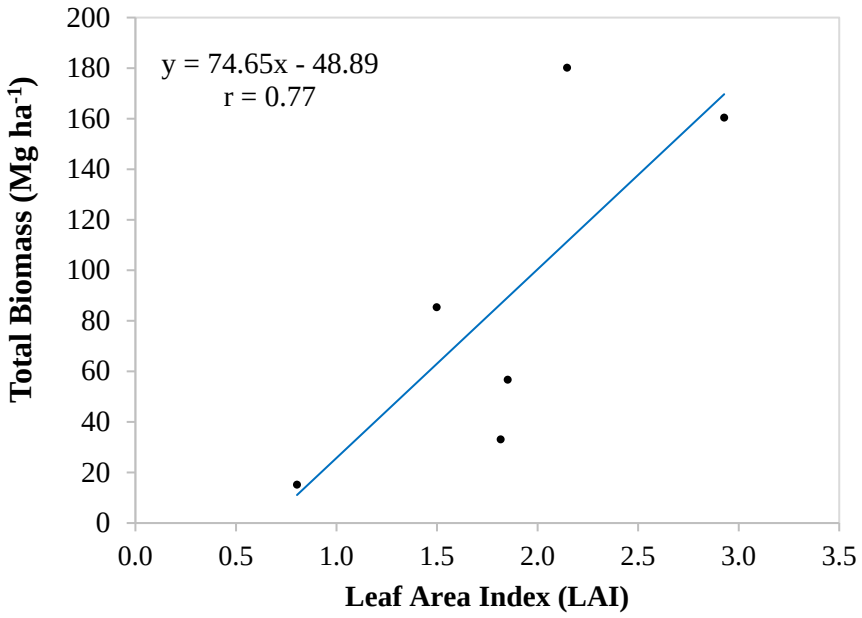

Fig. 3.6 Relationship between total biomass (Mg ha^{-1}) and LAI (m^2 m^{-2})

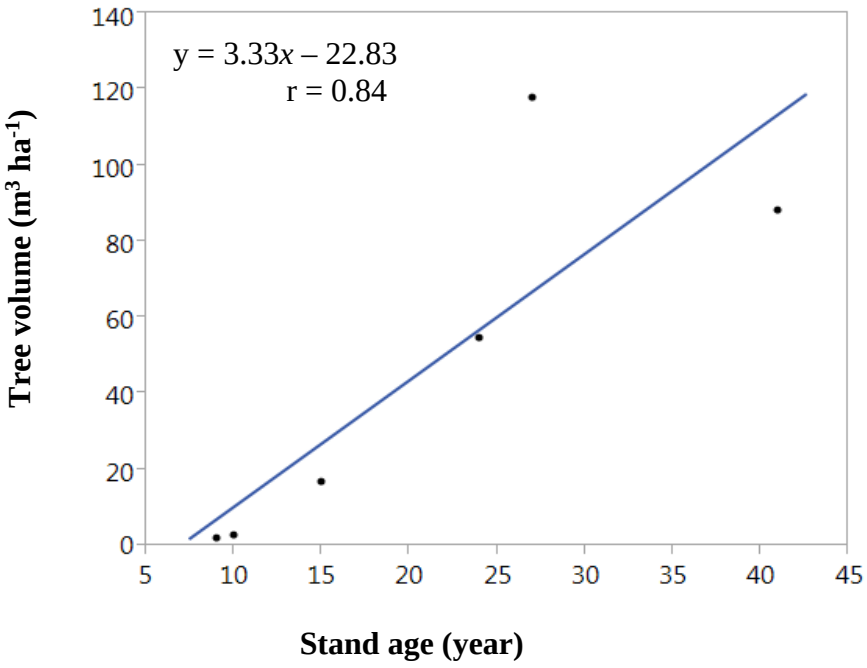

Fig. 3.7 Relationship between tree volume (m^3 ha^{-1}) and stand age (years).

3.5.5. Ecosystem Carbon and its dynamics

Ecosystem C is the sum of C from vegetation C, which was converted from total biomass using a conversion factor of 0.5, and SOC. After approximately a decade of abandonment, vegetation C densities in 9-year sites were 7.6 Mg C ha^{-1}. After four decades of abandonment, this value was 90.1 Mg C ha^{-1} (Table 3.6). Positive linear correlation between vegetation C and stand age was evident ($r = 0.95$; $P < 0.05$) (Fig. 3.8). Mean values of soil C ranged from 58.8 to 113.7 Mg C ha^{-1} but no trend of soil C was found over the time sequence.

Table 3.6 Means and standard deviations (in parentheses) values for vegetation, soil, and ecosystem C in abandoned croplands.

Site name	**Stand age**	**Carbon density to 45 cm depth**		
		Vegetation C	Soil C	Ecosystem C
	Year		*Mg C ha^{-1}*	
BSN-9	9	7.6 (6.0)	66.6 (13.0)	74.2 (15.0)
RED-10	10	16.6 (6.2)	113.7 (39.0)	130.3 (40.9)
RET-15	15	28.4 (12.13)	96.5 (29.4)	124.8 (33.3)
BSL-24	24	42.7 (39.4)	60.8 (11.5)	103.5 (38.2)
BSE-27	27	80.2 (35.8)	58.8 (12.5)	137.6 (33.0)
WLA-41	41	90.1 (72.7)	-[$$] -	- -

[$$] Cancelled soil sampling due to soil disturbance before the soils could be sampled.

Mean values of ecosystem C distribution in abandoned croplands ranged from 74.2 to 137.6 Mg C ha^{-1} (Table 3.6). It illustrates that mean values of ecosystem C changed with the mean values

of vegetation C, while soil C was almost consistent across time sequences. These results also indicate that vegetation C was the main source of contribution of ecosystem C under the natural succession of abandoned croplands.

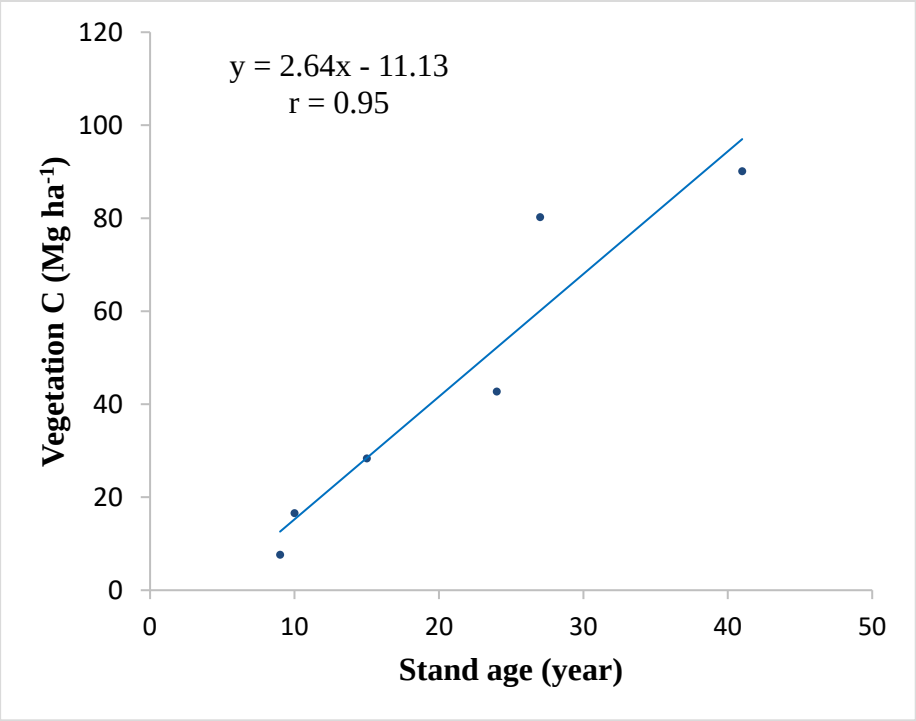

Fig. 3.8 Relationship between vegetation C (Mg C ha^{-1}) and stand age (year).

3.6. Discussion

Abandoned croplands in this study are characterized by thick Ap horizon (> 10 cm), low bulk density, and are predominantly loam textured Chernozemic soils. Mean concentration of SOC_{FM} is 62.0 Mg C ha^{-1} although it differs significantly between north and south sites. SOC density across the sites ranged from 44.2 to 86.9 Mg C ha^{-1} which is comparable to research outcomes in the same Ecozone and soil types where Pennock et al. (1994) reported C density ranged from 53 to 113 Mg C ha^{-1} to the same sample depth.

Differences in SOC levels could not be detected using a chronosequence approach. The overall difference in SOC between the north and south sites limited the utility of a combined chronosequence approach, and hence differences between paired sites was used to detect accumulation rate. In the first 15 cm depth the mean value of SOC density in abandoned cropland was 45.49 Mg C ha^{-1}.

The pair-comparison of abandoned and adjacent cultivated sites revealed a slight increase of SOC at the first sample depth (0 - 15 cm). However, large differences between soil C stock in the north and the south sites confounded the assessment of differences due to time since cropland abandonment. Our average accumulated rate of SOC after three decades of abandonment (0.35 Mg C ha^{-1} yr^{-1}) in Saskatchewan is higher than that in other studies but within the variability. In southern Ontario, Canada, Foote and Grogan (2010) estimated the SOC accumulation rates to be 0.08, 0.10, and 0.11 Mg C ha^{-1} yr^{-1} on Podzol, Brunisol, and Luvisol, respectively. The reported values by Foote and Grogan (2010) is in class with the SOC accumulation rate found in abandoned croplands of Minnesota sand soil (0.19 Mg C ha^{-1} yr^{-1}) reported by Johannes and Tilman (2000).

The dominant tree species in abandoned sites is trembling aspen (*P. tremuloides*). Total vegetative biomass could reach 180.2 Mg ha^{-1} after 41 years of abandonment. Total AGB was contributed mainly from litter and living trees. However, a linear relationship existed between stand age and living tree biomass only. Although herb, detritus, shrub, and litter biomass increased with stand age, a significant linear relation between them and stand age did not occur. However, total biomass, tree volume and vegetation C positively correlated with stand age. Ecosystem C reaches 137.6 Mg C ha^{-1} after four decades of abandonment, which is slightly lower than that in mature forest stands in the same ecozone (158 Mg C ha^{-1}) reported by Fitzsimmons et al. (2004).

For litter biomass, the mean values ranged from 4.6 to 19.8 Mg ha^{-1} for our study area. This is higher than the values reported by Zhang et al. (2008), which ranged from 3.2 to 16 Mg ha^{-1} for 0 to 25-year stands of predominately jack pine in the same ecozone. This might be attributed to the dissimilarities in litter properties, disturbance history, and associated decomposer community (Hilli et al., 2010; Laganiere et al., 2010). However, our range of values fell below the value on mature aspen stands in the Prince Albert National Park which was 31.76 Mg ha^{-1} (Gower et al., 1997).

The finding of AGB (6.2 – 127.2 Mg C ha^{-1}) in this study is comparable to 33.9 Mg ha^{-1} on poor sites of 15-year trembling aspen stands in British Colombia, Canada (Wang et al., 1995) and to the mean AGB in western Canadian aspen forest of 131 Mg C ha^{-1} (Hogg et al., 2005).

Mean values of vegetation C for 27- and 41-year stands found in this study were 80.2 and 90.1Mg C ha^{-1}, respectively. Those values are comparable to 60 Mg C ha^{-1} reported in Fitzsimmons et al. (2004) on forest stands (with DBH > 10 cm and without C from coarse roots). The lowest ecosystem C in the 9-year site (74 Mg C ha^{-1}) was approximately equal to ecosystem C in pasture (63 Mg C ha^{-1}) reported in the previous study in the same ecozone (Fitzsimmons et al., 2004). Moreover, our mean vegetation C value is comparable to the finding of Gower et al. (1997), who reported vegetation and detritus C in trembling aspen stand of 122.45 Mg C ha^{-1}.

Tree volumes ranged from 2.08 in the 9-year site to 117.9 m^3 ha^{-1} in the 27-year site. This range of values was within the 12 to 290 m^3 ha^{-1} for 40 year-stands reported by Nunifu (2009). Correspondingly, tree age, component, and density were found to be the main contributing factors to tree volume.

The chronosequence approach is a powerful tool for studying soil development and pedological investigation (Huggett, 1998). The approach has been used frequently for ecosystem C stock and change in abandoned croplands (Hooker and Compton, 2003; Howard and Lee, 2002; Johannes and Tilman, 2000; Johnston et al., 1996). In this study, the assumption of holding all soil-forming factors constant except time might be violated. The relationship between SOC stock and time since abandonment was not significant. Under cropland abandonment, SOC concentration may increase only at a certain depth (i.e. 0 - 15 cm) and was not evident in a complete pedon evaluation.

3.7. Conclusion

The abandoned cropland on Chernozemic soil in the Boreal Ecozone led to net sequestration of 90.1 Mg C ha^{-1} from vegetation C after four decades of regeneration. All biomass pools contributed to the increase of total biomass over the four decades of abandonment. However, aboveground biomass (+2.8 Mg C ha^{-1} yr^{-1}), especially tree biomass (1.9 Mg C ha^{-1} yr^{-1}), was the main C sink. The other proportions of C from herb, litter, shrub, detritus, and dead stand also contributed to vegetation C, but no significant trends were observed.

Under natural regeneration, such as trembling aspen regrowth, abandoned cropland could be a C sink in a shallow soil layer (i.e. < 15 cm). In the first decade of re-vegetation, mineral soil C was the main C sink accounting for 88.9% of ecosystem C. In the next three decades of abandonment, soil C proportion decreased (accounting for 41.27%) and was associated with a relative increase in vegetation C (accounting for 58.73%). Nevertheless, our study was challenged in finding abandoned fields for sampling. It also means that abandoned cropland in the research area is not dominant; and more work is needed for SOC accumulation rate under abandoned cropland.

Although the number of sample sites might limit the results of this study, this is the first estimate of ecosystem C in abandoned croplands for the Boreal Ecozone. This study could be an important component for broader estimations of C dynamics in comparable locations. The measurements of C from almost all C pools combined with related data (such as LAI) from abandoned lands can create a good field data source for biomass estimation at a broader scale. Hence, the next step in this study was to map abandoned cropland at a broader scale and to estimate time since abandonment using time-series remotely sensed data. Field measurements of almost all C pools served as initial field parameters for modelling (i.e. CBM-CFS) of C stocks and changes.

4. LAND-USE CHANGE AND ASSOCIATED CHANGES IN CARBON STORAGE IN THE AGRICULTURE-FOREST TRANSITION REGION OF THE BOREAL PLAINS ECOZONE, WESTERN CANADA

4.1. Preface

In Chapter 3, we saw that abandoned cropland on Chernozemic soils in the Boreal Plains Ecozone led to C accumulation in soil and vegetation. Therefore, it is important to include the land conversion in carbon budget modelling under LUCCs in an agricultural landscape. Abandoned cropland detected in Chapter 3 occurred at the field scale and is potentially linked to soil properties. Nevertheless, the associations between LUCCs and soil characteristics, such as soil texture, chemistry, drainage, and soil order, have not been evaluated. If such associations exist, this could be valuable information for estimating the likely area of change in the future. While Chapter 3 identified the potential of carbon sequestration in abandoned cropland in Saskatchewan, the main aim of this chapter is to quantify ecosystem carbon and characterize LUCCs and its associations with soil attributes in an agricultural landscape of the Boreal Plains Ecozone (BPE) in western Canada.

4.2. Abstract

Scientific interpretations of land-use and cover change and ecosystem C density are important for international reporting and management activities by governments. This study analyzes the land-use and cover change (LUCC), links between LUCC and soil characteristics, and estimates ecosystem C balance in the agricultural area of the BPE during the 1990 – 2000 period. The study results show that there was limited change in land-use with an integral change to approximately 6.5% of the total area. Of the two dominant conversions, forest to cropland was characterized by farm expansion on well-drained Chernozemic and Luvisolic soil orders; while cropland to abandoned cropland was associated with poorly drained and acidic parent materials. The simulation model estimated a net C sink of 0.76 ±0.3 Mg C ha^{-1} yr^{-1} for the agricultural region of the BPE during the research period.

4.3. Introduction

It has been well-documented that anthropogenic greenhouse gas (GHG) emissions can significantly contribute to global warming and climate change (Chase et al., 2000; Houghton, 1999a; IPCC, 2007b; Zwiers, 2002). Land-use change is one type of human activity that is causing change in both regional and global climates (Beringer et al., 2005; Claussen et al., 2001; Foley et al., 2003). Despite improvements in the quantification of cover changes for the boreal forest (Apps et al., 1993; Banfield et al., 2002; Bélanger and Pinno, 2008), only a few studies have examined land–use and cover change (LUCC) in the agricultural area of the BPE and the subsequent changes to C fluxes.

As part of Canada's commitment to the United Nations Framework Convention on Climate Change, AAFC conducted research to estimate C stock and changes in Canada`s agricultural region during 1990 and 2000 (Huffman et al., 2015). The results show an increase in perennial cover and estimated accumulated woody biomass of 16.8 Gg in the agricultural area of the BPE (Huffman et al., 2015). Overall, the GHG emission from Canada's cropland was estimated as a C sink in recent years (Environment Canada, 2013). This research investigates if more information can be extracted from the current data source by using new quantification and estimation approaches. Specifically, the goal is to determine if LUCC can be quantified based on total change, including losses and gains, in the area in each land category. The goal is to investigate at a larger spatial scale with more specific information. This research paper focuses on tracking the changes of land-use and cover with emphasis on size, shape, and relative location of land-use change to contribute to a better understanding of the possible causes of change in the BPE in Canada.

While many studies have focused on the effects of LUCC on soil characteristics (Pennock and van Kessel, 1997b; Six et al., 1998; van der Kamp et al., 1999) or other driving forces of LUCCs (Brown et al., 2005; Kuemmerle et al., 2009; Meyer and Turner, 1992; van Meijl et al., 2006), there has been little research to investigate soil characteristics as probable driving forces of land-use change in the BPE. Soil texture, chemical, drainage, and soil order characteristics are explored in this paper to determine if they are associated with specific land-use conversions including deforestation for cultivation and cropland abandonment.

Huffman et al. (2015) estimated overall C stock and change for the agricultural area of Canada by providing woody volume results for each ecozone, and linear growing rates. This paper explores the idea of combining root and soil C pools to contribute to greater certainty in these estimates. While modelling is a well-known approach to simulate the effects of LUCCs to C stock and its dynamics (Chiesi et al., 2005; Pueyo and Begueria, 2007), it has not been applied for C stock and dynamics in the agriculture area of the BPE. In this study, the CBM-CFS3 was used to simulate the dynamics of carbon in aboveground, belowground, litter, dead wood, and soil organic matter. CBM-CFS was developed under IPCC guidelines and has been officially applied to stimulate the dynamics of all Canadian forest C stocks required under the Kyoto Protocol (Kurz et al., 2009).

The focus throughout this study was to assess the C changes in the cultivated area of the BPE that contributed to the national C balance during 1990 - 2000. The specific objectives of the research were to (1) quantify LUCCs in the agricultural area of the Boreal Plains Ecozone, (2) explore any potential association between LUCCs and soil characteristics, and (3) simulate C stock and dynamics over a period of 15 years.

4.4. Materials and Methods

4.4.1. Study area

The research area was located in the BPE, one of the fifteen terrestrial ecozones in Canada, which covers parts of the three Prairies Provinces (Alberta, Saskatchewan, and Manitoba), Fig. 4.1. The BPE covers an area of 66.87 million ha, accounting for approximately 6.5% of the total area of Canada and the agricultural area accounts for approximately 20% or 13.37 million ha of the BPE (Huffman et al., 2006; Huffman et al., 2015; Statistics Canada, 2008). Cropland occupies less than 10 % of the boreal plains (Smith et al., 1998b).

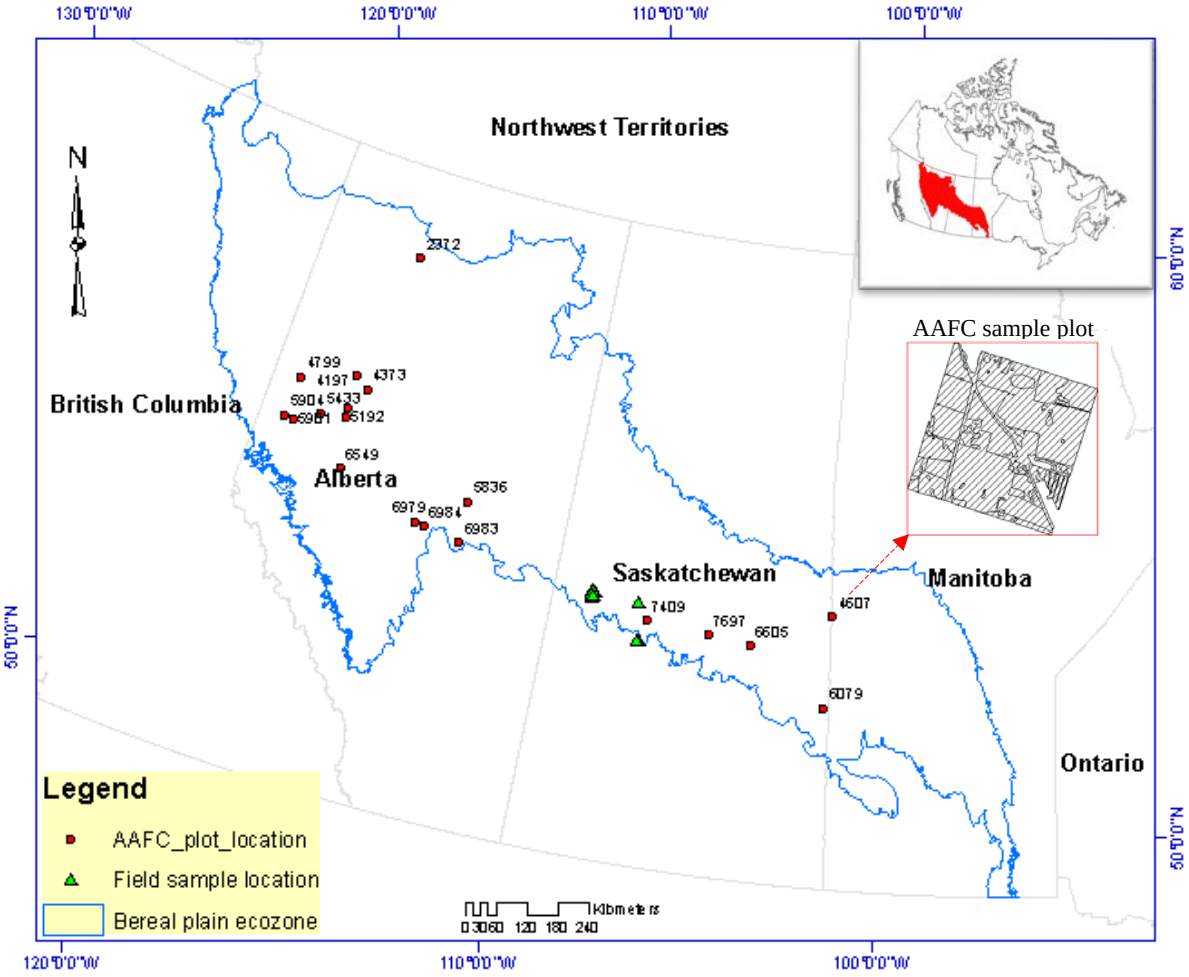

Fig. 4.1 Sample locations from AAFC (in red circle) and field data (green triangle) in the Boreal Plains Ecozone, Canada.

The main deciduous tree species in the area are trembling aspen (*P. tremuloides*), balsam poplar (*P. balsamifera*), and white birch (*B. papyrifera*) with white spruce (*P. glauca*), jack pine (*P. banksiana*), and tamarack (*L. laricina*) being the main coniferous species. Brunisols and Luvisols are the dominant soil orders although Dark Grey and Black Chernozems are present in the south.

Data collection and overall assumptions for the study LUCC data was extracted from AAFC data sources, and SOC data was compiled from the National Soil Database (NSDB). Age-yield assumptions were gathered from published data and field measurements.

The AAFC land-cover database contains 14 sample plots; one located in Manitoba (2 x 2 km), two in Saskatchewan (1 x 1 km) and 11 in Alberta (2 x 2 km). In each plot, land-use and land cover were sketched based on aerial photos to form series of polygons.

For the whole research region, the sample plots consisted of 1534 polygons with associated information on land-use (in attributes) over a total sample area of 6174.25 ha. This database was part of a larger study on estimation of C stock and change from woody biomass for Canada's cropland. In this study, random samples at the intersection points of the National Forest Inventory (NFI) were located and then paired with aerial photos of each location taken from the National Air Photo Library (NAPL). LUCCs during 1990 – 2000 were quantified using paired aerial photos and change detection on each plot (photo-plot) (Huffman et al., 2015).

LUCCs of the 1534 polygons were categorized into 13 groups (Table 4.1). In this table, forest cover is comprised of tree area greater than 1 ha and at least 25% crown closure. Tree cover is the area with trees that does not meet the forest criteria. Shrub cover is defined as a small woody plant area that would not be expected to meet the forest definition when mature (Huffman et al., 2015).

Table 4.1 Distribution and net change of land-use and covers during 1990 – 2000.

Land covers	1990		2000		Absolute net change
	ha	*%*	*ha*	*%*	*ha*
A.C[†]	131.46	2.13	171.29	2.77	39.83
Barren	17.85	0.29	17.85	0.29	0.00
Cropland	3891.61	63.03	3759.88	60.90	-131.73
Forest	1144.19	18.53	1162.44	18.83	18.25
Peat	0.00	0.00	0.65	0.01	0.65
Plantation	2.03	0.03	2.03	0.03	0.00
Settlement	225.05	3.65	248.44	4.02	23.39
Shrubs	52.00	0.84	50.39	0.82	-1.61
Trees	92.58	1.50	96.72	1.57	4.14
U.P[¶]	20.57	0.33	59.36	0.96	38.78
Unknown	0.00	0.00	23.08	0.37	23.08
Water	54.28	0.88	43.78	0.71	-10.50
Wetlands	542.62	8.79	538.34	8.72	-4.28
Total area	**6174.25**				

[†] Abandoned cropland; [¶] Unimproved pasture; Barren land, in this study, is defined as the soil exposed area with very low vegetation cover in agriculture region such as trail/pathway with pavement or gravel surfaces.

Soil attribute data was extracted for the 6174.25 ha from the National Soil Database (NSDB). The soil data packages consist of a map in shape format with a scale of 1:100,000 and soil attribute files, which include soil name, soil component, and proportion. The files are available online and free to access at http://sis.agr.gc.ca/cansis/nsdb/dss/v3/index.html. In NSDB data, each polygon is associated with more than one soil component (one to four components). It means NSDB is not spatially explicit. However, the highest area proportion (%) is in component 1 in all cases. Component 1 with the associated soil characteristics was used to join to the designated polygon for further data analysis. We assumed that soil characteristics in component 1 represent the characteristics of the whole polygon. Soil characteristics such as drainage, soil order, parent material texture, parent material chemical properties of each land parcel were extracted using GIS techniques such as attribute joining (map layer and soil component), map overlaying (soil map

layer and land-use layer). The further analyses were then conducted on parcel based data. Soil characteristics and area proportion (%) of the 14 sample plots are presented in Table 4.2.

Luvisolic and Chernozemic were the dominant soil orders in the sample plots, accounting for approximately 75% of the total area. For parent material texture, the three highest proportions found within the area were very fine, moderately fine, and fine texture. Well-drained and moderate well-drained areas accounted for greater than 70% of the entire area. The dominant chemistry of the parent material in the research plots was associated mainly with calcareous sediments, accounting for 90% of the total area.

Table 4.2 Soil characteristics of the 14 sample plots and area proportion in percentage.

Soil characteristics	Area proportion	Soil characteristics	Area proportion
	%		%
Soil Order		**Parent Material Texture**	
Brunisolic	5.89	Fine	28.54
Chernozemic	30.26	Medium	9.21
Gleysolic	7.85	Moderately Coarse	3.72
Luvisolic	44.45	Mesic (Organic)	6.60
Organic	6.60	Moderately Fine	14.74
Regosolic	4.17	Undifferentiated	1.87
Solonetzic	0.48	Very Coarse	5.89
Not applicable	0.31	Very Fine	29.12
		Not applicable	0.31
Drainage		**Parent Material Chemical**	
Imperfect	9.98	Medium Acid to Neutral	7.37
Moderately well	40.70		
Poor	6.02	Undifferentiated	1.87
Rapid	5.89	Moderately / Very Strongly Calcareous	41.92
Very poor	7.04		
Well-drained	30.07	Weakly Calcareous	48.17
Not applicable	0.31	Not applicable	0.67

The estimation of merchantable tree volume (age-yield curve) or mean annual increment (MAI) of woody biomass for different land covers was compiled using field and published data sources. For forest cover, the MAI value for the dominant Aspen-Spruce mixed-wood cover in the BPE (adapted from Kabzems et al. (1986)) was 3.28 m^3 ha^{-1} on well to imperfectly drained soils with soil texture from fine (clay) to coarse (loams). The age-yield assumption values of abandoned cropland, tree, and shrub were estimated from field measurements in 2012 at Bright Sand Lake, Saskatchewan. Tree height, DBH, stand age, and tree species were recorded. Biomass in different C pools was calculated and converted into merchantable volume. The estimation of MAI rate of abandoned cropland was 2.137 m^3 ha^{-1} $year^{-1}$, which corresponded with an estimated value (2.14 m^3 ha^{-1} $year^{-1}$) reported by JWRL (2013). For the MAI in trees, the current estimation of 1.75 m^3 ha^{-1} $year^{-1}$ was reported for stand age greater than 50 (JWRL, 2013). The estimated MAI value was 1.21 m^3 ha^{-1} $year^{-1}$ for stand age less than 50 years. Hence, MAI for trees was assumed differently for the two age groups using associated MAI values. It was assumed that MAI of shrub cover was 0.086 m^3 ha^{-1} $year^{-1}$. Assumptions of MAI in unimproved pasture and cropland were zero (i.e. yearly woody biomass gain and loss are equal). The assumption values used in this research are presented in Table 4.3.

In summary, input data included land cover, soil properties, and estimations of MAI of gross merchantable tree volume. LUCCs data during 1990 – 2000 were interpreted and mapped from the archived aerial photography in a plot size of 1x1 km or 2x2 km. Soil data in associated locations was extracted from the National Soil Database. Assumptions of yield volume as a function of time (year) were constructed from field and published data, for the boreal plains ecozone.

Table 4.3 Assumption of merchantable volume and mean annual increment (MAI) values of the different land covers.

Land covers	Number of plots	Stand age	Volume	Δ volume	Reference
		Year	m^3	$m^3\ ha^{-1}\ y^{-1}$	
Forest	16	60	196.80	3.280	1
Trees	16	60	81.25	1.610	2,3
Abandoned cropland	5	50	51.00	2.137	3
Shrub	4	30	7.35	0.086	3

1: Kabzems et al. (1986)
2: JWRL (2013)
3: Current study

4.4.2. Data analysis

Three different data analysis approaches were applied to achieve the research objectives. Cross-tabulation matrix was applied to quantify LUCCs and the characteristics based on the aerial photo change detection results. Cross tabulation (Chi-square test, χ^2) was used to examine the relationships between soil characteristics and types of cover change. Estimation of C stock and dynamics was conducted using the CBM-CFS3 model.

4.4.2.1. *Quantification and characteristics of LUCCs*

A general cross-tabulation matrix, adapted from Pontius et al. (2004), was utilized to present the magnitude of change and cover pattern between two points in time. In the cross-tabulation matrix, the rows represent land-cover categories in time-1 and the columns represent land-cover categories in time-2. Diagonal entries denote the persistence of a category. The other entries (off-diagonal) are the transitions among the land categories. Total area of a category in time-1 and time-2 is the sum of row and column, respectively. Lost area in a category is calculated by subtracting the persistence area from total area of the category in time-1 (row). Gained area in a category is calculated by subtracting the persistence area from total area in the same category in time-2 (column). Net change is the difference between loss and gain.

Although a cross-tabulation matrix is useful to present net change, it could not fully reflect the magnitude of change. A loss in a category could be compensated by a gain (in the same area)

in other locations, resulting in term swap, or a zero net change in the category. Swap is defined as two times the minimum of gain and loss (Pontius et al., 2004).

For the main cover categories, assessment of change was conducted to characterize and generalize some possible causes of change. For each plot, magnitude of change, change in area, change in shape, and relative location to field border of changed features was assessed using change detection techniques offered by ArcMap and by direct observation technique of pair-aerial photos. These observations were used to suggest the most likely causes of land-use change.

4.4.2.2. *LUCCs and soil characteristics*

Pertinent data from the AAFC's National Soil Database (NSDB) and LUCC database from 1990 – 2000 were collected and categorized. Parent material texture and chemical characteristics, as well as drainage and soil order data, were extracted and re-grouped. Soil texture was grouped into coarse, fine, and organic. Parent material chemical characteristics include acidic and calcareous classes. Soil drainage data consists of poorly drained and well-drained characteristics. No change was made to soil order. To examine the relationship between soil characteristics and LUCC, conversion types of forest to cropland (F2C), cropland to abandonment (C2A), and abandonment to cropland (A2C) and their associated soil attributes were extracted. In order to compare the distribution of each land category (e.g. Forest to forest vs. forest to cropland), cropland to cropland (C2C) and forest to forest (F2F) were also included. The chi-square test was used to examine associations of the land covers to the soil characteristics. In this study, we assumed that the area proportion of each land use category is equal to that of the occurrences. Since the polygons are small, they are treated as pixels for statistical analysis. Hence, the occurrences of the land use types were used rather than the area. The association between variables was tested using Pearson Chi-square test ($\chi 2$).

4.4.2.3. *Carbon stock simulation using CBM-CFS3 model*

Carbon stock and dynamics on the main LUCCs (non-forest cover) in the BPE were simulated using the CBM-CFS3 model. All software and research protocols were adapted from AAFC and the Canadian Forest Service (CFS). LUCCs were extracted from AAFC data for the simulation. Some records that could not interpret the associated land cover from aerial photos were grouped into unknown. Orchards and vineyards were included as C stock biomass and included in

the previous estimation (Huffman et al., 2015); however, those covers were not observed in the BPE. Our simulation did not account for C stock and dynamics of permanent forest cover, but rather included forest disturbances for cultivation. Despite the assumption that C accumulation in cropland and unimproved pasture was zero, these land covers were counted as they form part of the land-cover change in the agricultural region. As a result, three land-use and cover categories were established for simulation including abandoned cropland, shrub, tree and three associated transition covers namely forest, cropland, and unimproved pasture. Details on the area of each land category and its transition are presented in Table 4.4. Accordingly, the input data for simulation include six land-use and covers in a total area of 526.84 ha which accounts for 8.57% of total sample area.

Table 4.4 Transitions and associated area used for C balance estimation.

Land-use and cover	**A.C.**[†]	**Cropland**	**Forest**	**Shrubs**	**Trees**	**U.P.**[¶]	**Grand Total T1**
				ha			
A.C.	103.25	20.94	3.07		1.13		**128.40**
Cropland	63.56		85.60		1.95	38.37	**189.47**
Forest	0.00	34.25			8.69	4.02	**46.96**
Shrubs		0.76		50.39		0.15	**51.31**
Trees		4.88	1.18		83.16	1.17	**90.39**
U.P.	4.49	0.30	0.35		0.27	14.91	**20.31**
Grand Total T2	**171.29**	**61.13**	**90.20**	**50.39**	**95.20**	**58.62**	**526.84**

[†] Abandoned cropland; [¶] Unimproved pasture

In accordance with land-use and conversion data, some assumptions were compiled for stand age, event, historic disturbance, land class, previous disturbance, mask, non-forest cover, species, and age-yield (or MAI). Standing or inventory age was assumed to be age assigned by AAFC for different covers plus time step; where 0, 20, 60 were assigned for covers converted from cropland, abandoned cropland, and shrub/tree/forest, respectively, and time step was the random

number between time-2 (T2) minus time-1 (T2) plus 1 (random[T1 – (T2+1)]). Simulation time of 15 years, 1985 – 1999, was assumed. The tree species of unspecific hardwood were assumed for abandoned cropland and shrub, while trembling aspen was assumed for both tree and forest covers. Cropland and pasture were assumed for non-forest cover with the Dark Brown Chernozemic soil order. Default model assumptions were used for the remaining parameters.

The next step in data analysis was C simulation using the CBM-CFS3 model. Introduced by the Canadian Forest Service - Natural Resources Canada, this aspatial model allows estimate C stock and dynamics in five C pools based on both periodic measurements and annual merchantable volume increment (Kurz et al., 2009). Although the model was originally constructed for C accounting of forest ecosystems, the current version (CBM-CFS3) has the capacity to simulate C stock and changes in different land-use and disturbances. The conceptual design of the model involves the simulation of C entering into an ecosystem (vegetation growth) and the resulting C turnover or disturbances (decay and transfer). In this study, we replicated an approach introduced under a collaborative study between AAFC and CFS, which was aimed at estimation of C dynamics, and emissions and removals on agricultural woody land transitions.

The Recliner Tool is an open-source code module that creates the properly defined template input databases required for CBM-CFS3 simulation. Data Analysis was initiated by executing the Recliner Tool using the described input data and assumption files. From LUCCs and assumption input files, new database template files, as defined and required by CBM-CFS3 (*.mdb), were generated for each plot through a lookup table process. These new input data files were then input into the CBM-CFS3 simulation process. From a yield table, (merchantable production volume by a class for each species), equations were applied to each stand-level to convert merchantable into AGB (Boudewyn et al., 2007), BGB (Li et al., 2003b), as well as the other carbon pools (Kurz et al., 2009).

The outcomes of the model include annual estimation of C stocks and stock changes as well as their transfer inside and outside of the ecosystem. Carbon stock and change in the main pools were summarized and reported as AGB, BGB, soil organic matter, dead wood, and litter. As input data was in a number of data sets, the C changes in ecological system indicators of Net Primary Productivity (NPP), Heterotrophic Respiration (Rh), and Net Ecosystem Productivity

(NEP) were calculated based on the sum of estimated results from each record as follows (Kurz and Apps, 1999; Li et al., 2003b) as:

$$\mathbf{NPP} = \sum_{i=1}^{n} \boldsymbol{\eta_i} * (\boldsymbol{G_{t,i}} + \boldsymbol{L_{t,i}}) \quad \text{(Eq. 4.1)}$$

Where: NPP is Net Primary Production
η_i is area fraction associated with recode i
$G_{t,i}$ and $L_{t,i}$ are biomass increment and detrital input, respectively.

$$\mathbf{Rh} = \sum_{i=1}^{n} \boldsymbol{\eta_i} * \boldsymbol{Rh_{t,i}} \quad \text{(Eq. 4.2)}$$

Where: Rh is heterotrophic respiration
ηi is area fraction associated with recode i
Rht,i is heterotrophic respiration of recode i at time t

$$\mathbf{NEP = NPP - Rh} \quad \text{(Eq. 4.3)}$$

Where: NEP is Net Ecosystem Productivity

Among the reported values, positive values denote net ecosystem C uptake. Although uncertainty from input data (including soil and yield curves) may affect simulation results, the uncertainties of the land-use and cover in CBM-CFS3 model have been assessed and validated (Huffman et al., 2015; Kurz et al., 1996). Therefore, an uncertainty assessment was not included in this study.

In summary, the data analysis involves LUCCs quantification, the association between LUCCs and soil association using Chi-square test, and CBM-CFS3 simulation for C balance estimation. General procedure of data analysis is depicted in Fig. 4.2.

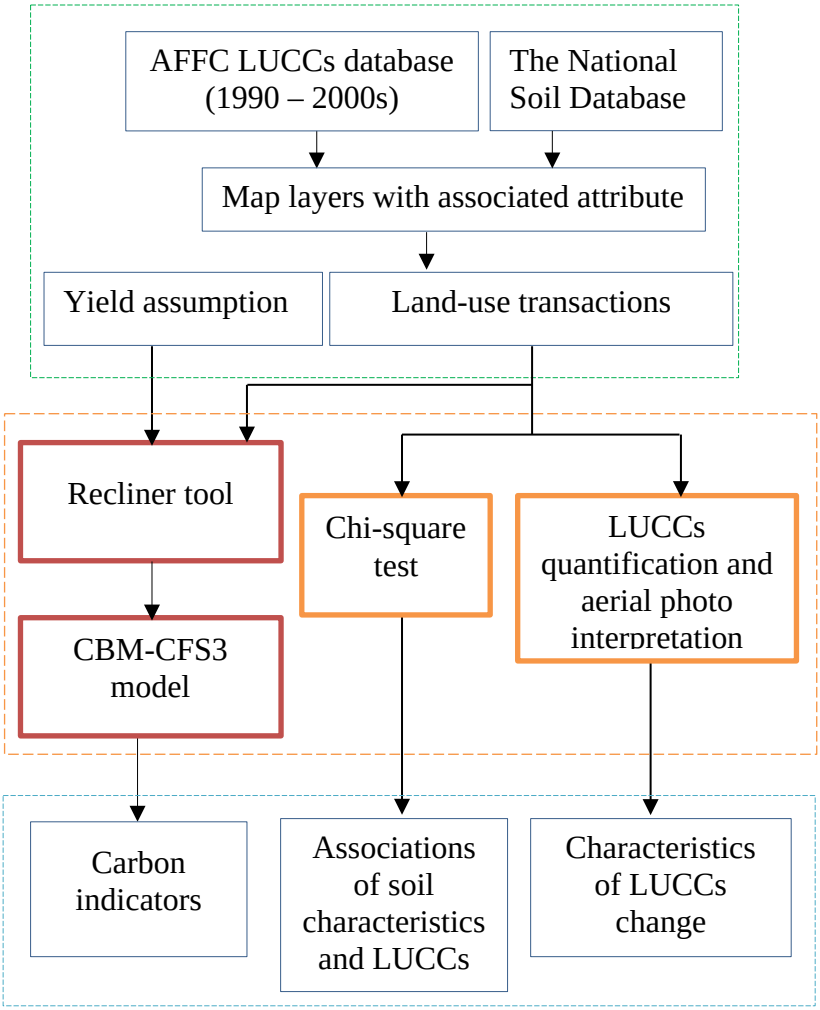

Fig. 4.2 Data analysis framework with input data (green dotted box), analysis methods (orange dotted box), and the expected outcomes (blue dotted box).

4.5. Results

4.5.1. Land-use and cover change during 1990 – 2000

The transitions among the land categories during 1990 – 2000 in the agriculture region of the BPE are presented in a cross-tabulation matrix (Table 4.5). In the matrix table, integral area in 1990 and 2000 are presented as Total T1 and Total T2, respectively. The diagonal entries show persistent area, while the off-diagonal entries are the conversion area between the land categories. In a total area of 6174.26 ha, cropland and forest were the dominant land covers in 1990, accounting for approximately 80%. After 10 years of conversion, cropland experienced the highest

conversions with cropland decreasing from 63.03% during 1990 to 60.9% in 2000. Area reduction in cropland was the consequence of cropland abandonment, forest expansion, settlement growth, and expansion of wetlands. The proportion of forest cover increased slightly from 18.53% to 18.83% during the research period. Slight gains also occurred to abandoned cropland, yielding an addition of about 40 ha after 10 years. Similarly, tree, and shrub covers experienced small changes between the two periods. No transition was recorded in barren, plantation, and shrub cover.

Table 4.5 Land-use and covers in the sample plots in time 1 (1990, T1) and time 2 (2000, T2).

Land-use and covers	A.C†	Barren	Cropland	Forest	Quarries	Plantations	Settlement	Shrubs	Trees	U.P¶	Unknown	Water	Wetlands	Total T1
						ha								
A.C†	103.25		20.94	3.07			3.06		1.13					**131.46**
Barren		17.85												**17.85**
Cropland	63.56		3657.81	87.01	0.65		21.28		1.95	38.37	0.63	4.99	15.35	**3891.61**
Forest			34.25	1069.95			1.90		8.69	4.02	21.84	1.32	2.22	**1144.19**
Plantations						2.03								**2.03**
Settlement			6.41	0.88			217.03			0.74				**225.05**
Shrubs			0.76				0.70	50.39		0.15				**52.00**
Trees			4.88	1.18			1.42		83.30	1.17			0.63	**92.58**
U.P¶	4.49		0.30	0.35			0.26		0.27	14.91				**20.57**
Water			16.73						0.09			37.47		**54.28**
Wetlands			17.79				2.80		1.28		0.61		520.14	**542.62**
Total T2	**171.29**	**17.85**	**3759.88**	**1162.44**	**0.65**	**2.03**	**248.44**	**50.39**	**96.72**	**59.36**	**23.08**	**43.78**	**538.34**	**6174.26**

† Abandoned cropland; ¶ Unimproved pasture

During the research period, the net change in land-use and cover was slight with the persistent area accounting for approximately 93.52 % of the landscape. However, the absolute changes shown in Table 4.5 may not reflect the magnitude of changes. In order to highlight the possible magnitude of disturbances that took place in each land category, a quantification approach was used which accounts for persistence and total change areas (Pontius et al., 2004).

Table 4.6 Area distribution and land-cover changes in the Boreal Plain Ecosystem during 1990 – 2000.

Land-use and covers	Gain	Loss	Total change	Swap	Absolute value of net change
			%		
A.C[†]	0.46	1.10	1.56	0.91	0.65
Barren	0.00	0.00	0.00	0.00	0.00
Cropland	3.79	1.65	5.44	3.31	2.13
Forest	1.20	1.50	2.70	2.40	0.30
Peat	0.00	0.01	0.01	0.00	0.01
Plantations	0.00	0.00	0.00	0.00	0.00
Settlement	0.13	0.51	0.64	0.26	0.38
Shrubs	0.03	0.00	0.03	0.00	0.03
Trees	0.15	0.22	0.37	0.30	0.07
U.P[¶]	0.09	0.72	0.81	0.18	0.63
Unknown	0.00	0.37	0.37	0.00	0.37
Water	0.27	0.10	0.37	0.20	0.17
Wetlands	0.36	0.29	0.66	0.59	0.07
Total	**6.48**	**6.48**			

[†] Abandoned cropland; [¶] Unimproved pasture

Table 4.6 shows the transition proportion of each land category for the research period relative to the total area (6174.25 ha). Land-use and cover transitions in the research area were small, accounting for 6.48% of the entire sample area. Changes in cropland cover contributed 5.44% to the total area and was the highest change among land categories. Swap area in cropland accounted for 3.31% and yielded an absolute net change value of 2.13% of the total area. Higher forest cover loss (1.5%) than gain (1.2%) was observed, leading to a total change of 2.7% of the

total area. Additionally, a high proportion in the swap area category indicates that the large loss of area was compensated by gain in other areas. Absolute net change of 0.3% of the total area clearly underestimates the disturbance that occurred during the research period. Similarly, abandoned cropland also experienced changes accounting for 1.56% of the total area. Swap percentage was high (0.9%) compared to the total change portion. Changes in the remaining land covers were slight, less than 1% total area. There was no change on wet land, plantation, and barren covers.

In conclusion, LUCCs in the agriculture area of the BPE experienced only slight change during 1990 – 2000. Changes occurred in almost all land covers but the survey recorded dominant changes in cropland, forest, and abandoned cropland with an increasing trend in the woody cover types.

4.5.2. Characteristics of cover change

Fig. 4.3 depicts the change detection approach using bi-temporal aerial photos. The land cover boundaries were delineated the current land-use based on aerial photos in 1988 (T1) and depicted in the yellow lines. The aerial photos in 2000 (T2) were then overlaid to delineate the polygons that experienced land-use change. An example of a land-use change site was depicted in Fig. 4.3 as in yellow polygon. It shows from this example that the size of change was relatively small compared to the entire field borders. Cropland to unimproved pasture (C2U) was the dominant conversion. The changes took place inside fields and adjacent to small water bodies suggesting that the conversions occurred mainly on lowland, where accessibility of farm machinery could be difficult. The same process was applied to 14 plots and the LUCC was recorded. The other five plots (AB6549, SK6079, AB4373, SK6605, AB5192) were unchanged. The characteristics of disturbed polygons are summarized in the Table 4.7.

In the entire time scale, land cover conversions were characterized by shape, size, and location (Table 4.7). Almost all changes were small in area, except for two large changes of forest to cropland (F2C) in AB2372 and AB6984 and cropland abandonment (C2A) in MB4607. Excluding one triangle-shaped change, all the major changes were of rectangular or irregular shaped forms, suggesting that change could be due to whole field conversion (rectangular) or field-edge modification (irregular). Cover change within the research area was also characterized by location in spatial relation to field border. Correspondingly, the proportion of whole field change

and edging change are roughly equal. Only one change took place in the center of a field (SK7409). Deforestation in the plots was associated with hedgerow or shelterbelt removal and forest to cropland conversion, which were located next to cropland area. Field merging and edging modifications were the major causes of hedgerow/shelterbelt harvesting. Abandoned croplands were found at field corners or adjacent to lowland wet areas. The overall inconvenience for farm machinery movement could be the main reason for cropland abandonment in the research area during 1990 – 2000. C2A and F2C conversions were the prominent conversions and while F2C conversion was affiliated with farm expansion, C2A conversion was difficult to understand based on the spatial pattern of conversion alone.

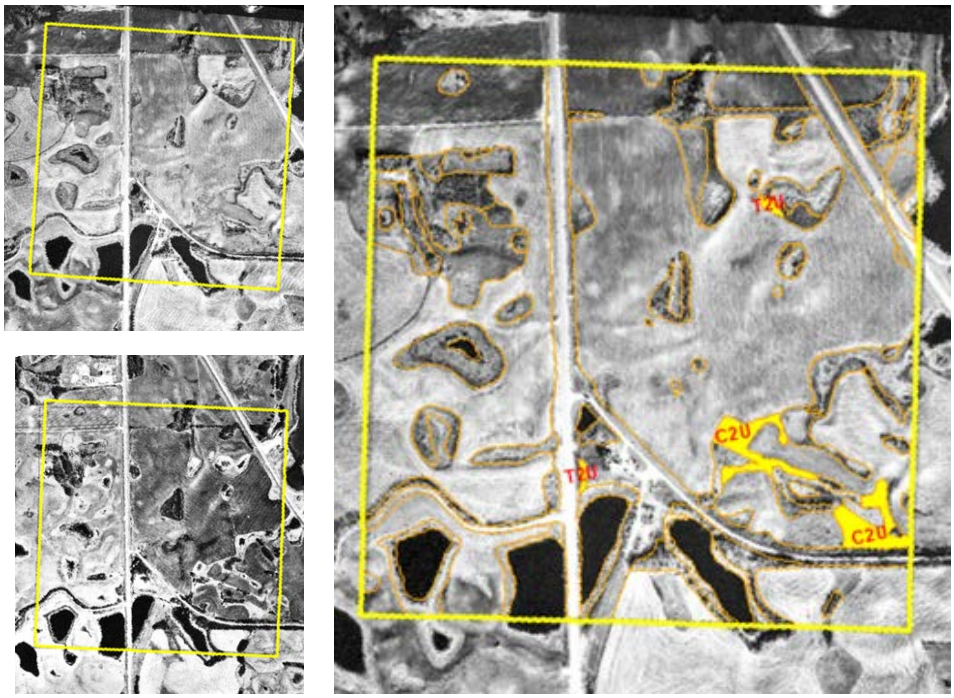

Fig. 4.3 An example of change detection and characteristics on the permanent sample plots using bi-temporal aerial photos for plot number 7409; aerial photo in 1988 (top left), 2000 (bottom left) and the changed polygons (in yellow).

Table 4.7 Characteristics of LUCC in the boreal plains ecozone; The major changes in each plot were coded with the associated change size, shape, and relative location.

Plot ID	Major change	Change size	Change shape	Location of change	Possible reasons for change
AB6979	A2C, F2C	S	I	E	Straighten field edges for efficient use of farm machinery
AB5904	U2C, T2U	M, S	R	W, E	Natural succession of pasture; farming expansion to adjacent areas or isolated polygons
AB5901	T2C	S	R	E	Deforestation of tree and hedgerows for field expansion
AB2372	F2C, F2T	L	R	W	Deforestation, shelterbelt removal for field expansion
AB5836	F2C	S	R	E	Field expansion
AB4197	C2A	M	T	E	Access of bigger machinery (farm with an airport)
AB4799	A2C	M. S	I	W, E	Hedgerow deforestation for field expansion
AB4976	F2C, T2C	M, S	R	W, E	Deforestation for field expansion
AB6983	C2A	M	R	W, E	Unknown
AB6984	F2C, C2U	L	R	W, E	Deforestation for field expansion
SK7697	U2T	S	R	W, E	Pasture abandoned; regeneration of tree at edging area along the farm hedgerow
SK7409	C2U	M, S	I	C	Lowland adjacent to wet area
AB5433	F2C, C2A	M, S	R	E	Expansion of cultivated area
MB4607	C2A, C2F	L, M, S	I	W	Unknown

L = Large (whole quarter section or more), M = Medium, S = Small, I = Irregular shape, R = rectangular like shape, T = Triangle like shape
W = Entire field, E = Edge of farm, C = Inside farm border; A2C = Abandonment to cropland, F2C = forest to cropland, U2C = unimproved pasture to cropland, T2U = tree to unimproved pasture, T2C = tree to cropland, F2T = forest to tree).

4.5.3. LUCCs and soil characteristics, 1990 - 2000

The association between LUCC and soil characteristics was examined for the main LUCC: forest to forest (F2F) and forest to cropland (F2C) and cropland to cropland (C2C) and cropland to abandonment (C2A).

The associations between changes of forest to forest (F2F) and forest to cropland (F2C), in regards to soil characteristics, are presented in Table 4.8. Conversion from forest to cropland (F2C) was more limited than persistence (F2F). A significant association was evident between F2C conversion and soil drainage and soil order. In relation to soil drainage, F2C conversion in well-drained sites (18.77%) was almost twice the occurrence in poorly drained sites (9.72%). In relation to soil order, no conversion of F2C was recorded in Brunisolic and Regosolic soil orders (0%). The distributions of F2C in Chernozemic, Gleysolic, and Luvisolic are 19.59%, 10.61%, and 19.56%, respectively. A small p-value in the chi-square test indicates that the distribution of F2C is not due to data variation (χ^2 (6, N = 469) = 21.46, P = 0.0015). In relation to parent material texture, the occurrence of F2C conversion found in both fine and coarse texture are about the same. Similarly, distribution of F2C is not significantly associated with parent material chemistry characteristics (χ^2 (1, N = 438) = 2.798, P = 0.0944). In summary, deforestation for cultivation during 1990 – 2000 in the BPE occurred dominantly on well-drained areas of Chernozemic and Luvisolic soil order.

Table 4.8 Distribution of forest remaining (F2F) and deforestation for cultivation (C2F) in different soil characteristics, 1990 - 2000.

Soil characteristics	Land-cover change		$\chi 2$	df	P-value
	F2F	F2C			
	%				
Parent material texture (N= 440)					
Coarse	83.08(54)	16.92(11)			
Fine	82.75(283)	17.25(59)	4.533	2	0.1037
Organic	96.97(32)	3.03(1)			
Drainage (N= 469)					
Well-drained	81.23(264)	18.77(61)	6.08	1	0.0137 *
Poorly drained	90.28(130)	9.72(14)			
Parent material chemistry (N= 438)					
Acid	100.00(14)	0.00(0)	2.798	1	0.0944
Calcareous	83.25(353)	16.75(71)			
Soil order (N= 469)					
Brunisolic	100.00(9)	0.00(0)			
Chernozemic	80.41(78)	19.59(19)			
Gleysolic	89.39(59)	10.61(7)			
Luvisolic	80.44(181)	19.56(44)	21.46	6	0.0015*
Organic	96.97(32)	3.03(1)			
Regosolic	100.00(30)	0.00(0)			
Solonetzic	55.56(5)	44.44(4)			

Note: Number in parentheses are the total number of conversions in each category;
* Significant at the 0.05 probability level; N is number of observation (polygon).

The area proportions associated with forest to cropland and forest to forest on different soil characteristics are presented in Table 4.9. The cover change categories were evident relative to soil drainage and parent material chemistry. Approximately double the number of occurrence of cropland abandonment (30.56%) occurred in poorly drained soil compared to well-drained (15.47%), suggesting that poorly drained soils are likely the significant driver of cropland abandonment. The relationship between soil drainage and cropland abandonment is significant at the 0.05 level. In relation to parent material chemistry, statistical results revealed a higher occurrence of abandoned cropland in acidic parent materials (50%) compared to that on calcareous

parent materials (19.57%) although the number in acidic parent materials encountered was quite low (n = 8).

Table 4.9 Distribution of cropland remaining (C2C) and cropland to abandonment (C2A) in different soil characteristics, 1990 - 2000.

Soil characteristics	Land-cover change		$\chi 2$	df	P-value
	C2C	C2A			
	%				
Parent material texture (N = 253)					
Coarse	80(24)	20(6)			
Fine	80.42(152)	19.58(37)	1.528	2	0.4657
Organic	68.42(13)	31.58(6)			
Drainage (N = 253)					
Well-drained	84.53(153)	15.47(28)	7.393	1	0.0065*
Poorly drained	69.44(50)	30.56(22)			
Parent material chemical (N = 253)					
Acid	50(4)	50(4)	4.38	1	0.0364*
Calcareous	80.43(185)	19.57(45)			
Soil order (N = 253)					
Brunisolic	100(2)	0(0)			
Chernozemic	86.25(69)	13.75(11)			
Gleysolic	65.63(21)	34.38(11)			
Luvisolic	82.18(83)	17.82(18)	10.094	6	0.1207
Organic	68.42(13)	31.58(6)			
Regosolic	6.4(12)	14.29(2)			
Solonetzic	60(3)	40(2)			

Note: Number in parentheses are the total number of conversions in each category;
* Significant at the 0.05 probability level; N is number of observation (polygon).

After abandonment, vegetation was established naturally in some fields but others were converted into cropland. Table 4.10 shows the proportion of occurrence of abandoned cropland to cropland (A2C) conversion and the association between variables. The land-cover change proportions of persistent abandoned cropland (A2A) and conversion of abandoned cropland to cropland (A2C) are approximately equal indicating that a significant proportion of abandoned

cropland was converted back into cropland after a certain time period. It was evident that A2C conversions took place mainly on well-drained soil (χ^2 (1, N = 35) = 4.375, P = 0.0365). The A2C conversion likely occurred on Luvisolic soils (accounting for 56% of polygons converted). Although high distribution of A2C conversion was observed, the association of this change to parent material texture was not evident (χ^2 (1, N = 35) = 0.686, P = 0.4074). Similarly, the association of land cover conversion and parent material was not found to be related (χ^2 (1, N = 35) = 0.721, P = 0.3957). Generally, the major distribution of A2C conversion was in well-drained and Luvisolic soil.

Table 4.10 Distribution of abandoned cropland remaining (A2A) and abandoned cropland to cropland (A2C) in different soil characteristics, 1990 - 2000.

Soil characteristics	Land-cover change		χ^2	df	P-value
	A2A	A2C			
	%				
Parent material texture (N = 35)					
Coarse	100.00(1)	0.00(0)	0.686	1	0.4074
Fine	58.82(20)	41.18(14)			
Drainage (N = 35)					
Well-drained	45.00(9)	55.00(11)	4.375	1	0.0365*
Poorly drained	80.00(12)	20.00(3)			
Parent material chemical (N = 34)					
Acid	100.00(1)	0.00(0)	0.721	1	0.3957
Calcareous	57.58(19)	42.42(14)			
Soil order (N = 35)					
Brunisolic	100.00(1)	0.00(0)	9.333	3	0.0252*
Gleysolic	100.00(6)	0.00(0)			
Luvisolic	44.00(11)	56.00(14)			
Regosolic	100.00(3)	0.00(0)			

Note: Number in parentheses are the total number of conversions in each category;
* Significant at the 0.05 probability level; N is number of observation (polygon).

In summary, more occurrences of deforestation were found on well-drained Chernozemic and Luvisolic soils. Abandoned cropland is significantly associated with poorly drained and (to a

lesser extent) acidic parent materials, and abandoned cropland in well-drained Luvisolic soil order was most likely to be re-converted to cultivation.

4.5.4. Carbon balance in the Boreal Plains Ecozone

The CBM-CFS3 model was used to simulate C stock and dynamics in the agriculture area of the Boreal Plains ecozone based on multiple data sources, including field data. In this model, C stock and dynamics, as the consequences of changes in land use and cover of both agriculture and forest, were included. Biomass C from stable forest and cropland were not included in the simulation, but changes from/to forest and cropland were included. Carbon stock and dynamics in all C pools, including root and soil pools, were reported.

Table 4.11 summarizes the simulation results on C stock and C change based on LUCCs during 1985 – 1999. The average ecosystem C was estimated at 256.2 Mg C ha^{-1}, inferring a stock of 555.9 Tg C for the BPE agriculture region (2.17 million ha). Among the C pools, the average C stock in AGB and BGB accounted for about 21.78% of the ecosystem C. The highest proportion of C stock was found in the soil pool, accounting for 45.51% of ecosystem C. The second highest C stock was the litter pool, accounting for 24.11%.

During the 15-year simulation, AGB and soil became a C sink while BGB, litter, and DOM were C sources. The highest annual accumulation rate of C was found in the soil pool, 0.83 Mg C ha^{-1} yr^{-1} (or 1801.1 Gg yr^{-1} for entire area), accounting for 45.51% ecosystem C. About one-tenth of that amount of C accumulated in the AGB pool, resulting in a total annual accumulation rate of about 0.08 Mg C ha^{-1} yr^{-1}. Of the three C sources, litter and dead wood pools released almost the same amount (0.26 Mg C ha^{-1} yr^{-1}), while the annual accumulation rate in BGB was small. Overall, abandoned cropland, shrub, and tree covers in the agriculture area of the BPE gained 0.32 Mg C ha^{-1} yr^{-1} (approximately 6.94 Tg C for the entire agriculture region a year).

Table 4.11 Summary of the simulation results on C stocks of abandoned cropland, shrubs, and trees for the period of 1985 – 1999.

Items	Unit	Carbon pools					Total Ecosystem
		Living biomass		Soil	Dead organic matter		
		Aboveground biomass	Belowground biomass		Dead wood	Litter	
C stock							
Max	Mg C ha^{-1}	47.38	12.03	120.60	24.20	64.36	259.37
Min		41.67	10.48	107.89	20.30	60.32	254.22
Average (Std.)		44.80 (±1.06)	10.99 (±0.47)	116.59 (±4.29)	22.02 (±1.24)	61.76 (±1.46)	256.16 (±1.65)
C stock change							
Max	Mg C ha^{-1} yr^{-1}	1.42	0.19	7.81[¥]	-0.17	0.13	1.32
Min		-4.01	-1.24	-0.41	-0.67	-1.88	-0.47
Average (Std.)		0.08 (±1.33)	-0.07 (±0.36)	0.83 (±2.03)	-0.26 (±0.12)	-0.26 (±0.49)	0.32 (±0.5)

[¥] The calculation of this impossibly high value was back-tracked and occurs in only one site (plot 2372, forest to cropland); input data and simulation procedures were thoroughly checked but no explanation was discovered and it was concluded that perhaps a processing error exists in the model.

The annual ecosystem C fluxes for the non-forest region of the BPE during 1985 - 1999 are presented in the

Fig. 4.4. It was estimated that the average C taken up from atmosphere, NPP, was 4.88±0.32 Mg C ha^{-1} yr^{-1}. This short-term C storage was then transformed through decomposition of DOM (heterotrophic respiration, Rh). Approximately 84.44% of C was released through heterotrophic respiration (Rh). This resulted in the net ecosystem C density of 0.76 ±0.3 Mg C ha^{-1} yr^{-1} accumulated mainly in soil and litter pools. However, under the effects of land-use conversions, including afforestation of abandoned farmlands, natural succession of tree and shrub covers, and deforestation of tree and forest for cultivation resulted in only 41.78% ecosystem C remaining in the Net Biome Productivity, NBP. It is noted that annual means and standard deviations of NPP, NEP, NBP, and heterotrophic respiration (Rh) are rounded to nearest 0.01 Mg

ha^{-1} yr^{-1}. Over the course of the simulation, the estimation results show that the highest C fluxes were associated with NPP and Rh, and trends of NEP and NBP were slightly positive. A small gap between NEP and NBP suggests a minor effect of LUCCs on C fluxes in the research region during the simulation years.

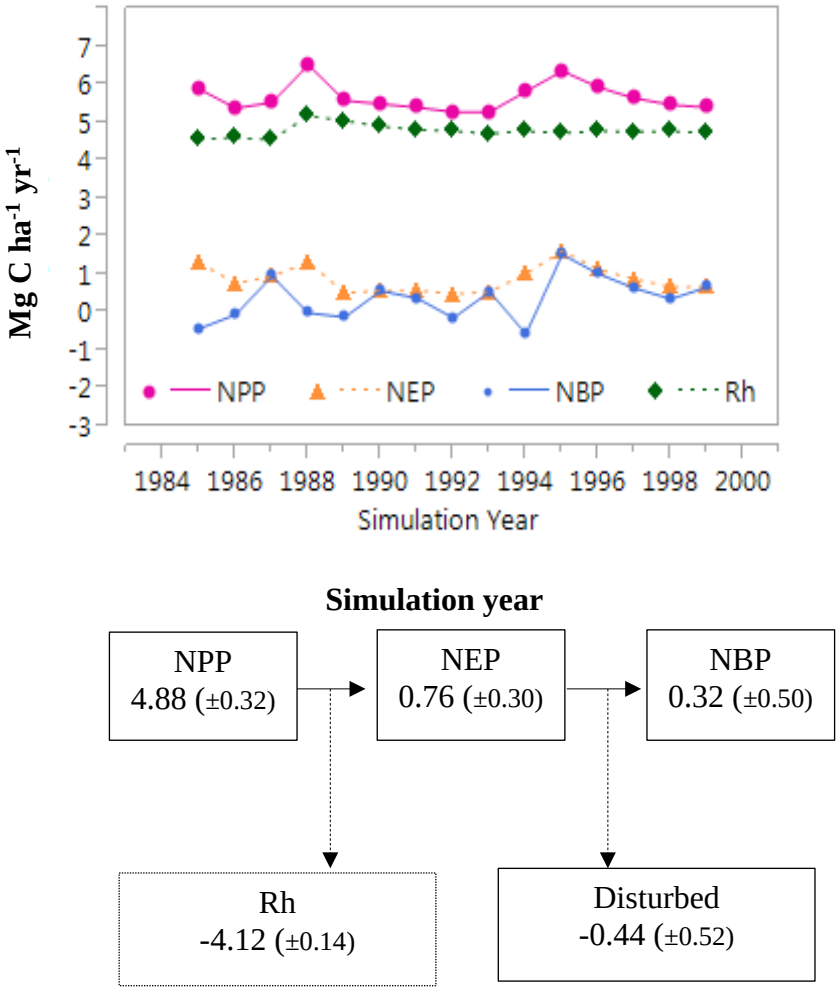

Fig. 4.4 Estimated ecosystem C fluxes per area unit (graph) and whole research region (diagram) for agriculture area of the boreal plains ecozone, Canada, during 1985 – 1999. NPP = Net Primary Productivity, NEP = Net Ecosystem Production, NBP = Net Biome Production, Rh = Heterotrophic Respiration.

4.6. Discussion

Our reported values on LUCCs support estimated values in a recent publication by Huffman et al. (2015) and our reporting approach and assumption on LUCCS between two points of time (10 years) include a total change from loss and gain and swapping area. The annual deforestation rate found during this research of -0.07% yr^{-1} was lower than that observed by Fitzsimmons (2002) at areas adjacent to Prince Albert National Park, central Saskatchewan (-0.19 to -0.43% yr^{-1}). Higher frequency of deforestation in the buffer zone of the protected area and higher deforestation rates during the 1960s could be the main reasons for the differences in deforestation rate. Furthermore, limited capacity for farming and low demand for settlement, such as road expansion, might also be contributing factors. Cropland experienced the highest change rate with annual loss and gain rate of 0.29% and 0.13%, respectively. This suggests a decreasing trend in cropland proportion in the agricultural portions of the BPE in association with an increased trend of abandoned cropland (1.11% gain). Our findings support a previous research outcome by Ramankutty and Foley (1999b) on LUCCs over several decades to 1992 that cropland area was stable over the past decades in North America.

LUCCs of the research area were associated with certain soil characteristics depending on conversion types. The associations of F2C conversion with soil drainage and soil order suggest that well-drained areas of Luvisolic soil order are more susceptible to deforestation for cultivation. The relationships between cropland-related conversions with soil drainage suggest that soil drainage is an important factor contributing to LUCC in the agriculture area of the boreal plains ecozone.

The examination of the spatial pattern of land-use change offered insights into the possible drivers for land-use change. The removal of hedgerows/shelterbelts and the smoothing of field boundaries, which support farm machinery movement, appeared to be the main reasons for woody vegetation loss in the research area during 1990 – 2000. C2A conversion was difficult to understand based on the spatial pattern of conversion alone.

Although the links between LUCC and soil attributes (from a 1:00,000 digital soil map) of drainage, soil order, chemical, and texture were examined, only the largest soil component in each polygon was included; meanwhile LUCC could occur on the other components. Further investigations of polygons where minor components are different soil properties, especially drainage and parent material chemical (pH) are needed to validate the current results. While soil map of drainage and pH used in this study is readily available with largest spatial scale in our research region, actual field truthing through on-the-ground observation should be considered.

Our estimated results on C stock were comparable to previous published results within the same ecozone. With regards to AGB carbon, the estimated result of 44.8 Mg C ha^{-1} was in the range reported by Fitzsimmons et al. (2004) for AGB carbon in the same ecozone, in which C densities in AGB of forest, pasture, and cultivated sites were 60, 1, and 4 Mg ha^{-1}, respectively. The CBM-CFS3 simulated an average rate of 0.08 Mg C ha^{-1} yr^{-1} for AGB accumulation for non-forest covers which was lower than results in the forest ecosystem (Chen and Luo, 2015). The average simulated soil C of 116.59 Mg ha^{-1} was comparable to the estimated range of 104 to 132 Mg C ha^{-1} for the three prairie provinces reported by Bhatti et al. (2002). Simulation results on soil C in this study were in close agreement with observations from Pennock and van Kessel (1997b) and Huang and Schoenau (1996) in central Saskatchewan.

The average NPP value of 4.88 Mg C ha^{-2} yr^{-1} resulting from abandoned cropland, shrub, and tree in the dominated Chernozemic soil was higher compared to NPP values reported for the boreal forest in the Luvisolic soil, which ranged from 1.2 to 4.0 Mg C ha^{-1} yr^{-1} (Gower et al., 2001; Li et al., 2003a; Liu et al., 2002; Ryan et al., 1997; Stinson et al., 2011). More The average NEP of 0.76 Mg C ha^{-1} yr^{-1} in this study was in range of previous values in studies of the same ecozone (Arevalo et al., 2011; Bond-Lamberty et al., 2004; Goulden et al., 2011). Heterotrophic respiration in agriculture areas affected by cover conversion yielded an average of 4.12 Mg C ha^{-1} yr^{-1} in this study.

Although our research provided initial outcomes on LUCCs associated with the characteristics of the agriculture area of the BPE, as well as initial simulation results on C stock and dynamics rate under multiple LUCCs transitions, the results can still be improved by enhancing the quality of the input data. For example, the distribution and number of plots relied

on the availability of pair-photo at the intersect points of the National Forest Inventory grid. Consequently, most of the sample plots were located in the province of Alberta and in the southern part of the boreal plains ecozone (Fig. 4.1). Hence, more sample plots are required at higher latitudes in Saskatchewan and Manitoba as different pattern changes between the north and south regions have been reported (Hobson et al., 2002). A further study with quantification of C stock on these permanent plots would verify and validate the estimated results.

Additionally, the pair-photography change detection technique used in this study offered types of conversion among land-cover categories, but the approach could not provide temporal information (year) of the events' occurrence because of the low temporal resolution of the data source. The time associated with each conversion event was assigned randomly within the two points of the simulation time. To overcome this challenge, time-series data of Landsat will be examined in the next section of this thesis, where the ready-to-use Landsat data allows users to track all conversion events with the associated years of changes (Huang et al., 2009; Kennedy et al., 2012). However, direct application of this data source may be challenging as this 30 m imagery may not capture changes in small size objects such as hedgerow or farm edging modifications in agricultural areas. The combination of historical air-photos for detecting change sites and time-series data for change time (where appropriate) should be considered.

While applications of multiple source data in a simulation model have been used, more effort is required to investigate the applicability with the CBM-CFS3 model. The model was originally designed for forest C simulation (Kurz et al., 2009) and the initial parameters and change rate, such as turnover, fall, and decay rate of the C pools, need to be adjusted (Amichev et al., 2012). Moreover, tree and forest cover in our simulation were assumed to be with the same species, trembling aspen. Since the difference in yield of woody biomass between tree species was minor in the short term (15 years), the effect of tree species overall could also be minor. More age-yield curves for associated tree species would be beneficial to support a longer simulation period.

4.7. Conclusions

LUCCs in the research area was small, accounting for approximately 6.5% of total research area. Almost all changes were small in area and associated with cultivation activities. Our results suggest that deforestation for cultivation was likely to occur on well-drained area of Luvisolic or

Chernozemic soil orders. On the contrary, abandoned cropland was associated with poorly drained and acid soil. The average C stock in the BPE resulting from abandoned cropland, tree, shrub, and unimproved pasture was 256.16 Mg C ha^{-1}, where the total C was distributed in living biomass, soil, and dead organic matter pools accounting for 21.78, 45.51, and 32.71%, respectively. Simulation results indicated that AGB and soil pools were C sinks of 0.08 and 0.83 Mg C ha^{-1} yr^{-1}, respectively, while BGB, litter and dead wood became C sources.

The research region was estimated a C sink of 0.32 Mg C ha^{-1} yr^{-1}. Assuming that 20% of the BPE is covered by agriculture and LUCCs in the agriculture region accounts for 6.5% of the region (or 882,050 ha), the accumulation potential of the region is 282,256 Mg C per year from 1990 to 2000 (or 1.04 Mt CO_2 equivalents).

5. LAND-USE AND COVER CHANGE DETECTION IN THE AGRICULTURAL-FOREST TRANSITION ZONE IN CENTRAL SASKATCHEWAN

5.1. Preface

Chapter 4 confirmed that LUCCs in the agriculture region of the boreal forest resulted in a C sink and that changes were broadly associated with soil characteristics. However, the C simulation model in Chapter 4 was based on randomized years of land-use and cover transition because time associated with each conversion (change year) could not be extracted in using the bi-temporal change detection technique (Chapter 3). Therefore, extracting information on time points when LUCCs took place is essential for seeking a higher estimation accuracy. Additionally, the previous studies relied on the data collected at a plot scale, which is not feasible for a broader scale study. In the current chapter, characteristics of LUCCs in the long term, including year of change for the full research area, were examined using remote sensing techniques. The study region was expanded into the Agri-Forest intersection region of the BPE. Mapping LUCCs and assessing the likely change patterns among land use types on the different soil classes were the main objectives of this chapter.

5.2. Abstract

Discrete changes in forest or agriculture are readily detectable using remote sensing data; however, aggregate changes through time across the agricultural-forest transition zone are more difficult to monitor. In this research, we explore how qualitative and quantitative changes have taken place in the boreal forest and the association between these changes and soil capability over a period of 27 years, from 1984 to 2011. For land-cover change, maps of disturbance and recovery were created using Landtrendr, a temporal segmentation algorithm. The maps were developed from 64 Landsat Thematic Mapper images and assessed for validity from 900 random points. The output map shows high accuracy (90% overall) and provides both spatial and temporal information of cover change, including both abrupt and longer-term or chronic disturbances as well as vegetation regrowth. The results show that approximately 60% forest and shrub area were

disturbed with different magnitudes. The major regrowth proportion (60% of the regrowth area) came from slow natural regeneration on undeveloped pasture. For land-use change, a post-classification change detection approach using Landsat images for the years of 1984 and 2011 was used. The overall accuracy of the output maps in 1984 and 2011 was 96.2% and 93.3%, respectively. The results revealed net change in the land-use categories. While slight change in annual cropping (-4.4% during the research period) was observed, substantial changes occurred in pasture (+76%) and summer fallow (-87.8%). During the 27-year period, shrub and forest both decreased, -31.6% and -16.4%, respectively. Conversion of summer fallow to annual cropland and pasture, annual cropland to pasture, and shrub to pasture were the main land use transitions over the research area. Our results also highlighted that changes in land-use differed across the CLI (Canada Land Inventory) soil capability classes. While substantial changes of summer fallow to annual cropland took place on higher soil capability land, annual cropland to pasture conversion was more likely on lower capability soil classes.

5.3. Introduction

Land-cover change is recognized to have a great impact on the global environment and climate change (Foley et al., 2005; Gibbard et al., 2005; Ojima et al., 1994; Vitousek, 1994). Quantification of land use and land cover has thus become a major subject and policy focus in the recent decades. Information on land-cover change is of particular importance for C accounting efforts as well as mitigation and adaptation actions under the United Nations Framework Convention on Climate Change (UNFCCC).

A considerable amount of research has focused on quantifying land use and cover change (LUCC) in forests, but less has been conducted within the Agri-Forest transition region. In Canada, it was estimated that the main drivers of land-cover change in the boreal forest include wildfire, harvesting, aspen dieback, and pathogens. Among these, insects caused the largest damage (20 million ha in 2013) and became the leading driver of disturbance of the boreal forest in Canada (Natural Resources Canada, 2016). Fire affects roughly 2 million ha annually across Canada (Masek et al., 2011). Hermosilla et al. (2015) indicated that disturbance by fire was estimated to affect nearly 345,000 thousand ha per year in Saskatchewan, accounting for approximately 70% of the total land-cover change in forests. Along the southern edge of the Canadian boreal forest,

severe drought has accelerated vegetation mortality, resulting in a massive dieback of trembling aspen that accounted for up to 35% of aspen biomass (Michaelian et al., 2011). Additionally, insect outbreaks and weather condition such as freeze-thaw events were also contributed to aspen dieback (Hogg et al., 2002; Hogg et al., 2008). Under one climate scenario (Christensen et al., 2007), aspen forest along the prairie-forest border (i.e., the Aspen Parkland) was expected to shift to the northeast rapidly through a process called "savanification" (Frelich and Reich, 2010). The deforestation rate in Canada has declined slightly over recent decades at a mean rate of 0.02% annually; however, the conversion of forest to agriculture remains the largest contributor to deforestation (Natural Resources Canada, 2015). Overall, these studies have provided insights into disturbances in forest landscapes but often at a fairly general level. Additional studies on comprehensive land-cover changes of the Agri-Forest transition on the southern boundary of the boreal forest of Canada are needed.

For land-use change within the agriculture region, the effects of multiple drivers, including intensification of agricultural production practices, the adoption of conservation technologies, and changing markets on land-use change on agriculture have received considerable attention (Lambin et al., 2001; Mottet et al., 2006; Tilman et al., 2011). Environmental characteristics that effect cultivation such as soil type, irrigation, and climate conditions are also important to land use decisions. In many cases, a certain land use transition are associated with differences in soil capability, which summarizes several key determinants of plant productivity (Bakker et al., 2011). Ideally, annual cropland is located on the soils with high capability for cropland production (Bakker et al., 2011). A recent study by Zhang et al. (2014) showed a substantial decrease of summer fallow coupled with a slight increase in annual crops and perennial crops, and transitions between summer fallow, annual cropland, and perennial crops depending on soil capability. This study provides significant insights into the changes in the Montane Cordillera ecozone, and suggests that a similar approach would be useful to explore land-use change in the Agri-Forest transition.

To monitor land-cover change, Earth Observation (EO) instruments offer the longest historical archive data (Wulder et al., 2008) and play an important role in the assessment and monitoring land use and cover change in spatial and temporal fashion. Landsat imagery is available in large volumes, offering free-of-charge data with a suitable spatial and temporal resolution. With

advances in image processing methods and computation capacity, the Landsat time series has been widely used for land use and cover change applications. Using satellite imagery, many previous studies have employed a variety of approaches mapping land-cover change (Cohen et al., 1995; Hame et al., 1998; Kennedy et al., 2010; Townshend and Justice, 1995). Accordingly, the application of multi-temporal data with trajectory analysis in the satellite time-series data shows greatest opportunity for land-use change and land cover monitoring (Coppin et al., 2004). The significant advantages of this approach over other techniques are that additional information on conversion and modification, such as rate, time, and extent of change can be derived (Kennedy et al., 2010). A more comprehensive understanding of land use and cover change can be achieved from this time series data than change detection of a bi-temporal change detection approach (Cohen et al., 2010; Müller et al., 2015). For these reasons, Landsat time-series data is definitely valuable for the study of the spatial, temporal, and severity change of land-cover change at the landscape scale.

For Landsat Time Series (LTS) data, two common techniques are normally used for analysis - image classification-based methods and trajectory-based change detection. In the first approach, the image of each time is classified and post-classification comparisons are then used to identify the changes. In the BPE of Canada, Schroeder et al. (2011) detected forest harvest and fire disturbances using a supervised minimum-distance-to-mean classifier and concluded that the accuracy of the output maps varies with different spectral variables (i.e., bands and indices). The accuracy of the output maps was also influenced by difficulties in detection of non-stand replacement and wetland misclassification. The advantages of this approach include a reduction in the time for radiometric calibration and atmospheric correction of the input images; however the lack of ground truth samples may introduce errors to final products via misclassification and misregistration (Coppin et al., 2004). In trajectory-based change detection, Kennedy et al. (2010) introduced a model using Landsat-based detection of trends in disturbance and recovery (Landtrendr). By applying temporal segmentation of spectral indices extracted from Landsat time-series data, the model allows us to capture all changes due to natural and artificial forest disturbances with associated characteristics (Griffiths et al., 2012; Kennedy et al., 2012; Meigs et al., 2011). Although, the trajectory-based change detection offers a robust approach for monitoring forest disturbance and recovery (Kennedy et al., 2007; Piciarelli et al., 2008), its applicability to a

more complex region such as the transition region of the boreal forest and cropland remains to be examined.

The first objective of this research was to map land-cover changes during 1984 - 2011 in the forest - cropland transition region of Saskatchewan. Landsat surface reflectance bands and suitable vegetation indices were prepared. The Landtrendr model was used for capturing the yearly cover changes. Segmentation of the temporal trajectories of the spectral data and the rates, location, and duration of any changes was extracted. Field data and finer spatial resolution images such as SPOT and aerial photos were used for validation. The second objective of this research was to quantify land-use change in study region and document the association between land-use change and soil capability classes. Multi-spectral images in the years of 1984 and 2011 were collected and classified. The post-classification technique was applied to detect changes. Maps of land use transitions were overlaid on soil capability map layer to assess the likely change patterns among land use types on the different soil classes.

5.4. Materials and Methods

5.4.1. Research location

The study area is located in the northwest area of the agriculture-boreal forest transition zone in Saskatchewan, Canada (Fig. 5.1), and covers an area of ~ 3700 km^2. Our previous research in this region found that land-use change occurred mainly between forest and cropland with deforestation for cultivation on well-drained Chernozemic soil orders and abandoned cropland on poorly drained and more acidic soil.

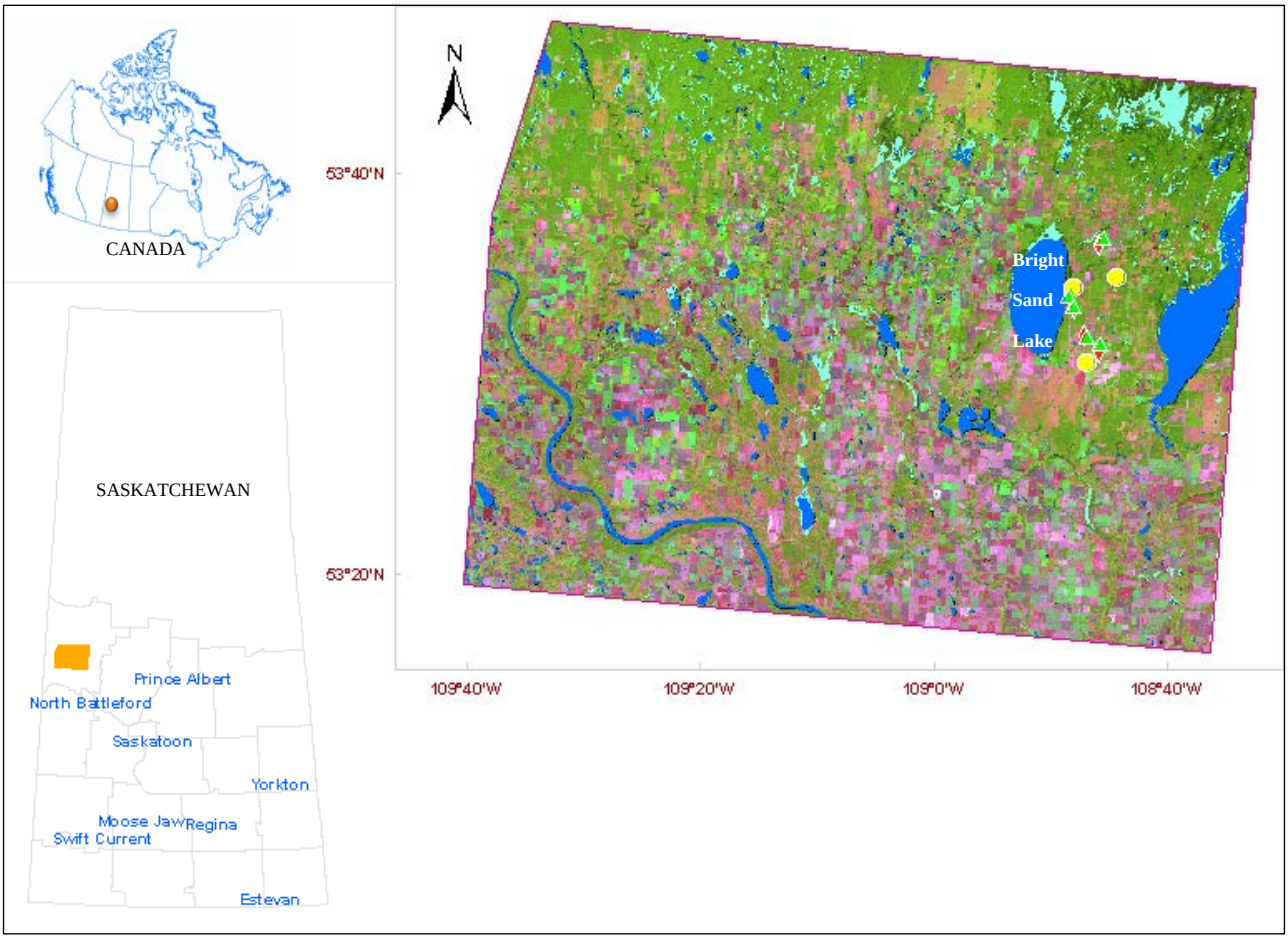

Fig. 5.1 The ground surface reflectance of the study area in RGB (543) and the sample locations on abandoned croplands (in red diamond), cropland (in yellow circle), and mature forest (in green triangles) used in previous research.

5.4.2. Data collection and pre-processing

5.4.2.1. *Landsat data collection and processing*

Annual Landsat images of the study area acquired between mid-July to August from 1984 to 2011 were collected from the archive of Landsat data of the United States Geological Survey (USGS, http://earthexplorer.usgs.gov/). The study region was in Landsat paths 39 and row 23. Since no cloud-free images were available for some years during mid-July to August, other cloud-free images from the adjacent footprint were also collected. Consequently, 64 scenes of the

pertinent images from four different Landsat footprints (WRS-2) were recorded. Details on the acquisition date and scene locations are presented in Fig. 5.2.

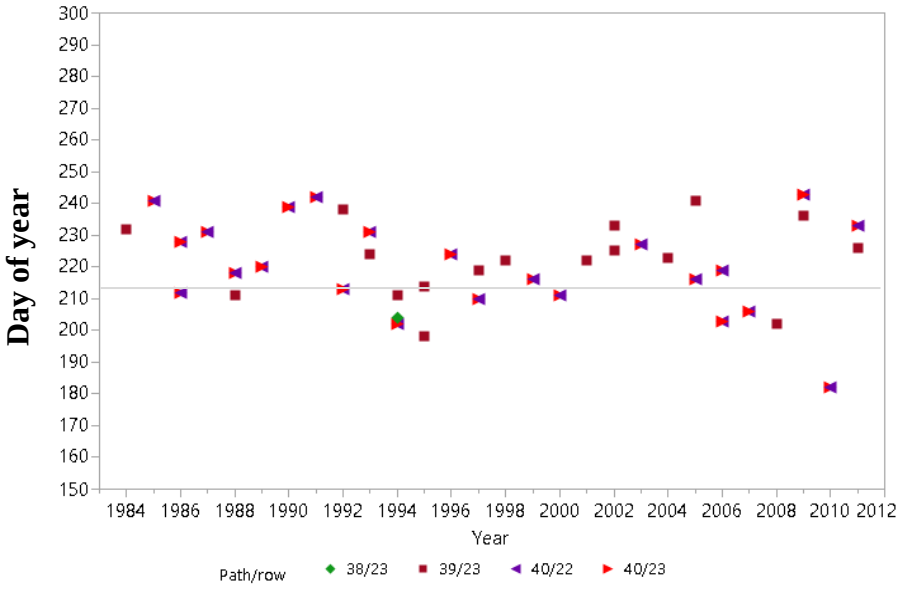

Year

Fig. 5.2 Acquisition dates (in Julian date) and paths of the Landsat Time Series Images from 1984 to 2011.

Landsat Surface Reflectance and cloud mask products were ordered through the USGS Earth Resources Observation and Science (EROS), Center Science Processing Architecture (ESPA) On Demand Interface (https://espa.cr.usgs.gov/). In these products, surface reflectance data were the products of Landsat Ecosystem Disturbance Adaptive Processing System (LEDAPS) and corrected by the Second Simulation of a Satellite Signal in the Solar Spectrum (6S) radiative transfer models. The products also include cloud and cloud shadow mask bands, which were calculated from the fmask algorithm (Zhu and Woodcock, 2012).

All images were acquired from the same source, in which orthorectification steps have been conducted. Quality verification was also conducted on each image on the percentage of cloud cover, geological and biological accuracies. Data collection procedure is depicted in Fig. 5.3.

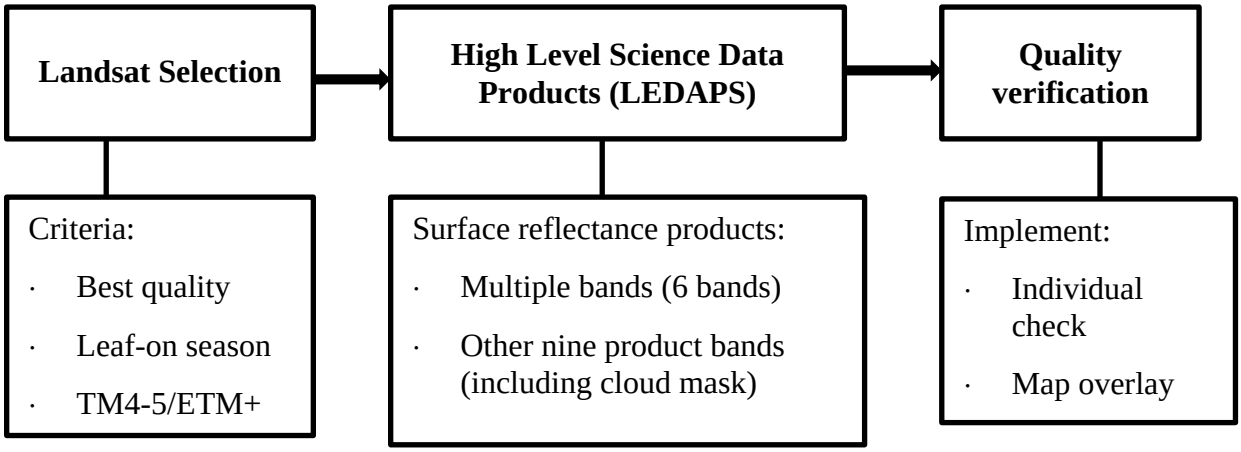

Fig. 5.3 Major steps for collecting archive Landsat time series data.

Because LEDAPS products are offered in an archive format, some data preparation steps were conducted, including layer stacking and image sub-setting. Consequently, a cloud mask band and six surface reflectance bands (1-5, and 7) of each scene were stacked into a single file then subset into the region of interest. All images were registered to the Universal Transverse Mercator (UTM) project system: zone 13, datum North_American_1983_CSRS, spheroid GSR 1980.

Landsat time-series has been considered as a good data source for capturing decadal changes to land surfaces (Liu et al., 2013a). However, the quality of a time – series stack for a specific area is normally restrained by environmental conditions, including illumination, phenology, atmospheric conditions, and acquisition date. Data normalization processing, adapted from Canty et al. (2004), was thus applied for reducing noise introduced from environmental conditions to an individual image.

5.4.2.2. *Ground truth data collection*

For land use map classification, ground-truth points for classification training and accuracy assessment were collected from aerial photos, field data, high-resolution Google Earth imagery, and existing land cover maps. For the 1984 land use map, paper aerial photos taken in 1980 and archived at the University of Saskatchewan Library were scanned and geo-referenced for ground-truthing. Different Landsat Thematic Mapper (Landsat TM) multispectral bands were also used to generate classification training and testing points with the assumption that the time lag between 1984 imagery, and the ground truth collection was not significantly different. For the 2011 land

use map, high-resolution orthophotos taken during 2008-2011, collected from the Saskatchewan Geospatial Imagery Collaborative (SGIC, www.flysask2.ca), were used. High-resolution air photos available on Google Earth, the Landsat TM multispectral bands, and the AAFC Annual Crop Inventory maps from 2011-2014 (Agriculture and Agri-Food Canada, 2014) were also used for reference to enhance the accuracy of the ground truth points. Field measurements were conducted in 2012 during the growing season as reported in chapter 3 of this dissertation. The field samples include five forest, four abandoned cropland, and four cropland parcels. Details on field data collection were presented in 3.4.1. Land covers and the dominant vegetation of the adjacent sample parcels were recorded from field trips for classification purpose.

5.4.2.3. *Meteorological data*

It was evident that variations of vegetation indices were partially explained by temporal precipitation and temperature (Ding et al., 2007; Kawabata et al., 2001). Therefore, historical data of precipitation and temperature during 1984 – 2011 was obtained from Butte St-Pierre weather station (Environment Canada, which is available at http://climate.weather.gc.ca/). Daily data recodes were collected and reconstructed into average monthly temperature and precipitation for research purposes. Meteorological data (original data) was decomposed into three different components, which are seasonal, trend, and remainder (Fig. 5.4).

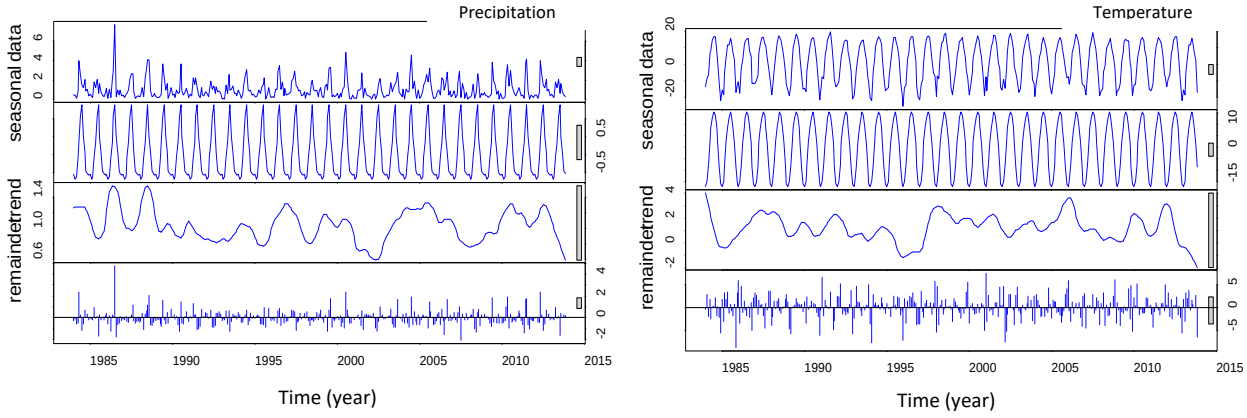

Fig. 5.4 Trends of precipitation (left) and temperature (right) for Bright Sand Lake area.

The Butte St-Pierre weather station was chosen for meteorological data collection as it is closest to the research region. From monthly average, the temporal patterns of temperature and

precipitation were extracted using a decompose model in R, an open-source software (Fig. 5.4). It is noted in Fig. 5.4 that data is monthly average input values; seasonal is the pattern that repeats with fixed period of time; trend is major temporal pattern over time; remainder is the residuals of the time series after allocation into the trend and seasonal components. This information, especially trend, is important for interpreting the temporal spectral trajectories of a vegetation index.

5.4.2.4. *Soil capability*

A GIS data set of soil capability and associated attribute data from the Canada Land Inventory (CLI) was collected from Agriculture and Agri-Food Canada (2014). This GIS data set was created from a comprehensive multi-disciplinary land inventory of rural Canada. Based on soil characteristics such as texture, slope, and drainage, the CLI soil capability for agriculture was classified into seven classes. Class 1 has no significant limitation for crops. Classes 2 to 4 have moderate limitations for annual crops and pasture. Class 5 has severe limitations and can only be used for forage crops under improvement practices. Class 6 has very severe limitation and improvement practices are not feasible. Classes 7 and O (Organic Soils) have no capability for arable culture or permanent pasture.

The current data sets include a digital map layer of CLI coverage and a soil component attribute table (e.g. soil class, sub-class, areal proportion). Each polygon refers to one CLI soil unit, which link to at least one soil component. Although the areal proportion of each component was determined, the spatial location of the each component was not identified. For example, CLI soil unit number 18 (a polygon), has three components (from 1 to 3 in attribute table); component 1 is soil class 3 and accounts for 80% of total area of the soil unit, component 2 is soil class 4 and accounts 10% the total area, and component 3 is soil class 5 and accounts for the remainder. To facilitate our investigation on land-use change on soil capability, the associated component which has the highest areal portion (normally from component 1) for each polygon was used.

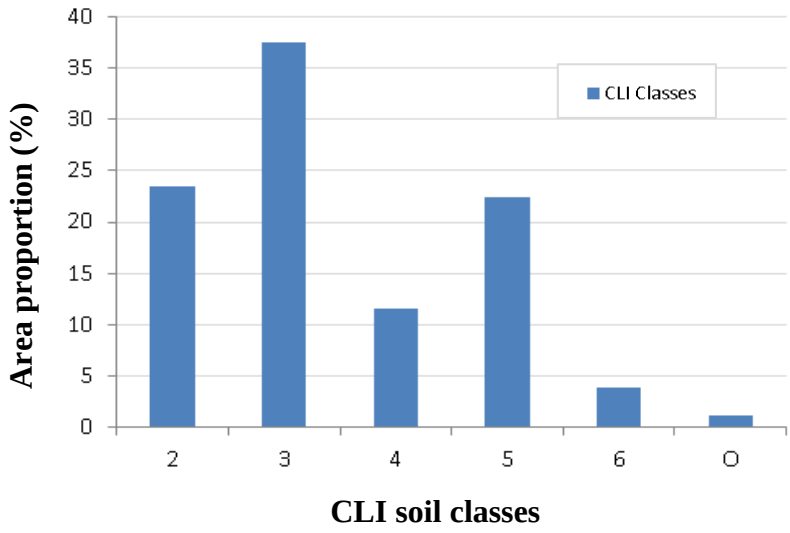

Fig. 5.5 The distribution of CLI classes in the research area.

The soil map includes six different CLI Classes, but the major area portion of the interested covers was distributed on five Classes (2-6). CLI Classes 2, 3 and 5 were the dominant soil classes (Fig. 5.5). Among them, the highest area proportion was on Class 3, approximately 139,000 ha (37%). Area of CLI Classes 2 and 5 shared about the same portion (roughly 23%). The area of Class 4 was 43,000 ha (11.5%). The area of Class 6 was relatively small (3.8%). There are no polygons dominated by soil capability classes 1 and 7 in our research area. Class O (organic soil) accounts for a very small portion.

5.4.3. Cover change detection using Landtrendr

Land cover in this study refers to the physical material at the surface of the earth, for example, bare ground, crops, shrub/trees, and forest. Monitoring the differences of an object or phenomenon at different times is termed change detection (Singh, 1989). Land use involves the management and modification undertaken by humans on the land in the service of their economic activities. Forest, annual cropland, summer fallow, and perennial/pasture are examples of land use types.

The first part includes an overview of the Landtrendr model and the segmentation procedure will be provided. The section also covers some associated information on parameters used to execute the model and accuracy assessment processes; change detection analysis, describes

how to generate the disturbance maps on forest and shrub covers as well as the recovery maps for forest, shrub, and croplands. The second part covers the steps required to create two land use maps of 1984 and 2011 in the whole region including ground truth point collection, classifier selection, and accuracy assessment procedures. Post-classification and change detection of the land use maps in 1984 and 2011 are included in this part. Generally, the first part focuses on methods to assess qualitative change in cover, especially in the forest region. The second part aims at the quantitative change in land use during the research period.

5.4.3.1. *Overview on Landtrendr model*

In order to track land-cover change using temporal Landsat data or time-series data, Kennedy et al. (2010) introduced a package of algorithms to detect trends in forest disturbance and recovery, which they called the Landtrendr model. Landtrendr is a set of the change detection algorithm via temporal segmentation and fitting of the Landsat time series, which used in this study to monitor land-cover change in the forest region. Landtrendr is scrip-based model running on basic operation of Interactive Data Language (IDL). Four steps are required to execute the model: (1) data preparation, (2) folder structure, (3) parameter setting, and (4) model execution.

In data preparation, multispectral bands of annual archived Landsat images retrieved for each growing season and which had low cloud cover percentages were prepared. Additionally, cloud cover and vegetation indices associated with the annual multispectral bands were also included. The folder structure is required for an automated process implemented in the scrip-based model to extract variables such as year, names of input indices, and names of output map layers.

In the model, different vegetation indices were extracted from the Landsat time-series stack to form a temporal trajectory for each pixel location. The vegetation index values from the separated image were gathered and stored in pixel-based trajectory imagery or a pixel's temporal profile (i.e., the source stack). From the model parameter option, segmentation can be executed on different indices, including Normalized Difference Vegetation Index (NDVI), Normalized Burn Ratio Index (NBR), and Tasselled Cap indices (Brightness, Greenness, Wetness). Although NBR was designed to determine burn severity (Cocke et al., 2005; Escuin et al., 2008), it was also suggested that it could be applied to land cover classification (Li et al., 2014). In the Landtrendr model, previous work indicated a stronger relationship between NBR and the interpreted

vegetation covers compared to that of the NDVI (Kennedy et al., 2010), and that NBR was the most responsive to forest disturbances and recoveries (Cohen et al., 2010). The NBR index was therefore used for segmentation process. The final step, model execution, is conducted on a script in IDL interface. The outputs of this process are in band sequential raster format.

The main purpose of segmentation is to identify the year that a change event occurred. A segmentation function was applied as a function of time and relied on NBR index values, and then regression and point-to-point fitting approaches were applied to each segment. Note that the terms used in this section are depicted in Fig. 5.6. Subsequently, the annual fitted values, which are the simplification of the source stack, were generated and fitted stacks were created for further analysis (Kennedy et al., 2010). From the curve fitting outputs, other map layers can be extracted including disturbance and recovery regions, the duration of each segment, the magnitude of a trend/change, and the important years in describing the trend. Once the change points were defined from segmentation, the tasseled cap indices were imposed to form curve fitting outputs. The tasseled cap indices were transformed from Landsat bands into three components of soil brightness (TC_b), vegetation greenness (TC_g), and soil vegetation wetness (TC_w) (Crist, 1985). My preliminary evaluation suggested that TC_w was the most sensitive index to the temporal change. The wetness index was widely used to detect forest disturbances (Frazier et al., 2015; Masek et al., 2008; Senf et al., 2015).

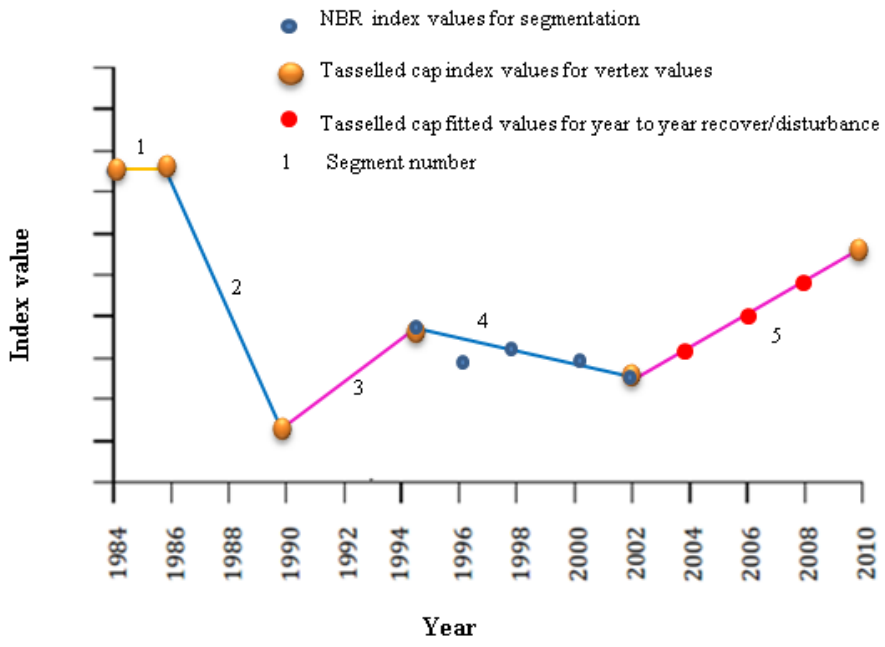

Fig. 5.6 Temporal segmentation concept for land-cover change detection with an example of five change events in land during 1984 - 2011 (no change: orange line (1); disturbance: blue lines (2, 4); recovery or regrowth: purple lines (3, 5)).

The segmentation process was conducted from pixel to pixel on raw index values (such as NBR) values (blue dot) to identify the change events over time; from those events, tasselled cap values (Brightness, Greenness, Wetness) were imposed to calculate curve fitting (segment, lines) and vertex values (tasselled cap indices, orange dots) and fitted values (red dots).

The process of generating disturbance and recovery maps relied on the changes in index values. However, direct interpolation of disturbance magnitude might be constrained by the range of a certain index. A process to convert these data ranges into a changed percentage was conducted. Accordingly, the high (HighVal) and low index values (LowVal) were converted into 0% cover (bare ground) and 100% cover (closed canopies), respectively. To do this, reference values (HighVal/LowVal) were gathered based on both fitted stack scene and field sampling/image interpolation. Cover percentage of each pixel was calculated as (Kennedy et al., 2012):

$$\textbf{PercentCover} = \left(\frac{TCw - LowVal}{HighVal - LowVal}\right)\mathbf{100} \quad \text{(Eq. 5.1)}$$

Where:
TCw is Tasseled Cap wetness
LowVal is the value TCw associated with bare soil samples
HighVal is the value TCw associated with closed canopy samples

For each pixel, relative disturbance magnitude was extracted from fitted stack and defined as:

$$\textbf{Magnitude}_{Rel.} = \left(\frac{\textbf{PercentCover}_{PreDist.} - \textbf{PercentCover}_{PostDist.}}{\textbf{PercentCover}_{PreDist.}}\right) \quad \text{(Eq. 5.2)}$$

Where:
MagnitudeRel. is relative disturbance magnitude.
PercentCoverPredist. is the percentage cover before a disturbance event.
PercentCoverPostDist is the percentage cover after a disturbance event.

Map labeling scripts were composed to extract disturbance and recovery areas under defined criteria. The defined criteria in this study include disturbance/recovery magnitude and disturbance/recovery duration. Fig. 5.7 details the terms used in this section. Only pixels with a disturbance/recovery magnitude greater than 10% over one-year or 3% over a 20-year duration, or sliding scale for the years in-between, were mapped. Although all disturbances can be mapped, disturbances of a minor magnitude might be difficult to validate and hence the cover percentages of a disturbance events smaller than 10% was excluded and assigned as no change. A similar protocol was applied to the whole research region using the same parameters, and any pixels not meeting the above conditions were filtered to no-change.

Disturbance duration is defined as the number of years that a disturbance event lasts and calculated by the start minus the end year of the segment (Fig. 5.7). Similarly, pixels that gained cover percentage greater than 5% were mapped regardless of recovery duration. Forest and shrub disturbance duration can occur in one year (such as forest clear-cut) or be spread over decades (such as tree mortality or interaction among disturbances) but recovery duration normally occurs over a decade or more. Therefore, only recovery duration greater than 4 years was included. It is

noted that cover loss and gain could occur in the same location. Forest clear-cut followed by forest regeneration is an example. The information on changes (i.e. year, magnitude of disturbance/recovery) was thus mapped and reported separately.

Due to the complexity of cover change in the transition region, only certain covers were included for reporting. Specifically, disturbances on Forest and Shrub and recovery on Forest, Shrub, and Annual Croplands were summarized.

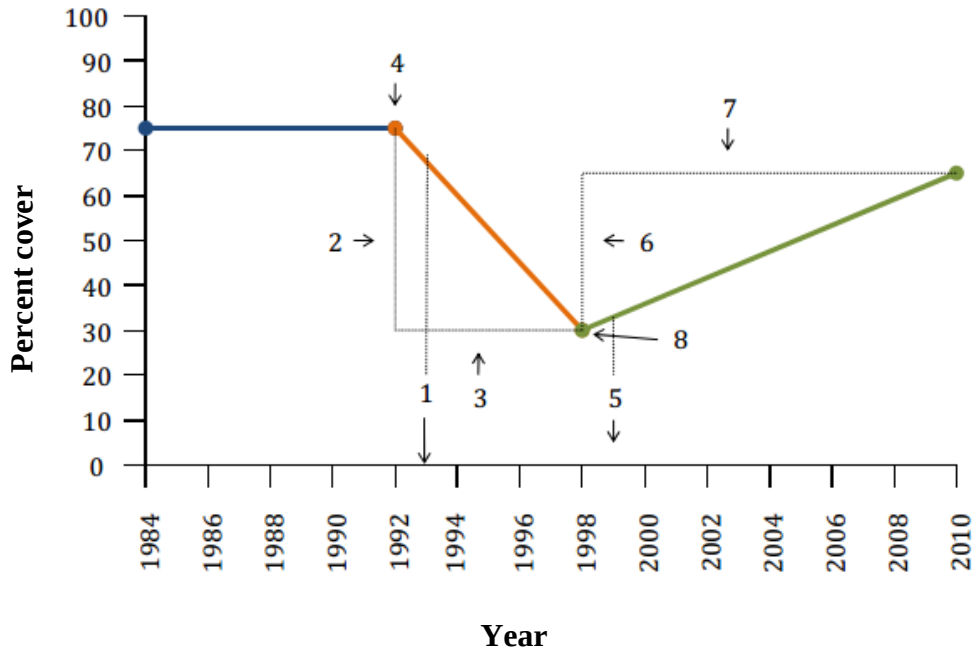

Fig. 5.7 Land-cover change detection and labeling. 1: disturbance year; 2: magnitude of disturbance; 3: disturbance duration; 4: pre-disturbance value; 5: post-disturbance start year; 6: recovery magnitude; 7: recovery duration; 8: initiate-regrowth value.

5.4.3.2. *Accuracy assessment*

Accuracy assessment is a process to compare the classified map to ground truth data which is assumed to be correct (disturbed year in this case). The main aim of the process is to access how well the segmentation process accomplished the task. The procedure includes generating a set of random points, updating each random point's value from ground truth and classified map, and performing accuracy assessment. From the output map of disturbed year, 20 random points were generated on each year-class (a single year) or 500 random points in total for 25 years (during

1984 – 2011). Additionally, another 400 random points were generated to assess the performance of the model on forest and non-forest separation. Disturbed year estimated by the model was updated for the random points using Spatial Analyst Tool on ArcMap (Extract Multi-Value to Points). Subsequently, ground truth data was updated using multi-source data. These sources include (1) historical aerial photos (2) field study, and (3) SPOT imagery. The first source includes aerial photographs acquired in 1980 and archived in the University of Saskatchewan Library and aerial photos taken during 2011 from The Saskatchewan Geospatial Imagery Collaborative (SGIC, FlySas2.ca). Field data were collected from a field study in 2012. SPOT satellite image acquired in 2006 and archived by the Natural Resource Canada database (Geobase.ca); Furthermore, Google Earth map, time series TC_w trajectories (source stack), and Landsat multi-spectral bands were also referenced (in some cases) for accuracy assessment.

In some recent studies, time-series data observation based on archival Google Earth data, such as TimeSync tool, has been used as a supporting tool for cover change validation (Cohen et al., 2010; Kennedy et al., 2010; Kennedy et al., 2015). In our case, temporal aerial photographs available on Google Earth are very sparse and the field sample points are small; therefore, multi-source data were used for accuracy assessment.

From the sample locations, comparisons between the ground truth (disturbed year) with those in the predicted map on disturbed year were noted and summarized in an error matrix. Statistical results such as user's accuracy and producer's accuracy, user's accuracy, and kappa coefficient (K_{hat}) were also computed (discussed below).

5.4.4. Land-use change during 1984-2011 using bi-temporal change detection

To detect land-use change between 1984 and 2011, two land use maps were created for a post-classification change-detection process. For land use maps, Landsat TM images, which were acquired during the growing season (both in August), were used for classification. The class number and typology were defined based on our field work, the EOSD Land Cover Classification Scheme (Wulder and Nelson, 2003), and existing AAFC cropland maps (Agriculture and Agri-Food Canada, 2014). Five land use classes were defined, which are forest, shrub, pasture, cropland, and fallow (i.e., summer fallow or essentially bare soil). In the forest region, forest class includes predominantly forested or treed areas where tree canopies cover more than 10% of the total area.

Shrub class is defined as the predominantly woody vegetation of low height (+/- 2m), which may include woody vegetation in wetlands and regenerating forest. The Pasture class includes tame grasses and perennial crops. Grassland or native grasses occur only in a small portion in the research area and are included in Pasture class. Cropland includes annual crops of cereals, pulses, oilseeds, and others. Fallow is agriculture fields that were tilled and left unsown for the growing season. Changes in water bodies, wetlands, and resident/built-up areas were grouped into "others" class for reporting purposes and excluded from the classification process. However, these classes were reserved in classification maps for visualization purpose. In summary, the classification scheme in the research area includes forest, shrub, pasture, cropland, and fallow.

For image classification and accuracy assessment purposes, ground truth points were collected mainly from the aerial photographs. For 1984, a total of 671 sample points covering all land use classes of the research area were collected from aerial photographs. The sample points were also checked using different Landsat band combinations (RGB composite of three bands, i.e. 5, 4, 3 or 7, 3, 2). About 50% of those data points were randomly selected to calibrate the classification. The remaining points were used for accuracy assessment purposes. For 2011, training samples were collected based mainly on visual interpretation of aerial photographs. These training points were then compared with reference data from other data sources including field data, Google Earth, and existing land cover maps. Over the study area, 675 sample points were collected for five land use classes. In each cover category, about 50% of data points were used to calibrate the classification, and the remaining points were used for accuracy assessment.

A Maximum Likelihood classifier was adopted to create the land use maps. This classifier was chosen as it is one of the most efficient parametric classifiers used for supervised classification (Bolstad and Lillesand, 1991). The classification process was conducted on ArcMap, and a 3x3 majority filter was applied to reduce noise in the classified maps. The Jeffrey_Matusita distance (Richards and Jia, 2006) was used to assess the capability of separation among the training signatures. The distance values ranged from 1.7 to 2.0 except for the separation between forest and shrub (1.5). This indicates that the training samples are sufficient to process the classification step.

Accuracy assessment is an important step in evaluating the classification results. This step refers to the degree of correspondence between the ground truth data and the predicted or classified

maps. Error matrices were used to perform accuracy assessment for the two classified maps. The accuracy of the output maps were measured by user's accuracy, producer's accuracy, and kappa values. User’s accuracy corresponds to errors of commission (inclusion), where pixels that belong to another class are labeled as belonging to the class in question. Producer's accuracy corresponds to omission (exclusion) and represents pixels that belong to a given class but which are not classified into that class. Another measurement of map accuracy, the kappa coefficient (K_{hat}), was also used to distinguish the differences between actual agreement and the agreement expected by chance. This coefficient shows the extent to which the correct values of an error matrix are due to "true" versus "chance" agreement (Foody, 2002; Jensen, 2005).

To detect changes in land use, post-classification comparison methods were used to map the area that had changed between the two periods with the defined "from-to" land covers with associated area coverage from the two classified maps. The cover categories adapted from vector map layers, which are water bodies, wetland, and built up areas, were grouped into one class, "others". Cloud cover area in 2011 Landsat image was also masked and grouped into "others" for the both maps. From the change map, a contingency matrix table summarizing the change pathways was constructed for reporting.

5.4.5. Land-use change and soil capability

From the previous step, a map showing the changes among land use types between the two times was generated. To investigate the influence of soil on land-use change, a map layer of soil capability for agriculture was overlaid on the land-use change map using the Intersect Tool of ArcMap software. The area proportion of the soil classes over the research region was summarized and the distribution of land use in 1984 and 2011 on each soil class was extracted for reporting. Land-use changes between 1984 and 2011 on CLI Classes were also investigated.

Previous results indicated that the research area experienced a considerable land-use change in fallow and pasture, and these changes also interacted with changes in cropland. Investigating land use transitions among fallow, cropland, and pasture was thus our focus. To assess the possible effects of soil classes on each transition type (such as cropland to pasture or fallow to pasture), the area proportion of a given transition type on each soil class was calculated. In general, the areal percentage of six cover transition types (fallow to cropland, fallow to pasture,

cropland to fallow, cropland to pasture, pasture to fallow, and pasture to cropland) on five soil classes (i.e., classes 2 to 6) were computed.

5.5. Results

5.5.1. Spectral trajectory and accuracy

During a research period of 27 years, 64 LEDAPS products of the Landsat images were collected with the cloud-free cover greater than 50%. Because of the high cloud cover found in certain years (such as 1985, 1992, 1993, 2003, and 2010), two scenes or more were used to fill these areas.

Using segmentation and regression fitting approaches on Normalized Burn Ratio (NBR), changes in land covers were successfully captured by the Landtrendr model (Fig. 5.8). In forest region, short abrupt change of forest cover due to clear-cut and recovery process after disturbance was well captured by the model (Fig. 5.8-A). The same results were achieved on long-duration disturbance and stable forest. In the non-forest cover, permanent cropland is characterized by level fitting line (i.e., no-change) with a high variation of source values around the mean (Fig. 5.8-B). Spectral profile of non-disturbed shrub shows a slight increase in trend over time with low variation (Fig. 5.8-C). Deforestation for cropland or abandoned cropland was captured by the model (Fig. 5.8-D, Fig. 5.8-E). From the fitted line, characteristics of cover disturbance/recovery, such as time, magnitude, and duration, can also be mapped. Additionally, long-term stable forest cover was well separated.

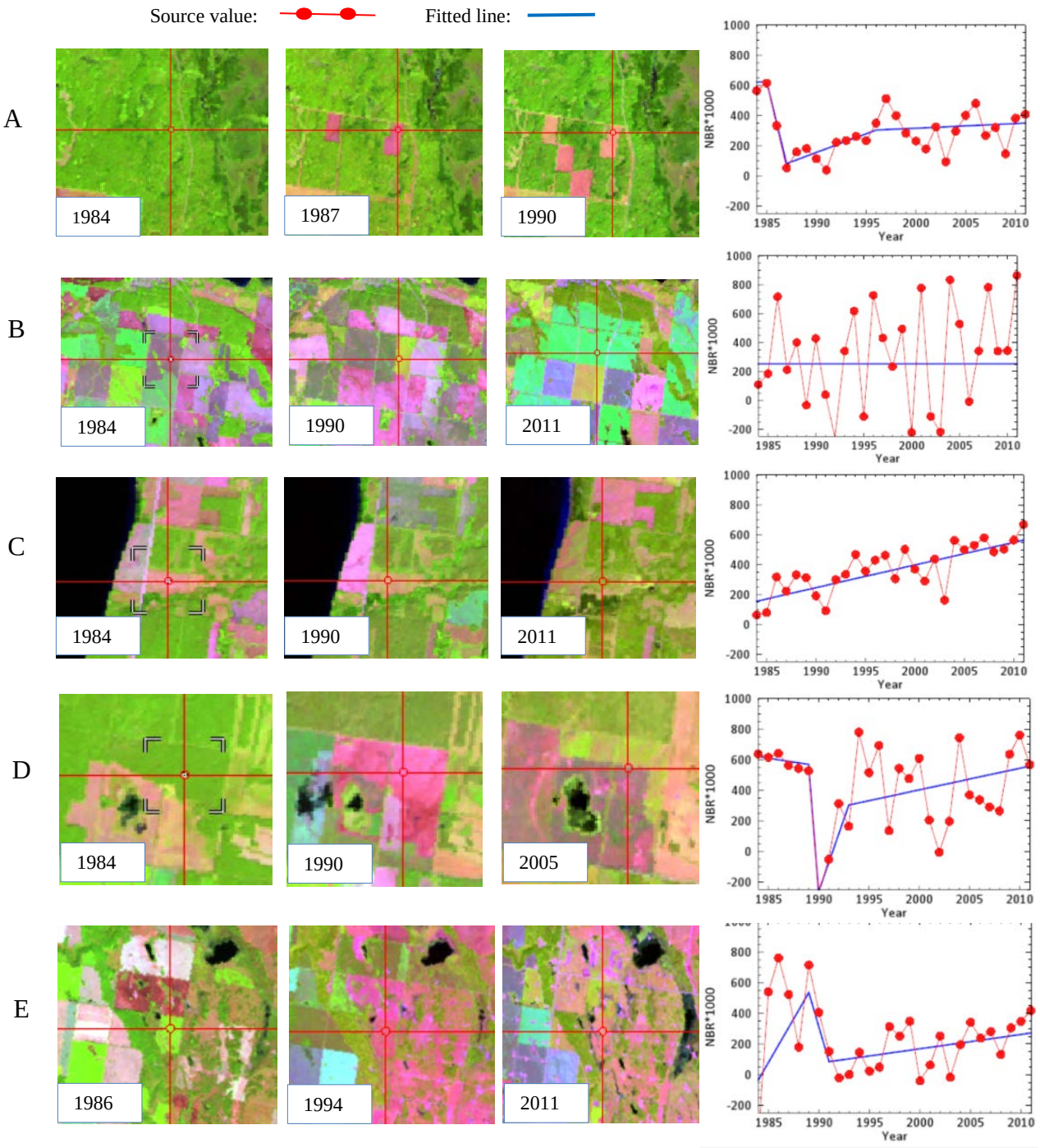

Fig. 5.8 Examples of Landtrendr model trajectory using Normalized Burn Ratio (NBR) derived from Landsat bands 4 and 7; A: Forest disturbance followed by slow recovery; B: Permanent cropland; C: Long-duration recovery; D: Forest disturbance followed by cropland; E: Abandoned cropland.

The Landtrendr model yielded a reliable map of forest disturbance in the Agri-Forest transition region with the overall accuracy of 90% (Table 5.1 and Table 5.2). The Commission and Omission errors in Non-forest (NF) and Stable forest (SF) were low, ranging from 4 to 15%. Commission errors were varied with the highest value of 40% in 1994 and lowest of 0% in 1986 and 1987. The highest Omission errors ranged from 0 to 39%, and the highest error value found in 1986 (39%). The detail on accuracy assessment is presented in Table 5.2.

Table 5.1 The Accuracy assessment results in the disturbance map showing commission and omission errors (SF= Stable forest; NF = Non-forest).

Disturbed year	**Commission error**	**Omission error**
	%	
1985	30	0
1986	0	39
1987	0	26
1988	10	10
1989	0	5
1990	20	6
1991	10	28
1992	5	0
1993	5	0
1994	40	25
1995	10	10
1996	15	0
1997	20	11
1998	5	14
1999	25	0
2000	5	14
2001	5	0
2002	10	5
2003	0	0
2005	10	0
2006	30	0
2007	35	0
2008	5	10
2009	15	6
2010	10	0
SF	9.5	4
NF	4	15
Overall accuracy: 90%		

Table 5.2 Confusion matrix resulting from the validation of the predicted disturbance map.

Disturbed year	Ground truth																											Total
	1985	1986	1987	1988	1989	1990	1991	1992	1993	1994	1995	1996	1997	1998	1999	2000	2001	2002	2003	2005	2006	2007	2008	2009	2010	SF	NF	
1985	14	1	1	0	1	0	1	0	0	2	0	0	0	0	0	0	0	0	0	0	0	0	0	0	0	0	0	20
1986	0	20	0	0	0	0	0	0	0	0	0	0	0	0	0	0	0	0	0	0	0	0	0	0	0	0	0	20
1987	0	0	20	0	0	0	0	0	0	0	0	0	0	0	0	0	0	0	0	0	0	0	0	0	0	0	0	20
1988	0	1	1	18	0	0	0	0	0	0	0	0	0	0	0	0	0	0	0	0	0	0	0	0	0	0	0	20
1989	0	0	0	0	20	0	0	0	0	0	0	0	0	0	0	0	0	0	0	0	0	0	0	0	0	0	0	20
1990	0	2	0	0	0	16	1	0	0	0	0	0	0	0	0	0	0	0	0	0	0	0	0	0	0	0	1	20
1991	0	0	0	0	0	0	18	0	0	0	0	0	0	0	0	0	0	0	0	0	0	0	0	0	0	0	2	20
1992	0	0	0	0	0	0	0	19	0	0	0	0	0	0	0	0	0	0	0	0	0	0	0	0	0	0	1	20
1993	0	1	0	0	0	0	0	0	19	0	0	0	0	0	0	0	0	0	0	0	0	0	0	0	0	0	0	20
1994	0	2	0	0	0	1	2	0	0	12	0	0	0	0	0	0	0	0	0	0	0	0	0	0	0	0	3	20
1995	0	0	0	0	0	0	0	0	0	0	18	0	0	1	0	0	0	0	0	0	0	0	0	0	0	0	1	20
1996	0	0	0	0	0	0	1	0	0	1	1	17	0	0	0	0	0	0	0	0	0	0	0	0	0	0	0	20
1997	0	1	0	0	0	0	0	0	0	0	1	0	16	1	0	0	0	0	0	0	0	0	0	0	0	0	1	20
1998	0	0	0	1	0	0	0	0	0	0	0	0	0	19	0	0	0	0	0	0	0	0	0	0	0	0	0	20
1999	0	0	3	0	0	0	0	0	0	0	0	0	1	0	15	1	0	0	0	0	0	0	0	0	0	0	0	20
2000	0	0	0	0	0	0	0	0	0	0	0	0	1	0	0	19	0	0	0	0	0	0	0	0	0	0	0	20
2001	0	0	0	0	0	0	0	0	0	1	0	0	0	0	0	0	19	0	0	0	0	0	0	0	0	0	0	20
2002	0	0	0	0	0	0	0	0	0	0	0	0	0	1	0	1	0	18	0	0	0	0	0	0	0	0	0	20
2003	0	0	0	0	0	0	0	0	0	0	0	0	0	0	0	0	0	0	20	0	0	0	0	0	0	0	0	20
2005	0	0	0	0	0	0	0	0	0	0	0	0	0	0	0	0	0	1	0	18	0	0	0	0	0	0	1	20
2006	0	3	1	0	0	0	0	0	0	0	0	0	0	0	0	0	0	0	0	0	14	0	0	0	0	0	2	20
2007	0	1	1	0	0	0	1	0	0	0	0	0	0	0	0	0	0	0	0	0	0	13	0	1	0	0	3	20
2008	0	0	0	0	0	0	0	0	0	0	0	0	0	0	0	1	0	0	0	0	0	0	19	0	0	0	0	20
2009	0	1	0	1	0	0	1	0	0	0	0	0	0	0	0	0	0	0	0	0	0	0	0	17	0	0	0	20
2010	0	0	0	0	0	0	0	0	0	0	0	0	0	0	0	0	0	0	0	0	0	0	2	0	18	0	0	20
SF	0	0	0	0	0	0	0	0	0	0	0	0	0	0	0	0	0	0	0	0	0	0	0	0	0	181	19	200
NF		0	0	0	0	0	0	0	0	0	0	0	0	0	0	0	0	0	0	0	0	0	0	0	0	8	192	200
Total	14	33	27	20	21	17	25	19	19	16	20	17	18	22	15	22	19	19	20	18	14	13	21	18	18	189	226	900

SF= Stable forest; NF = Non-forest

5.5.2. Change pattern in forest and shrub

The summary of the area on each cover and associated proportion of change is presented in Table 5.3. It is estimated in forest and shrub that approximately 75 thousand ha was disturbed under different magnitudes (corresponding to 38% the total area). Of the main covers, nearly two thirds of the disturbed area took place in the forest, and the remaining portion occurred in the shrub cover. Forest clear-cuting for logging and farming were evident. The total regrowth area during the research period is about 76,000 ha. Of the regrowth area, nearly half was contributed from pasture cover. Forest and shrub also contributed approximately 30% and 20% regrowth area, respectively.

Table 5.3 Disturbance and recovery area during 1984 – 2011.

Covers	1984	Disturbance	Proportion	Recovery	Proportion
	ha	*ha*	*%*	*ha*	*%*
Forest	80,265.3	45,569.5	56.8	22,050.7	27.5
Shrub	49,366.2	29,842.7	60.5	16,972.3	34.4
Pasture	70,939.4			37,223.6	52.5
Total	**200,570.9**	**75,412.3**	**100**	**76,246.7**	**100**

The disturbed locations are depicted in Fig. 5.9. The disturbance map reveals that forest disturbance took place mainly in the northwest and center regions (in green colour code) during the 1980s. Fig. 5.9-A highlights an example of forest disturbance regions that occurred during 1986-1988. The rectangular shape of the disturbed patch in this example suggests forest harvesting and logging operational activities (in green). In the next decade (the 1990s), the disturbances spread all over research region and adjacent to non-forest cover. Those disturbed regions are more associated with shrub cover. From 2000-2011, cover disturbances took place mainly in the north and northeast region. Fig. 5.9-B shows an example of a large patch disturbed in 2004 located close to cropland and pasture. Fig. 5.9-C shows the disturbed patches during 2004 (orange) and 2011 (red). Some disturbed patches in the rectangular shape shown during 1985. Disturbance activities continued to occur in 1990, 1995, and 2006 with a similar size and shape suggesting forest

disturbances for cultivation (Fig. 5.9-D). The disturbance time map also shows that disturbance of most of the small patches occurred during the 1980s, and many sizable disturbed patches occurred in more recent decades.

The disturbance magnitude is highlighted in Fig. 5.10. The high-magnitude disturbances (i.e., major cover changes associated with clear cutting) occurred in large patches in the forest region and were spatially clustered at the fringe areas between forest and cropland (in yellow to red). Fig.5.10-A is an example of high-magnitude disturbance; the patches in red and yellow are likely associated with forest stand removal while patches in blue and cyan, which experienced relatively lower-magnitude disturbance, may be signs of selective harvesting. Fig. 5.10-B shows an example of forest disturbance for cultivation characterized by a regular shape and high-magnitude disturbance (greater than 80%, in red). This capture also highlights the harvesting roads, which are a relatively higher-magnitude disturbance (continuous lines) (Fig. 5.10-C). Fig. 5.10-D is an example of forest disturbances for cultivation (red), which lead to removal of vegetation cover and exposed bare soil and result in the maximum disturbance magnitude. This is different to that in the previous example (Fig. 5.10-C), where land surface was probably covered by understory and debris left after harvesting activities. Low-magnitude disturbance presents mainly in the northwest region, where the dense canopy is dominant, and relatively higher-magnitude disturbance appears in the center region.

The greatest tree recovery during the research period was captured by the model and the year that trees initiated the greatest rate of recovery are presented in Fig. 5.11. Recovery year examined only from 1985 to 2007 as a regrowth duration less than 4 years was excluded. Recovery (green) took place mainly in north part of research area during the 1980s. During the 1990s, substantial recovery turned up in many parts of research areas, clustering to the northwest, southwest, and northeast regions (Fig. 5.11-A). Fig. 5.11-B and Fig. 5.11-C are examples of vegetation recovery initiated in 2003 after forest disturbances and natural succession in pasture after 1987, respectively. Another example of vegetation recovery during 1985-1990 from a cultivated region is presented in Fig. 5.11-D.

The magnitude of recovery is relatively low. Fig 5.12 shows that vegetation recovery took place all over the research region. Very low-magnitude recovery under natural regrowth within the

dense forest or shrub shows up at the northwest region (dark blue). High-magnitude recovery is located mainly on shrub and pasture dominated areas (light cyan). Fig. 5.12-A shows regrowth patches after forest harvesting activities (dark blue or light cyan) as well as no recovery (in grey). The disturbances in the forest for cultivation as in Fig. 5.12-B shows as both no regrowth (grey) and very high-magnitude recovery (in red). Trajectory analysis revealed that this change was the consequences of quick regrowth in a short time period of annual crops (data not show). An example of regrowth after forest harvesting is presented in Fig. 5.12-C. It appears that natural regrowth brings about lower recovery magnitude in the forest, but this may not be the case in the agriculture region because high regrowth magnitude also appears in some unimproved pasture regions. Fig.5.12-D includes no regrowth detected by the model under forest to pasture conversion (at the center of the capture, in the grey rectangle).

The disturbed areas in function of time over the research period (1985-2011) is summarized in Fig. 5.13-A. In forest cover, the mean annual disturbed area is 1752 ha per year, corresponding to 0.02 % of the forest area analyzed. Over time, the total disturbed area fluctuated and reached a peak in 1990, marked as the largest disturbances in a year (approximately five thousand ha). Another increasing trend was initiated during the period of 1992 - 2003 with a peak in 2003 (approximately four thousand ha). In terms of area, forest disturbances during the following years (2004-2011) were much low. The disturbance area initiated before 1985 accounts considerable portion, 37% (or 17309 ha). In the shrub cover, the mean disturbed area over the research period is 1147 ha per year, relatively smaller than that in forest cover. This area is equivalent to 0.03% of the total examined shrub area. The yearly disturbed area of shrubs increases gradually during 1986 – 1990 and dropped in the following years. An increasing trend initiated in 1995 and ended with a peak value of 2.1 thousand ha in 2000; the disturbed area since 2001 was relatively low without an obvious trend. In general, the trend in disturbance in this cover over the research period is similar to that in the forest.

The magnitude of disturbance in the forest and shrub is grouped in 10% interval and presented in the Fig. 5.13-B. In forest cover, more than a half of the disturbed area experienced low-magnitude disturbance (<30 %). The low-magnitude disturbed area is nearly 33 thousand ha, corresponding to 72% of the total forest disturbed area. In the shrub cover, the disturbed area

associated with the magnitude of 20-50% is dominant, but the differences within the area between the magnitude groups are well-defined.

Disturbance patch size is an important indicator for characterizing fragmentation and disturbance regimes; this information, therefore, was extracted. The statistical data show that the mean disturbed patch size values for forest and shrub are 0.65 and 0.40 ha, respectively (data not shown). Although the means of disturbed patch size are different among the land covers, no obvious pattern in each cover over time was observed. In order to highlight anthropogenic disturbances, we excluded patch size less than 5 ha as most of these patches were associated with low magnitude disturbances. In forest cover, disturbed patch size during 1985-2004 fluctuated around a mean value of 11 ha. However, the mean patch size values in the following years dramatically increased, especially in 2005, 2007, 2009, and 2011 (Fig. 5.14-A). The mean patch size during 2005-2011 is 26 ha with the peak value of 47 ha in 2005. The mean disturbed patch size of the shrub is stable over the research period with no obvious pattern. Fig. 5.14-B illustrates the disturbed duration in the two covers. It is obvious from the figure that disturbance duration ranges from 1 to 27 years for all covers, but the 1 - 3 year is the prevalent group. The area proportion associated with this duration group accounts for 52% and 55% in the forest and shrub cover, respectively.

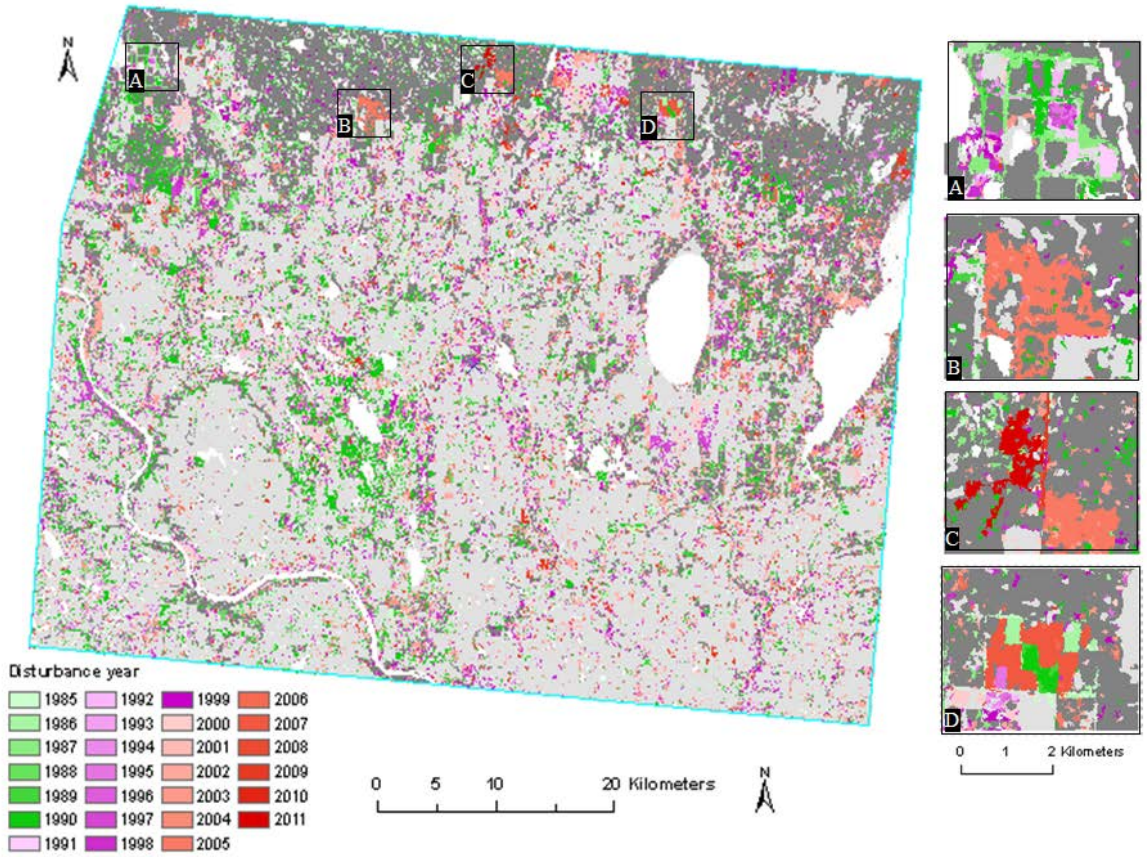

Fig. 5.9 Maps of disturbance year (highlight colours); water bodies in white, non-forest in light grey, no-change forest in dark grey.

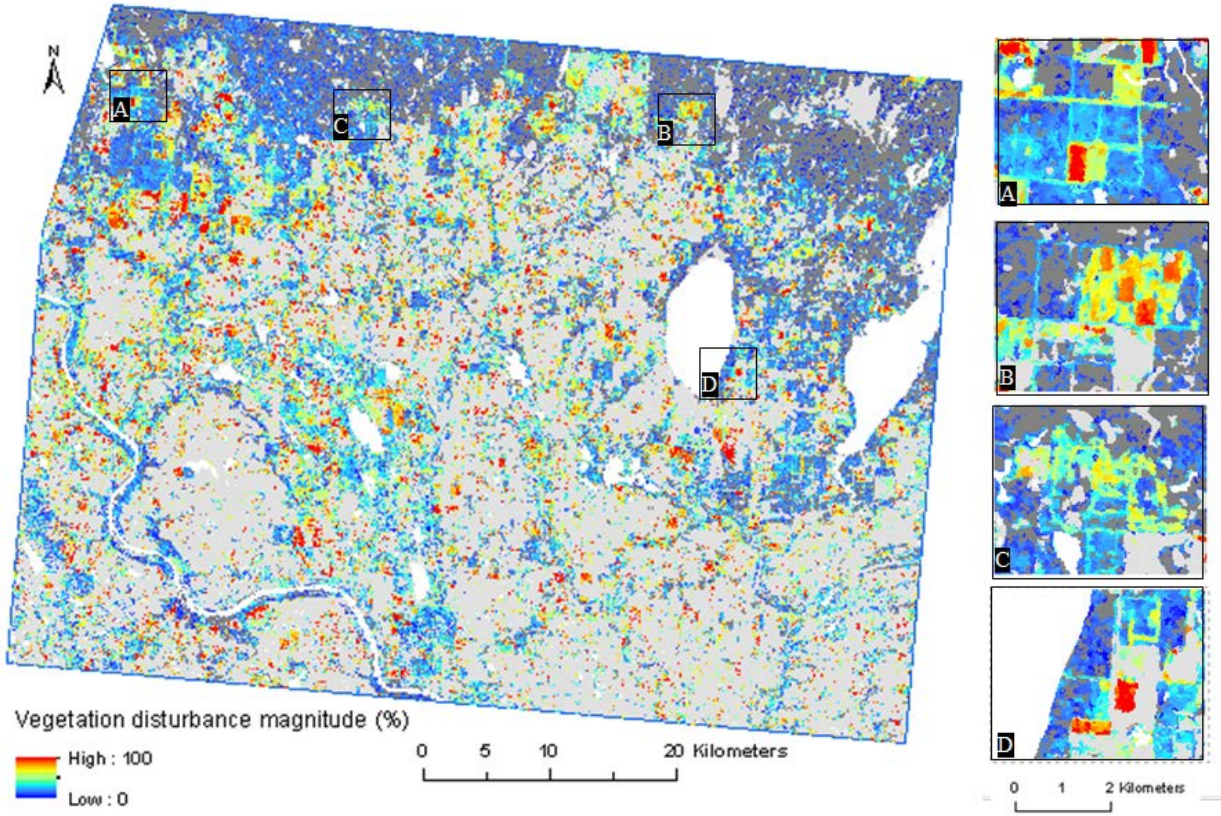

Fig. 5.10 Maps of disturbance magnitude (highlight colours); water bodies in white, non-forest in light grey, no-change forest in dark grey.

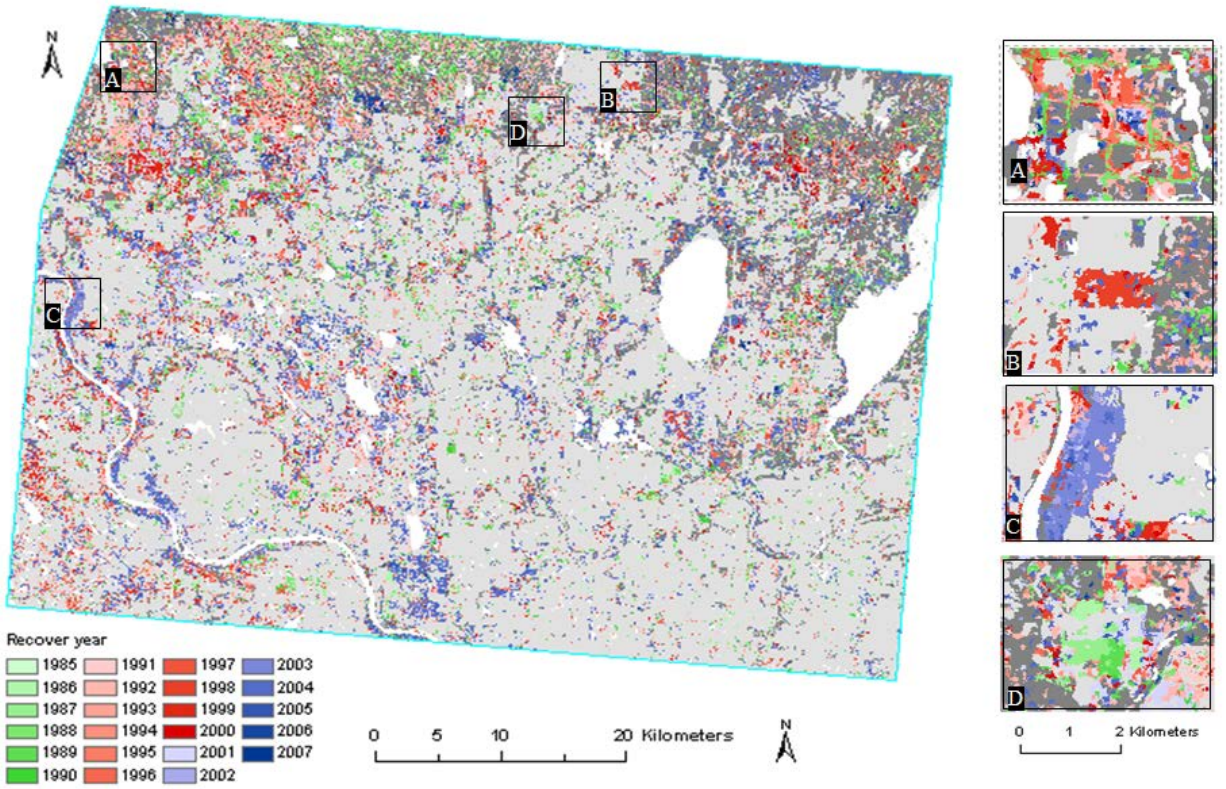

Fig. 5.11 Maps of recovery year (highlight colours); water bodies in white, non-forest in light grey, no-change forest in dark grey.

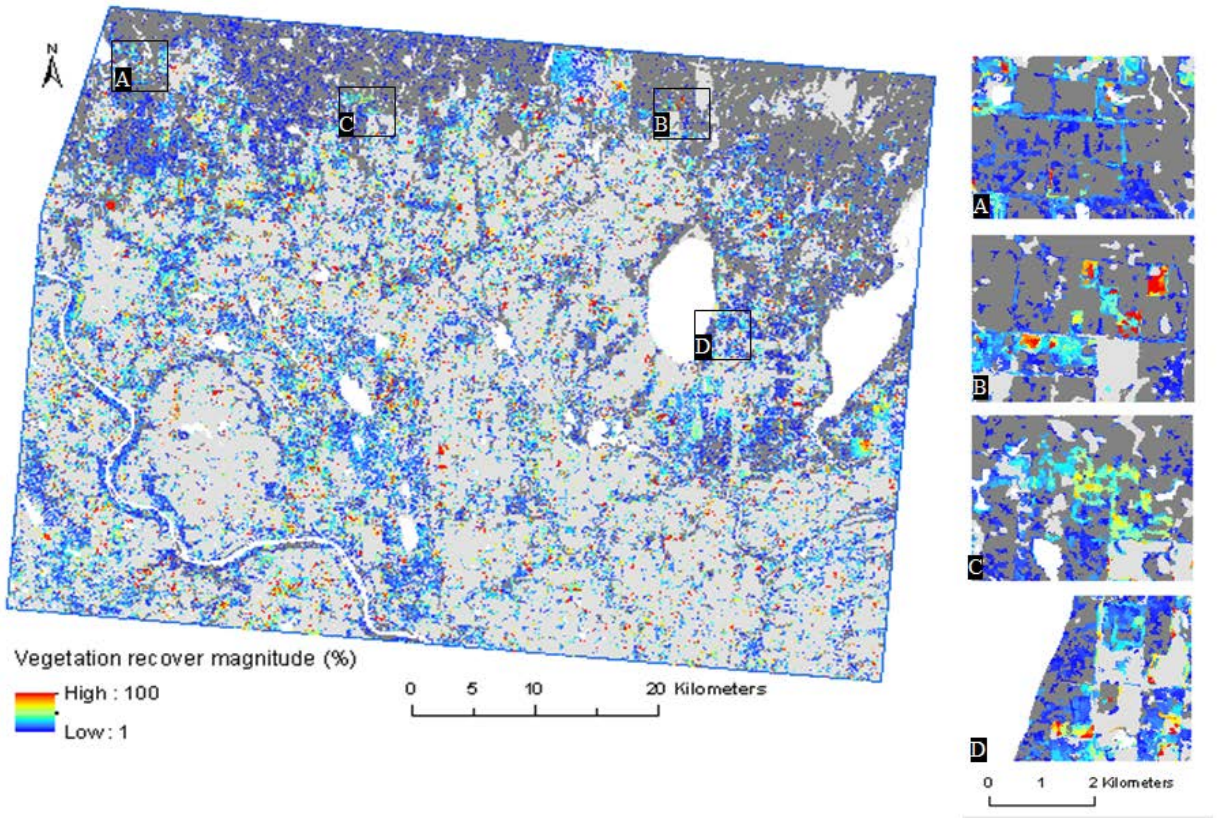

Fig. 5.12 Maps of recovery magnitude (highlight colours); water bodies in white, non-forest in light grey, no-change forest in dark grey.

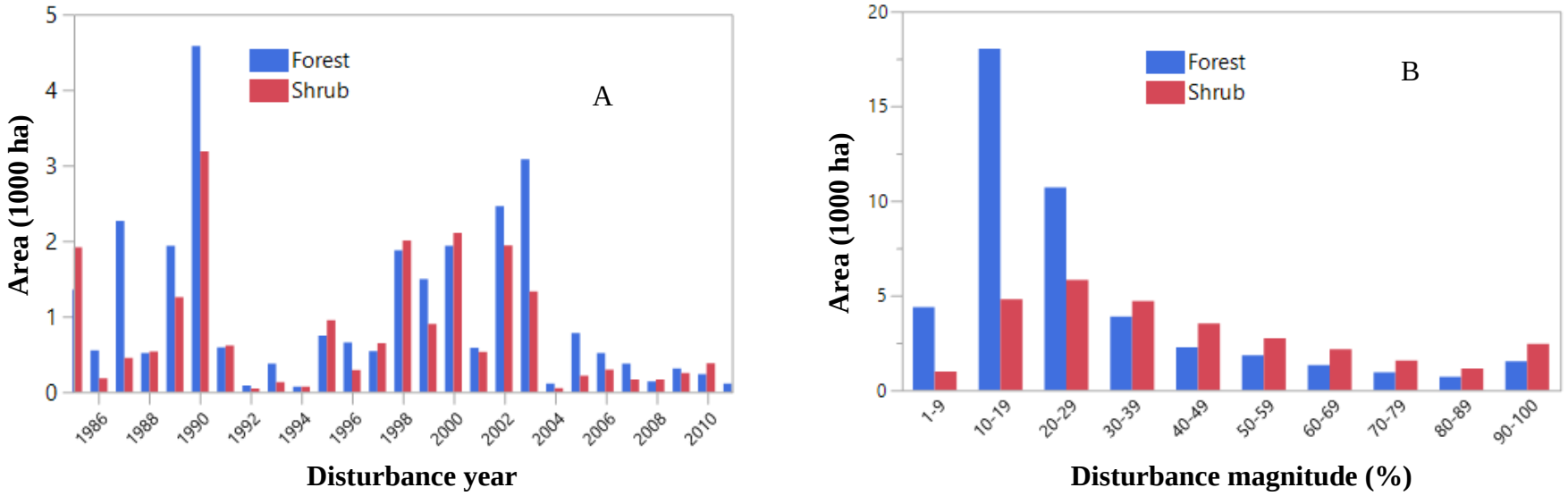

Fig. 5.13 Disturbance characteristics of forest and shrub during 1985 – 2011: (A) Total disturbance area by year; (B) Total disturbed area associated with different magnitude of disturbance classes.

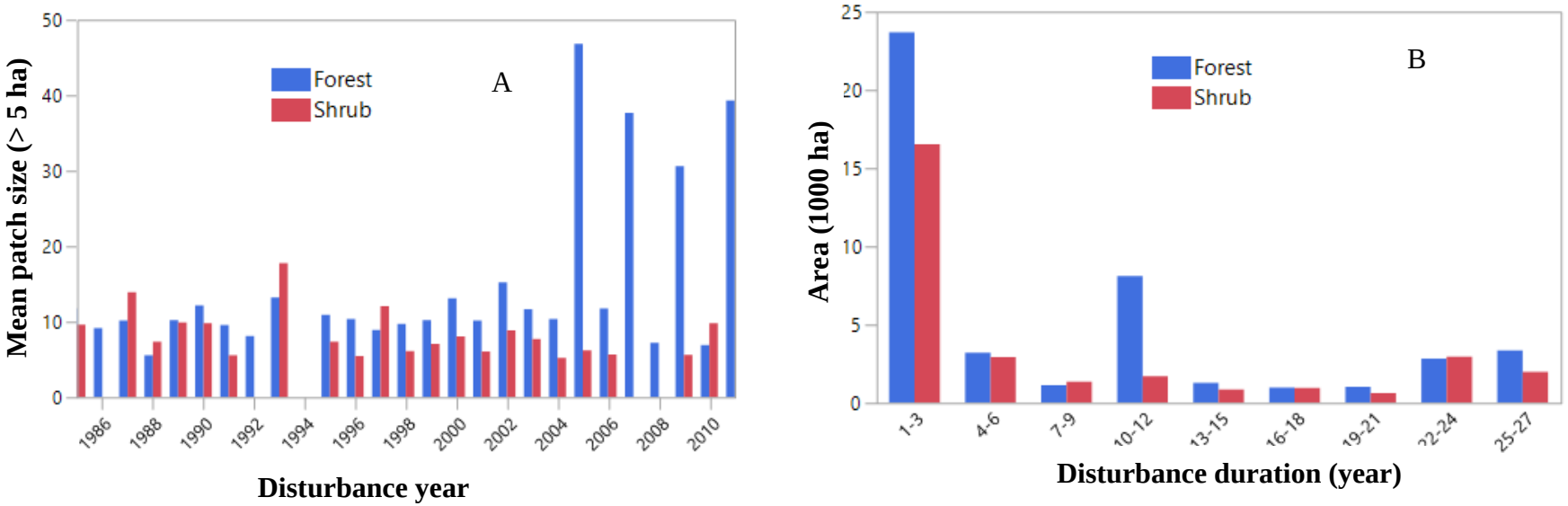

Fig. 5.14 Disturbance characteristics of forest and shrub during 1985 – 2011: (A) Mean disturbance patch size over the research period; (B) Total disturbed area for different duration of disturbance classes.

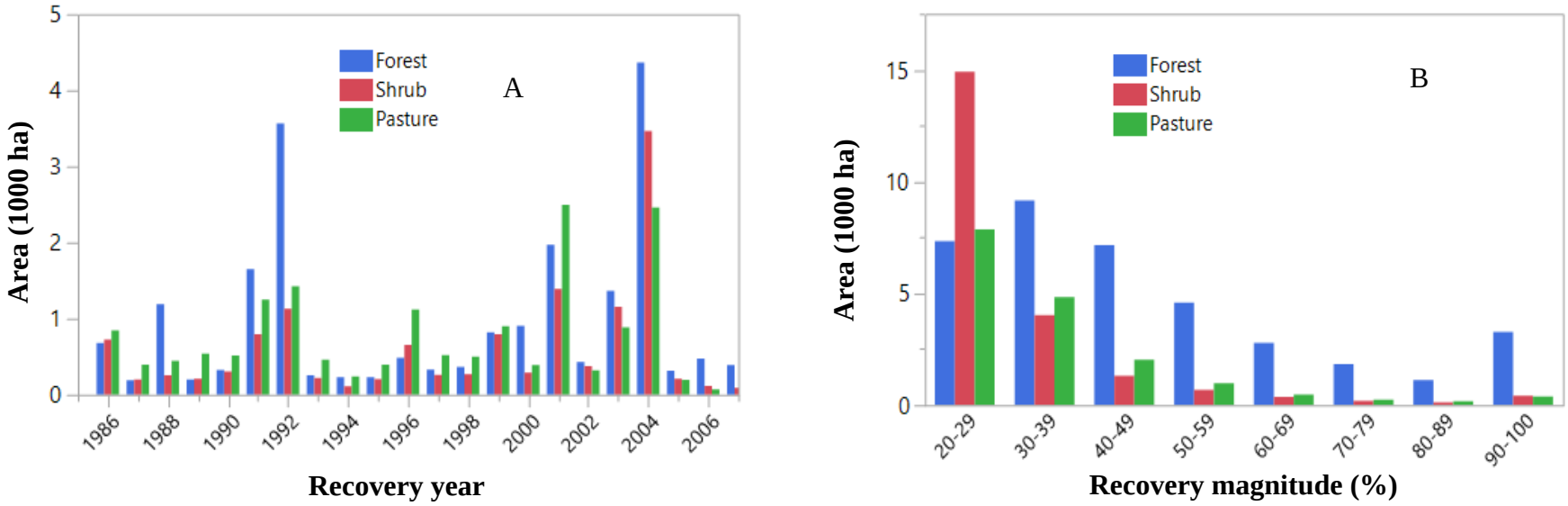

Fig. 5.15 Recovery characteristics of forest, shrub, and pasture during 1985 – 2011: (A) Area distribution over time period, (B) Area distribution on the different recovery magnitude classes.

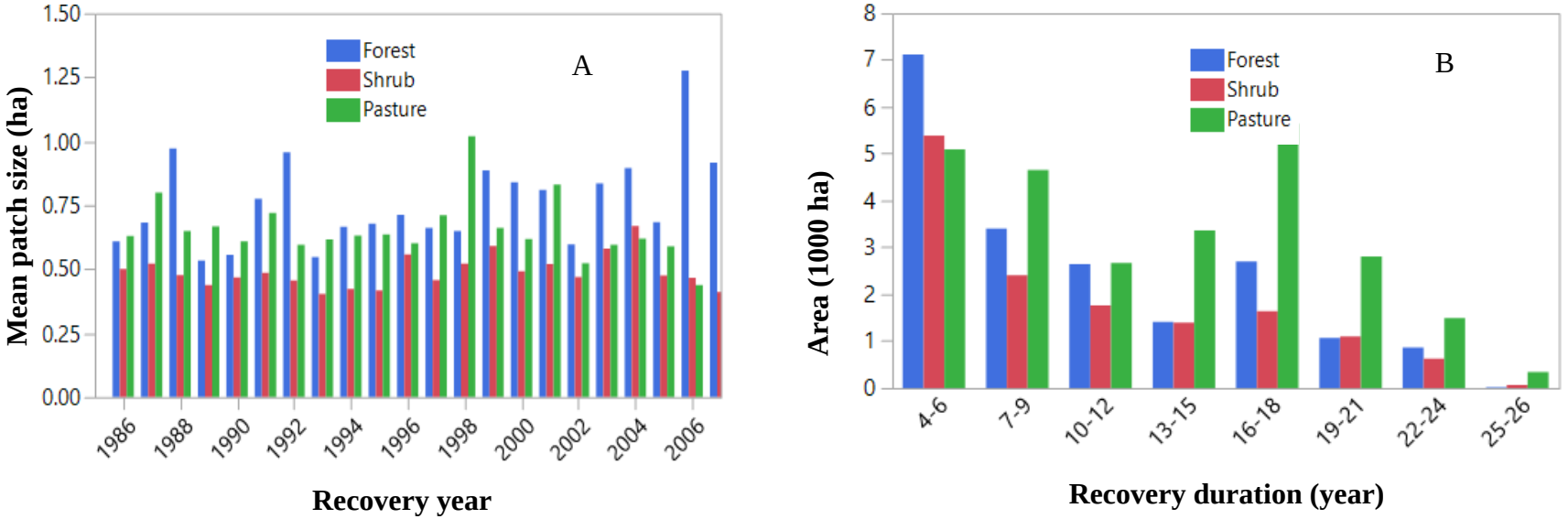

Fig. 5.16 Recovery characteristics of forest, shrub, and pasture during 1985 – 2011: (A) Mean recovery patch size over the research period, (B) Area distribution on different recovery duration classes.

Vegetation recovery could take place in forest and shrub (after disturbance events) and non-forest through natural succession (mainly from pasture). Therefore, recovery characteristics in the forest, shrub, and pasture during 1985-2011 were summarized (Fig. 5.15). The recovery area of the three covers fluctuated over the research period 1985-2007 with the mean of 920, 707, and 1551 ha per year in the forest, shrub, and pasture, respectively (Fig. 5.15-A). In the forest, the recovery area has fluctuated since 1986 with peaks in 1992 (nearly 4 thousand ha). Forest recovery area during the next period (1992 to 1997).

Forest recovery area gradual increased and got peak in 2004 (approximately 4.4 thousand ha), The area of recovered initiated during 2005-2007 is comparatively small. The pattern of recovery of the shrub is similar to pasture with a peak value in 2004 of 3.5 thousand ha. Fig. 5.15-B illustrates recovery magnitude (%) in the three different covers. While the area of shrub and pasture covers is clustered in the recovery magnitude class of 20-29%, the area proportion of forest cover recovery is distributed equally among the first three groups. In the pasture, recovery initiated before 1985 was 20.1 thousand ha, accounting for 56% total recovery area for pasture. After 1985, the recovered areas initiated in 1992, 2001, and 2004 are dominant, with areas of 1.4, 2.5, and 2.4 thousand ha respectively. The mean regrowth area in the remaining years is 1.5 thousand ha.

The average patch size values for recovery of the three covers ranged from 0.3 to 1.3 ha (Fig. 5.16-A). Mean patch size of forest cover fluctuated greatly between 0.5 to 1.3 ha, while these values in pasture ranged between 0.4 and 1.06 ha. Mean patch size of shrub was in the range of 0.4 to 0.6 ha, and the variation among the values in shrub is more stable than that in forest and pasture covers. Recovery duration ranged from 1 to 27 years, but the duration less than four years may not be important to a land-cover change study and therefore only recovery durations greater than four years were included. The area distribution of recovery duration groups is presented in Fig. 5.16-B. Of the 22 thousand ha of recovery in the forest, the highest area shows in the first group (4-6 years), which accounts for about 35% area.. A similar pattern was observed in the 17 thousand ha of shrub cover. In the pasture, not much difference was observed among the duration groups, and most of the recovery region (60%) associated with long duration (more than 12 years).

5.5.3. Land-use change and soil classes

5.5.3.1. *Land use classification and accuracy*

The overall accuracies for the two classified maps, 1984 and 2011, were 96.2% and 93.3% and the kappa values were 0.95 and 0.91, respectively (Table 5.4). In the table, producer's and user's accuracies were calculated and presented for all land use categories. The number of ground truth points used for accuracy assessment were also included in the table. For 1984 classified map, the accuracies were high, ranging from 92.54% (pasture) to 98.4% (forest) for producer's accuracy; and 89.19% (fallow) to 99.42% (cropland) for user's accuracies. For the land use map in 2011, producer's and user's accuracies were also high, ranging from 77.8% (shrub) to 98.1% (forest). Relatively lower producer's accuracy of shrub class was due to the misclassification of shrub into pasture and forest classes.

Our research approach distinguished five main land use classes for 1984 and 2011 over an area of approximately 373,000 ha. The land-use classification maps of 1984 and 2011 are summarized in Table 5.5 and in Fig. 5.17 and Fig. 5.18. Annual cropland, which is located mainly in the southwestern part, was the dominant cover in 1984, corresponding to 23.7%. The forest is the second largest area, accounting for about the same portion as annual cropland, 21.5% in 1984, and the forest cover is located mainly in the northern part of the research area. Over the research period, there was a slight decline in the area of forest to 18.1% after about three decades of change. In 1984, pasture accounted for a comparably small portion and was located mainly on areas adjacent to forest or water bodies. This land use expanded considerably relative to other land uses, resulting in an increase from 19% in 1984 to 33.6% in 2011, becoming the dominant land use in 2011. Shrub occupied a proportionally small area (13.3%) during 1984 and decreased to 9.1% in 2011. However, the extent changes are not obvious on the land use maps because this class has relatively small patch size. The fallow class, which intermingled with cropland, accounted for 6.6% in 1984. At the end of the research period, the proportion of fallow was 0.8%, and has almost disappeared from the land use map in 2011. The "other" class, which includes water, wetland, developed/residential, and roads, occupied approximately 59 thousand ha or 15.8% of the total area.

Table 5.4 Classification accuracy results for the land use maps of 1984 and 2011.

Land use	1984			2011		
	n	Producer's accuracy	User's accuracy	n	Producer' accuracy	User's accuracy
		(%)			*(%)*	
Fallow	34	97.06	89.19	25	92.0	79.3
Cropland	175	98.29	99.42	140	92.1	96.3
Pasture	67	92.54	98.41	97	96.9	92.2
Shrub	30	83.33	89.29	27	77.8	91.3
Forest	64	98.40	91.43	54	98.1	96.4
	Overall accuracy		96.2%	Overall accuracy		93.3%
	Kappa		0.95	Kappa		0.91

Table 5.5 Land use classification results for 1984 and 2011.

Land use	1984		2011	
	Area	Proportion	Area	Proportion
	ha	*%*	*ha*	*%*
Fallow	24,643.4	6.6	3,013.3	0.8
Cropland	88,182.4	23.7	84,325.7	22.6
Pasture	70,961.8	19.0	125,307.4	33.6
Shrub	49,406.0	13.3	33,774.9	9.1
Forest	80,699.0	21.7	67,471.3	18.1
Others	58,833.9	15.8	58,833.9	15.8
Total	**372,726.5**	**100**	**372,726.5**	**100**

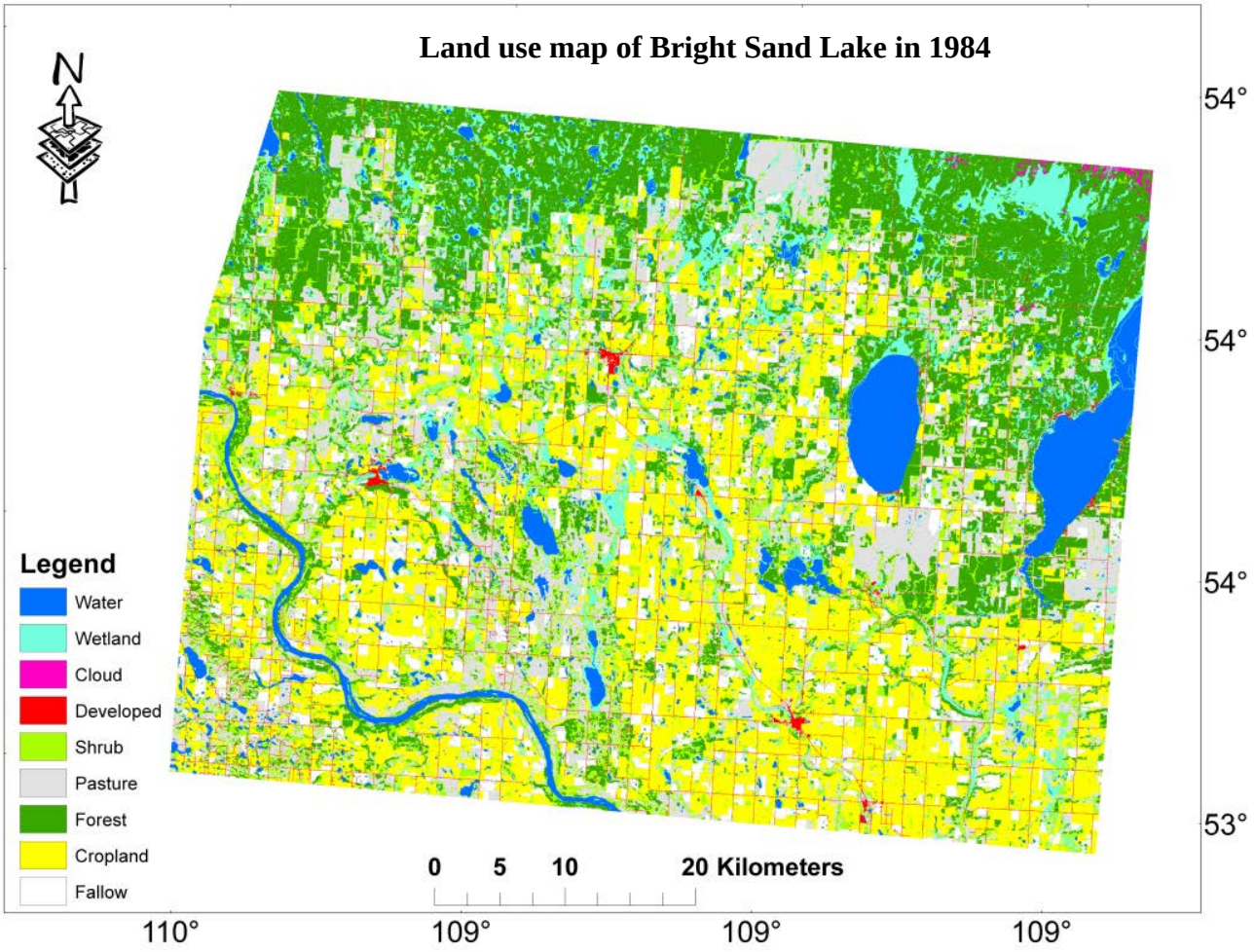

Fig. 5.17 Classification results of the land use in 1984 at Bright Sand Lake, Saskatchewan.

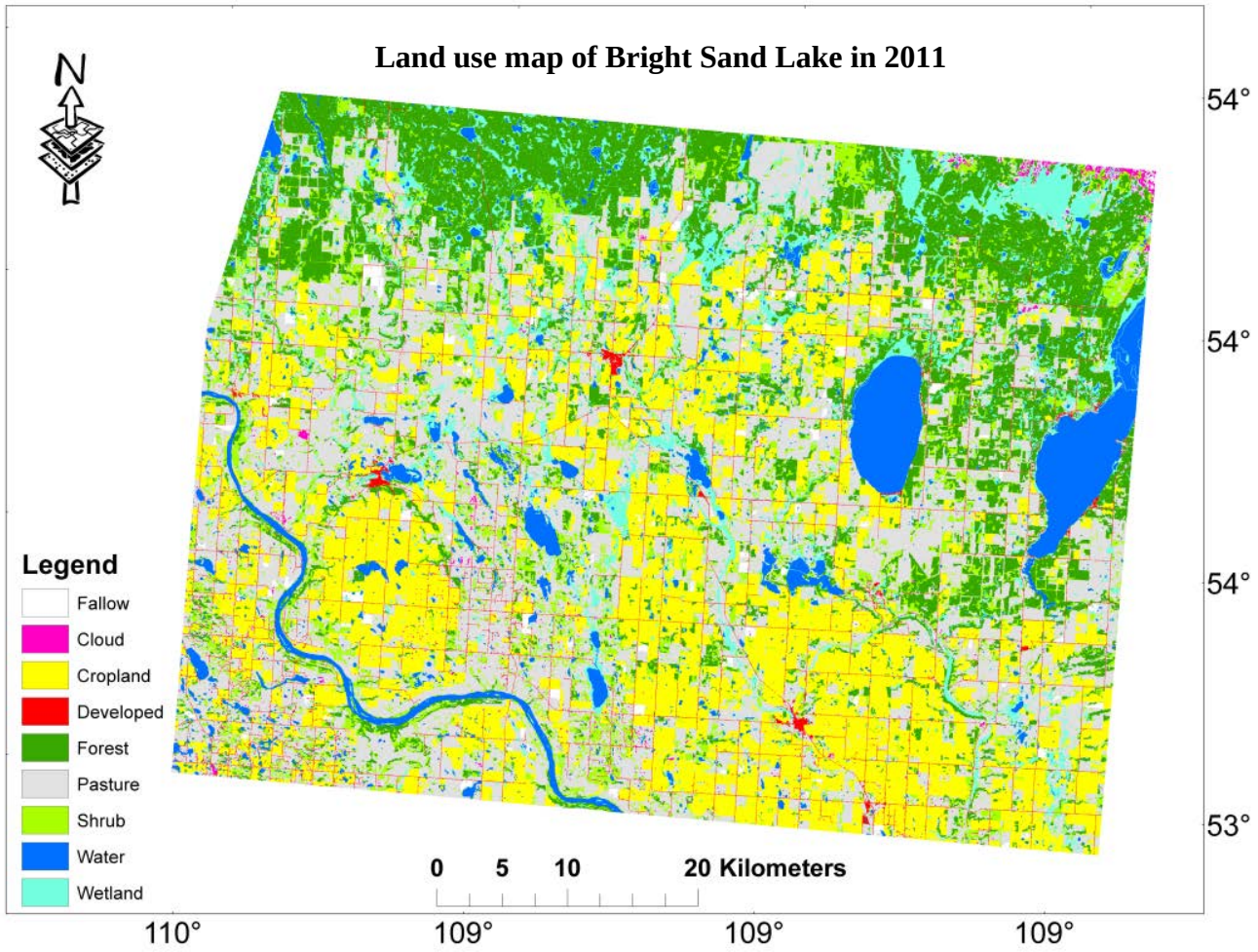

Fig. 5.18 Classification results of the land use in 2011 at Bright Sand Lake, Saskatchewan.

5.5.3.2. *Land-use change during 1984-2011*

Transitions among land use classes between the two points of time are presented in Table 5.6. In the matrix table, the area transitions of the five entered land use classes were presented with a total area of 313,892.5 ha. The five land use classes are Fallow (summer fallow), Cropland (annual crops), Pasture, Shrub, and Forest. The diagonal values show the area that did not change over the research period. The off-diagonal values indicate area converted from one land use to the other ("from" and "to" conversion). The consequence of changes, including the total area in 2011, expansion area, reduction area, are included in this table. The area in 1984 was used as a basis to calculate the proportion of changes (percentage of expansion and reduction).

Pasture experienced the greatest change during the period; while approximately 70% of this land remained unchanged, 29% (in 1984) of the area was converted into other classes (mainly to cropland). At the same time, a considerable expansion of pasture (more than 75 thousand ha) was also recorded, resulting in a substantial increment in the land use class. The increment in pasture came mainly from cropland (25% in 2011) and shrub (17% in 2011). Consequently, pasture became the dominant land use in 2011, accounting for approximately 40% of the entire research region.

In cropland, a total of approximately 52 thousand ha (60%) did not change while a considerable area (more than 30 thousand ha) was converted into pasture (35%). Over the period, cropland expanded more than 32 thousand ha, and this area is equivalent to 37% of the total cropland area in 1984. The highest proportion was from fallow (38%) and pasture (32%). Expansion of cropland to forest and shrub was relatively small, accounting 1252 ha and 2668 ha, respectively. However, all the above transitions caused in a slightly net change of cropland with a decline of approximately 4 thousand ha over the period.

Fallow experienced the highest change in terms of area proportion, a reduction of 98% of its original area. Although expansion is observed, the additional area to fallow was relatively small. Consequently the fallow class, which accounted for more than 24 thousand ha in 1984, declined to 3 thousand ha in the end of the research period (1% total area in 2011). The cessation of summer fallow practices in the last decades could be the main cause of this transition and considerable area

proportion of the class (50%) was transferred to cropland in 2011. Additionally, a remarkable transition from fallow to pasture was also observed.

The transitions of shrub and other land use categories were noticeable, but the most active exchanges were between shrub and pasture. During the period, approximately 75 thousand ha (44% in 1984) of shrub was converted into pasture, and this causes the largest area reduction in this land use category. Conversely, nearly 7 thousand ha of pasture (20% in 2011) and more than 12.5 thousand ha of forest (37% in 2011) were converted into shrub, respectively. The transition caused a net decline of 15.6 thousand ha in shrub.

Forest experienced relatively small change compared to other classes with approximately 70% area marked as no change. The highest loss of forest was to pasture (14% in 1984) and shrub (15% in 1984) while the gain of forest area came mainly from the shrub (10% in 2011). Consequently, the expansion of 13 thousand ha and reduction of 26 thousand in forest resulted in a net decrease of 13 thousand ha. In short, land-use change s during 1984 and 2011 at Bright Sand Lake of Saskatchewan was remarked by some major conversions such as (1) fallow, cropland, shrub, and forest to pasture, (2) fallow and pasture to cropland, and (3) forest to shrub.

Table 5.6 Land use transition between 1984 and 2011.

Land use		1984					Total 2011	Expansion area‡
		Fallow	Cropland	Pasture	Shrub	Forest		
		ha						
2011	Fallow	501.0	1,576.5	456.3	283.9	195.6	3,013.3	2,512.3 (10%)
	Cropland	12,406.3	51,806.6	10,341.7	7,750.5	2,020.5	84,325.7	32,519.1 (37%)
	Pasture	10,632.1	30,879.1	50,522.4	21,749.9	11,523.9	125,307.4	74,785.0 (105%)
	Shrub	548.1	2,668.1	6,841.2	11,236.5	12,481.0	33,774.9	22,538.4 (46%)
	Forest	555.9	1,252.0	2,800.2	8,385.1	54,478.1	67,471.3	12,993.2 (16%)
	Total 1984	24,643.4	88,182.4	70,961.8	49,406.0	80,699.0	313,892.5	
	Reduction area	24,142.4 (98%)	36,375.8 (41%)	20,439.4 (29%)	38,169.5 (77%)	26,221.0 (32%)		

‡ Percentage values were calculated by taking expansion/reduction value in each land use class divided by area of that class in 1984 to show the magnitude of reduction/expansion.

5.5.3.3. *Land use transition associated with CLI classes*

To assess the influence of CLI soil classes on land-use change, the distribution of CLI classes over the research area and the distribution of selected land-use transition on CLI classes were analyzed. The general distribution of land use classes during 1984 and 2011 on CLI soil classes across the research area is presented in Fig. 5.19. Among the six different CLI classes, the cropland and pasture classes were distributed mainly in classes 2, 3, and 5 while forest was distributed broadly in soil classes 3, 4, and 5. Shrub was distributed on almost all soil classes except for class O.

Changes in land-use on soil classes were quite dynamic across the research region. In pasture, the no-change area was mostly in class 3 (41%) and 5 (33%). The conversion of pasture to cropland occurred on almost all soils, including classes 2 (33%), 3 (33%), and 5 (27%) while the expansion on shrub was mainly on soil classes 5 and 3 (35% in each class). Conversely, the conversion of pasture to cropland was concentrated on soil class 2 (38%) and 3 (33%). This reveals that changes in pasture were influenced by soil classes because pasture on more highly rated soils was converted into cropland while cropland on less fertile soils were converted into pasture. Additionally, land-use changes "from" and "to" pasture did not result in considerable changes in area proportion among the soil classes, but the absolute change in area on soil classes 2, 3, and 5 were positive in the end period (Fig. 5.19).

Cropland experienced a slight decrease in the total area during the research period due to the substantial conversion "to" pasture. At the same time, the area of this class also added "from" fallow and pasture. Fallow to cropland conversion occurred in the main on class 2 (54%) and class 3 (28%). This transition indicated that the more fertile soil (class 2) in fallow was converted into cropland through the reduction in summer fallow practice while the less suitable soil was converted to pasture use. Forest to cropland accounted for a very small proportion, and these transitions took place on soil classes 2 and 3 mainly (70%). Overall, land-use change associated with cropland resulted in positive area change in soil classes 2 and 4 and negative changes on soil classes 3, 5, and 6.

A noticeable change occurred in shrub during the research period. In parallel to the conversion of shrub to pasture, pasture to shrub and forest to shrub also contributed considerably

to changes in shrub area. Of the pasture to shrub conversion, 40% of the converted area (2862 ha) took place on soil class 3, and 32% (2159 ha) occurred on soil class 5, and area proportions of the other soil classes in relation to this transition were relatively small. Forest to shrub conversion turned up in all soil classes, but the transition occurred dominantly on class 3 (53%), 4 (11%), and 5 (21%). It is reasonable that this transition was less related to soil classes, which were also soil capability for agriculture, as forest harvesting (not for cultivation) was the cause of this change.

To highlight the major land-use transitions (in terms of area) on soil classes, the spatial extent of the selected transitions are mapped and presented in Fig. 5.20. Because all land-use transitions can be mapped, the overlaying of all land-use transition classes on a soil map may not be an effective way to highlight the meaningful changes. Some transitions may cause a permanent change of land use (such as forest to cropland) while other transitions result in a temporary change only (such as fallow to cropland). To simplify the output map and focus more on permanent transitions, fallow and cropland were merged into cropland (in map legend), and only selected conversions were presented, including cropland to pasture, pasture to cropland, forest to shrub, forest to pasture, and forest to cropland. Moreover, two other transition groups, namely cropland and pasture to forest and cropland and pasture to shrub, were included.

Overall, cropland to pasture was the dominant transition, and the transition was located randomly over the research area. Cropland and pasture to forest (dark green), which indicates the vegetation gain during the period, was characterized by small patches located edging to forest (data not shown). Similar spatial distribution was observed in cropland and pasture to shrub transition. Forest to cropland accounted for a very small area, but this transition includes both large (northwest region) and small patch sizes. These could be the consequence of both farm expansion (small area) and deforestation (large patch size). Forest to pasture took place mainly in the north and northwest parts of the study area. Most of forest disturbance patches occurred immediately adjacent to cropland or pasture. Similarly, forest to shrub distributed mainly at the transition region with the relatively larger patch size. Evidence from aerial photos suggests that these shrub patches were the consequences of natural regrowth after forest harvesting. Pasture to cropland shows a random pattern with considerable patch size. In general, cropland to pasture, forest to shrub, forest to cropland, and forest to pasture are the most obvious transitions, which were characterized by large

patch size and area, and the figure also suggests that loss would be greater than gain in woody biomass.

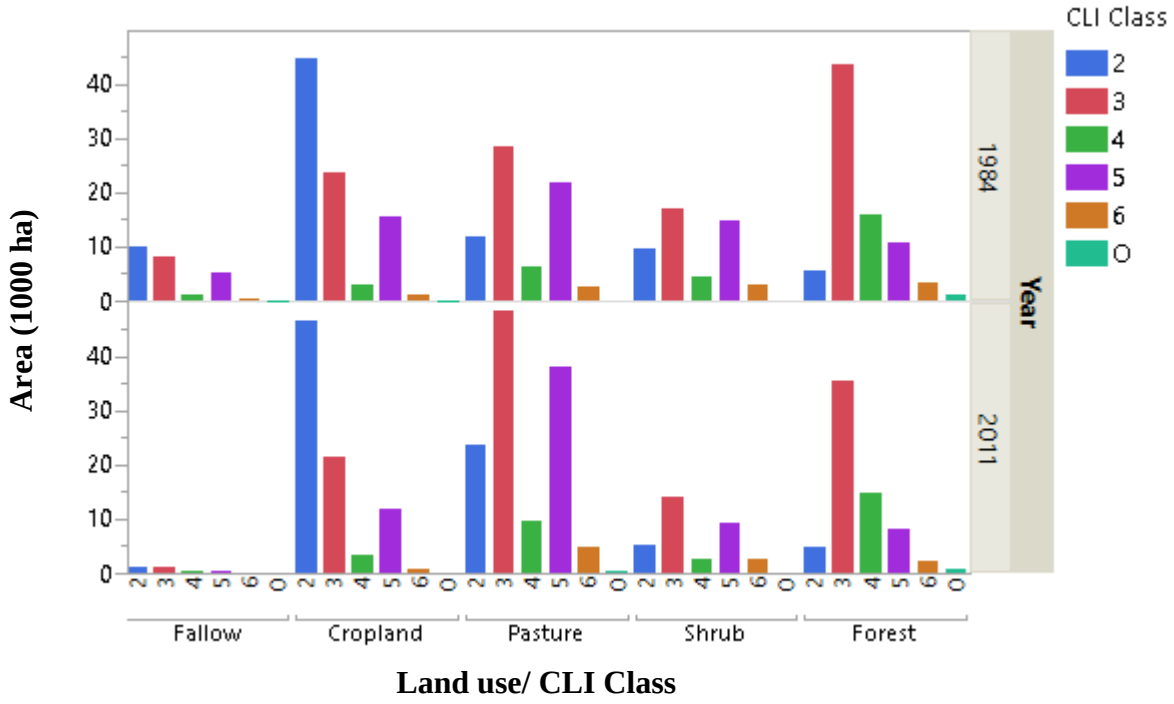

Fig. 5.19 Specific land use transitions on CLI classes at Bright Sand Lake, Saskatchewan.

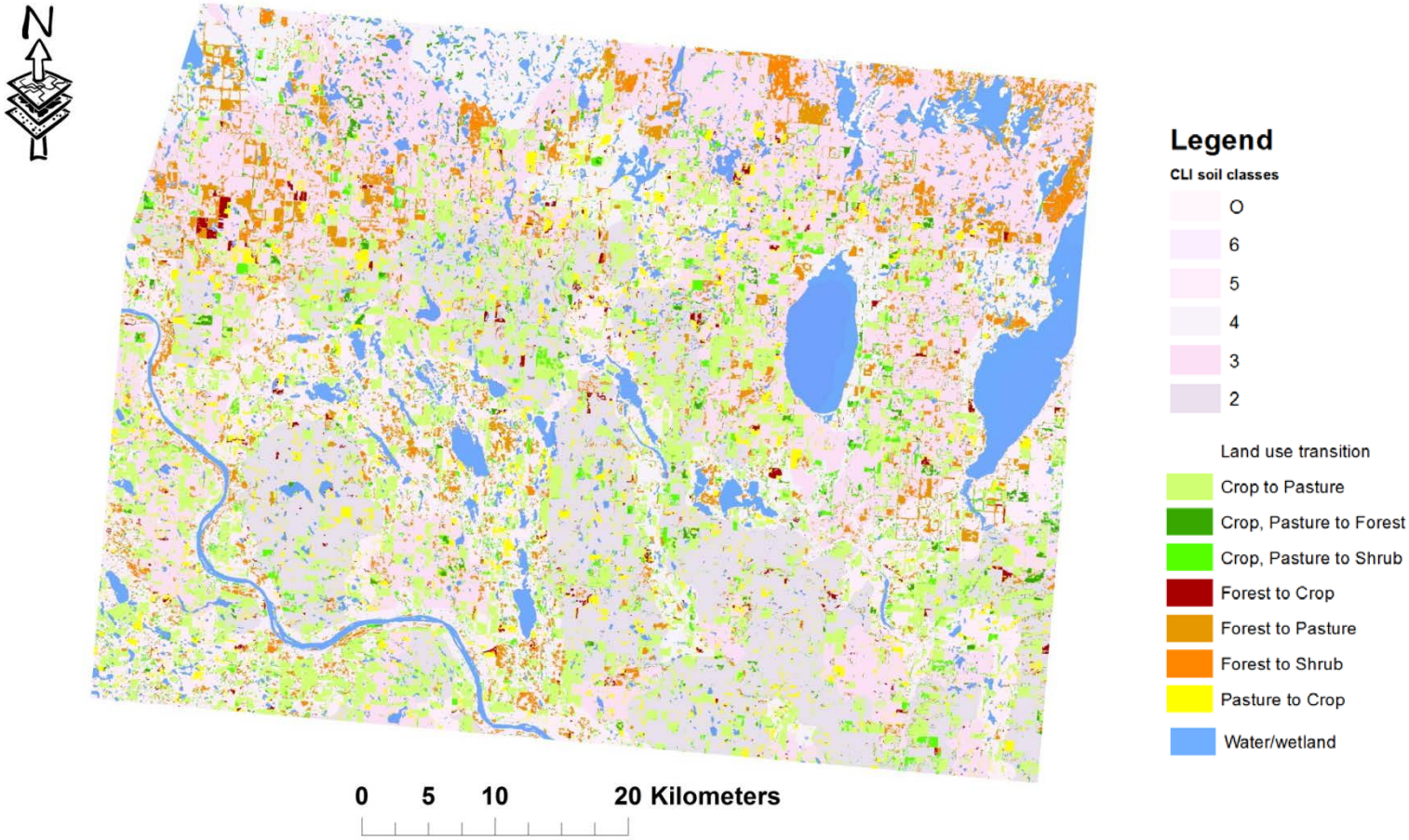

Fig. 5.20 Selected land use transitions during 1984 – 2011 at Bright Sand Lake, Saskatchewan.

5.6. Discussion

In this paper, we applied Landtrendr model, a spectral trend based analysis, to 27 years Landsat TM data to detect and characterize changes in the forest, shrub, and pasture over the agricultural-forest transition area in central Saskatchewan. To achieve the research objectives, 64 Landsat TM products acquired during 1984-2011 were collected. Data pre-processing includes cloud masking, mosaic, and data normalization over the research area of 3700 km^2. The assessment results indicate that the model has a high capacity for capturing cover changes with high spatial and temporal accuracy (Table 5.2). Additionally, the model provides some attributes of change including magnitude, patch size, duration of a disturbance and regrow event.

The overall accuracy of the disturbance map is high (90%). Although the commission and omission errors of some classes were greater than 25%, the majority ranged from 0% to 25%. The highest commission errors were in 1986, 1987, and 1991 classes. High omission errors in the first years of the time series are likely caused by the performance of the fitting algorithm; it is probable that high index values in the first years of the time series were considered as outliers. For 1988 – 2011 classes, misclassifications were associated with differences in image acquisition dates, which are strongly associated with phenology and illumination changes. High cloud cover percentage in some images (such as 1985, 1987, 1994) yielded lower accuracy. It is likely that changes in illumination caused by cloud cover strongly affected the data signals although contaminated pixels were carefully masked. The overall accuracy of 90% in our disturbance map is lower than that of Griffiths et al. (2012), who obtained an overall accuracy of 95.72% using the same approach. The complexity in land covers of the Agri-Forest transition region could be an additional reason.

Although identifying drivers of cover changes is not our main aim in this study and beyond the scope of this study, some potential drivers from previous research can be mentioned. Current studies suggest that cover changes in research area might be associated with some disturbed agents, including drought, pests, deforestation for cultivation, and fire (Brandt et al., 2003; Hermosilla et al., 2015; Hogg et al., 2005). Our disturbance map reveals that high magnitude disturbance regions, which cause considerable stand replacement, occurred mainly in the north part of the research area (Fig. 5.7). The available ground truth points (from aerial photos) and disturbed patch size and shape also suggest evident of forest harvesting and deforestation for cultivation. It seems that the

major cause of stand replacement in the agricultural-forest transition area is different to that in the northern region, where forest fire is the major cause of forest disturbance (Hermosilla et al., 2015). In short, high disturbance magnitude during the research period induced stand replacement, resulting in cover changes.

The output map also highlights the lower disturbance magnitude, which is characterized by no-stand replacement and relatively longer duration of disturbance. This largely occurred during 1990 and in the period from 1998 to 2003. Relating this changing pattern to the weather record (Fig. 5.4) suggests that precipitation and temperature might have contributed to the changes as some current research shows strong correlation evident between climatic variation and vegetation growth, including aspen stands (Hogg et al., 2008; Huang et al., 2010b). Through investigations the impacts of climate moisture index, a measure of drought severity or water stress induced by low soil moisture, on aspen productivity in the western Canadian interior, Hogg et al. (2013) reported that droughts cause multi-year decreases in aspen growth. Change detection results in our study did not separate causes of disturbance, but relatively high disturbed area initiated during the severe drought during 2001 -2003 might be a sign of climate impact on vegetation growth (Fig. 5.13). In another study, Michaelian et al. (2011) also reported that drought was the main cause of massive mortality and dieback of aspen in the transition region between boreal forest and prairie, western Canada in the last decades. It was also evident from the study that the severe drought during 2001-2003 caused the mortality and dieback of aspen. Additionally, pests (insect outbreak and fungal pathogens) might have also played a role in intensifying and prolonging the growth reductions of aspen stands as their populations are sensitive to climatic variations (Volney and Fleming, 2000). Brandt et al. (2003) addressed pests, such as tent caterpillar and root diseases as one of the major agents (after age and drought) affecting trembling aspen health, which induces damages such as crown dieback and severe stem lean, in the Prairie Provinces of Canada. Similarly, while short duration disturbances (less than 2 years) associated with abrupt changes such as stand replacement, long duration disturbances (greater than 3 years) were evident in non-replaced stands.

Landsat time series in a temporal segmentation algorithm of Landtrendr is a successful approach for studying land-cover change of in forest region. Collecting ground truth data for validation was one of the challenges in this study, so only disturbance magnitude greater than 20%

in forest region was validated and accuracy assessment has been done for pasture and shrub. In the agriculture region, changes in land-use and land cover were not fully captured by the Landtrendr model. Regrowth after cropland abandonment, for instance, was confounded with summer fallow practices or more intensive cropland over time. The research results of qualitative change maps in the forest region and quantitative change maps may be used to help in understanding the impacts of past environmental changes and farmer decisions in controlling the dynamics on land-cover changes. Our future work will focus on the identification of the drivers and impacts of land-cover change in the case study area. Detailing trends of land-use change in the agriculture region in relation to the limited factors available in the CLI soil capability classes.

The conversion of summer fallow to annual cropland on more fertile soils was the dominant change during the research period. Similar finding was reported by Zhang et al. (2014) in a study in Montane Cordillera ecozone, Alberta.

5.7. Conclusion

The results from this study demonstrate that land-cover change in the Agri-Forest transition the boreal forest of Canada changed dramatically during 1984-2011, and changes in agriculture varied with soil capability. This research is the first detailed cover changes in forest and shrub covers and land-use changes in the transition region between prairie and boreal forest.

More than a half of the forest was disturbed and most of the area occurred during 1987-1990 and 1998-2001, but one third of the area experienced low magnitude disturbance. Substantial highs in disturbed patch size associated with the forest harvesting in the recent year (2005-2011) was observed, and short disturbance duration (less than 3 years, indicating forest harvest) is dominant.

An approximately two-thirds of the shrub area was disturbed with relatively high magnitude. The average disturbed patch size was stable throughout the period, and most area was associated with short duration disturbance.

Recovery initiated during 1990-1992 and 2001-2004 was dominant for all covers. While most of the forest and shrub area experienced short recovery duration (less than 6 years), recovery area in pasture was distributed equally on most of the year groups. Recovery patch size and magnitude were low in general.

Over the research area, total area of summer fallow decreased dramatically between 1984 and 2011, and most of the area were converted to cropland and pasture. Transition of summer fallow to annual crops declined from better to poorer soil capability land.

More than one-third of cropland area was converted into pasture, and more transitions to pasture occurred on soils of poorer capability. Considerable area of shrub was converted into pasture. While a small portion of forest (2.7%) was converted into cropland and summer fallow, a considerable area portion of the cover was converted into pasture (14%).

The current study area of ~ 3700 km^2 is still small compared to the entire agriculture area in the BPE; therefore, expanding the study to other regions would be helpful in explaining land-use and cover changes.

6. SYNTHESIS AND CONCLUSIONS

Land use and land-use change have contributed significantly to CO_2 concentration in the atmosphere. Terrestrial ecosystems exchange C with the atmosphere through processes such as photosynthesis and respiration. According to one current estimation, total worldwide C in soil and biomass is 1912.2 Gt C, and 74% of the quantity stored in soil organic C (Scharlemann et al., 2014). However, when the land is disturbed, the stored C (and other GHGs) will be released to the atmosphere and become a C source. During 2004-2015, the total global C emissions were estimated to be 10.89 Gt C yr^{-1}; vegetation and soil were a C sink (land sink) of 2.98 Gt C yr^{-1} and also a C source of 0.92 Gt C yr^{-1}, resulting in a net sink approximately 2.06 Gt C yr^{-1} (Le Quéré et al., 2015). In 2012, Canada contributed 1.6% of the worldwide GHG emissions (CAIT, 2015). Carbon balance under land use, land-use change and forestry category acts as a C source of 72 Megaton CO_2 equivalents (Mt CO_2 eq) in 2014, accounting for approximately 9.8% the total Canadian GHG emissions (Environment and Climate Change Canada, 2016). Although the current estimation has provided a general view of C stock and its dynamics, the estimated outcomes have a large uncertainty, and further studies on C emission at different spatial scales on land-use change are needed (Houghton et al., 2012; Huffman et al., 2015; Lal, 2008).

My overall project had three parts. In the first part, I completed a field sampling project to provide data on the C changes associated with cropland abandonment in the boreal plains ecozone of Central Saskatchewan. This type of land use conversion had not been previously studied in this region, and is required for national C reporting purposes. In the second study I used data provided by AAFC on land-use change for nineteen sample plots from the BPE for the period from 1990 to 2000 to model the effect of these changes on ecosystem C. The C stock simulation was completed with the CBM-CFS model of the Canadian Forest Service, and the data for cropland abandonment from the first study was used in this simulation. In the final study the research on land-use change and land-cover change was scaled up to a larger area of approximately 4150 km^2. This study focused primarily on innovative remote sensing methods to improve our estimates of land cover

and land-use change. In this section I will synthesize the results of this final study with the C change values presented in the earlier studies.

6.1. Summary of Findings

Land use conversion can be a C source or C sink (Houghton, 1995). The abandonment of cropland, for example, could act as an ecosystem C sink. After several years of abandonment, early successional vegetation will begin to grow and increase the rate of C sequestration, primarily by increasing belowground and aboveground biomass. Abandoned cropland in European Russia, Ukraine, and Belarus, for instance, has accumulated ecosystem C at a rate of 0.77 Mg C ha^{-1} yr^{-1} (Schierhorn et al., 2013). In Canada, abandonment of cropland has been widespread in eastern and central Canada since the 1950s (Ramankutty and Foley, 1999b). Benjamin et al. (2005) investigated the vegetation composition of abandoned cropland and Foote and Grogan (2010) quantified C sequestration in different soil orders. In the western part of Canada, afforestation on marginal lands, including abandoned cropland, shows very high potential for C sequestration in willow plantations, which could accumulate up to 4.6 Mg C ha^{-1} yr^{-1} in the BPE (Amichev et al., 2012). In the same ecozone, a recent study also suggests the potential of C removal under the forest/shrub transition in the agriculture area (Huffman et al., 2015). However, information on the extent, C stocks, and the potential for C sequestration in both ecosystem and individual pools under natural regeneration to forest or shrub has not been investigated explicitly. Additionally, under the IPCC guidelines for national greenhouse gas inventories, abandoned lands are also suggested for inclusion (IPCC, 2006). A study in the BPE is particularly important to provide primary information on abandoned cropland and role that the land could play in Canadian C budget.

In 2012, I completed a field study to investigate the spatial distribution of abandoned cropland within the BPE of Central Saskatchewan. The main objective of this study was to determine C stock, distribution, and changes at specific research sites. Archived aerial photos acquired during 1960 - 2000 were collected and overlaid on a GIS software (ArcMap) to detect fields. Six old fields were identified at the three main regions (Bright Sand Lake, Witchekan Lake, and Redberry) with the period since cultivation ceased ranging from 9 to 41 years. The sites have the same soil order (Chernozem), dominant tree species (trembling aspen, *populus tremuloides*),

disturbance history (cultivated), and ecozone (BPE), but they differ in stand ages. Field data on SOC and biomass from distinct pools (tree, shrub, herb, dead wood, litter, and soil) were collected.

My results provide a new view of the extent of abandoned cropland, including field characteristics, C density in different C pools, as well as C accumulation rate over time. The total abandoned area is 123 ha, and the average field size is 21 ha. The area of abandoned land is relatively small compared to that of the cultivated area, although the current approach (aerial photo detection) may underestimate the actual situation. Carbon density in the soil pool to 45 cm depth of the abandoned cropland ranged from 58.8 to 113.7 Mg C ha^{-1} with a mean value of 79.3 Mg C ha^{-1}. A very high variation of C density among sites was observed. Soil organic carbon accumulated mainly in the first 15-cm depth. It was evident that SOC accumulation occurred after abandonment with a mean of 0.35 Mg C ha^{-1} yr^{-1}. The SOC accumulation rate seems to decrease with time, but more sample points are needed for a reliable conclusion. Carbon stock in vegetation ranges from 7.6 to 90.1 Mg ha^{-1} and tree biomass is the major contribution. Ecosystem C, which is the addition of C from all C pools, changed from 74.2 Mg C ha^{-1} from the 9-year site to 137.6 Mg C ha^{-1} in the 27 year-site. C in abandoned cropland was accumulated in all pools, but C accumulation occurred mainly in the vegetation pool. In general, cropland abandonment in the BPE of Saskatchewan is not common; nonetheless, it shows high potential for C sequestration due to higher biomass productivity under trembling aspen regeneration.

The outcome of our first study on abandoned cropland contributed new information on C density and distribution in each pool. The accumulation rate of C from each pool is also important for ecosystem C estimation at larger spatial scales. A single land-use change, such as cropland abandonment, accounts a small portion of the changes. Quantification of C resulting from interactions of all land-use types at a larger spatial scale is thus important for having a broad view about land-use change and the C budget in an ecozone. In Canada, quantification of C stock and dynamics is required for all managed land as part of Canada's commitment to the UNFCCC. Across the country, AAFC conducted a study to quantify the contribution that agriculture land makes to the national C balance (Huffman et al., 2015). Although the contribution of C from woody biomass is minor in the agricultural region, research results from national C balance studies show a positive change in C sequestered from woody biomass in the agriculture region of the boreal plains ecozone during 1990 - 2000.

My second study focused on quantifying the land-use change and associated ecosystem C balance at a series of research plots in the agriculture area of the BPE during 1990 – 2000. The total area of change (addition of losses and gains) was quantified instead of net change (subtraction of the two periods) for each land use category. A single transition in land use could result from many factors and I explored the links between land-use change and soil characteristics. This could help to assess if a soil characteristic(s) can be used as a predictor for future land-use change. Carbon balance was estimated by a model (CBM-CFS3) that includes C stock and dynamics in all carbon pools.

To achieve the research objectives, data were collected from multiple sources, including reference data, field sampling, and archive data. The data on land-use transitions were extracted from the AAFC data, and soil organic C was compiled from the National Soil Database (NSDB). The assumptions on tree age and biomass yield (or age-yield assumption) for different land-use categories were gathered from published data and field measurements. Chi-square test ($\chi 2$) was used to examine the relationships between soil characteristics and land-use change. Carbon stock and dynamics were simulated by a C inventory based model, CBM-CFS3. The pilot area used for modelling was 6174.25 ha, accounting for 0.02 % the total area of the ecozone (2.17 million ha).

Our research shows that among the thirteen land-use types, the conversions occurred mainly on cropland, abandoned cropland, and unimproved pasture. While substantial positive net changes in the pasture and abandoned cropland were observed, cropland area slightly decreased during the two periods. The increase of pasture was converted mainly from cropland and forest while the increase in abandoned cropland was from cropland and pasture. Overall, land-use change in the Boreal Plains ecozone was minor with the total change in each category less than 6% of the original area. Nevertheless, an increasing trend in the forest/shrub cover types was observed.

Cropland to pasture conversion occurred in relatively small areas located adjacent to water bodies or low-lying field areas and could be a result of navigation difficulties caused by the ever-increasing size of farm machinery. Cropland abandonment was found at field corners or next to lowland or wet areas but was difficult to explain based on spatial pattern of conversion only. The statistical results also indicated that poorly drained soils are more likely to be abandoned. Additionally, cropland was more likely abandoned in soils developed on acidic parent material.

Deforestation (forest to cropland) in the BPE was most likely in well-drained areas of Chernozemic and Luvisolic soil orders. No association was evident between deforestation and soil texture or soil chemistry.

The conversion of cropland to abandoned account 1.6 % of the original land use during the 10-year period. The conversion was significantly associated with poorly drained soil and acidic parent material. At the same period, approximately 16 % of abandoned cropland was converted to cropland and the transition was significantly regulated by drainage condition. The well-drained Luvisol soil order was most common for this type of conversion, while soil texture and acidity were not found to be associated with the conversion.

The total area of the 14 sample plots was 6174.25 ha, and the area of transition to forest/shrub accounted for 8% of the sample area (467.92 ha). The non-forest area of the BPE as a whole is 28.64 million ha; if we extrapolate the area of forest/shrub transition to the ecozone as a whole, this equals 2.17 million ha. Over the CBM-CFS simulation period (15 years), aboveground biomass and soil pools became a C sink, while belowground, dead wood, and litter was a C source. The aboveground pool accumulated C at a rate of about +0.08 Mg C ha^{-1} yr^{-1}. The accumulation rate in the soil pool was +0.83 Mg C ha^{-1} yr^{-1}. Of the three C sources, litter and dead wood pools released the same amount (-0.26 Mg C ha^{-1} yr^{-1}), while the annual emission rate in the belowground biomass was small (-0.07 Mg C ha^{-1} yr^{-1}). Knowing that the average NEP is 0.76 Mg C ha^{-1} yr^{-1}, we estimated that the transition to forest/shrub (2.17 million ha) in the agriculture region of the boreal plains ecozone accumulated 1649.2 Gg C yr^{-1}. Similarly, the average NBP is 0.32 Mg C ha^{-1} yr^{-1}; this translates into 282 Mg C per year from 1990 to 2000 for the whole research region (or 1.04 Mt CO_2 equivalents with a conversion factor of 3.67).

While emission from land use, land-use change, and forestry sector in Canada acted as a C net source of 72 million tons CO_2 equivalents in 2014 (Environment and Climate Change Canada, 2016), the transition to forest/shrub in the agriculture region of the BPE became a C net sink of 1.04 million tonne CO_2 equivalent per year. However, the annual C removal from the study region is relatively small, offsetting 0.015% of the total national greenhouse gas emission in land use, land-use change, and forestry sector.

In the previous study, land-use change, soil characteristics, and C stocks and dynamics in the agriculture-forest transition region were investigated using plot-scale input data. The advantages of using this data source include: (1) detailed information on land-use transitions, (2) an ability to associate change with soil characteristics, and (3) an ability to integrate C balance estimation systems. Nonetheless, ten years is a short period to monitor changes of land use and the area of plots was very small.

In my third study, I used Landsat data to explore land use and cover change at a larger spatial scale. The main objectives of the study include (1) assess land-cover change in a forest – cropland intersection region of Saskatchewan during 1984 - 2011, (2) mapping land-use change, and (3) investigating the association between soil capability for agriculture and land-use change. To achieve the first research objective, Landsat time-series data were prepared for a temporal trajectories change detection model, Landtrendr. The rate, location, and duration of any changes were extracted by temporal segmentation algorithm. The output maps were validated by field data, finer spatial resolution images such as SPOT, and aerial photos. The results of this component include areas, locations, and rates of land-cover changes at the regional scale.

For the second objective, a bi-temporal change in agriculture region was examined. Multi-spectral images in the years of 1984 and 2011 were collected and classified. Post-classification technique was applied to detect changes. Ground truth points collected from field surveys, and aerial photo interpolations were used to validate the output maps. For the third objective, a GIS data set of soil capability (or Canada Land Inventory - CLI) was collected from Agriculture and Agri-Food Canada (2014). The content of the map layer reflects rates of soil capability for agriculture (from most suitable [class 1] to no capability for arable culture [class 7]). Map overlaying of soil capability map and land use transition map were conducted on ArcMap software. This allows documenting the distribution of land use conversions on soil capability class and assessing the potential influence of soil capability on each type of land use transition.

The approach yielded a land-cover change map with high accuracy (90% overall). Both spatial and temporal information of cover change, including abrupt and chronic disturbances as well as ongoing vegetation regrowth were obtained. In the study region approximately 60% of the area of forest and shrub were disturbed with different magnitudes and less than 35% of the area

was mapped as regrowth with low magnitude. The major regrowth proportion (60% of the regrowth area) came from slow natural regeneration on undeveloped pasture.

The post-classification change detection approach resulted in land-use maps, which include the consequences of land-cover changes, with high accuracies (greater than 93%). Substantial net areal changes occurred in the summer fallow (-87%), pasture (+77%), and shrub (-32%). Changes in net area of cropland and forest were small, -4.4% and -16.4%, between the two points of time, respectively. The total disturbed area accounted for 46.3% with many conversions among the types of land-use. In relation to soil capability, the cropland and pasture classes distributed primarily in classes 2, 3, and 5 while forest distributed broadly on soil classes 3, 4, and 5. Shrubs were distributed on almost all soil classes except for class O. Substantial changes of summer fallow to annual cropland took place on the better soil capability (soil class 2), but annual cropland to pasture conversion was more likely on less fertile soil classes (soil class 3). The conversion from shrub to pasture was mainly on less fertile soil (classes 3 and 5). Forest to cropland accounted for a very small proportion, and these transitions occurred in soil classes 2 and 3 mainly (70%). Forest to shrub conversion (forest harvesting) occurred in all soil classes, but the transition occurred dominantly on class 3 (53%) and 5 (21%).

Over the research area, each transition type was characterized by a different spatial distribution. Cropland to pasture, for instance, was located randomly over the research area. Cropland/pasture to forest, which indicates vegetation gain during the period, was characterized by the small patches located on the edge of large forested patches. Similar spatial distribution was observed in cropland/pasture to shrub transition. The forest to cropland transition area was relatively small, but this transition includes both large and small patch sizes. Changes by farm expansion (small area) and deforestation (large patch size) could be the reasons. Most of the disturbed shrub and forest patches occurred immediately adjacent to cropland or pasture. Forest to shrub transitions had relatively larger patch size, and evidence from aerial photos suggests that these shrub patches were the consequences of natural regrowth after forest harvesting. In general, cropland to pasture, forest to shrub, forest to cropland, and forest to pasture were the most obvious transitions, which were characterized by large patch size, and the study outcome suggests that loss of woody biomass would be greater than gain.

From the land-use map, C stocks in the whole research area were estimated. On each land-use type, C density value was estimated based on our current field study and publication data conducted in the same ecoregion and sample depth (Table 6.1). Total ecosystem C for each land-use type was calculated by multiplying C density to the associated area. Accordingly, the research region experienced a decline in ecosystem C from 34.9 Tg C in 1984 to 33.8 Tg C in 2011 (1 Tg = 1 million Mg). This primary results suggest that C accumulation in the agriculture region during the last decades did not compensate the C loss under forest and shrub disturbances, including deforestation. Consequently, total C stocks in 2011 is lower than that in 1984 indicating C source of 1.1 Tg for the Agri-Forest transition region in the last three decades.

Table 6.1 Estimation of carbon stocks in the research area in 1984 and 2011.

Land use	C density	Total area		Total C stock		References†
		1984	2011	1984	2011	
	Mg C ha^{-1}	*1000 ha*	*1000 ha*	*Tg C*		
Forest	178.4	80.7	67.5	14.4	12.0	1, 3, 4, 5, 6, 10
Shrub	91.9	49.4	33.8	4.5	3.1	2, 3, 4, 6,7, 8, 9
Pasture	88.2	71.0	125.3	6.3	11.1	1, 4, 8
Cropland	86.7	88.2	84.3	7.6	7.3	1, 3, 4, 7
Fallow	83.7	24.6	3.0	2.1	0.3	11
Total		**313.9**	**313.9**	**34.9**	**33.8**	

† 1: Arevalo et al. (2011); 2: Bhatti et al. (2002) 3: current study; 4: Fitzsimmons et al. (2004); 5: Gower et al. (1997); 6: Kurz et al. (2013); 7: Pennock and van Kessel (1997b); 8: Pinno and Wilson (2011); 9: Stinson et al. (2011) 10: Seedre et al. (2014); 11: VandenBygaart et al. (2003)

Land-use transitions at a landscape scale can be a C source or sink depending on the changed area in each land-use type and the associated C change. To explore the potential effects of all changes in land-use on total C during 1984 - 2011, some estimated values collected from field measurements and publications were used. We assumed that land-use changes might cause long-term changes in soil C (>13 years) but changes in biomass C can be short (single change) or long-term (>13 years) depending on the transition. Additionally, the land use transition occurred one time in the middle of our research period (1998), and C gain from a forward transition is equal to C loss in the backward transition (and vice versa). The amount of C loss under forest to cropland, for example, is equal to the C gain from cropland to forest. Accordingly, the dominant land-use transitions were included, and the area in each transition reflects the net change area. The C loss in each transition category is denoted in negative value (-).

Table 6.2 Estimation of total C change under land-use conversions during 1984 – 2011.

Land-use transition	Area change	Soil C change	Biomass C change			Total C change	References‡
	1000 ha	*Mg ha^{-1} yr^{-1}*	*Mg ha^{-1}*	*Mg ha^{-1} yr^{-1}*	*Year*	*Gg*	
Fallow to Cropland	10.8	0.3	0.0	0.0	1	42.2	1, 4
Fallow to Forest	0.4	0.3	37.1	2.9	13	14.8	3, 10
Fallow to Pasture	10.2	0.4	1.0	1.0	1	68.4	3, 8
Fallow to Shrub	0.3	0.2	12.4	1.0	13	4.0	2, 6, 10
Cropland to Pasture	20.5	0.4	3.0	3.0	1	179.1	3, 9, 10
Forest to Cropland	0.8	-0.5	-50.0	-50.0	1	-43.4	3, 9, 10
Shrub to Cropland	5.1	-0.3	-9.5	-9.5	1	-64.8	7, 9, 10
Forest to Pasture	8.7	0.0	-53.0	-53.0	1	-462.4	3
Forest to Shrub	4.1	0.0	-40.0	-40.0	1	-163.8	5
Shrub to Pasture	14.9	0.0	-8.5	-8.5	1	-126.7	3, 10
Total						**-552.7**	

‡ 1: Boehm et al. (2004); 2: Foote and Grogan (2010); 3: Fitzsimmons et al. (2004); McConkey et al. (2000); 5: Peng et al. (2002) ; 6: Pinno and Wilson (2011); 7: Pennock and van Kessel (1997b); 8: Smith et al. (2001); 9: Wei et al. (2014); 10: Current study.

We estimate that the land-use change in the Agri-Forest transition region is a net C source of 552.7 Gg C (1 Gg = 1000 Mg) during 1984 - 2011. This means that human induced land-use change might be a source 20.5 Gg C per year for entire research area or 0.07 Mg C ha^{-1} yr^{-1}. With this estimated rate, an amount of 409.4 Gg C is expected to be released from the research area in the next 20 years. Our study also reveals that greatest source of C was forest to pasture conversion; therefore efforts to increase C storage should be placed on the priority on reducing forest to pasture conversion in the transition region. Expanding the study to other regions as well as using empirical model to simulate temporal dynamics of C from all pools would improve our understanding on effects of land-use change in the Agri-Forest transition on ecosystem C.

6.2. Conclusion

My research demonstrated that abandoned croplands in the Chernozemic soil order of the Boreal Plains Ecozone of Saskatchewan, Canada have significant potential for C sequestration. Ecosystem C ranges from 74.02 to 137.6 Mg C ha^{-1} (to 45 cm soil depth), and C accumulation rate was estimated to be 0.36 Mg C ha^{-1} yr^{-1} within 9 to 27-year sites. While high variation was observed in soil C (58.8 to 113.7 Mg C ha^{-1}) over the time sequences, vegetation C increased continuously after abandonment, ranging from 7.6 to 90.1 Mg C ha^{-1}. Years since abandonment was a good predictor of C stocks in tree biomass and AGB.

LUCCs in the agriculture region of the BPE was minor, accounting for approximately 6.5% during 1990 – 2000. Investigating transitions among 13 land-use categories, we found that the major changes occurred in cropland, unimproved pasture, and abandoned cropland with increasing trends in woody cover types. Cropland abandonment was most prevalent on poorly drained soils and acidic parent material. Deforestation for agriculture was most likely on well-drained areas of Chernozemic and Luvisolic soil orders. Under the land-use transitions, agriculture region of the BPE is a C sink of 1.04 Mt CO_2 eq per year, equivalent to approximately 0.015% GHGs released from land use, land-use change and forestry sector.

In the whole Agri-Forest transition region, summer fallow to annual cropland and pasture, annual cropland to pasture, and shrub to pasture were the major LUCCs, and the conversions were associated with soil capability. A large proportion of shrub and forest was disturbed, but stand replacements were more likely to occurr in the most recent years (2005 - 2011). Given that the entire boreal transition zone of Saskatchewan, Canada, is 4,986,400 ha (Hobson et al., 2002), annual C emission from LUCCs can be estimated at 349,048 Mg C, or 1.28 Mt CO_2 eq. As forest to pasture is the dominant conversion in the region, limiting deforestation, especially on well-drained Chernozemic and Luvisolic soils, should be a priority option for combating effects of global climate change.

6.3. Future research

Although quantification of carbon stocks and dynamics due to LUCCs has been studied over many decades, this research provides the first insight into the role of LUCCs in mitigating GHG emission in Agi-Forest transition of the Boreal Plains Ecozone, Canada. Some existing knowledge gaps have been addressed, including C stocks and dynamics under cropland abandonment. The findings through this work were the grounds to identify future research.

The manual approach on abandoned cropland detection using digital aerial photography can be expensive and labour intensive for a broader spatial scale study. To identify the region of interest, future research should adopt the use of a no-charge satellite imagery such as Landsat. Semi-automatic techniques on mapping cropland abandonment using aerial photography such as object-based classification and change detection (Li and Shao, 2014) should be applied. It is worth noting from our approach that the older abandoned sites were more difficult to identify due to the lack of pair-photos; therefore, prior knowledge (from farmers or researchers) on abandoned fields is of crucial importance.

Carbon stocks found in this study would be valuable for further C dynamics estimation using models, especially in empirical yield-curve models. The current estimation of C dynamics in abandoned cropland (Chapter 3) relied on limited field samples (six abandoned fields) and vegetation regeneration period (9 to 41 years). Linear relationships between vegetation C and stand age suggested that vegetation C may continue to increase after 41 years of regeneration. Consequently, vegetation C sequestered during the period greater than four decades since regeneration was not included in this estimation. More field data collections on expanded area and various stand ages are needed to enhance the estimation accuracy.

While this study has focused intensively on changes in C stock in abandoned cropland with stand age (Chapter 3), some factors that potentially drive C dynamics such as structure, farming practice history, or climate (Goulden et al., 2011; Silver et al., 2000), have not been assessed. Therefore, a study identifying factors controlling C stocks and dynamics in abandoned cropland is essential for carbon management.

Huffman et al. (2015) emphasized the need for a long-term study on LUCCs in the agriculture region. Indeed, LUCCs in a period of 10 years (1990 - 2000) might not be long enough

to reveal certain changes, which need longer time period to show entire conversions such as cropland to forest. Updating current land-use on the existing sample plots using air-photos would be an effective approach for monitoring LUCCs in the agriculture region.

CBM-CFS3 was used, for the first time, for estimation of ecosystem C fluxes on agriculture landscape. Applications of this model on similar landscapes are needed to assess the model performance. The time points that each land-use change occurred were assigned randomly, as the information on conversion year could not be derived from the pair-photos data. Additionally, the homogeneity in vegetation structure was assumed in this study (Chapter 4). Hence, a study allowing utilization of current datasets (multiple sources) with time-series data such as Landsat, which can offer the characteristics of LUCCs such as magnitude, time, location, and duration, would be very useful for C balance estimation of the entire Agri-Forest transition region based on CBM-CFS3.

7. LITERATURE CITED

Aber, J.D. 1979. Foliage-height profiles and succession in northern hardwood forests. Ecology: 18-23.

Agriculture and Agri-Food Canada. 2014. Geospatial products – all maps, data and applications. Agri-Geomatics Service. http://www.agr.gc.ca/eng/?id=1343066456961#a9. (accessed July 10, 2015).

Aide, T.M., J.K. Zimmerman, J.B. Pascarella, L. Rivera and H. Marcano-Vega. 2000. Forest regeneration in a chronosequence of tropical abandoned pastures: Implications for restoration ecology. Restoration Ecology 8: 328-338.

Allen, D.E.A., M.J.A. Pringle, K.L.A. Page and R.C.A. Dalal. 2010. A review of sampling designs for the measurement of soil organic carbon in Australian grazing lands. The rangeland Journal 32: 227-246.

Allen, M.R., D.J. Frame, C. Huntingford, C.D. Jones, J.A. Lowe, M. Meinshausen et al. 2009. Warming caused by cumulative carbon emissions towards the trillionth tonne. Nature 458: 1163-1166.

Amichev, B.Y., W.A. Kurz, C. Smyth and K.C.J. Rees. 2012. The carbon implications of large-scale afforestation of agriculturally marginal land with short-rotation willow in Saskatchewan. GCB Bioenergy 4: 70-87.

Amichev, B.Y., M.J. Bentham, S.N. Kulshreshtha, C.P. Laroque, J.M. Piwowar and K.C.J. Van Rees. 2016. Carbon sequestration and growth of six common tree and shrub shelterbelts in Saskatchewan, Canada. Canadian Journal of Soil Science 97: 368-381.

Apps, M.J., W.A. Kurz, R.J. Luxmoore, L.O. Nilsson, R.A. Sedjo, R. Schmidt et al. 1993. Boreal forests and tundra. Water Air and Soil Pollution 70: 39-53.

Arevalo, C.B.M., J.S. Bhatti, S.X. Chang and D. Sidders. 2009. Ecosystem carbon stocks and distribution under different land-uses in north central Alberta, Canada. Forest Ecology and Management 257: 1776-1785.

Arevalo, C.B.M., J.S. Bhatti, S.X. Chang and D. Sidders. 2011. Land use change effects on ecosystem carbon balance: From agricultural to hybrid poplar plantation. Agriculture, Ecosystems & Environment 141: 342-349.

Ash, J. and C. Helman. 1990. Floristics and vegetation biomass of a forest catchment, Kioloa, south coastal New South Wales. Cunninghamia 2: 167-182.

Baccini, A. 2004. Forest biomass estimation over regional scales using multisource data. Geophysical Research Letters 31: 2-5.

Bakker, M.M., E. Hatna, T. Kuhlman and C.A. Mücher. 2011. Changing environmental characteristics of European cropland. Agricultural Systems 104: 522-532.

Banfield, G.E., J.S. Bhatti, H. Jiang and M.J. Apps. 2002. Variability in regional scale estimates of carbon stocks in boreal forest ecosystems: results from West-Central Alberta. Forest Ecology and Management 169: 15-27.

Batjes, N.H. 1996. Total carbon and nitrogen in the soils of the world. European Journal of Soil Science 47: 151-163.

Beare, M.H., R.W. Parmelee, P.F. Hendrix, W.X. Cheng, D.C. Coleman and D.A. Crossley. 1992. Microbial and faunal interactions and effects on litter nitrogen and decomposition in agroecosystems. Ecological Monographs 62: 569-591.

Bélanger, N. and B.D. Pinno. 2008. Carbon sequestration, vegetation dynamics and soil development in the Boreal Transition ecoregion of Saskatchewan during the Holocene. Catena 74: 65-72.

Benjamin, K., G. Domon and A. Bouchard. 2005. Vegetation composition and succession of abandoned farmland: effects of ecological, historical and spatial factors. Landscape Ecology 20: 627-647.

Berg, B., M.P. Berg, P. Bottner, E. Box, A. Breymeyer, R.C. Deanta et al. 1993. Litter mass-loss rates in pine forests of europe and eastern unitedstates: Some relationships with climate and litter quality. Biogeochemistry 20: 127-159.

Beringer, J., F.S. Chapin Iii, C.C. Thompson and A.D. McGuire. 2005. Surface energy exchanges along a tundra-forest transition and feedbacks to climate. Agricultural and Forest Meteorology 131: 143-161.

Bhatti, J.S., M.J. Apps and C. Tarnocai. 2002. Estimates of soil organic carbon stocks in central Canada using three different approaches. Canadian Journal of Forest Research 812: 805-812.

Boddy, L., E.M. Owens and I.H. Chapela. 1989. Small scale variation in decay rate within logs one year after felling: Effect of fungal community structure and moisture content. FEMS Microbiology Letters 62: 173-183.

Boehm, M. and S. Kulshreshtha. 2000. Summerfallow reduction on the prairies and mitigation of greenhouse gas emissions. Unpublished.

Boehm, M., B. Junkins, R. Desjardins, S. Kulshreshtha and W. Lindwall. 2004. Sink potential of Canadian agricultural soils. Climatic Change 65: 297-314.

Bolstad, P.V. and T.M. Lillesand. 1991. Rapid maximum-likelihood classification. Photogrammetric Engineering and Remote Sensing 57: 67-74.

Bonan, G.B. 1997. Effects of land use on the climate of the United States. Climatic Change 37: 449-486.

Bond-Lamberty, B., C. Wang and S.T. Gower. 2002. Annual carbon flux from woody debris for a boreal black spruce fire chronosequence. Journal of Geophysical Research-Atmospheres 108.

Bond-Lamberty, B., C. Wang and S.T. Gower. 2004. Net primary production and net ecosystem production of a boreal black spruce wildfire chronosequence. Global Change Biology 10.

Boudewyn, P., X. Song, S. Magnussen and M.D. Gillis. (2007). Model-based, volume-to-biomass conversion for forested and vegetated land in Canada. Natural Resources Canada (accessed

Boulanger, Y. and L. Sirois. 2006. Postfire dynamics of black spruce coarse woody debris in northern boreal forest of Quebec. Canadian Journal of Forest Research 36: 1770-1780.

Brandt, J.P., H.F. Cerezke, K.I. Mallett, W.J.A. Volney and J.D. Weber. 2003. Factors affecting trembling aspen (*Populus tremuloides Michx.*) health in the boreal forest of Alberta, Saskatchewan, and Manitoba, Canada. Forest Ecology and Management 178: 287-300.

Brassard, B.W., H.Y.H. Chen, Y. Bergeron and D. Pare. 2011. Coarse root biomass allometric equations for *Abies balsamea, Picea mariana, Pinus banksiana, and Populus tremuloides* in the boreal forest of Ontario, Canada. Biomass & Bioenergy 35: 4189-4196.

Bremer, E., H.H. Janzen and R.H. McKenzie. 2002. Short-term impact of fallow frequency and perennial grass on soil organic carbon in a Brown Chernozem in southern Alberta. Canadian Journal of Soil Science 82: 481-488.

Brink, A.B. and H.D. Eva. 2009. Monitoring 25 years of land cover change dynamics in Africa: A sample based remote sensing approach. Applied Geography 29: 501-512.

Brown, D.G., K.M. Johnson, T.R. Loveland and D.M. Theobald. 2005. Rural land-use trends in the conterminous United States, 1950–2000. Ecological Applications 15: 1851-1863.

Brown, K. 2006. Re-presenting GIS Geographical Journal 172: 264-265.

Brown, S. and A.E. Lugo. 1990. Tropical secondary forests. Journal of Tropical Ecology 6: 1-32.

Brown, S., J. Mo, J.K. McPherson and D.T. Bell. 1996. Decomposition of woody debris in Western Australian forests. Canadian Journal of Forest Research 26: 954-966.

Busing, R.T. 2005. Tree mortality, canopy turnover, and woody detritus in old cove forests of the southern Appalachians. Ecology 86: 73-84.

Cairns, M.a., S. Brown, E.H. Helmer and G.a. Baumgardner. 1997. Root biomass allocation in the world's upland forests. Oecologia 111: 1-11.

CAIT. 2015. Total GHG emissions including Land-use change and forestry. World Resources Institute. http://cait.wri.org/historical. (accessed June 6, 2016).

Canty, M.J., A.A. Nielsen and M. Schmidt. 2004. Automatic radiometric normalization of multitemporal satellite imagery. Remote Sensing of Environment 91: 441-451.

Carmona, M.R., J.J. Armesto, J.C. Aravena and C.A. Perez. 2002. Coarse woody debris biomass in successional and primary temperate forests in Chiloe Island, Chile. Forest Ecology and Management 164: 265-275.

Cerri, C.E.P., M. Easter, K. Paustian, K. Killian, K. Coleman, M. Bernoux et al. 2007. Simulating SOC changes in 11 land use change chronosequences from the Brazilian Amazon with RothC and Century models. Agriculture Ecosystems & Environment 122: 46-57.

Chase, T.N., R.A. Pielke Sr, T.G.F. Kittel, R.R. Nemani and S.W. Running. 2000. Simulated impacts of historical land cover changes on global climate in northern winter. Climate Dynamics 16: 93-105.

Chen, H.Y.H. and Y. Luo. 2015. Net aboveground biomass declines of four major forest types with forest ageing and climate change in western Canada's boreal forests. Global Change Biology 20: 3675-3684.

Chen, J.M. and J. Cihlar. 1995. Plant canopy gap-size analysis theory for improving optical measurements of leaf-area index. Applied Optics 34: 6211-6222.

Chiesi, M., F. Maselli, M. Bindi, L. Fibbi, P. Cherubini, E. Arlotta et al. 2005. Modelling carbon budget of Mediterranean forests using ground and remote sensing measurements. Agricultural and Forest Meteorology 135: 22-34.

Cho, M.A., A. Skidmore, F. Corsi, S.E. Van Wieren and I. Sobhan. 2007. Estimation of green grass/herb biomass from airborne hyperspectral imagery using spectral indices and partial least squares regression. International Journal of Applied Earth Observation and Geoinformation 9: 414-424.

Christensen, J.H., B. Hewitson, A.C. A. Busuioc, X. Gao, R.J. I. Held, R.K. Kolli et al. 2007. Regional climate projections. In: Climate Change 2007:The Physical Science Basis. Contribution of Working Group I to the Fourth Assessment Report of the Intergovernmental Panel on Climate Change., [S. Solomon, D. Qin, M. Manning, M. Marquis, K. Averyt, M. M. B. Tignor, H. L. Miller and Z. L. Chen (eds.)], Cambridge University Press, NY, USA. p. 847-940.

Claussen, M., V. Brovkin and A. Ganopolski. 2001. Biogeophysical versus biogeochemical feedbacks of large-scale land cover change. Geophysical Research Letters 28: 1011-1014.

Cocke, A.E., P.Z. Fule and J.E. Crouse. 2005. Comparison of burn severity assessments using Differenced Normalized Burn Ratio and ground data. International Journal of Wildland Fire 14: 189-198.

Cohen, W.B., T.A. Spies and M. Fiorella. 1995. Estimating the age and structure of forests in a multi-ownership landscape of western Oregon, U.S.A. International Journal of Remote Sensing 4: 721-746.

Cohen, W.B., Z. Yang and R. Kennedy. 2010. Detecting trends in forest disturbance and recovery using yearly Landsat time series: 2. TimeSync — Tools for calibration and validation. Remote Sensing of Environment 114: 2911-2924.

Coleman, K., D.S. Jenkinson, G.J. Crocker, P.R. Grace, J. Klir, M. Korschens et al. 1997. Simulating trends in soil organic carbon in long-term experiments using RothC-26.3. Geoderma 81: 29-44.

Coleman, K. and D.S. Jenkinson. 1999. RothC-26.3 - A model for the turnover of carbon in soil: Model description and windows users guide. Lawes Agricultural Trust Harpenden. http://www.rothamsted.ac.uk/sites/default/files/users/kcoleman/RothC_guide_WIN.pdf. (accessed March 16, 2014).

Coops, N.C., R.H. Waring and J.J. Landsberg. 2001. Estimation of potential forest productivity across the Oregon transect using satellite data and monthly weather records. International Journal of Remote Sensing 22: 3797-3812.

Coops, N.C., J.D. White and N.A. Scott. 2002. Assessment of regional forest and scrub productivity using a coupled vegetation process model with remote sensing. Geocarto International 17: 5-14.

Coppin, P., I. Jonckheere, K. Nackaerts, B. Muys and E. Lambin. 2004. Digital change detection methods in ecosystem monitoring: A review. International Journal of Remote Sensing 25: 1565-1596.

Couteaux, M.M., P. Bottner and B. Berg. 1995. Litter decomposition, climate and litter quality. Trends in Ecology & Evolution 10: 63-66.

Covington, W.W. 1981. Changes in forest floor organic-matter and nutrient content following clear-cutting in northern hardwoods. Ecology 62: 41-48.

Cox, P.M., R.A. Betts, C.D. Jones, S.A. Spall and I.J. Totterdell. 2000. Acceleration of global warming due to carbon-cycle feedbacks in a coupled climate model. Nature 408: 184-187.

Crist, E.P. 1985. A TM tasseled cap equivalent transformation for reflectance factor data. Remote Sensing of Environment 17: 301-306.

Cronan, C.S. 1990. Patterns of organic-acid transport from forested watersheds to aquatic ecosystems. In: E. M. Perdue and E. T. Gjessing, editors, Organic Acids in Aquatic Ecosystems. p. 245-260.

Crowley, T.J. 2000. Causes of climate change over the past 1000 years. Science 289: 270-277.

de Gruijter, J.J., A.B. McBratney, B. Minasny, I. Wheeler, B.P. Malone and U. Stockmann. 2016. Farm-scale soil carbon auditing. Geoderma 265: 120-130.

De Jong, S.M., E.J. Pebesma and B. Lacaze. 2003. Aboveground biomass assessment of Mediterranean forests using airborne imaging spectrometry: The DAIS peyne experiment. International Journal of Remote Sensing 24: 1505-1520.

Dignac, M.F., H. Knicker and I. Kogel-Knabner. 2002. Effect of N content and soil texture on the decomposition of organic matter in forest soils as revealed by solid-state CPMAS NMR spectroscopy. Organic Geochemistry 33: 1715-1726.

Ding, M., Y. Zhang, L. Liu, W. Zhang, Z. Wang and W. Bai. 2007. The relationship between NDVI and precipitation on the Tibetan Plateau. Journal of Geographical Sciences 17: 259-268.

Drake, J.B., R.O. Dubayah, D.B. Clark, R.G. Knox, J.B. Blair, M.A. Hofton et al. 2002. Estimation of tropical forest structural characteristics using large-footprint lidar. Remote Sensing of Environment 79: 305-319.

EEA. 2014. Annual European Union greenhouse gas inventory 1990–2012 and inventory report 2014. European Environment Agency. http://www.eea.europa.eu/publications/european-union-greenhouse-gas-inventory-2014. (accessed January 10, 2015).

Ellert, B.H., H.H. Janzen, A.J. VandenBygaart and E. Bremer. 2006. Measuring changes in soil organics carbon storage. In: Soil Sampling and Methods of Analysis, [M. R. Carter and E. G. Gregorich (eds.)], CRC Press. p. 25-37.

Environment and Climate Change Canada. 2016. National Inventory Report 1990-2014: Greenhouse Gas Sources and Sinks in Canada. Public Inquiries Centre. https://www.ec.gc.ca/ges-ghg/default.asp?lang=En&n=662F9C56-1. (accessed January, 12, 2016).

Environment Canada. 2013. National Inventory Report 1990–2011: Greenhouse Gas Sources and Sinks in Canada. Environment Canada. https://www.ec.gc.ca/ges-ghg/. (accessed June 5, 2014).

EPA. 2014. Inventory of U.S. Greenhouse Gas Emissions and Sinks. US Environmental Protection Agency. http://www.epa.gov/. (accessed March 22, 2013).

Escuin, S., R. Navarro and P. Fernandez. 2008. Fire severity assessment by using NBR (Normalized Burn Ratio) and NDVI (Normalized Difference Vegetation Index) derived from LANDSAT TM/ETM images. International Journal of Remote Sensing 29: 1053-1073.

European Community. 2009. Directive 2009/28 on the promotion of the use of energy from renewable sources: Article 2. Definitions. European Union. http://eur-lex.europa.eu/legal-content/EN/TXT/PDF/?uri=CELEX:32009L0028&from=en. (accessed April 20, 2015).

Falloon, P. and P. Smith. 2002. Simulating SOC changes in long-term experiments with RothC and CENTURY: model evaluation for a regional scale application. Soil Use and Management 18: 101-111.

Falloon, P., P. Smith, R.I. Bradley, R. Milne, R. Tomlinson, D. Viner et al. 2006. RothC UK – a dynamic modelling system for estimating changes in soil C from mineral soils at 1-km resolution in the UK. Soil Use and Management 22: 274-288.

Federici, S., F.N. Tubiello, M. Salvatore, H. Jacobs and J. Schmidhuber. 2015. New estimates of CO_2 forest emissions and removals: 1990-2015. Forest Ecology and Management 352: 89-98.

Finegan, B. 1984. Forest succession. Nature 312: 109-114.

Fitzsimmons, M. 2002. Estimated rates of deforestation in two boreal landscapes in central Saskatchewan, Canada. Canadian Journal of Forest Research 32: 843-851.

Fitzsimmons, M. 2003. Effects of deforestation and reforestation on landscape spatial structure in boreal Saskatchewan, Canada. Forest Ecology and Management 174: 577-592.

Fitzsimmons, M.J., D.J. Pennock and J. Thorpe. 2004. Effects of deforestation on ecosystem carbon densities in central Saskatchewan, Canada. Forest Ecology and Management 188: 349-361.

Flannigan, M., B. Stocks, M. Turetsky and M. Wotton. 2009. Impacts of climate change on fire activity and fire management in the circumboreal forest. Global Change Biology 15: 549-560.

Foley, J.A., M.H. Costa, C. Delire, N. Ramankutty and P. Snyder. 2003. Green surprise? How terrestrial ecosystems could affect earth's climate. Frontiers in Ecology and the Environment 1: 38-44.

Foley, J.A., R. DeFries, G.P. Asner, C. Barford, G. Bonan, S.R. Carpenter et al. 2005. Global consequences of land use. Science 309: 570-574.

Foody, G.M. 2002. Status of land cover classification accuracy assessment. Remote Sensing of Environment 80: 185-201.

Foote, R.L. and P. Grogan. 2010. Soil carbon accumulation during temperate forest succession on abandoned low productivity agricultural lands. Ecosystems 13: 795-812.

Frazier, R.J., N.C. Coops and M.A. Wulder. 2015. Boreal shield forest disturbance and recovery trends using Landsat time series. Remote Sensing of Environment 170: 317-327.

Frelich, L.E. and P.B. Reich. 2010. Will environmental changes reinforce the impact of global warming on the prairie-forest border of central North America? Frontiers in Ecology and the Environment 8: 371-378.

Frey, B.R., V.J. Lieffers, E.H. Hogg and S.M. Landhäusser. 2004. Predicting landscape patterns of aspen dieback: mechanisms and knowledge gaps. Canadian Journal of Forest Research 34: 1379-1390.

Fukushima, Y., T. Hiura and S. Tanabe. 1998. Accuracy of the MacArthur-Horn method for estimating a foliage profile. Agricultural and Forest Meteorology 92: 203-210.

Gaboury, S., J.F. Boucher, C. Villeneuve, D. Lord and R. Gagnon. 2009. Estimating the net carbon balance of boreal open woodland afforestation: A case-study in Quebec's closed-crown boreal forest. Forest Ecology and Management 257: 483-494.

Gallardo, J.F., J. Saavedra, T. Martinpatino and A. Millan. 1987. Soil organic matter determination. Communications in Soil Science and Plant Analysis 18: 699-707.

Gellrich, M., P. Baur, B. Koch and N.E. Zimmermann. 2007. Agricultural land abandonment and natural forest re-growth in the Swiss mountains: A spatially explicit economic analysis. Agriculture, Ecosystems & Environment 118: 93-108.

Gibbard, S., K. Caldeira, G. Bala, T.J. Phillips and M. Wickett. 2005. Climate effects of global land cover change. Geophysical Research Letters 32.

GISTEMP Team. 2016. GISS Surface Temperature Analysis (GISTEMP). NASA Goddard Institute for Space Studies. http://data.giss.nasa.gov/gistemp/. (accessed May 10, 2016).

Goodale, C.L., M.J. Apps, R.A. Birdsey, C.B. Field, L.S. Heath, R.A. Houghton et al. 2002. Forest carbon sinks in the northern hemisphere. Ecological Applications 12: 891-899.

Goulden, M.L., A.M.S. McMillan, G.C. Winston, A.V. Rocha, K.L. Manies, J.W. Harden et al. 2011. Patterns of NPP, GPP, respiration, and NEP during boreal forest succession. Global Change Biology 17: 855-871.

Goward, S., T. Arvidson, D. Williams, J. Faundeen, J. Irons and S. Franks. 2006. Historical record of Landsat global coverage: Mission operations, NSLRSDA, and international cooperator stations. Photogrammetric Engineering and Remote Sensing 72: 1155-1169.

Gower, S.T., J.G. Vogel, J.M. Norman, C.J. Kucharik, S.J. Steele and T.K. Stow. 1997. Carbon distribution and aboveground net primary production in aspen, jack pine, and black spruce stands in Saskatchewan and Manitoba, Canada. Journal of Geophysical Research 102: 29029–29041.

Gower, S.T., O. Krankina, R.J. Olson, M. Apps, S. Linder and C. Wang. 2001. Net primary production and carbon allocation patterns of boreal forest ecosystems. Ecological Applications 11: 1395-1411.

Grewal, K.S., G.D. Buchan and R.R. Sherlock. 1991. A comparison of three methods of organic carbon determination in some New Zealand soils. Journal of Soil Science 42: 251-257.

Griffiths, P., T. Kuemmerle, R.E. Kennedy, I.V. Abrudan, J. Knorn and P. Hostert. 2012. Using annual time-series of Landsat images to assess the effects of forest restitution in post-socialist Romania. Remote Sensing of Environment 118: 199-214.

Groen, T., G.J. Nabuurs and M.J. Schelhaas. 2006. Carbon accounting and cost estimation in forestry projects using CO2Fix V.3. Climatic Change 74: 269-288.

Grünzweig, J.M., D.W. Valentine and F.S. Chapin. 2015. Successional changes in carbon stocks after logging and deforestation for agriculture in interior Alaska: Implications for boreal climate feedbacks. Ecosystems 18: 132-145.

Guariguata, M.R. and R. Ostertag. 2001. Neotropical secondary forest succession: changes in structural and functional characteristics. Forest Ecology and Management 148: 185-206.

Guo, L.B. and R.M. Gifford. 2002. Soil carbon stocks and land use change: a meta analysis. Global Change Biology 8: 345-360.

Gupta, R.K., T.S. Prasad and D. Vijayan. 2000. Relationship between LAI and NDVI for IRS LISS and Landsat TM bands. Advances in Space Research 26: 1047-1050.

Hagemann, U., M.T. Moroni, J. Gleissner and F. Makeschin. 2010. Accumulation and preservation of dead wood upon burial by bryophytes. Ecosystems 13: 600-611.

Hame, T., I. Heiler and J. San Miguel-Ayanz. 1998. An unsupervised change detection and recognition system for forestry. International Journal of Remote Sensing 19: 1079-1099.

Hanninen, H. 2006. Climate warming and the risk of frost damage to boreal forest trees: identification of critical ecophysiological traits. Tree Physiology 26: 889-898.

Hansen, J., R. Ruedy, M. Sato and K. Lo. 2010. Global surface temperature change. Reviews of Geophysics 48: RG4004.

Hansen, J., M. Sato and R. Ruedy. 2012. Perception of climate change. Proceedings of the National Academy of Sciences of the United States of America 109: 2415-2423.

Hansen, M.C., D.P. Roy, E. Lindquist, B. Adusei, C.O. Justice and A. Altstatt. 2008. A method for integrating MODIS and Landsat data for systematic monitoring of forest cover and change in the Congo Basin. Remote Sensing of Environment 112: 2495-2513.

Hansen, M.C., P.V. Potapov, R. Moore, M. Hancher, S.A. Turubanova, A. Tyukavina et al. 2013. High-resolution global maps of 21st-century forest cover change. Science 342: 850-853.

Harmon, M.E. and J. Sexton. 1996. Guidline for measurements of woody detritus in forest ecosystems. U.S. LTER Network Office, Universtiy Washington, Sealtle, WA, U.S.A.

Harmon, M.E., O.N. Krankina and J. Sexton. 2000. Decomposition vectors: a new approach to estimating woody detritus decomposition dynamics. Canadian Journal of Forest Research 30: 76-84.

Hasegawa, K., H. Matsuyama, H. Tsuzuki and T. Sweda. 2010. Improving the estimation of leaf area index by using remotely sensed NDVI with BRDF signatures. Remote Sensing of Environment 114: 514-519.

Helmisaari, H.-S. and L. Hallbäcken. 1999. Fine-root biomass and necromass in limed and fertilized Norway spruce (*Picea abies (L.) Karst.*) stands. Forest Ecology and Management 119: 99-110.

Hermosilla, T., M.A. Wulder, J.C. White, N.C. Coops and G.W. Hobart. 2015. Regional detection, characterization, and attribution of annual forest change from 1984 to 2012 using Landsat-derived time-series metrics. Remote Sensing of Environment 170: 121-132.

Hilli, S., S. Stark and J. Derome. 2010. Litter decomposition rates in relation to litter stocks in boreal coniferous forests along climatic and soil fertility gradients. Applied Soil Ecology 46: 200-208.

Hobbie, S.E. 1996. Temperature and plant species control over litter decomposition in Alaskan tundra. Ecological Monographs 66: 503-522.

Hobson, K.A., E.M. Bayne and S.L.V. Wilgenburg. 2002. Large-scale conversion of forest to agriculture in the boreal plains of Saskatchewan. Conservation Biology 16: 1530-1541.

Hogg, E.H., J.P. Brandt and B. Kochtubajda. 2002. Growth and dieback of aspen forests in northwestern Alberta, Canada, in relation to climate and insects. Canadian Journal of Forest Research 32: 823-832.

Hogg, E.H., J.P. Brandt and B. Kochtubajda. 2005. Factors affecting interannual variation in growth of western Canadian aspen forests during 1951-2000. Canadian Journal of Forest Research 35: 610-622.

Hogg, E.H., J.P. Brandt and M. Michaellian. 2008. Impacts of a regional drought on the productivity, dieback, and biomass of western Canadian aspen forests. Canadian Journal of Forest Research 38: 1373-1384.

Hogg, E.H., A.G. Barr and T.A. Black. 2013. A simple soil moisture index for representing multi-year drought impacts on aspen productivity in the western Canadian interior. Agricultural and Forest Meteorology 178–179: 173-182.

Hooker, T.D. and J.E. Compton. 2003. Forest ecosystem carbon and nitrogen accumulation during the first century after agriculture abandonment. Ecological Applications 13: 299-313.

Houghton, R.A., R.D. Boone, J.R. Fruci, J.E. Hobbie, J.M. Melillo, C.A. Palm et al. 1987. The flux of carbon from terrestrial ecosystems to the atmosphere in 1980 due to changes in land use geographic distribution of the global flux. Tellus Series B Chemical and Physical Meteorology 39: 122-139.

Houghton, R.A. 1995. Land-use change and the carbon cycle. Global Change Biology 1: 275-287.

Houghton, R.A. 1999a. The U.S. carbon budget: Contributions from Land-Use Change. Science 285: 574-578.

Houghton, R.A. 1999b. The annual net flux of carbon to the atmosphere from changes in land use 1850-1990. Tellus Series B-Chemical and Physical Meteorology 51: 298-313.

Houghton, R.A. and C.L. Goodale. 2004. Effects of land-use change on the carbon balance of terrestrial ecosystems. In: Ecosystems and Land Use Change, [R. S. DeFries, G. P. Asner and R. A. Houghton (eds.)], Amer Geophysical Union, Washington. p. 85-98.

Houghton, R.A. 2005. Aboveground forest biomass and the global carbon balance. Global Change Biology 11: 945-958.

Houghton, R.A. 2007. Balancing the global carbon budget. Annual Review of Earth and Planetary Sciences 35: 313-347.

Houghton, R.A., J.I. House, J. Pongratz, G.R. van der Werf, R.S. DeFries, M.C. Hansen et al. 2012. Carbon emissions from land use and land-cover change. Biogeosciences 9: 5125-5142.

Howard, L.F. and T.D. Lee. 2002. Upland old-field succession in southeastern New Hampshire. Journal of the Torrey Botanical Society 129: 60-76.

Huang, C., S.N. Goward, J.G. Masek, F. Gao, E.F. Vermote, N. Thomas et al. 2009. Development of time series stacks of Landsat images for reconstructing forest disturbance history. International Journal of Digital Earth 2: 195-218.

Huang, C., S.N. Goward, J.G. Masek, N. Thomas, Z. Zhu and J.E. Vogelmann. 2010a. An automated approach for reconstructing recent forest disturbance history using dense Landsat time series stacks. Remote Sensing of Environment 114: 183-198.

Huang, J., J.C. Tardif, Y. Bergeron, B. Denneler, F. Berninger and M.P. Girardin. 2010b. Radial growth response of four dominant boreal tree species to climate along a latitudinal gradient in the eastern Canadian boreal forest. Global Change Biology 16: 711-731.

Huang, W.Z. and J.J. Schoenau. 1996. Forms, amounts and distribution of carbon, nitrogen, phosphorus and sulfur in a boreal aspen forest soil. Canadian Journal of Soil Science 76: 373-385.

Hudak, A.T., E.K. Strand, L.A. Vierling, J.C. Byrne, J.U.H. Eitel, S. Martinuzzi et al. 2012. Quantifying aboveground forest carbon pools and fluxes from repeat LiDAR surveys. Remote Sensing of Environment 123: 25-40.

Huffman, T., R. Ogston, T. Fisette, B. Daneshfar, P.Y. Gasser, L. White et al. 2006. Canadian agricultural land-use and land management data for Kyoto reporting. Canadian Journal of Soil Science 86: 431-439.

Huffman, T., J. Liu, M. McGovern, B. McConkey and T. Martin. 2015. Carbon stock and change from woody biomass on Canada's cropland between 1990 and 2000. Agriculture, Ecosystems & Environment 205: 102-111.

Huggett, R. 1998. Soil chronosequences, soil development, and soil evolution: a critical review. Catena 32: 155-172.

Hyde, P., R. Dubayah, W. Walker, J. Blair, M. Hofton and C. Hunsaker. 2006. Mapping forest structure for wildlife habitat analysis using multi-sensor (LiDAR, SAR/InSAR, ETM+, Quickbird) synergy. Remote Sensing of Environment 102: 63-73.

Indorante, S.J., L.R. Follmer, R.D. Hammer and P.G. Koenig. 1990. Particle-size analysis by a modified pipetty procedure. Soil Science Society of America Journal 54: 560-563.

IPCC. 2001. Contribution of Working Group I to the Third Assessment Report of the Intergovernmental Panel on Climate Change. In: Climate Change 2001: The Scientific Basis, [J. T. Houghton, Y. Ding, D.J. Griggs, M. Noguer, P.J. van der Linden, K. M. X. Dai and C. A. Johnson (eds.)], Cambridge University Press, Cambridge, United Kingdom and New York, NY, USA.

IPCC. 2003. Forest land. In: Good practice guidance for land use, land-use change and forestry, [J. Penman, M. Gytarsky, T. Hiraishi, T. Krug, D. Kruger, R. Pipatti, L. Buendia, K. Miwa, T. Ngara, K. Tanabe and F. Wagner (eds.)], IPCC National Greenhouse Gass Inventory Programme, Hayama, Japan.

IPCC. 2006. Agriculture, forestry and other land use. In: 2006 IPCC Guidelines for National Greenhouse Gas Inventories, [Eggleston H.S., L. Buendia, K. Miwa, T. Ngara and K. Tanabe (eds.)], National Greenhouse Gas Inventories Programme, IGES, Japan.

IPCC. 2007a. Synthesis report: Contribution of working groups I, II and III to the fourth assessment report of the intergovernmental panel on climate change. In: Climate Change 2007, [Core Writing Team, R.K. Pachauri and L.A. Meyer (eds.)], IPCC Geneva, Switzerland.

IPCC. 2007b. Summary for policymakers. In: Climate Change 2007: Mitigation of Climate Change, [Metz B., O.R. Davidson, P.R. Bosch, R. Dave and L.A. Meyer (eds.)], Cambridge University Press, Cambridge, United Kingdom and New York, NY, USA.

IPCC. 2013. Summary for policymakers. In: Climate Change 2013: The Physical Science Basis. Contribution of Working Group I to the Fifth Assessment Report of the Intergovernmental Panel on Climate Change, [Stocker T.F., D. Qin, G.-K. Plattner, M. Tignor, J. B. S.K. Allen, A. Nauels, Y. Xia, V. Bex and P.M. Midgley and G.-K. P. D. Qin, M. Tignor, S.K. Allen, J. Boschung, A. Nauels, Y. Xia, V. Bex and P.M. Midgley (eds.)], Cambridge University Press, Cambridge, United Kingdom and New York, NY, USA.

Jackson, R., J. Canadell, J. Ehleringer, H. Mooney, O. Sala and S. ED. 1996. A global analysis of root distributions for terrestrial biomes. Oecologia 108.

Janisch, J.E. and M.E. Harmon. 2002. Successional changes in live and dead wood carbon stores: implications for net ecosystem productivity. Tree Physiology 22: 77-89.

Jenkins, J.C., D.C. Chojnacky, L.S. Heath and R.A. Birdsey. 2003. National-scale biomass estimators for united states tree species. Forest Science 49: 12-35.

Jenkinson, D. and J. Rayner. 1977. The turnover of soil organic matter in some of the roti-iamsted classical experiments. Soil Science 123: 298-305.

Jenkinson, D.S., J. Meredith, J.I. Kinyamario, G.P. Warren, M.T.F. Wong, D.D. Harkness et al. 1999. Estimating net primary production from measurements made on soil organic-matter. Ecology 80: 2762-2773.

Jensen, J.R. 2005. Introductory digital image processing. In: Digital Change Detection, [(eds.)], Prentice Education, Inc, New Jersey. p. 471-487.

Jobbagy, E.G. and R.B. Jackson. 2000. The vertical distribution of soil organic carbon and its relation to climate and vegetation. Ecological Applications 10: 423-436.

Johannes, K.H.M. and D. Tilman. 2000. Dynamics of soil nitrogen and carbon accumulation for 61 years after agricultural abandonment. Ecology 81: 88-98.

Johnson, C.E., C.T. Driscoll, T.J. Fahey, T.G. Siccama and J.W. Hughes. 1995. Carbon dynamics following clear-cutting of a northern hardwood forest. In: Carbon Forms and Functions in Forest Soils, [W. W. McFee, J. M. Kelly and J. M. Bigham (eds.)]. p. 463-488.

Johnston, M.H., P.S. Homann, J.K. Engstrom and D.F. Grigal. 1996. Changes in ecosystem carbon storage over 40 years on an old-field/forest landscape in east-central Minnesota. Forest Ecology and Management 83: 17-26.

Jonckheere, I., S. Fleck, K. Nackaerts, B. Muys, P. Coppin, M. Weiss et al. 2004. Review of methods for in situ leaf area index determination: Part I. Theories, sensors and hemispherical photography. Agricultural and Forest Meteorology 121: 19-35.

Ju, W. and J.M. Chen. 2005. Distribution of soil carbon stocks in Canada's forests and wetlands simulated based on drainage class, topography and remotely sensed vegetation parameters. Hydrological Processes 19: 77-94.

JWRL. 2013. Woody Matter Volume on Agriculture Land Use Change Plots. JWRL Geomatics Inc. AAFC, Canada.

Kabzems, A., A.L. Kosowan and W.C. Harris. 1986. Mixedwood section in an ecological perspective, Saskatchewan. Saskatchewan Parks and Renewable Resources. http://cfs.nrcan.gc.ca/pubwarehouse/pdfs/19648.pdf. (accessed March 2, 2012).

Kalyn, A.L. and K.C.J. Van Rees. 2006. Contribution of fine roots to ecosystem biomass and net primary production in black spruce, aspen, and jack pine forests in Saskatchewan. Agricultural and Forest Meteorology 140: 236-243.

Kawabata, A., K. Ichii and Y. Yamaguchi. 2001. Global monitoring of interannual changes in vegetation activities using NDVI and its relationships to temperature and precipitation. International Journal of Remote Sensing 22: 1377-1382.

Keenleyside, C. and G. Tucker. 2010. Farmland Abandonment in the EU: an Assessment of Trends and Prospects. Report prepared for WWF. Institute for European Environmental Policy. http://www.ieep.eu/assets/733/Farmland_abandonment_in_the_EU_-_assessment_of_trends_and_prospects_-_FINAL_15-11-2010_.pdf. (accessed May 6, 2013).

Kennedy, R.E., W.B. Cohen and T.A. Schroeder. 2007. Trajectory-based change detection for automated characterization of forest disturbance dynamics. Remote Sensing of Environment 110: 370-386.

Kennedy, R.E., Z. Yang and W.B. Cohen. 2010. Detecting trends in forest disturbance and recovery using yearly Landsat time series: 1. LandTrendr — Temporal segmentation algorithms. Remote Sensing of Environment 114: 2897-2910.

Kennedy, R.E., Z.Q. Yang, W.B. Cohen, E. Pfaff, J. Braaten and P. Nelson. 2012. Spatial and temporal patterns of forest disturbance and regrowth within the area of the Northwest Forest Plan. Remote Sensing of Environment 122: 117-133.

Kennedy, R.E., Z. Yang, J. Braaten, C. Copass, N. Antonova, C. Jordan et al. 2015. Attribution of disturbance change agent from Landsat time-series in support of habitat monitoring in the Puget Sound region, USA. Remote Sensing of Environment 166: 271-285.

Kirschbaum, M.U.F. 1995. The temperature-dependence of soil organic matter decomposition, and the effect of global warming on soil organic C storage. Soil Biology & Biochemistry 27: 753-760.

Kirschbaum, M.U.F. 2000. Will changes in soil organic carbon act as a positive or negative feedback on global warming? Biogeochemistry 48: 21-51.

Knohl, A., O. Kolle, T.Y. Minayeva, I.M. Milyukova, N.N. Vygodskaya, T. Foken et al. 2002. Carbon dioxide exchange of a Russian boreal forest after disturbance by wind throw. Global Change Biology 8: 231-246.

Korol, R.L., K.S. Mimer and S.W. Running. 1996. Testing a mechanistic model for predicting stand and tree growth. Forest Science 42.

Krankina, O.N. and M.E. Harmon. 1995. Dynamics of the dead wood carbon pool in northwestern Russian boreal forests. Water Air and Soil Pollution 82: 227-238.

Kucharik, C.J., J.M. Norman and S.T. Gower. 1998. Measurements of branch area and adjusting leaf area index indirect measurements. Agricultural and Forest Meteorology 91: 69-88.

Kuemmerle, T., D. Mueller, P. Griffiths and M. Rusu. 2009. Land use change in southern Romania after the collapse of socialism. Regional Environmental Change 9: 1-12.

Kurganova, I., V.L. de Gerenyu and Y. Kuzyakov. 2015. Large-scale carbon sequestration in post-agrogenic ecosystems in Russia and Kazakhstan. Catena 133: 461-466.

Kurz, W.A., S.J. Beukema and M.J. Apps. 1996. Estimation of root biomass and dynamics for the carbon budget model of the Canadian forest sector. Canadian Journal of Forest Research 26: 1973-1979.

Kurz, W.A. and M.J. Apps. 1999. A 70-year retrospective analysis of carbon fluxes in the Canadian forest sector. Ecological Applications 9: 526-547.

Kurz, W.A., C.C. Dymond, T.M. White, G. Stinson, C.H. Shaw, G.J. Rampley et al. 2009. CBM-CFS3: A model of carbon-dynamics in forestry and land-use change implementing IPCC standards. Ecological Modelling 220: 480-504.

Kurz, W.A., C.H. Shaw, C. Boisvenue, G. Stinson, J. Metsaranta, D. Leckie et al. 2013. Carbon in Canada's boreal forest — A synthesis. Environmental Reviews 21: 260-292.

Kuzyakov, Y., P.W. Hill and D.L. Jones. 2007. Root exudate components change litter decomposition in a simulated rhizosphere depending on temperature. Plant and Soil 290: 293-305.

Laganiere, J., D. Pare and R.L. Bradley. 2010. How does a tree species influence litter decomposition? Separating the relative contribution of litter quality, litter mixing, and forest floor conditions. Canadian Journal of Forest Research 40: 465-475.

Lal, R. 2005. Forest soils and carbon sequestration. Forest Ecology and Management 220: 242-258.

Lal, R. 2008. Sequestration of atmospheric CO_2 in global carbon pools. Energy & Environmental Science 1: 86-100.

Lambert, M.C., C.H. Ung and F. Raulier. 2005. Canadian national tree aboveground biomass equations. Canadian Journal of Forest Research 35: 1996-2018.

Lambin, E.F., B.L. Turner, H.J. Geist, S.B. Agbola, A. Angelsen, J.W. Bruce et al. 2001. The causes of land-use and land-cover change: moving beyond the myths. Global Environmental Change-Human and Policy Dimensions 11: 261-269.

Lambin, E.F. and P. Meyfroidt. 2011. Global land use change, economic globalization, and the looming land scarcity. Proceedings of the National Academy of Sciences of the United States of America 108: 3465-3472.

Landsberg, J. 2003. Modelling forest ecosystems: state of the art, challenges, and future directions. Canadian Journal of Forest Research 33: 385-397.

Landsberg, J.J. and R.H. Waring. 1997. A generalised model of forest productivity using simplified concepts of radiation-use efficiency, carbon balance and partitioning. Forest Ecology and Management 95: 209-228.

Langley, J.A. and B.A. Hungate. 2003. Mycorrhizal controls on belowground litter quality. Ecology 84: 2302-2312.

Le Quéré, C., R. Moriarty, R.M. Andrew, G.P. Peters, P. Ciais, P. Friedlingstein et al. 2014. Global carbon budget 2014. Earth System Science Data Discussions 7: 521-610.

Le Quéré, C., R. Moriarty, R.M. Andrew, J.G. Canadell, S. Sitch, J.I. Korsbakken et al. 2015. Global carbon budget 2015. Earth System Science Data 7:349-396.

Leifeld, J., M. Zimmermann, J. Fuhrer and F. Conen. 2009. Storage and turnover of carbon in grassland soils along an elevation gradient in the Swiss Alps. Global Change Biology 15: 668-679.

Leite, C., L. Fernando, d.S. Mendonça, Eduardo, O.d.A. Machado, P. Luiz et al. 2004. Simulating trends in soil organic carbon of an Acrisol under no-tillage and disc-plow systems using the Century model. Geoderma 120: 283-295.

Lemke, R.L., A.J. VandenBygaart, C.A. Campbell, G.P. Lafond, B.G. McConkey and B. Grant. 2012. Long-term effects of crop rotations and fertilization on soil C and N in a thin black Chernozem in southeastern Saskatchewan. Canadian Journal of Soil Science 92: 449-461.

Lepers, E., E.F. Lambin, A.C. Janetos, R. DeFries, F. Achard, N. Ramankutty et al. 2005. A synthesis of information on rapid land-cover change for the period 1981-2000. Bioscience 55: 115-124.

Levy, P.E., M.G.R. Cannell and A.D. Friend. 2004. Modelling the impact of future changes in climate, CO_2 concentration and land use on natural ecosystems and the terrestrial carbon sink. Global Environmental Change 14: 21-30.

Li, P., L. Jiang and Z. Feng. 2014. Cross-comparison of vegetation indices derived from landsat-7 enhanced thematic mapper plus (ETM plus) and landsat-8 operational land imager (OLI) sensors. Remote Sensing 6: 310-329.

Li, X.X. and G.F. Shao. 2014. Object-based land-cover mapping with high resolution aerial photography at a county scale in Midwestern USA. Remote Sensing 6: 11372-11390.

Li, Z., M.J. Apps, E. Banfield and W.A. Kurz. 2002. Estimating net primary production of forests in the Canadian prairie provinces using an inventory-based carbon budget model. 169: 161-169.

Li, Z., M.J. Apps, W.A. Kurz and E. Banfield. 2003a. Temporal changes of forest net primary production and net ecosystem production in west central Canada associated with natural and anthropogenic disturbances. Canadian Journal of Forest Research 2351: 2340-2351.

Li, Z., W.A. Kurz, M.J. Apps and S.J. Beukema. 2003b. Belowground biomass dynamics in the Carbon Budget Model of the Canadian Forest Sector: recent improvements and implications for the estimation of NPP and NEP. Canadian Journal of Forest Research 33: 126-136.

Liu, J., J.M. Chen, J. Cihlar and W. Chen. 2002. Net primary productivity mapped for Canada at 1-km resolution. Global Ecology and Biogeography 11: 115-129.

Liu, L., H. Tang, P. Caccetta, E.A. Lehmann, Y. Hu and X. Wu. 2013a. Mapping afforestation and deforestation from 1974 to 2012 using Landsat time-series stacks in Yulin District, a key region of the Three-North Shelter region, China. Environmental Monitoring and Assessment 185: 9949-9965.

Liu, W., D. Schaefer, L. Qiao and X. Liu. 2013b. What controls the variability of wood-decay rates? Forest Ecology and Management 310: 623-631.

Lu, D., P. Mausel, E. Brondízio and E. Moran. 2004. Change detection techniques. International Journal of Remote Sensing 25: 2365-2401.

Lu, D. 2005. Aboveground biomass estimation using Landsat TM data in the Brazilian Amazon. International Journal of Remote Sensing 26: 2509-2525.

Lu, D. 2006. The potential and challenge of remote sensing based biomass estimation. International Journal of Remote Sensing 27: 1297-1328.

Lu, D., M. Batistella and E. Moran. 2008. Integration of landsat TM and SPOT HRG images for vegetation change detection in the Brazilian Amazon. Photogrammetric Engineering and Remote Sensing 74: 421-430.

Luckai, N., G.R. Larocque, L. Archambault, D. Pare, R. Boutin and A. Groot. 2012. Using the Carbon Budget Model of the Canadian Forest Sector (CBM-CFS3) to examine the impact of harvest and fire on carbon dynamics in selected forest types of the Canadian Boreal shield. Forestry Chronicle 88: 426-438.

Luther, J., R. Fournier, D. Piercey, L. Guindon and R. Hall. 2006. Biomass mapping using forest type and structure derived from Landsat TM imagery. International Journal of Applied Earth Observation and Geoinformation 8: 173-187.

Madugundu, R., V. Nizalapur and C.S. Jha. 2008. Estimation of LAI and above-ground biomass in deciduous forests: Western Ghats of Karnataka, India. International Journal of Applied Earth Observation and Geoinformation 10: 211-219.

Majdi, H., K. Pregitzer, A.-S. Morén, J.-E. Nylund and G. I. Ågren. 2005. Measuring fine root turnover in forest ecosystems. Plant and Soil 276: 1-8.

Martin, J.L., S.T. Gower, J. Plaut and B. Holmes. 2005. Carbon pools in a boreal mixedwood logging chronosequence. Global Change Biology 11: 1883-1894.

Masek, J.G., C.Q. Huang, R. Wolfe, W. Cohen, F. Hall, J. Kutler et al. 2008. North American forest disturbance mapped from a decadal Landsat record. Remote Sensing of Environment 112: 2914-2926.

Masek, J.G., W.B. Cohen, D. Leckie, M.A. Wulder, R. Vargas, B. de Jong et al. 2011. Recent rates of forest harvest and conversion in North America. Journal of Geophysical Research-Biogeosciences 116.

Masera, O.R., J.F. Garza-Caligaris, M. Kanninen, T. Karjalainen, J. Liski, G.J. Nabuurs et al. 2003. Modeling carbon sequestration in afforestation, agroforestry and forest management projects: the CO2FIX V.2 approach. Ecological Modelling 164: 177-199.

McConkey, B., C. Liang, G. Padbury, D. Pennock and W. Lindwall. 2000. Measuring Soil Carbon Change on Cropland: The Prairie Soil Carbon Balance Project. Unpublished.

McConkey, B.G., B.C. Liang, C.A. Campbell, D. Curtin, A. Moulin, S.A. Brandt et al. 2003. Crop rotation and tillage impact on carbon sequestration in Canadian prairie soils. Soil and Tillage Research 74: 81-90.

McCullough, D.G., R.A. Werner and D. Neumann. 1998. Fire and insects in northern and boreal forest ecosystems of North America. Annual Review of Entomology 43: 107-127.

Meentemeyer, V. 1978. Macroclimate and lignin control of litter decomposition rates. Ecology 59: 465-472.

Meersmans, J., M.P. Martin, F. De Ridder, E. Lacarce, J. Wetterlind, S. De Baets et al. 2012. A novel soil organic C model using climate, soil type and management data at the national scale in France. Agronomy for Sustainable Development 32: 873-888.

Meigs, G.W., R.E. Kennedy and W.B. Cohen. 2011. A Landsat time series approach to characterize bark beetle and defoliator impacts on tree mortality and surface fuels in conifer forests. Remote Sensing of Environment 115: 3707-3718.

Metherell, A.K., L.A. Harding, C.V. Cole and W.J. Parton. 1993. CENTURY Soil organic matter model environment. Technical documentation. Agroecosystem version 4.0. Great Plains System Research Unit Tech. USDA-ARS. ftp://daac.ornl.gov/data/model_archive/CENTURY/century_vemap_m4/comp/Century_Users_Manual_V4.pdf. (accessed November 12, 2012).

Metsaranta, J.M. and W.A. Kurz. 2012. Inter-annual variability of ecosystem production in boreal jack pine forests (1975-2004) estimated from tree-ring data using CBM-CFS3. Ecological Modelling 224: 111-123.

Meyer, W.B. and B.L. Turner. 1992. Human-population growth and global land-use cover change. Annual Review of Ecology and Systematics 23: 39-61.

Michaelian, M., E.H. Hogg, R.J. Hall and E. Arsenault. 2011. Massive mortality of aspen following severe drought along the southern edge of the Canadian boreal forest. Global Change Biology 17: 2084-2094.

Miegroet, H.V. and M. Olsson. 2011. Ecosystem disturbance and soil organic carbon - a review. In: Soil carbon in sensitive European ecosystems: From science to land management, [R. Jandl, M. Rodeghiero and M. Olsson (eds.)], John Wiley & Sons, Ltd, Chichester, UK. p. 85-117.

Miklos, M., M.G. Short, A.B. McBratney and B. Minasny. 2010. Mapping and comparing the distribution of soil carbon under cropping and grazing management practices in Narrabri, north-west New South Wales. Australian Journal of Soil Research 48: 248-257.

Mohren, G.M.J. and C.G.M.K. Goldewijk. 1990. CO2FIX: A dynamic model of the CO2-fixation in forest stands. Research Institute for Forestry and Urban Ecology. http://dataservices.efi.int/casfor/downloads/co2fix1_2_manual.pdf. (accessed January 22, 2013).

Mokany, K., R.J. Raison and A.S. Prokushkin. 2006. Critical analysis of root : shoot ratios in terrestrial biomes. Global Change Biology 12: 84-96.

Moran, E.F., E.S. Brondizio, J. Tucker, M.C. Silva-Forsberg, I.C. Falesi and a.S. McCracken. 2000. Strategies for Amazonian ForestRestoration: Evidence for Afforestationin Five Regions of the BrazilianAmazon. In: Amazonia at the Crossroads: the challenge of sustainabledevelopment., [A. Hall (eds.)], London, Institute of Latin AmericanStudies. p. 129-149.

Moroni, M.T. 2006. Disturbance history affects dead wood abundance in Newfoundland boreal forests. Canadian Journal of Forest Research 36: 3194-3208.

Moroni, M.T., C.H. Shaw and P. Otahal. 2010. Forest carbon stocks in Newfoundland boreal forests of harvest and natural disturbance origin I: field study. Canadian Journal of Forest Research 40: 2135-2145.

Mottet, A., S. Ladet, N. Coque and A. Gibon. 2006. Agricultural land-use change and its drivers in mountain landscapes: A case study in the Pyrenees. Agriculture Ecosystems & Environment 114: 296-310.

Müller, H., P. Rufin, P. Griffiths, A.J. Barros Siqueira and P. Hostert. 2015. Mining dense Landsat time series for separating cropland and pasture in a heterogeneous Brazilian savanna landscape. Remote Sensing of Environment 156: 490-499.

Murty, D., M.U.F. Kirschbaum, R.E. McMurtrie and A. McGilvray. 2002. Does conversion of forest to agricultural land change soil carbon and nitrogen? Global Change Biology 8: 105-123.

Mustafa, Y.T., P.E. Van Laake and A. Stein. 2011. Bayesian network modeling for improving forest growth estimates. IEEE Transactions on Geoscience and Remote Sensing 49: 639-649.

Nabuurs, G.J., M.J. Schelhaas and A. Pussinen. 2000. Validation of the European Forest Information Scenario Model (EFISCEN) and a projection of Finnish forests. Silva Fennica 34: 167-179.

Nabuurs, G.J., R. Paivinen and H. Schanz. 2001. Sustainable management regimes for Europe's forests - a projection with EFISCEN until 2050. Forest Policy and Economics 3: 155-173.

Nabuurs, G.J. and M.J. Schelhaas. 2002. Carbon profiles of typical forest types across Europe assessed with CO2FIX. Ecological Indicators 1: 213-223.

Nalder, I.A. and H.G. Merriam. 1995. Simulating carbon dynamics of the boreal forest in Pukaskwa National Park. Water Air and Soil Pollution 82: 283-298.

Natural Resources Canada. 2015. Deforestation in Canada: Key myths and facts. http://www.nrcan.gc.ca/forests/fire-insects-disturbances/deforestation/13419. (accessed April 28).

Natural Resources Canada. 2016. The state of Cananda's forest 2015. Canadian Forest Service. http://cfs.nrcan.gc.ca/pubwarehouse/pdfs/36553.pdf. (accessed July 12, 2016).

Nave, L.E., E.D. Vance, C.W. Swanston and P.S. Curtis. 2010. Harvest impacts on soil carbon storage in temperate forests. Forest Ecology and Management 259: 857-866.

Neilson, E.T., D.A. MacLean, F.R. Meng and P.A. Arp. 2007. Spatial distribution of carbon in natural and managed stands in an industrial forest in New Brunswick, Canada. Forest Ecology and Management 253: 148-160.

Nepstad, D.C., A. Verissimo, A. Alencar, C. Nobre, E. Lima, P. Lefebvre et al. 1999. Large-scale impoverishment of Amazonian forests by logging and fire. Nature 398: 505-508.

Nichol, J.E. and M.L.R. Sarker. 2011. Improved Biomass Estimation Using the Texture Parameters of Two High-Resolution Optical Sensors. IEEE Transactions on Geoscience and Remote Sensing 49: 930-948.

NIES. 2014. National GHGs Inventory Report of JAPAN. National Institute for Environmental Studies. http://www.cger.nies.go.jp/en/activities/supporting/publications/report/index.html. (accessed January 10, 2015).

Niu, X. and S.W. Duiker. 2006. Carbon sequestration potential by afforestation of marginal agricultural land in the Midwestern U.S. Forest Ecology and Management 223: 415-427.

Nobre, C.A., P.J. Sellers and J. Shukla. 1991. Amazonian deforestation and regional climate change. Journal of Climate 4: 957-988.

Nunifu, T.K. 2009. Compatible diameter and height increment models for lodgepole pine, trembling aspen, and white spruce. Canadian Journal of Forest Research 39: 180-192.

Nuutinen, T. and S. Kellomaki. 2001. A comparison of three modelling approaches for large-scale forest scenario analysis in Finland. Silva Fennica 35.

Ojima, D.S., K.A. Galvin and B.L. Turner. 1994. The global impact of land-use change. Bioscience 44: 300-304.

Ojima, D.S., W.J. Parton, R. McKeown and W.M. Pulliam. 2002. Century Carbon Model. Ecology Laboratory. USA. http://www.nrel.colostate.edu/projects/century5/. (accessed September 22, 2012).

Pan, Y., R.A. Birdsey, J. Fang, R. Houghton, P.E. Kauppi, W.A. Kurz et al. 2011. A large and persistent carbon sink in the World's forests. Science 333: 988-993.

Parton, W.J., D.S. Schimel, C.V. Cole and D.S. Ojima. 1987. Analysis of factors controlling soil organic levels of grasslands in the Great Plains. Soil Science Society of America Journal 51: 1173-1179.

Peng, C. and M.J. Apps. 1998. Simulating carbon dynamics along the boreal forest transect: Case study (BFTCS) in central Canada. Global Biogeochemical Cycles 12: 393-402.

Peng, C., H. Jiang, M.J. Apps and Y. Zhang. 2002. Effects of harvesting regimes on carbon and nitrogen dynamics of boreal forests in central Canada: a process model simulation. Ecological Modelling 155: 177-189.

Peng, C. and X. Wen. 2006. Forest simulation models. In: Computer Applications in Sustainable Forest Management, [G. Shao and K. Reynolds (eds.)], Springer Netherlands. p. 101-125.

Peng, C. and M.J. Apps. 1997. A coupled century model-gis approach for evaluation of the sustainability of Canadian boreal forests under a changing environment. Integrating Spatial Information Technologies for Tomorrow. GIS World Inc., Vancouver, Canada.

Pennock, D.J., D.W. Anderson and E. De Jong. 1994. Landscape-scale changes in indicators of soil quality due to cultivation in Saskatchewan, Canada. Geoderma 64: 1-19.

Pennock, D.J. and C. van Kessel. 1997a. Clear-cut forest harvest impacts on soil quality indicators in the mixedwood forest of Saskatchewan, Canada. Geoderma 75: 13-32.

Pennock, D.J. and C. van Kessel. 1997b. Effect of agriculture and of clear-cut forest harvest on landscape-scale soil organic carbon storage in Saskatchewan. Canadian Journal of Soil Science 77: 211-218.

Piciarelli, C., C. Micheloni and G.L. Foresti. 2008. Trajectory-based anomalous event detection. IEEE Transactions on Circuits and Systems for Video Technology 18: 1544-1554.

Piirainen, S., L. Finer, H. Mannerkoski and M. Starr. 2007. Carbon, nitrogen and phosphorus leaching after site preparation at a boreal forest clear-cut area. Forest Ecology and Management 243: 10-18.

Pinno, B.D., S.D. Wilson, D.F. Steinaker, K.C.J. Van Rees and S.A. McDonald. 2010. Fine root dynamics of trembling aspen in boreal forest and aspen parkland in central Canada. Annals of Forest Science 67.

Pinno, B.D. and S.D. Wilson. 2011. Ecosystem carbon changes with woody encroachment of grassland in the northern Great Plains. Ecoscience 18: 157-163.

Pontius, R.G., E. Shusas and M. McEachern. 2004. Detecting important categorical land changes while accounting for persistence. Agriculture, Ecosystems & Environment 101: 251-268.

Post, W., W. Emanuel, P. Zinke and A. Stangenberger. 1982. Soil carbon pools and world life zones. Nature 298: 156-159.

Post, W.M. and K.C. Kwon. 2000. Soil carbon sequestration and land-use change: processes and potential. Global Change Biology 6: 317-327.

Potithepa, S., N.K. Nasaharab, H. Muraokac, S. Nagaia and R. Suzukia. 2010. What is the actual relationship between LAI and VI in a deciduous broadleaf forest? In: K. Kajiwara, K. Muramatsu, N. Soyama, T. Endo, A. Ono and S. Akatsuka, editors, Technical Commission VIII Symposium Networking the World with Remote Sensing ISPRS, Japan.

Powell, S.L., D. Pflugmacher, A.a. Kirschbaum, Y. Kim and W.B. Cohen. 2007. Moderate resolution remote sensing alternatives: a review of Landsat-like sensors and their applications. Journal of Applied Remote Sensing 1: 1-16.

Powell, S.L., W.B. Cohen, S.P. Healey, R.E. Kennedy, G.G. Moisen, K.B. Pierce et al. 2010. Quantification of live aboveground forest biomass dynamics with Landsat time-series and field inventory data: A comparison of empirical modeling approaches. Remote Sensing of Environment 114: 1053-1068.

Prescott, C.E., L.L. Blevins and C.L. Staley. 2000. Effects of clear-cutting on decomposition rates of litter and forest floor in forests of British Columbia. Canadian Journal of Forest Research 30: 1751-1757.

Price, D.T., C.H. Peng, M.J. Apps and D.H. Halliwell. 1999. Simulating effects of climate change on boreal ecosystem carbon pools in central Canada. Journal of Biogeography 26: 1237-1248.

Proisy, C., P. Couteron and F. Fromard. 2007. Predicting and mapping mangrove biomass from canopy grain analysis using Fourier-based textural ordination of IKONOS images. Remote Sensing of Environment 109: 379-392.

Pueyo, Y. and S. Begueria. 2007. Modelling the rate of secondary succession after farmland abandonment in a Mediterranean mountain area. Landscape and Urban Planning 83: 245-254.

Qureshi, A., Pariva, R. Badola and S.A. Hussain. 2012. A review of protocols used for assessment of carbon stock in forested landscapes. Environmental Science & Policy 16: 81-89.

Rabenhorst, M.C. 1988. Determination of organic and carbonate carbon in calcareous soils ssing dry combustion. Soil Science Society of America Journal 52: 965-968.

Ramankutty, N. and J.A. Foley. 1999a. Estimating historical changes in global land cover: Croplands from 1700 to 1992. Global Biogeochemical Cycles 13: 997-1027.

Ramankutty, N. and J.A. Foley. 1999b. Estimating historical changes in land cover: North American croplands from 1850 to 1992. Global Ecology and Biogeography 8: 381-396.

Ravindranath, N.H. and M. Ostwald. 2007. Methods for estimating soil organic carbon. Springer Netherlands.

Ravindranath, N.H. and M. Ostwald. 2008. Carbon Inventory Methods: Handbook for Greenhouse Gas Inventory, Carbon Mitigation and Roundwood Production Projects. Springer, London.

Ray, D.K., U.S. Nair, R.O. Lawton, R.M. Welch and R.A. Pielke. 2006. Impact of land use on Costa Rican tropical montane cloud forests: Sensitivity of orographic cloud formation to deforestation in the plains. Journal of Geophysical Research-Atmospheres 111.

Richards, J.A. and X. Jia. 2006. Remote Sensing Digital Image Analysis. 4th ed. Springer-Verlag: Berlin/Heidelberg, Germany.

Romanyà, J., J. Cortina, P. Falloon, K. Coleman and P. Smith. 2000. Modelling changes in soil organic matter after planting fast-growing Pinus radiata on Mediterranean agricultural soils. European Journal of Soil Science 51: 627-641.

Rossel, R.A.V., D.J. Brus, C. Lobsey, Z. Shi and G. McLachlan. 2016. Baseline estimates of soil organic carbon by proximal sensing: Comparing design-based, model-assisted and model-based inference. Geoderma 265: 152-163.

Russell, M.B., S. Fraver, T. Aakala, J.H. Gove, C.W. Woodall, A.W. D'Amato et al. 2015. Quantifying carbon stores and decomposition in dead wood: A review. Forest Ecology and Management 350: 107-128.

Ryan, M.G., M.B. Lavigne and S.T. Gower. 1997. Annual carbon cost of autotrophic respiration in boreal forest ecosystems in relation to species and climate. Journal of Geophysical Research-Atmospheres 102: 28871-28883.

Sader, S.A. 1989. Tropical forest biomass and successional age class relationships to a vegetation index derived from Landsat TM data. Remote Sensing of Environment 28: 143-156.

Sala, O.E., M.E. Biondini and W.K. Lauenroth. 1988. Bias in estimates of primary production: An analytical solution. Ecological Modelling 44: 43-55.

Sanquetta, C.R., A.P. Corte and F. da Silva. 2011. Biomass expansion factor and root-to-shoot ratio for Pinus in Brazil. Carbon Balance and Management 6: 1-8.

Santatonio, D., R.K. Hermann and W.S. Overton. 1977. Root biomass studies in forest ecosystems. Pedobiologia 17.

Scharlemann, J.P.W., E.V.J. Tanner, R. Hiederer and V. Kapos. 2014. Global soil carbon: understanding and managing the largest terrestrial carbon pool. Carbon Management 5: 81-91.

Schelhaas, M.J., G.J. Nabuurs, M. Sonntag and A. Pussinen. 2002. Adding natural disturbances to a large-scale forest scenario model and a case study for Switzerland. Forest Ecology and Management 167: 13-26.

Schelhaas, M.J., P.W.v. Esch, T.A. Groen, B.H.J.d. Jong, M. Kanninen, J. Liski et al. 2004. CO2FIX V 3.1 - A modelling framework for quantifying carbon sequestration in forest ecosystems. ALTERRA. http://www.cifor.org/library/1750/co2fix-v-3-1-a-modelling-

framework-for-quantifying-carbon-sequestration-in-forest-ecosystems/. (accessed August 8, 2013).

Schelhaas, M.J., J. Eggers, M. Lindner, G.J. Nabuurs, A. Pussinen, R. Päivinen et al. 2007. Model documentation for the European Forest Information Scenario model (EFISCEN 3.1.3). Alterra. http://www.efi.int/files/attachments/publications/efi_tr_99_2016_verkerk_et_al.pdf. (accessed June 10, 2014).

Schierhorn, F., D. Muller, T. Beringer, A.V. Prishchepov, T. Kuemmerle and A. Balmann. 2013. Post-Soviet cropland abandonment and carbon sequestration in European Russia, Ukraine, and Belarus. Global Biogeochemical Cycles 27: 1175-1185.

Schroeder, T.A., M.A. Wulder, S.P. Healey and G.G. Moisen. 2011. Mapping wildfire and clearcut harvest disturbances in boreal forests with Landsat time series data. Remote Sensing of Environment 115: 1421-1433.

Seedre, M., B.M. Shrestha, H.Y.H. Chen, S. Colombo and K. Jogiste. 2011. Carbon dynamics of North American boreal forest after stand replacing wildfire and clearcut logging. Journal of Forest Research 16: 168-183.

Seedre, M., A.R. Taylor, H.Y.H. Chen and K. Jogiste. 2012. Deadwood density of five boreal tree species in relation to field-assigned decay class. Forest Science 59: 253-260.

Seedre, M., A.R. Taylor, B.W. Brassard, H.Y.H. Chen and K. Jõgiste. 2014. Recovery of ecosystem carbon stocks in young boreal forests: a comparison of harvesting and wildfire disturbance. Ecosystems 17: 851-863.

Seidel, D., S. Fleck, C. Leuschner and T. Hammett. 2011. Review of ground-based methods to measure the distribution of biomass in forest canopies. Annals of Forest Science 68: 225-244.

Senf, C., D. Pflugmacher, M.A. Wulder and P. Hostert. 2015. Characterizing spectral-temporal patterns of defoliator and bark beetle disturbances using Landsat time series. Remote Sensing of Environment 170: 166-177.

Serra, P., X. Pons and D. Sauri. 2003. Post-classification change detection with data from different sensors: some accuracy considerations. International Journal of Remote Sensing 24: 3311-3340.

Shakun, J.D., P.U. Clark, F. He, S.A. Marcott, A.C. Mix, Z. Liu et al. 2012. Global warming preceded by increasing carbon dioxide concentrations during the last deglaciation. Nature 484: 49-54.

Shorohova, E. and E. Kapitsa. 2016. The decomposition rate of non-stem components of coarse woody debris (CWD) in European boreal forests mainly depends on site moisture and tree species. European Journal of Forest Research 135: 593-606.

Silver, W.L., R. Ostertag and A.E. Lugo. 2000. The potential for carbon sequestration through reforestation of abandoned tropical agricultural and pasture lands. Restoration Ecology 8: 394-407.

Simard, D.G., J.W. Fyles, D. Paré and T. Nguyen. 2001. Impacts of clearcut harvesting and wildfire on soil nutrient status in the Quebec boreal forest. Canadian Journal of Soil Science 81: 229-237.

Singh, A. 1989. Digital change detection techniques using remotely-sensed data. International Journal of Remote Sensing 10: 989-1003.

Six, J., E.T. Elliott, K. Paustian and J.W. Doran. 1998. Aggregation and soil organic matter accumulation in cultivated and native grassland soils. Soil Science Society of America Journal 62: 1367-1377.

Smith, P., J.U. Smith, D.S. Powlson, W.B. McGill, J.R.M. Arah, O.G. Chertov et al. 1997. A comparison of the performance of nine soil organic matter models using datasets from seven long-term experiments. Geoderma 81: 153-225.

Smith, P., D.S. Powlson, M.J. Glendining and J.U. Smith. 1998a. Preliminary estimates of the potential for carbon mitigation in European soils through no-till farming. Global Change Biology 4: 679-685.

Smith, R.E., H. Veldhuis, G.F. Mills, R.G. Eilers, W.R. Fraser and G.W. and Lelyk. 1998b. Terrestrial Ecozones, Ecoregions, and Ecodistricts of Manitoba. Agriculture and Agri-Food Canada. http://sis.agr.gc.ca/cansis/publications/ecostrat/provDescriptions/mbteee/mbteee_report.pdf. (accessed February 15, 2013).

Smith, W.N., R.L. Desjardins and B. Grant. 2001. Estimated changes in soil carbon associated with agricultural practices in Canada. Canadian Journal of Soil Science 81: 221-227.

Smyth, C.E., W.A. Kurz and J.A. Trofymow. 2011. Including the effects of water stress on decomposition in the Carbon Budget Model of the Canadian Forest Sector CBM-CFS3. Ecological Modelling 222: 1080-1091.

Soenen, S.A., D.R. Peddle, R.J. Hall, C.A. Coburn and F.G. Hall. 2010. Estimating aboveground forest biomass from canopy reflectance model inversion in mountainous terrain. Remote Sensing of Environment 114: 1325-1337.

Soil Classification Working Group. 1987. The Canadian System of Soil Classification. Second ed. Agriculture Canada Publication, Ottawa, Ontario, Canada.

Song, C., C.E. Woodcock, K.C. Seto, M.P. Lenney and S.A. Macomber. 2001. Classification and change detection using Landsat TM data: when and how to correct atmospheric effects? Remote Sensing of Environment 75: 230-244.

Soudani, K., C. François, G. le Maire, V. Le Dantec and E. Dufrêne. 2006. Comparative analysis of IKONOS, SPOT, and ETM+ data for leaf area index estimation in temperate coniferous and deciduous forest stands. Remote Sensing of Environment 102: 161-175.

Spies, T.A., J.F. Franklin and T.B. Thomas. 1988. Coarse woody debris in douglas-fir forests of western Oregon and Washington. Ecology 69: 1689-1702.

Ståhl, G., B. Boström, H. Lindkvist, A. Lindroth, J. Nilsson and M. Olsson. 2004. Methodological options for quantifying changes in carbon pools in Swedish forests. Studia Forestalia Suecica 214: 46.

Stanek, W. and D. State. 1978. Equations predicting primary productivity (biomass) of trees, shrubs and lesser vegetation based on current literature. Environment Canada. https://cfs.nrcan.gc.ca/publications?id=3991. (accessed May 21, 2012).

Statistics Canada. 2008. Total farm area, land tenure and land in crops, by province (Census of Agriculture, 1986 to 2006). Statistics Canada. http://www40.statcan.gc.ca/l01/cst01/agrc25a-eng.htm. (accessed March 26, 2013).

Steele, S.J., S.T. Gower, J.G. Vogel and J.M. Norman. 1997. Root mass, net primary production and turnover in aspen, jack pine and black spruce forests in Saskatchewan and Manitoba, Canada. Tree Physiology 17: 577-587.

Sterling, S.M., A. Ducharne and J. Polcher. 2013. The impact of global land-cover change on the terrestrial water cycle. Nature Climate Change 3: 385-390.

Stinson, G., W.A. Kurz, C.E. Smyth, E.T. Neilson, C.C. Dymond, J.M. Metsaranta et al. 2011. An inventory-based analysis of Canada's managed forest carbon dynamics, 1990 to 2008. Global Change Biology 17: 2227-2244.

Sun, G., K.J. Ranson and V.I. Kharuk. 2002. Radiometric slope correction for forest biomass estimation from SAR data in the Western Sayani Mountains, Siberia. Remote Sensing of Environment 79: 279-287.

Takeda, T., H. Oguma, T. Sano, Y. Yone and Y. Fujinuma. 2008. Estimating the plant area density of a Japanese larch (*Larix kaempferi Sarg*.) plantation using a ground-based laser scanner. Agricultural and Forest Meteorology 148: 428-438.

Tans, P. and E. Dlugokencky. 2015. Trends in atmospheric carbon dioxide. National Oceanic and Atmospheric Administration, Earth System Research Laboratory. http://www.esrl.noaa.gov/gmd/ccgg/trends/global.html#global_growth. (accessed September 20, 2015).

Ter-Mikaelian, M.T. and M.D. Korzukhin. 1997. Biomass equations for sixty-five North American tree species. Forest Ecology and Management 97: 1-24.

Thomsen, I.K., P. Schjønning, B. Jensen, K. Kristensen and B.T. Christensen. 1999. Turnover of organic matter in differently textured soils: II. Microbial activity as influenced by soil water regimes. Geoderma 89: 199-218.

Thurig, E. and M.J. Schelhaas. 2006. Evaluation of a large-scale forest scenario model in heterogeneous forests: a case study for Switzerland. Canadian Journal of Forest Research 36: 671-683.

Tian, X., Z.B. Su, E.X. Chen, Z.Y. Li, C. van der Tol, J.P. Guo et al. 2012. Estimation of forest above-ground biomass using multi-parameter remote sensing data over a cold and arid area. International Journal of Applied Earth Observation and Geoinformation 14: 160-168.

Tilman, D., C. Balzer, J. Hill and B.L. Befort. 2011. Global food demand and the sustainable intensification of agriculture. Proceedings of the National Academy of Sciences of the United States of America 108: 20260-20264.

Tinker, D.B. and D.H. Knight. 2001. Temporal and spatial dynamics of coarse woody debris in harvested and unharvested lodgepole pine forests. Ecological Modelling 141: 125-149.

Tømmervik, H. 2003. Monitoring vegetation changes in Pasvik (Norway) and Pechenga in Kola Peninsula (Russia) using multitemporal Landsat MSS/TM data. Remote Sensing of Environment 85: 370-388.

Townshend, J.R.G. and C.O. Justice. 1995. Spatial variability of images and the monitoring of changes in the Normalized Difference Vegetation Index. International Journal of Remote Sensing 16: 2187-2195.

Tubiello, F.N., M. Salvatore, A.F. Ferrara, J.I. House, S. Federici, S. Rossi et al. 2015. The contribution of agriculture, forestry and other land use activities to global warming, 1990-2012. Global Change Biology 21: 2655-2660.

Tucker, C.J. and P.J. Sellers. 1986. Satellite remote sensing of primary production. International Journal of Remote Sensing 7: 1395-1416.

UNEP. 2014. Assessing global land use: Balancing consumption with sustainable supply. United Nations Environment Programme. http://www.unep.org/resourcepanel/Portals/50244/publications/Full_Report-Assessing_Global_Land_UseEnglish_(PDF).pdf. (accessed Septemper 22, 2015).

van der Kamp, G., W.J. Stolte and R.G. Clark. 1999. Drying out of small prairie wetlands after conversion of their catchments from cultivation to permanent brome grass. Hydrological Sciences Journal 44: 387-397.

van der Werf, G.R., J.T. Randerson, L. Giglio, G.J. Collatz, M. Mu, P.S. Kasibhatla et al. 2010. Global fire emissions and the contribution of deforestation, savanna, forest, agricultural, and peat fires (1997-2009). Atmospheric Chemistry and Physics 10: 11707-11735.

van Meijl, H., T. van Rheenen, A. Tabeau and B. Eickhout. 2006. The impact of different policy environments on agricultural land use in Europe. Agriculture, Ecosystems & Environment 114: 21-38.

VandenBygaart, A.J., E.G. Gregorich and D.A. Angers. 2003. Influence of agricultural management on soil organic carbon: A compendium and assessment of Canadian studies. Canadian Journal of Soil Science 83: 363-380.

VandenBygaart, A.J. and D.A. Angers. 2006. Towards accurate measurements of soil organic carbon stock change in agroecosystems. Canadian Journal of Soil Science 86: 465-471.

VandenBygaart, A.J., B.G. McConkey, D.A. Angers, W. Smith, H. de Gooijer, M. Bentham et al. 2008. Soil carbon change factors for the Canadian agriculture national greenhouse gas inventory. Canadian Journal of Soil Science 88: 671-680.

Vitousek, P.M. 1994. Beyond global warming - Ecology and global change. Ecology 75: 1861-1876.

Volney, W.J.A. and R.A. Fleming. 2000. Climate change and impacts of boreal forest insects. Agriculture, Ecosystems & Environment 82: 283-294.

Walther, G.R., E. Post, P. Convey, A. Menzel, C. Parmesan, T.J.C. Beebee et al. 2002. Ecological responses to recent climate change. Nature 416: 389-395.

Wang, D.L. and D.W. Anderson. 1998. Direct measurement of organic carbon content in soils by the Leco CR-12 carbon analyzer. Communications in Soil Science and Plant Analysis 29: 15-21.

Wang, J.R., A.L. Zhong, P. Comeau, M. Tsze and J.P. Kimmins. 1995. Aboveground biomass and nutrient accumulation in an age sequence of Aspen (*Populus-tremuloides*) stands in the Boreal White and Black Spruce zone, British-Columbia. Forest Ecology and Management 78: 127-138.

Wang, Q., S. Adiku, J. Tenhunen and A. Granier. 2005. On the relationship of NDVI with leaf area index in a deciduous forest site. Remote Sensing of Environment 94: 244-255.

Wang, X., J. Wang and J. Zhang. 2012. Comparisons of three methods for organic and inorganic carbon in calcareous soils of northwestern China. PLoS ONE 7: e44334.

Weggler, K., M. Dobbertin, E. Jüngling, E. Kaufmann and E. Thürig. 2012. Dead wood volume to dead wood carbon: the issue of conversion factors. European Journal of Forest Research 131: 1423-1438.

Wei, X., M. Shao, W. Gale and L. Li. 2014. Global pattern of soil carbon losses due to the conversion of forests to agricultural land. Scientific Reports 4: 4062.

White, J.D., N.C. Coops and N.A. Scott. 2000. Estimates of New Zealand forest and scrub biomass from the 3-PG model. Ecological Modelling 131: 175-190.

Wulder, M. A. and T. Nelson. 2003. EOSD land cover classification legend report. Canadian Forest Service, Pacific Forestry Centre, Victoria, British Columbia, Canada. https://cfs.nrcan.gc.ca/publications?id=33752. (accessed July 10, 2013).

Wulder, M.A., J.C. White, S.N. Goward, J.G. Masek, J.R. Irons, M. Herold et al. 2008. Landsat continuity: Issues and opportunities for land cover monitoring. Remote Sensing of Environment 112: 955-969.

Wulder, M.A., J.C. White, G. Stinson, T. Hilker, W.A. Kurz, N.C. Coops et al. 2010. Implications of differing input data sources and approaches upon forest carbon stock estimation. Environmental Monitoring and Assessment 166: 543-561.

Wulder, M.A., J.C. White, R.F. Nelson, E. Næsset, H.O. Ørka, N.C. Coops et al. 2012. Lidar sampling for large-area forest characterization: A review. Remote Sensing of Environment 121: 196-209.

Xie, Y., Z. Sha and M. Yu. 2008. Remote sensing imagery in vegetation mapping: a review. Journal of Plant Ecology 1: 9-23.

Yatskov, M., M.E. Harmon and O.N. Krankina. 2003. A chronosequence of wood decomposition in the boreal forests of Russia. Canadian Journal of Forest Research 33: 1211-1226.

Yuan, Z.Y. and H.Y.H. Chen. 2010. Fine root biomass, production, turnover rates, and nutrient contents in boreal forest ecosystems in relation to species, climate, fertility, and stand age: Literature Review and Meta-Analyses. Critical Reviews in Plant Sciences 29: 204-221.

Zell, J., G. Kändler and M. Hanewinkel. 2009. Predicting constant decay rates of coarse woody debris—A meta-analysis approach with a mixed model. Ecological Modelling 220: 904-912.

Zhang, C.F., R.C. Jamieson, F.R. Meng, R.J. Gordon, J. Bhatti and C.P.A. Bourque. 2011. Long-term forest-floor litter dynamics in Canada's boreal forest: Comparison of two model formulations. Ecological Modelling 222: 1236-1244.

Zhang, D., D. Hui, Y. Luo and G. Zhou. 2008. Rates of litter decomposition in terrestrial ecosystems: global patterns and controlling factors. Journal of Plant Ecology 1: 85-93.

Zhang, X., T. Huffman, J. Liu and H. Liu. 2014. Soil capability as a predictor of cropland change in Alberta, Canada from 1988 to 2010. Soil Use and Management 30: 403-413.

Zheng, D., L.S. Heath and M.J. Ducey. 2008. Spatial distribution of forest aboveground biomass estimated from remote sensing and forest inventory data in New England, USA. Journal of Applied Remote Sensing 2: 021502-021502.

Zheng, G., J. Chen, Q. Tian, W. Ju and X. Xia. 2007. Combining remote sensing imagery and forest age inventory for biomass mapping. Journal of Environmental Management 85: 616-623.

Zhu, Z. and C.E. Woodcock. 2012. Object-based cloud and cloud shadow detection in Landsat imagery. Remote Sensing of Environment 118: 83-94.

Zwiers, F.W. 2002. Climate change: The 20-year forecast. Nature 416: 690-691.